



## **Book of Abstracts**

18<sup>th</sup> Annual Conference on  
Engineering of Functional Interfaces  
and  
3<sup>rd</sup> International SIIRI Symposium

Hannover, 2026

Session	Author	Title	Page
	Prof. Kunimoto	Electrochemical Deposition for Functional Surfaces and Interfaces: Principles, Applications, and Analysis	1
A 1	Zach	Silk fibroin-riboflavin substrates for transient magnesium temperature sensors	2
A 2	Welden	How viruses gate a sensor: Modelling C-V response of TMV modified EISCAPs and experimental data	3
A 3	El-Jamal	pH Sensitive Hydrogels for Plasmonic-based Biofluid Sensing	4
A 4	Achtsnicht	Surface treatment using plasma sterilization - generation, application and mechanisms of action	5
A 5	Nagao	Dynamic Reconstruction of Anodized Fe-Co-Ni Spinel Oxide Functional Interfaces during the Oxygen Evolution Reaction (OER)	6
A 6	Alsholi	A Synthetic Receptor Approach for the Rapid Identification of Clinical Cancer Biomarkers	7
A 7	Özsoylu	Template-bacteria-free engineering of biomimetic polymer interfaces for selective E. coli capture and detection	8
A 8	Atanasova	Combinatorial Screening of Anodic Ti-Hf Oxides for Memristive Switching Properties	9
A 9	Batool	Design and Implementation of a Catheter-Integrated Biosensor Based on Molecularly Imprinted Polymers for Histamine Detection	10
A 10	Drexler	Electrospinning of PDMS Elastomer for Hydrophobic Surface Coatings	11
A 11	Garg	Non-Enzymatic Creatinine Detection Using Electroactive Molecularly Imprinted Polymers: Toward Point-of-Care Sensing	12
A 12	Duitscher	Temporally and spatially resolved pH in commensal and pathogenic oral biofilms in vitro	13
A 13	Iken	Effect of UV irradiation on the flatband voltage of chemical sensors with field-effect structures	14
A 14	Biswas	Spin-Dependent Wetting of Chiral Molecules via CISS	15
A 15	Karschuck	Building a portable measurement platform to detect per- and polyfluoroalkyl substances (PFAS) in soil and wastewater	16
A 16	Angerer	Raman-Based Visualization of Diffusion-Driven Delamination at Metal-Polymer-Interfaces of Active Implantable Medical Devices (AIMDs)	17
A 17	Lehnert	Effectiveness of deconvolution methods for surface reconstruction in AFM	18
A 18	Malekahmadi	Biofilm-Dependent MG-63 Responses in the 3D INTER <sub>6</sub> ACT-B Peri Implant Model	19
A 19	Wiebe	BDNF-optimized mesenchymal stem cells for therapeutic application in the inner ear	20
A 20	Badagnani de Carvalho	Development of flexible polyimide devices incorporated with polyvinylidene fluoride for applications as piezoelectric sensors and supercapacitors	21
A 21	Reiter	Neodymium-Samarium alloys with improved mechanical properties	22
A 22	Knoll	Device-to-device matching of extended-gate field-effect transistors with atomic-layer deposited high-k Ta2O5 as pH-sensitive material	23
A 23	Heine	Titanium-hydrogel-interaction in a peri-implant <i>in-vitro</i> model	24
A 24	Li	Structural and Electrochemical Investigation of Electrodeposited PEDOT:PSS Microelectrodes	25
A 25	Janzen	Surface functionalization with photoelectrons	26

A 26	Guzman-Landero	Development of Molecularly Imprinted Polymers as an Indirect Sensing Approach for Spore-Forming Bacteria Detection	27
A 27	Schäffl	Modular Raman Image Analysis of Calcium-Crosslinked Alginate Hydrogels	28
A 28	Konrad	PEDOT:PDA as a promising new polymer for the development of MIPs in electrochemical sensors	29
B 1	Zengin	Enhanced corrosion stability of Scandium-rich Magnesium alloy thin films in simulated body fluid	30
B 2	Kimoto	Studying of Organic Semiconductors in Light-Addressable Potentiometric Sensors (LAPS)	31
B 3	Börnert	PECVD Preparation of Silicon Carbide Layers as passivating contacts for POLO Solar Cells	32
B 4	Singla	Ultrasensitive Electrochemical Detection of Penicillin G Using Electroactive Molecularly Imprinted Polymers for Sepsis Monitoring	33
B 5	Kumar	Superparamagnetic Iron Oxide Nanoparticles in Niosomal Systems for Biomedical Applications	34
B 6	Ayouch	ML-based porous metamaterials design for hip implant stability	35
B 7	Sun	Influence of various oxygen levels on tissue-biofilm interaction in an implant-tissue-oral-bacterial-biofilm model	36
B 8	Vu	Investigation of TiNx Thin film Deposited by Ion Beam Deposition and Sputtering for electronic and bioelectronic applications	37
B 9	Yousaf	Melt Electrowritten Fibrous Scaffolds for Bone Tissue Engineering: From Architectural Design to Dynamic Cell Culture	38
B 10	Gaikwad	An Advanced Three-Dimensional Peri-implant Tissue Model to Investigate Host-Microbe Interactions	39
B 11	Nawaz	Diabetes-Associated Host Dysregulation at the Peri-Implant Tissue Interface in an Immunocompetent 3D Cell Culture Model	40
B 12	Schulz	Interface-induced shear control for enhanced flow of shear-thinning silicones in micro-annular printheads	41
B 13	Tragoudas	Computational modeling of stent failure during crimping and deployment in coronary arteries	42
B 14	Nguyen	Biodegradable nanoMIP Interfaces Enable Selective IL-6 Detection in Human Perilymph	43
B 15	Christmann	Microwave-Assisted Preparation of Bone Regeneration Materials	44
B 16	Bogaardt	Direct Detection of <i>Staphylococcus aureus</i> via Microparticle Imprinted Polymers	45
B 17	Miller	Biocompatible surface modification of dental implants	46
B 18	Roger	Optimized implants through control of stem and immune cells: modulation of TAK1 activity	47
B 19	Höchel	Simulation of Biofilm Growth and Drug-Induced Degradation	48
B 20	Devkota	Photovoltaic-Driven Organo-Electronic Ion Pump for Wireless Retinal Ionic Stimulation	49
B 21	Molasarvestani	Development of an integration process for a high-density electrode array for future retinal implant	50
B 22	Fuenzalida	Electrostatics of Thin-Film MOS Devices for Gas Electroadsorption	51
B 23	Dhanjai	Single Enzyme Nanocapsules for Highly Stable & Robust Bio-sensing	52
B 24	Püttmann	Characteristic pH profiles in a dual-species biofilm model associated with musculoskeletal implant infections	53

B 25	Bode	Electrospun SLIPS as Anti-Adhesive Biomaterial Coatings: Effects on Wettability and Biological Interactions	54
B 26	Brüning	Bioimpedance Model Fitting for Clinical Biomarker Quantification	55
B 27	Guo	A CFD–DEM Framework for Predicting Thermo-Mechanical Drying Behaviour of mRNA-LNP Vaccine Droplets	56
B 28	Greul	The Corrosion of Titanium Dental Implants in Dental Hygiene Products	57
B 29	Lukina	Influence of Thiol-Based Self-Assembled Monolayers on the Electrochemical Behavior of Combinatorial Ag-Cu Thin Films	58
C 1	Engelmann	Insights in Biomedical Applications of Magnetic Nanoparticles from Nonequilibrium Dynamic Relaxation Simulations	59
C 2	Beging	Impact of ionophore concentration on sensor performance of Na <sup>+</sup> -ion sensitive field-effect capacitors	60
C 3	Łuczak	Analysing functionalisation of FETs used in biosensing with KPFM	61
C 4	Hauseder	Towards tunable biomineralization Morphology studies of calcium carbonate formation in silk-based solutions	62
C 5	Bakhshi Schani	A multiplexed impedimetric biosensor platform for lung-disease biomarker detection in exhaled breath condensate	63
C 6	Liu	Innovative Sensing to Optimise Parkinson’s Disease Management	64
C 7	Braemer	In vitro investigation of electrospun PVDF-TrFE fiber mats regarding their influence on electrical impedance and cell proliferation	65
C 8	Chowdhury	Long-Term Human Brain-Slice Electrophysiology using a Flexible Microelectrode Interface	66
C 9	Dosdogru	Qualification of a Swellable Hydrogel–Silicone Bimorph for Implantable Actuation	67
C 10	Duan	Medium-dependent Mg ion release and biological responses to WE43 magnesium alloy	68
C 11	Tiwari	Double-Imprinted nanoMIPs for Targeted Drug Delivery in NSCLC	69
C 12	Frings	Accurate concentration prediction in multispecies bacterial samples using FTIR spectroscopy and deep learning	70
C 13	Mattauch	Effective contact-area investigation in polymer-based TENGs	71
C 14	Evers	Finite element modelling for gentle removal of total hip arthroplasties by means of induction heating	72
C 15	Furtado	Green Chemistry Meets Thermal Sensing: Sustainable Metal MIP–based Sensors for L-Leucine Detection	73
C 16	Leuker	Mussel-Inspired Nanoprecipitation Coatings for Complex Geometries	74
C 17	Käsehagen	MatrixModel: Building a Computational Model of the HSPC Niche	75
C 18	Baron	Adjacent Hydrogel Thin-Films for a competitive cell culture assay	76
C 19	Lohar	Establishment of personalized immunocompetent 3D peri-implant-mucosa models using patient-derived macrophages	77
C 20	Hofinger	Systematic study of Ytterbium influence in binary alloying systems	78
D 1	Onken	Fully Additive Neural Implants ... and understanding why they fail	79
D 2	Arndt	Continuous Millifluidic Synthesis of ZnO Nanostructures	80
D 3	Blank	Corrosion Sensing for Cochlear Implants	81

D 4	Boukari	Streptavidin-based anti-adhesive biofunctionalization for dental implants	82
D 5	Börmann-El Kholy	Advancing a multi-sensor array platform for real-time drinking water quality surveillance	83
D 6	Chen	Evaluation of Host Responses to Biofilms with Distinct Pathogenic Potential Using a 3D Macrophage-Containing INTER <sub>6</sub> ACT Model	84
D 7	Guo	Controlling Adhesion of Bacteria and Host Tissue Cells by Polyelectrolyte Multilayer Coatings on Titanium-based Biomaterials	85
D 8	Tamjdtash	Adhesion characteristics of <i>Candida albicans</i> on polymer-based materials	86
D 9	Gellert	Development of an electrochemically synthesized RNA sensor	87
D 10	Reus	Plasma-Engineered Coatings for the Reduction of Biomaterial Adhesion	88
D 11	Di Scala	A Biosensor with Simplified Target Recognition for Early Detection of Leprosy from Serum of Household Contacts	89
D 12	Knabel	Additively manufactured drug delivery implants made from photo crosslinked methacrylated pullulan	90
D 13	Schneider	New platform for microfluidic structuring in glass	91
D 14	Thomsen	Hormone-Driven Modulation of Implant-Associated Biofilms	92
D 16	Fang	Photoelectrochemical sensing and mapping of flow velocity in microfluidics	93
D 17	Brockert	Creating biomimetic 3D in vitro models of the bone-marrow / implant interface	94
D 18	Zerrik	Direct 3D Printing of Soft Neural Implants onto Flexible PCB Substrates	95
D 19	Ehlers	Fabrication and preliminary optimization of an in situ written PEGDA membrane in a quartz glass microfluidic chip	96
D 20	Awerbuch	Bacteria-surface interaction on smooth and rough titanium: Correlation between surface characteristics and bacterial adhesion	97

# Electrochemical Deposition for Functional Surfaces and Interfaces: Principles, Applications, and Analysis

Masahiro Kunimoto<sup>1</sup>

[m.kunimoto@waseda.jp](mailto:m.kunimoto@waseda.jp)

<sup>1</sup>Waseda Center for a Carbon Neutral Society, Waseda University, Okubo 3-4-1, Shinjuku, Tokyo, 169-8555, Japan

**Abstract:** This tutorial presents the fundamentals of electrochemical deposition process as an advanced industrial technique for the creation of functional surfaces and interfaces. The operating principle of electrochemical deposition is based on both electrochemistry and crystallization, requiring interdisciplinary knowledge of these areas. Furthermore, electrochemical deposition has a wide range of applications and has recently emerged as an important design guideline for controlling interfaces, particularly in energy-related technologies. This talk describes the fundamental aspects of the technique in a systematic manner, also highlighting recent progress in the analysis of electrochemical deposition phenomena.

**Keywords:** electrochemical deposition, crystallization, spectroscopy, multi-scale simulation

Electrochemical deposition is a versatile technique that integrates electrochemical reactions with crystallization processes, enabling the formation of metal or alloy thin films on substrates and the creation of interfaces between distinct phases with unique surface functionalities. Originally developed as an industrial method to provide mechanically and/or chemically durable coatings on engineering materials, it is now widely recognized as an indispensable technology for the fabrication of precise electronic components and as a key methodology for preparing functional electrodes in advanced devices such as batteries and sensors.

Against this background, significant efforts have been devoted to improving the controllability of electrochemical deposition. Such control requires a mechanistic understanding of the underlying processes and, consequently, a solid foundation in electrochemistry, which involves both mass transfer and reaction, and crystallization kinetics. Electrochemistry deals with reduction and oxidation reactions driven by potential differences at interfacial regions, whether externally applied or internally generated, and provides a fundamental framework based on thermodynamics, reaction rate theory, and electromagnetism. Crystallization kinetics, governed by supersaturation, interfacial interactions between deposits and substrates play a central role in determining the mechanical, chemical, and optical properties of deposited materials as well as the characteristics of the resulting interfaces.

A key challenge lies in identifying and controlling the fundamental parameters that govern these coupled processes. When appropriately understood and regulated based on sound theoretical principles, electrochemical deposition offers a powerful framework for the rational design of functional interfaces. In this tutorial, we highlight the physical

models underlying electrochemistry and crystallization kinetics and provide a systematic perspective that enables a clear understanding of both the governing principles and the practical, experience-based aspects of the technique.

Furthermore, electrochemical deposition concepts are increasingly recognized as essential in the development of next-generation energy storage technologies for sustainable power systems. In battery systems, uncontrolled electrodeposition can induce irregular morphological evolution of electrodes, leading to severe performance degradation and, in some cases, critical safety issues. Over the years, electrochemical engineering has established effective strategies to control such phenomena, giving rise to the concept of “kinetic interfacial design” as a guiding principle for practical applications. This presentation highlights representative examples of kinetically governed electrode behaviour and discusses solution strategies from the viewpoint of electrochemical deposition, illustrating how fundamental understanding can be translated into practical design guidelines.

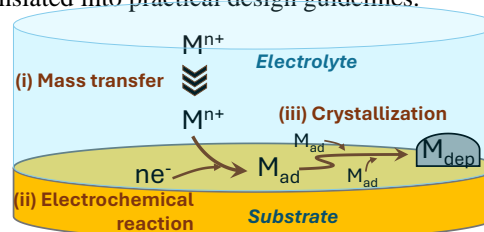


**Figure 1:** The art of electrochemical deposition: (i) mass transfer + (ii) electrochemical reaction + (iii) crystallization.

## Acknowledgements

This study was financially supported in part from the “Adaptive and Seamless Technology Transfer Program through Target-driven R&D (A-STEP, JPMJTR202K)” of the Japan Science and Technology Agency (JST), Japan.

# Silk fibroin–riboflavin substrates for transient magnesium temperature sensors

M. Zach<sup>1,2</sup>, S. Achtsnicht<sup>1</sup>, M. Welden<sup>1</sup>, M. Rodrigues<sup>3</sup>, B. Isella<sup>3</sup>, A. Kopp<sup>3,4</sup>, M. Keusgen<sup>2</sup>, M. J. Schöning<sup>1,5</sup>

[zach@fh-aachen.de](mailto:zach@fh-aachen.de)

<sup>1</sup>Institute of Nano- and Biotechnologies (INB), FH Aachen University of Applied Sciences, Campus Jülich, Heinrich-Mußmann-Str. 1, 52428 Jülich, Germany

<sup>2</sup>Institute of Pharmaceutical Chemistry, Marburg University, Wilhelm-Roser-Str. 2, 35037 Marburg, Germany

<sup>3</sup>Fibrothelium GmbH, Philipsstr. 8, 52068 Aachen, Germany

<sup>4</sup>Meotec GmbH, Philipsstr. 8, 52068 Aachen, Germany

<sup>5</sup>Institute of Biological Information Processing (IBI-3), Forschungszentrum Jülich GmbH, Wilhelm-Johnen-Str., 52425 Jülich, Germany

**Abstract:** A new research strategy for biocompatible, implantable temperature sensors is presented. The resistance temperature detectors (RTDs) are made of silk fibroin with incorporated riboflavin (SFRF) and magnesium (Mg)-based alloys. Goal of this study is to investigate sensor performance in the physiologically relevant temperature range between 30 °C and 42.9 °C.

**Keywords:** temperature sensor, bioabsorbable, silk-fibroin, riboflavin, magnesium alloy

## Introduction

Implantable and bioresorbable sensors are of great interest for continuous monitoring of postoperative healing processes, such as those following skin grafts, as they would eliminate the need for an additional surgical removal [1,2]. Here, the first 72 hours are crucial for the healing process [2]. Magnesium can be used as a temperature-dependent resistive material because it is both biocompatible and bioabsorbable, as previous studies have already demonstrated [3]. This study examines SFRF as a new biocompatible and bioabsorbable substrate material for Mg-based RTDs, to overcome limitations that arise when using polylactic acid (PLA) with different encapsulation materials.

## Results and Discussion

As shown in Figure 1, meander-shaped Mg-based RTDs were deposited via thin-film technology onto a SFRF substrate. Performance and lifetime of the sensors were characterized under ambient air conditions between 30 °C and 42.9 °C. The RTDs on SFRF exhibited a resistance temperature coefficient of approximately 0.003 °C<sup>-1</sup> which is fully comparable to values achieved for Mg-based RTDs on PLA.

## Conclusions

The sensors were successfully characterized at ambient air conditions between 30 °C and 42.9 °C. A comparison between the sensor performance of Mg-based RTDs on SFRF and those on a PLA substrate clearly demonstrates SFRF's suitability as substrate material. The key advantage of SFRF over PLA is that it allows for the use of natural

encapsulation materials with greater temperature stability, such as carnauba wax or poly(lactic-co-glycolic) acid (PLGA).

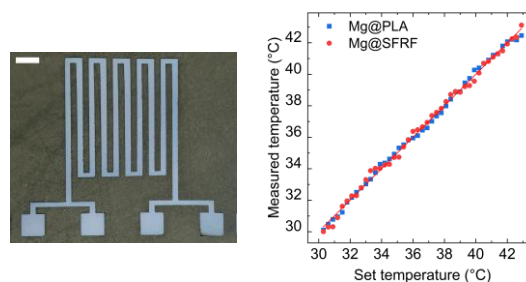


**Figure 1** Mg-based RTD on SFRF substrate (left); the white bar corresponds to 2 mm. Measured temperature (right) with RTD on PLA (blue) and SFRF (red) vs. set temperature; linear regression for both RTDs is overlapping.

## References

- [1] P. Ayisha Sana, K. P. Khadeeja Thanha, K. Pramod. *Asia-Pac. J. Chem. Eng.* **20** (2025) 6. doi: 10.1002/apj.70094
- [2] D. Özsoylu, K. A. Janus, S. Achtsnicht, T. Wagner, M. Keusgen, M. J. Schöning. *Sens. Actuators Rep.* **6** (2023) 100163. doi: 10.1016/j.sn.2023.10063
- [3] K. A. Janus, S. Achtsnicht, A. Drinic, A. Kopp, M. Keusgen, M. J. Schöning. *Appl. Res.* **3** (2024) 3. doi: 10.1002/appl.202300102

## Acknowledgements

This work was funded by the Deutsche Forschungsgemeinschaft (DFG: German Research Foundation) – 548199022. H. Iken is acknowledged for technical support.

# How viruses gate a sensor: Modelling C-V response of TMV-modified EISCAPs and experimental data

M. Welden<sup>1</sup>, A. Poghossian<sup>2</sup>, C. Wege<sup>3</sup>, M. J. Schöning<sup>1,4</sup>

[m.welden@fh-aachen.de](mailto:m.welden@fh-aachen.de)

<sup>1</sup>Institute of Nano- and Biotechnologies (INB), FH Aachen University of Applied Sciences, Campus Jülich, Heinrich-Mußmann-Str. 1, 52428 Jülich, Germany

<sup>2</sup>MicroNanoBio, Von-Guericke-Allee 1, 53125 Bonn, Germany

<sup>3</sup>Institute of Biomaterials and Biomolecular Systems, University of Stuttgart, Pfaffenwaldring 57, 70569 Stuttgart, Germany

<sup>4</sup>Institute of Biological Information Processing (IBI-3), Forschungszentrum Jülich GmbH, Wilhelm-Johnen-Str., 52425 Jülich, Germany

**Abstract:** Plant viruses are a major cause of crop losses, making early and reliable detection essential. This work presents a capacitive model of electrolyte-insulator-semiconductor (EISCAP) sensors for label-free detection of negatively charged *tobacco mosaic virus* (TMV) particles, modelled as nanoscale local gates. The impact of TMV surface coverage on capacitance-voltage characteristics of SiO<sub>2</sub>-gate EISCAPs was studied theoretically and experimentally.

**Keywords:** capacitive field-effect biosensor; plant virus particles; *tobacco mosaic virus*; capacitive model; virus coverage; label-free detection

## Introduction

Plant viruses significantly impact global agriculture, causing annual losses of up to \$60 billion and threatening food security. Early, reliable detection combined with pre-symptomatic intervention is essential to limit their spread.

Capacitive field-effect biosensors based on electrolyte-insulator-semiconductor capacitors (EISCAPs) enable label-free detection of virus particles via their intrinsic charge. This work presents a capacitive model of an EISCAP sensor loaded with negatively charged *tobacco mosaic virus* (TMV) particles [1].

## Results and Discussion

In the model, adsorbed TMV particles (Figure 1) act as nanoscale local gates that modulate the semiconductor space-charge region. This results in shifts of the capacitance-voltage (*C-V*) characteristics, with signal amplitudes depending on the surface coverage. Simulations indicate an approximately linear relationship between TMV coverage and both capacitance change and voltage shift in the depletion region.

Experimental results obtained with SiO<sub>2</sub>-gate EISCAP sensors confirmed these predictions. TMV adsorption induced concentration-dependent *C-V* shifts; quantitative analysis using scanning electron microscopy revealed a strong correlation between surface coverage and sensor response.

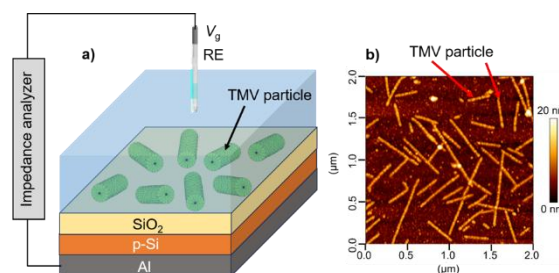


**Figure 1:** Schematic EISCAP structure (a) and atomic force microscopy image of the SiO<sub>2</sub>-gate surface loaded with TMV particles [1].

## Conclusions

The findings highlight the key role of virus surface coverage in EISCAP sensor performance and demonstrate the potential of this approach for rapid, label-free, and quantitative in-field detection of plant viruses.

## References

- [1] M. Welden, A. Poghossian, C. Wege, M. J. Schöning. *Anal. Bioanal. Chem.* (2026) doi: 10.1007/s00216-026-06468-4

## Acknowledgements

This work was funded by the Deutsche Forschungsgemeinschaft (DFG: German Research Foundation)–446507449. The authors thank D. Rolka, H. Iken and T. Karschuck for technical support and S. Felekyan for simulations.

# pH Sensitive Hydrogels for Plasmonic-based Biofluid Sensing

Kaussar El-Jamal<sup>1,2</sup>, Ammar Ahmed<sup>1,2</sup>, Nils Heine<sup>2,3</sup>, Katharina Doll-Nikutta<sup>2,3</sup>, Maria Leilani Torres-Mapa<sup>1,2</sup>, Alexander Heisterkamp<sup>1,2</sup>

el-jamal@iqo.uni-hannover.de

<sup>1</sup>Institute of Quantum Optics (IQO), Gottfried Wilhelm Leibniz University Hannover, Hannover, Germany

<sup>2</sup>Lower Saxony Center for Biomedical Engineering, Implant Research and Development, Hannover, Germany

<sup>3</sup>Department of Prosthetic Dentistry and Biomedical Materials Science, Hannover Medical School, Hannover, Germany

**Abstract:** We present the development of a plasmonic hydrogel-based pH sensor functionalized with MAA and DMAEMA for monitoring physiologically relevant pH fluctuations in biofluids, where the hydrogels exhibit reversible volumetric swelling responses. To enable optical detection, gold nanoparticles were embedded into the polymer matrix via UV photoreduction. This approach yields an active sensing platform capable of detecting nanoscale changes as the polymer responds to varying pH levels. Ongoing studies focus on optimizing the sensor performance toward smart diagnostic pH monitoring for future applications in dental implants.

**Keywords:** pH responsive hydrogels, optical biosensing, dental implant diagnostic, UV photoreduction, smart biomaterials

## Introduction

Tightly regulated pH levels are essential in maintaining normal physiological functions in the human body. Any deviations from physiological pH can indicate or lead to a dysfunction in metabolic activities<sup>[1]</sup>. Hydrogels are soft, flexible three-dimensional polymer networks capable of absorbing and retaining large amounts of water. An optical readout is provided through integrating gold nanoparticles within the hydrogel matrix<sup>[2]</sup>.

## Results and Discussion

An elevation in pH level results in a swelling of the hydrogel leading to a weight increase associated with a shift to shorter wavelengths in the absorption spectra. When functionalized with dimethylaminoethyl methacrylate (DMAEMA), the hydrogels exhibited a reversed swelling effect compared to methacrylic acid (MAA) as a function of varying pH levels. The observed blue shifts of the peak absorbance in response to the expansion of the polymers were attributed to the spacing of gold nanoparticles and the changes in local refractive index.

The swelling behavior of hydrogels was tested in different biologically relevant conditions such as synthetic sweat, synthetic saliva, and bacterial culture medium and the expected trend was observed across all hydrogels. Figure 1 shows the weight increase of approximately 130% when the pH of synthetic saliva is elevated from pH=4 to pH=8. In this regard, the sensors were able to capture pH changes in the various biofluids and accordingly exhibit the increase in swelling accompanied with blue shifts as a result of the pH level elevation. Simultaneously, repeatability and reusability tests conducted over multiple cycles demonstrated reliable performance of the hydrogels.

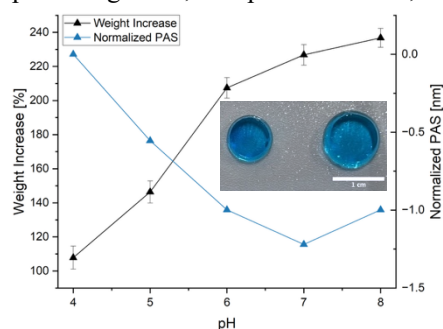


**Figure 1:** Weight increase vs. normalized peak absorption shift as a function of pH level in synthetic saliva. ( $n=2$ )

## Conclusions

The presented hydrogel platform allowed successful optical monitoring of pH-responsive swelling behavior. Future efforts are directed toward the optimization and integration of these hydrogel systems with optical fiber-based diagnostics for localized pH sensing in dental implant environments.

## References

- [1] M. T. Ghoneim et al., "Recent Progress in Electrochemical pH-Sensing Materials and Configurations for Biomedical Applications," *Chem. Rev.*, vol. 119, no. 8, pp. 5248–5297,
- [2] Y.-R. Toh, P. Yu, X. Wen, J. Tang, and T. Hsieh, "Induced pH-dependent shift by local surface plasmon resonance in functionalized gold nanorods," *Nanoscale Res. Lett.*, vol. 8, no. 1, p. 103, Dec. 2013, doi: 10.1186/1556-276X-8-103.

## Acknowledgements

Funded by the Deutsche Forschungsgemeinschaft (DFG, German Research Foundation) - SFB/TRR-298-SIIRI-Project-ID 426335750 – EXC 2122: PhoenixD – Project-Nb 390833453

# Surface treatment using plasma sterilization - generation, application and mechanisms of action

S. Achtsnicht<sup>1</sup>, H. Geissler<sup>2</sup>, M. J. Schöning<sup>1,3</sup>

achtsnicht@fh-aachen.de

<sup>1</sup>Institute of Nano- and Biotechnologies (INB), FH Aachen University of Applied Sciences, Campus Jülich, Heinrich-Mußmann-Str. 1, 52428 Jülich, Germany

<sup>2</sup>SIG Combibloc Systems GmbH, Rurstraße 58, 52441 Linnich, Germany

<sup>3</sup>Institute of Biological Information Processing (IBI-3), Forschungszentrum Jülich GmbH, Wilhelm-Johnen-Str., 52425 Jülich, Germany

**Abstract:** Using plasma for sterilizing food packaging represents an interesting alternative to established industrial methods, such as the use of gaseous hydrogen peroxide. What are the typical input parameters that influence the sterilization process and, consequently, its effectiveness? This contribution provides a brief overview of these factors.

**Keywords:** plasma; sterilization; inactivation; atmospheric cold plasma

## Introduction

In addition to the use of chemical-based methods (e.g., hydrogen peroxide, ethylene oxide), thermal methods (moist and dry heat), and radiation-based methods (e.g., UV, X-ray), plasma sterilization processes have recently been increasingly employed in the field of food technology. This work will focus on plasmas generated by dielectric discharge at temperatures below 150 °C to ensure compatibility with the packaging material to be sterilized.

## Results and Discussion

Dielectric barrier discharge (DBD) and atmospheric low-pressure plasma jet (APPJ) are the most extensively studied methods of plasma generation in process engineering and the food industry. It should be noted that some of the individual components formed in the plasma are very short-lived or undergo direct interactions. The reason for this lies in particular in the significantly higher pressure compared to plasmas generated in ultra-high vacuum. In plasma sterilization processes, reactive oxygen and nitrogen species (RONS) are considered the primary inactivation factors, in contrast to other components that are formed, such as UV photons.

In general, the effectiveness of plasma sterilization depends on various factors:

- (1) System configuration; this includes not only the plasma source (electrode geometry/material, voltage, frequency) but also gas parameters (e.g., composition, operating pressure, gas flow rate, humidity).
- (2) Plasma treatment; size of the surface to be sterilized, volume, treatment duration, and post-treatment time for evaluating sterilization efficacy.
- (3) Influence of the item being sterilized; surface type, roughness, interaction between the surface

and plasma (components), catalytic effects, temperature, moisture/biofilm formation.

However, the inactivating effect (efficacy) of plasma sterilization is also influenced by the type of bacteria or spores themselves: RONS cause chemical bonds to break and lead to erosion of the cell membrane. This results in lipid peroxidation, the denaturation of proteins and enzymes, and the oxidation of amino acids (enzyme inactivation) both here and within the cell. Furthermore, the resulting RONS can damage the cell's DNA/RNA; it is known that these interact directly with factors related to survival and proliferation. Different cell types are affected to varying degrees by oxidative stress; conversely, a small amount of additional oxidative stress can contribute to increased cell growth, and apoptosis/necrosis is only initiated once a critical threshold is exceeded.

## Conclusions

The use of plasma – particularly non-thermal plasma – as a sterilization method represents an interesting alternative to traditional sterilization methods. However, a wide range of interactions must be taken into account when selecting appropriate parameters and evaluating efficiency.

# Dynamic Reconstruction of Anodized Fe-Co-Ni Spinel Oxide Functional Interfaces during the Oxygen Evolution Reaction (OER)

Tomoya Nagao<sup>1</sup>, Sho Kitano<sup>2</sup>, Mana Iwai<sup>2</sup>, Koji Fushimi<sup>2</sup>, Hiroki Habazaki<sup>2</sup>

nagao.tomoya.d4@elms.hokudai.ac.jp

<sup>1</sup>Graduate School of Chemical Sciences and Engineering, <sup>2</sup>Division of Applied Chemistry, Faculty of Engineering, Hokkaido University, Sapporo 060-8628, Japan

**Abstract:** Dynamic reconstruction of Fe-Co-Ni-based catalysts under OER conditions is crucial for catalytic activation, yet its correlation with valence changes remains unclear. Here, an anodized Fe-Co-Ni spinel oxide ECPA film derived from a metal fluoride precursor was investigated as a model catalytic interface. Integrated *in situ* Raman spectroscopy, XRD, and XAFS revealed transformation of low-crystallinity spinel oxides into non-layered  $\gamma$ -Ni<sub>1-x-y</sub>Fe<sub>x</sub>Co<sub>y</sub>OOH. The analyses establish a valence–structure–activity relationship: Ni and Co drive reconstruction and act as OER-active sites, whereas Fe stabilizes the reconstructed structure.

**Keywords:** OER; Anodizing; *in situ* Raman spectroscopy; XRD; XAFS

## Introduction

Transition-metal oxide electrocatalysts often undergo potential-dependent structural and electronic changes under OER conditions. Such dynamic reconstruction can generate the catalytically active phase, but correlating structural transformation, metal valence changes, and catalytic activation under identical electrochemical conditions remains challenging. To overcome this issue, we focused on an electrocatalyst prepared by anodizing (ECPA) from an anodized metal fluoride precursor [1]. The ECPA film consists of ultrasmall low-crystallinity Fe-Co-Ni spinel oxides, enabling nearly complete reconstruction into an OER-active metal oxyhydroxide phase. Here, *in situ* Raman spectroscopy, *in situ* XRD, and *in situ* XAFS were integrated to clarify the valence–structure–activity relationship during OER.

## Results and Discussion

The ECPA film was prepared by anodizing Kovar (Fe-16.3 wt% Co-29.7 wt% Ni) at 10 V for 60 min in ethylene glycol containing 0.54 M NH<sub>4</sub>F and 2.5 M H<sub>2</sub>O, followed by electrochemical activation in 1.0 M KOH. *In situ* Raman spectroscopy revealed that spinel oxides in the ECPA film reversibly transform into  $\gamma$ -Ni<sub>1-x-y</sub>Fe<sub>x</sub>Co<sub>y</sub>OOH under anodic polarization. The spinel-related Raman peak at 690 cm<sup>-1</sup> decreased with increasing potential, whereas  $\gamma$ -Ni<sub>1-x-y</sub>Fe<sub>x</sub>Co<sub>y</sub>OOH peaks at 474 and 554 cm<sup>-1</sup> appeared and increased. *In situ* XRD revealed a broad diffraction feature corresponding to in-plane ordering of edge-sharing octahedral sites, while the diffraction peak associated with layered stacking was absent, indicating the formation of non-layered  $\gamma$ -Ni<sub>1-x-y</sub>Fe<sub>x</sub>Co<sub>y</sub>OOH. Figure 1 shows the correlation between spinel Raman intensity and metal K-edge shifts obtained from *in situ* XAFS measurements. The Ni and Co K-edge positions shifted to higher energy as the spinel Raman peak decreased,

indicating that oxidation of Ni<sup>2+</sup> to Ni<sup>3+</sup> and Co<sup>2+</sup> to Co<sup>3+</sup> drives the structural transformation. At higher potentials, the continued positive shifts suggest the generation of highly oxidized Ni and Co species that act as the active sites for the OER. In contrast, Fe showed only a gradual shift, suggesting that Fe stabilizes the reconstructed structure rather than acting as the main redox-active site.

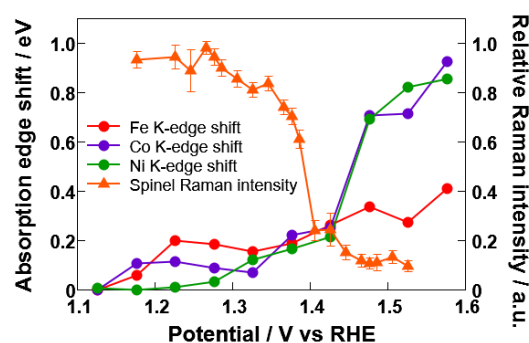


**Figure 1:** Correlation between metal K-edge shifts and spinel Raman intensity in the ECPA film during OER.

## Conclusions

Integrated *in situ* analyses elucidated the dynamic reconstruction of anodized Fe-Co-Ni spinel oxide into non-layered  $\gamma$ -Ni<sub>1-x-y</sub>Fe<sub>x</sub>Co<sub>y</sub>OOH during OER. This transformation is driven by Ni and Co oxidation, while Fe stabilizes the reconstructed structure.

## References

- [1] Z. Xiong, D. Quintero, S. Kitano, T. Nagao, et al. *Electrochim. Acta* 491, 144352 (2024). <https://doi.org/10.1016/j.electacta.2024.144352>

## Acknowledgements

This work was supported by JST SPRING (JPMJSP2119), JSPS KAKENHI (23H00224), and the ARIM Program of MEXT, Japan.

# A Synthetic Receptor Approach for the Rapid Identification of Clinical Cancer Biomarkers

Ahmad Alsholi<sup>1</sup>, Stephen Lyons<sup>2</sup>, Claire Hart<sup>2</sup>, Robert Bristow<sup>2</sup>, Ashwin Sachdeva<sup>2</sup>, Marloes Peeters<sup>1</sup>

ahmad.alsholi@postgrad.manchester.ac.uk, Marloes.peeters@manchester.ac.uk

<sup>1</sup>Department of Chemical Engineering and Analytical Science, School of Engineering, The University of Manchester, Manchester M13 9PL, United Kingdom

<sup>2</sup>Division of Cancer Sciences, The University of Manchester, Manchester M13 9NT, United Kingdom

**Abstract:** Current cancer biomarkers often rely on costly sequencing or unreliable antibodies. Therefore, we developed molecularly imprinted polymers (nanoMIPs) targeting a novel epitope of a cancer protein. Using solid-phase synthesis, we fabricated homogenous nanoparticles under 100 nm, ideal for biosensing applications. They demonstrated binding affinities comparable to natural antibodies. Future work will focus on developing an optical biosensor, benchmarking its performance against traditional antibodies.

**Keywords:** artificial antibody; epitope imprinting; cancer detection; molecularly imprinted polymers

## Introduction

Cancer is a highly heterogeneous disease, making precision medicine essential for optimising targeted treatments [1]. As such, there is a critical demand for robust materials capable of detecting specific genetic mutations in tumours to guide clinical decisions. Current diagnostics including genetic sequencing and traditional antibodies suffer from high costs, complexity, and batch-to-batch variability [2]. To overcome these limitations, this research develops advanced molecularly imprinted nanoparticles (nanoMIPs) for an optical biosensing platform. These highly specific, cost-effective artificial receptors provide robust alternatives to conventional tools, enabling rapid and accurate screening to guide targeted clinical therapies.

## Results and Discussion

To evaluate the synthetic receptors, nanoMIPs were successfully synthesised against a novel short peptide sequence representing the target biomarker using a solid-phase approach [3]. Dynamic Light Scattering (DLS) and Scanning Electron Microscopy (SEM) confirmed the fabrication of homogenous, spherical nanoparticles. The targeted nanoMIPs exhibited an average diameter of 60 nm and a hydrodynamic diameter ( $D_h$ ) under 80 nm (see Figure 1), a size range crucial for biosensing applications. Binding affinity and thermodynamics were evaluated using Surface Plasmon Resonance (SPR), Bilayer Interferometry (BLI), and Isothermal Titration Calorimetry (ITC). Quantitative binding analysis revealed consistent dissociation constants ( $K_D$ ) in the micromolar range [2], recording 7.91  $\mu\text{M}$  for SPR, 8.46  $\mu\text{M}$  for BLI, and 2.25  $\mu\text{M}$  for ITC. This validation confirms their strong target capture capabilities, proving these synthetic receptors perform comparably to traditional commercial antibodies.

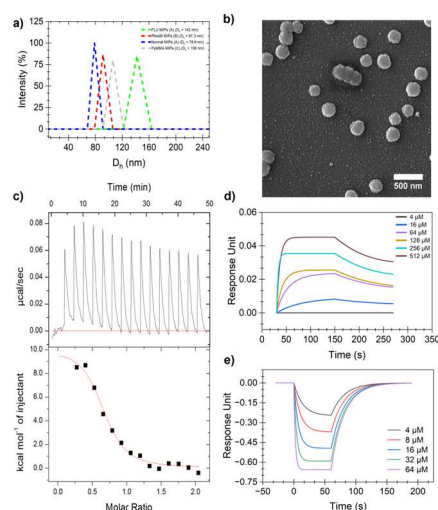


**Figure 1:** Normal MIPs were tested for a) DLS presenting  $D_h$ . b) SEM image showing spherical morphology. c) ITC showing affinity and stoichiometry. d & e) BLI and SPR showing binding kinetics, respectively.

## Conclusions

The successful solid-phase synthesis of homogenous, nanoscale MIPs has provided a robust synthetic receptor with binding affinities comparable to traditional antibodies. These materials hold strong potential for detecting mutations in heterogeneous tumours, ultimately optimising precision cancer treatments.

## References

- [1] DOI: 10.1017/pcm.2023.23
- [2] DOI: 10.1002/advs.202309976
- [3] DOI: 10.1038/nprot.2016.030

## Acknowledgements

The authors gratefully acknowledge the financial support provided by The University of Manchester and the Manchester Cancer Research Centre, United Kingdom.

# Template-bacteria-free engineering of biomimetic polymer interfaces for selective *E. coli* capture and detection

D. Özsoylu<sup>1</sup>, E. Börmann-El Kholy<sup>1</sup>, P. Wagner<sup>2</sup>, M. J. Schöning<sup>1,3</sup>

[oezsoylu@fh-aachen.de](mailto:oezsoylu@fh-aachen.de)

<sup>1</sup>Institute of Nano- and Biotechnologies (INB), FH Aachen University of Applied Sciences, Campus Jülich, Heinrich-Mußmann-Str. 1, 52428 Jülich, Germany

<sup>2</sup>Department of Physics and Astronomy, Laboratory for Soft Matter and Biophysics, KU Leuven, Celestijnenlaan 200D, B-3001, Leuven, Belgium

<sup>3</sup>Institute of Biological Information Processing (IBI-3), Forschungszentrum Jülich GmbH, Wilhelm-Johnen-Str., 52425 Jülich, Germany

**Abstract:** Selective bacterial recognition remains challenging due to limitations of biological receptors and conventional imprinting approaches. Here, we present a template-bacteria-free strategy combining photolithographic surface imprinting and molecular imprinting to create biomimetic polymer interfaces. Importantly, lipopolysaccharide-functionalized stamps introduced chemical recognition, yielding synergistic physical–chemical binding and enhanced capture efficiency (imprinting factor up to 6.5) and decent selectivity. The approach provides a scalable platform for robust, low-cost biosensing and environmental monitoring.

**Keywords:** surface-imprinted polymers; molecular imprinting; *E. coli* detection; lipopolysaccharides; biomimetic interfaces; biosensors

## Introduction

Selective capture of bacteria at engineered interfaces is essential for biosensing and environmental monitoring. While biological receptors such as antibodies offer high specificity, they suffer from limited stability and high costs [1]. Synthetic alternatives, particularly molecularly imprinted polymers (MIPs), provide robust and scalable recognition platforms. Surface-imprinted polymers (SIPs) enable direct whole-bacteria detection through shape-selective cavities but conventional fabrication relies on whole bacterial templates, leading to poor reproducibility and biosafety concerns [2]. Template-bacteria-free approaches using photolithographic mimics address these issues by allowing controlled and reproducible interface design, though they primarily offer physical recognition. Here, we introduce a dual-mode strategy combining geometry-based surface imprinting with molecular imprinting of lipopolysaccharides (LPS), enabling synergistic physical and chemical recognition without using whole bacterial templates [1].

## Results and Discussion

The dual-mode imprinting strategy was exemplarily demonstrated with selective detection of *E. coli* bacteria, by first fabricating photolithographic mimics and then, introducing lipopolysaccharide (LPS)-based molecular recognition. The resulting surfaces exhibited well-defined, high-density cavities that integrate geometric matching with molecular recognition.

This synergy led to significantly enhanced bacterial capture (imprinting factor up to 6.5) and improved

selectivity toward *E. coli*, as demonstrated against non-target microorganisms with mismatched size and shape.

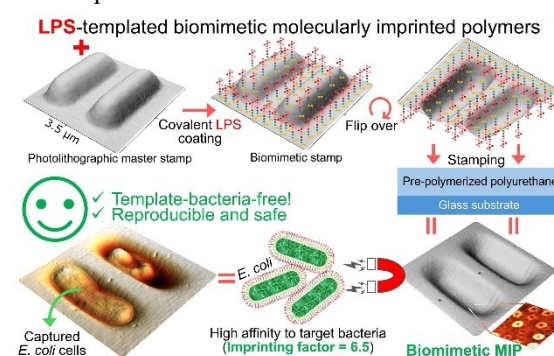


**Figure 1:** Dual-mode (geometry + LPS) imprinting concept for template-free bacterial recognition.

## Conclusions

This work highlights the critical role of combining physical and chemical cues in designing highly efficient and selective functional interfaces.

## References

- [1] Özsoylu *et al.*, *Chem. Eng. J.* **531** (2026) 173963. doi: 10.1016/j.cej.2026.173963R.
- [2] Özsoylu *et al.*, *Biosens. Bioelectron.* **261** (2024) 116491. doi: 10.1016/j.bios.2024.116491.

## Acknowledgements

This work was funded by the European Commission and the German Federal Ministry of Education and Research (BMBF, project no. 03F0902A) and the Research Foundation Flanders (FWO, grant G0G3321N) within the AquaticPollutants ERA-NET Cofund (No. 869178, ARENA project).

# Combinatorial Screening of Anodic Ti-Hf Oxides for Memristive Switching Properties

Elena Atanasova<sup>1\*</sup>, Alexey Minenkov<sup>2</sup>, Andreas Greul<sup>1</sup>, Achim Walter Hassel<sup>1,3</sup>, Andrei Ionut Mardare<sup>1,4\*</sup>

\*[elena.atanasova@jku.at](mailto:elena.atanasova@jku.at)

<sup>1</sup>Institute of Chemical Technology of Inorganic Materials, Johannes Kepler University Linz, Altenberger Str. 69, 4040, Linz, Austria

<sup>2</sup>Christian Doppler Laboratory for Nanoscale Phase Transformations, Center for Surface and Nanoanalytics, Johannes Kepler University Linz, Altenberger Str. 69, 4040, Linz, Austria

<sup>3</sup>Faculty of Medicine and Dentistry, Danube Private University, Steiner Landstraße 124, 3500, Krems an der Donau, Austria

<sup>4</sup>National Institute for Lasers, Plasma and Radiation Physics, Atomistilor Str. 409, 077125, Magurele, Romania

**Abstract:** This work investigates anodically formed Ti-Hf mixed oxides for their resistive switching behaviour. The memristive devices were fabricated via a sputtered combinatorial Ti-Hf alloy library with compositions ranging from 15-90 at. % Hf. The devices show forming-free, volatile, analog switching with self-rectification and composition-dependent behavior. The increase in Hf content raises the SET voltage, while lowering the RESET voltage, and improving the high resistive state to low resistive state (HRS/LRS) ratio. Electrical characterization and Transmission Electron Microscopy (TEM) indicate interfacial resistive switching based on Schottky emission. This highlights the use of Ti-Hf anodic memristors as tuneable materials for neuromorphic applications.

**Keywords:** anodic memristors; resistive switching; interfacial switching;

## Introduction

Memristors are metal-insulator-metal (MIM) devices, which can retain and recall their resistance states. This property makes them attractive for memory and neuromorphic electronics. Anodization offers a controllable and low-cost route for the fabrication of the insulating layer. TiO<sub>2</sub> supports oxygen-vacancy-driven switching, while HfO<sub>2</sub> improves stability and lowers leakage. Creating a mixed oxide enables compositionally tuned interfacial switching [1,2].

## Results and Discussion

All anodically formed Ti-Hf mixed oxide devices across the 15-90 at. % Hf library were electrically investigated and showed electroforming-free, volatile, analog switching with strong self-rectification. The observed switching behaviour was composition-dependent. The increase in Hf content raised the SET voltages, lowered the RESET voltages, and improved the overall HRS/LRS ratios. Among all compositions, the Hf-rich region, more specifically the Ti-75 at. % Hf device, offered the best ratio of stable switching and reliable endurance. TEM analysis revealed an approximately 20 nm oxide with amorphous and polycrystalline regions, as can be seen in Figure 1 (a) and (b). Furthermore, conduction analysis confirmed Schottky emission, supporting interfacial, filament-free switching [2].

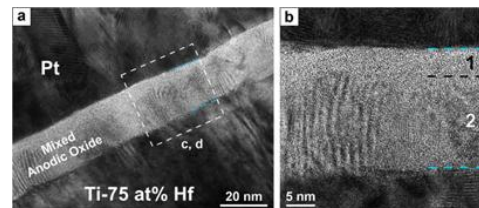


Figure 1: A summary of TEM characterization of the Ti-75 at% Hf specimen. (a) overview of the MIM structure (b) magnified image of the anodic active layer [2].

## Conclusions

Ti-Hf mixed anodic oxides show compositionally tuneable, forming-free, and analog memristive behavior with intrinsic self-rectification. The Hf-rich region, (50-90 at. % Hf), showed superior switching, high HRS/LRS ratios, and stable endurance, making these devices promising for low-power neuromorphic computing.

## References

- [1] E. Atanasova et al, Mater. Adv. 3,7, 1357-1377, (2026)
- [2] E. Atanasova et.al, ACS Appl. Electron. Mater. 8, 2, 813-823 (2026)

## Acknowledgements

This research was funded in whole or in part by the State of Upper Austria through the Linz Institute of Technology [project COMSENS, LIT-2023-12-SEE-111].

# Design and Implementation of a Catheter-Integrated Biosensor Based on Molecularly Imprinted Polymers for Histamine Detection

Bushra Batool<sup>1</sup>, Soroush Bakhshi Sichani<sup>1</sup>, Jan Tack<sup>1</sup>, and Patrick Wagner<sup>1</sup>

[bushra.batool@kuleuven.be](mailto:bushra.batool@kuleuven.be)

<sup>1</sup> KU Leuven, Laboratory for Soft Matter and Biophysics, Celestijnenlaan 200D, 3001 Leuven, Belgium

**Abstract:** The elevated level of histamine in the irritable bowel syndrome (IBS) patients motivated us to develop a catheter based biomimetic sensor functionalised with molecularly imprinted polymers (MIPs) coated on gold electrodes. MIPs are man-made biomimetic receptors famous for their stability and reusability. Their polymer network has recognition sites complementary to histamine and can be used for the fabrication of bioreceptors for selective histamine detection by impedance spectroscopy in complex biological fluids. And in addition, these MIP-based biosensors would be reliable, economic and sustainable for the detection of analyte concentration from picomolar to milli molar range.

**Key Words:** histamine detection; catheter sensors; gastrointestinal disorders; molecularly imprinted polymers

## Introduction

In the functional gastrointestinal (GI) disorders for instance IBS include symptoms such as abdominal pain, change in bowel habits, bloating, and abdominal distension. IBS is a heterogeneous entity resulting from many different overlapping factors such as inflammation, neuroimmune interactions, gut microbiota, environmental pollution, and an abnormal gut-brain axis. Immune cells (mast cells) release different inflammatory chemicals like histamine that play a key role in the pathogenesis of IBS [1]. Current diagnostic procedures are invasive and limited. We propose a minimally invasive approach using catheter-based impedance sensors functionalized with molecularly imprinted polymers (MIPs) for detecting histamine concentrations from  $10^{-9}$  M to  $10^{-3}$  M range directly in the complex media [2].

## Results and Discussion

In this sensor different electrode combinations are present to determine clearest correlation between a given histamine concentration and the corresponding increase of the impedance signal. The responses of electropolymerized pyrrole MIP-coated gold electrodes to the target analyte (histamine), pseudo-analyte (histidine) for selectivity testing, and NIP-coated reference electrodes for non-specific adsorption are shown in **Figure 1a**. The binding mechanisms between analyte and the MIP, involving  $\pi$ - $\pi$  interactions and H-bonding, are illustrated in **Figure 1b**. Impedance spectroscopy and equivalent-circuit modelling showed that histamine binding to MIP-functionalised electrodes increases interfacial resistance. To mimic intestinal conditions, histamine concentrations from  $10^{-9}$  to  $10^{-3}$  M in  $1\times$  PBS were measured at 37 °C across different pH levels in a dummy model. The sensor showed the saturation up to the detection limit down to 10 nM, covering the

physiological range (up to  $>1$   $\mu$ M) relevant for IBS diagnosis.

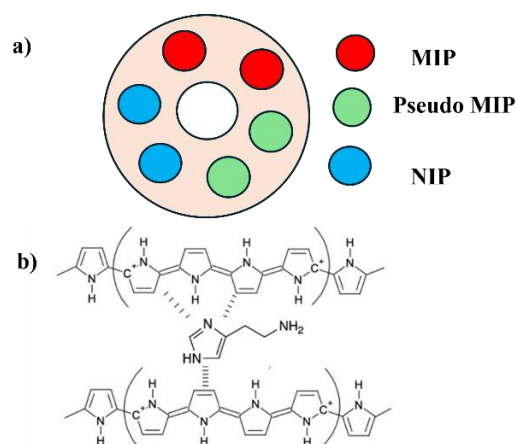


**Figure 1:** a) Different electrode combinations. b) Binding mechanism between histamine and MIP through  $\pi$ - $\pi$  interactions and H-bonding.

## Conclusions

The minimal invasive catheter-based impedimetric sensor for the detection of small histamine concentration up to  $10^{-9}$  M range in complex media facilitates the diagnosis of irritable bowel syndrome and could be of interest for pharmaceutical and medical researchers.

## References

- [1] A. Fabisiak, *et al.*, J. Neurogastroenterol. Motil. 23, 341–348 (2017).
- [2] G. Wackers, *et al.*, ACS Sens. 6, 100–110 (2021).

## Acknowledgements

Financial support from the Punjab (Pakistan) Educational Endowment Fund (PEEF) is gratefully acknowledged.

# Electrospinning of PDMS Elastomer for Hydrophobic Surface Coatings

Jan Drexler<sup>1</sup>, Tom Bode<sup>1</sup>, Marc Mueller<sup>1</sup>, Gerrit Paasche<sup>2</sup>, Birgit Glasmacher<sup>1</sup>

drexler@imp.uni-hannover.de

<sup>1</sup>Institute for Multiphase Processes, Leibniz University Hannover, An der Universität 1, 30823 Garbsen, Germany

<sup>2</sup>Department of Otorhinolaryngology, Hannover Medical School, Carl-Neuberg-Straße 1, 30625 Hannover, Germany

**Abstract:** Fibrosis around cochlear implant electrodes increases impedance, motivating the development of antifibrotic surface modifications. This study investigates electrospun PDMS fibers as porous coatings, focusing on curing state and solvent effects. Fiber formation and shape retention was possible for curing states preceding the gel point, while solvent choice governed morphology and diameter. Controlled processing enabled tunable PDMS nonwovens with potential for biomedical applications.

**Keywords:** Electrospinning; Hydrophobic surface coating; Silicone; Cochlear implants

## Introduction

The impedance of cochlear implants is adversely affected by fibrosis surrounding the electrode array [1]. Potential strategies for reducing fibrosis include surface microstructuring and the use of hydrophobic materials [2]. A potential approach to combine these strategies is to apply highly porous coatings made of electrospun poly(dimethylsiloxane) (PDMS) fibers to the electrodes. However, electrospinning PDMS elastomer poses a fundamental processing challenge. Cured elastomers are insoluble and lack the flow properties required for electrospinning, while the prepolymers typically exhibit low glass transition temperatures and remain liquid at ambient conditions. Consequently, maintaining the structural integrity of deposited fibers necessitates in situ curing of the elastomer system during electrospinning. In addition, solvents must be added to ensure sufficient charge carrier density.

This study investigates the influence of solvent selection and curing degree on electrospun fibers from Sylgard 184 silicone elastomer. In situ curing was implemented by combining infrared radiation and a heated plate collector.

## Results and Discussion

The success of electrospinning PDMS strongly depends on the curing state of the elastomer system. Over wide timescales of the curing process, only electrospinning occurred, accompanied by minor changes in viscosity and negligible elasticity. As the curing reaction approached the gel point, a clear increase in viscosity was observed, and elastic behavior became detectable by rheological measurements. This transition corresponded to the shift from electrospinning to electrospinning. Successful electrospinning was achieved using hexane (HEX), chloroform, tetrahydrofuran (THF), and acetone (AC) as solvents. In contrast, more polar solvents than acetone did not yield homogeneous mixtures with the prepolymer.

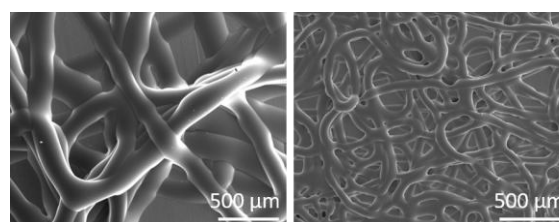


**Figure 1:** Electrospun nonwovens of PDMS in hexane (left) and tetrahydrofuran (right) exhibited a distinct fiber morphology and connected fiber interspaces.

Solvent conductivity significantly influenced fiber diameter distribution, as the nonpolar PDMS prepolymer contains almost no intrinsic charge carriers. Measured fiber diameter decreased with increasing solvent polarity, yielding  $210 \pm 26 \mu\text{m}$  (HEX),  $70 \pm 18 \mu\text{m}$  (THF) and  $24 \pm 5 \mu\text{m}$  (AC). Solvent choice also influenced structural integrity of the fibers. Fibers electrospun from HEX and THF demonstrated good structural integrity, whereas sagging occurred for fibers spun from AC.

## Conclusions

Precise control of curing time combined with appropriate solvent selection enables the fabrication of electrospun PDMS nonwovens with well-defined fiber geometries and interconnected porosity. Future work will focus on evaluating the effect of surface coatings on fibroblast growth.

## References

- [1] C. Newbold, S. Mergen, R. Richardson, et al. Cochlear Impl Inter 15, 4 (2014). DOI 10.1179/1754762813Y.0000000050
- [2] U. Reich, P.P. Mueller, E. Fadeeva, et al. J Biomed Mater Res 87(B), 1 (2008). DOI 10.1002/jbm.b.31084

## Acknowledgements

This study was funded by the German Research Foundation (DFG) - 60443918.

# Non-Enzymatic Creatinine Detection Using Electroactive Molecularly Imprinted Polymers: Toward Point-of-Care Sensing

Saweta Garg<sup>1</sup>, Ahmad Alshohli<sup>1</sup>, Giuliana de Melo Cossani<sup>1,2</sup>, Pankaj Singla<sup>1</sup>, Robert D. Crapnell<sup>3</sup>, Craig E. Banks<sup>3</sup>, Marloes Peeters<sup>1\*</sup>

Marloes.peeters@manchester.ac.uk

<sup>1</sup> Department of Chemical Engineering and Analytical Science, School of Engineering, University of Manchester, Manchester M20 4BX, United Kingdom

<sup>2</sup> Department of Chemical Engineering, University of São Paulo, São Paulo, Brazil

<sup>3</sup> Faculty of Science and Engineering, Manchester Metropolitan University, Manchester M1 5GD, United Kingdom

**Abstract:** Creatinine (Cr) is a key biomarker for assessing renal function, with abnormal levels indicating kidney disease. Conventional detection methods rely on centralized laboratories and sophisticated instrumentation; while accurate, they are not suitable for rapid point-of-care (PoC) diagnostics. This study presents a low-cost electrochemical sensor based on creatinine-imprinted electroactive molecularly imprinted polymer nanoparticles (Cr-eMIPs), which combine enzyme-like affinity with low cost, robustness, and simple fabrication. Cr-eMIPs were drop-cast onto disposable screen-printed electrodes (SPEs) to enable Cr detection over a wide range (1-120  $\mu\text{M}$ ) with a low detection limit ( $\sim 11 \mu\text{M}$ ). The sensor shows high sensitivity, strong selectivity against common interferents, and excellent stability ( $>6$  months). It was validated in artificial urine and human serum samples (20-200  $\mu\text{M}$ ), with future benchmarking against commercial assays, demonstrating strong potential for PoC kidney diagnostics.

**Keywords:** electroactive molecularly imprinted polymer nanoparticles (eMIPs), screen printed electrode (SPEs), conductive polymers, Polypyrrole (PPy)

## Introduction

Chronic kidney disease (CKD) affects  $\sim 788$  million people worldwide and is a major cause of morbidity and mortality. Abnormal creatinine levels ( $<40 \mu\text{M}$  or  $>150 \mu\text{M}$ ) are linked to renal and muscular disorders, emphasizing the need for reliable quantification.[1-2] Conventional tests are simple but not selective (e.g., Jaffe's reaction), while advanced methods (HPLC, LC-MS/MS) are accurate but too complex and costly for PoC use.[3] Molecularly imprinted polymers (MIPs) offer a promising alternative due to their low cost, high stability, reusability, and excellent selectivity for target molecules.[4] In this work, we developed a Cr-eMIPs SPEs based sensor for rapid ( $<30$  s), sensitive, and selective electrochemical detection of Cr, enabling next-generation non-enzymatic monitoring for CKD management.

## Results and Discussion

eMIPs produced through free-radical polymerization were characterized using different techniques.[5] DLS and TEM showed an average particle size of  $122 \pm 0.9$  nm and  $54 \pm 4$  nm respectively. Then, Cr-eMIPs SPEs were incubated with Cr (20-120  $\mu\text{M}$ ) for 1 min and cyclic voltammograms (CV) were recorded. CV results observed the linear decrease in current with the increasing concentration of Cr (Figure 1a). Moreover, the sensor, combining high selectivity (no interference with interferents) and sensitivity, was tested in Cr spiked artificial urine (A.U) samples, with LOD of  $10.57 \mu\text{M}$  (1b).

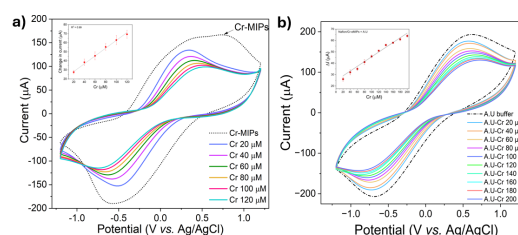


**Figure 1:** CV of Cr-eMIPs in the presence of Cr (1-120) and (b) CV of Cr-eMIPs in A.U samples; inset is CC of Cr at x-axis vs.  $\Delta I$  at y-axis ( $n=3$ ).

## Conclusions

The developed Cr-eMIP sensor enables sensitive and selective Cr detection over a clinically relevant range using a low-cost, disposable platform. It demonstrates excellent stability, robustness, and reliable performance in complex biological samples such as A.U and human serum. CKD Patient serum and urine samples will be tested using this sensor, highlighting its potential for PoC kidney function monitoring.

## References

1. Ayli BI et al., (2026). *Journal of Medicine and Palliative Care*, 7(2), 415-23.
2. Dagle T et al., (2018). *The New England Journal of Medicine*, 379(1), 61-73.
3. Srisawasdi, P et al., (2010). *Journal of Clinical Laboratory Analysis*, 24(3), 123-133.
4. S. Garg et al., *Macromolecules*. 1 (2025) 1157-68.
5. S. Garg et al., (2024), *Small*. 20(46),2403320.

## Acknowledgements

Authors would like to thank UKRI IAA grant (623) for the partial salary support for Saweta Garg.

# Temporally and spatially resolved pH in commensal and pathogenic oral biofilms *in vitro*

Maya Duitscher<sup>1,2</sup>, Nils Heine<sup>1,2</sup>, Meike Stiesch<sup>1,2</sup>, Katharina Doll-Nikutta<sup>1,2</sup>

duitscher.maya@mh-hannover.de

<sup>1</sup>Department of Prosthetic Dentistry and Biomedical Materials Science, Hannover Medical School, Carl-Neuberg-Straße 1, 30625 Hannover, Germany

<sup>2</sup>Implant-associated Infections, Lower Saxony Centre for Biomedical Engineering, Implant Research and Development (NIFE), Stadtfelddamm 34, 30625 Hannover, Germany

**Abstract:** Peri-implant infections are caused by shifts in the bacterial composition leading to a domination of pathogenic species. These shifts are accompanied by changes in bacterial metabolism, making them suitable targets for early detection strategies. This study measured the pH and metabolites inside commensal and pathogenic multispecies biofilms cultivated in both static and dynamic conditions using advanced imaging and assays. Analysis revealed reduced acidification in pathogenic biofilms. Additionally, indole and gingipain were identified as promising biomarkers for early detection of oral dysbiosis.

**Keywords:** oral biofilms, pH value, metabolite analysis, *in vitro* models

## Introduction

Biofilms in the oral cavity contain diverse microbes that interact through complex metabolic pathways. The onset of diseases such as periodontitis and peri-implantitis are caused by a shift in the bacterial compositions from commensal to pathogenic species, correlating with disease progression [1]. Accompanied by this are changes in secreted metabolites, posing a promising target for early disease detection [2]. Within the present study, differences in oral *in vitro* multispecies biofilm pH and associated molecules in correlation to commensal and pathogenic species under static and dynamic cultivation conditions have been evaluated to form the knowledge base for dysbiosis sensor development.

## Results and Discussion

Commensal biofilms showed stronger acidification compared to pathogenic biofilms under static conditions due to elevated levels in acidifying commensal species.

In the HOBIC model, an early drop in pH was followed by partial neutralization, with the most acidic layer at the biofilm-surface-interface caused by lactate-producing early colonizers. Even though lactate levels were higher in pathogenic biofilms, no relation to pH development could be found, suggesting lactate to be unfit as biomarker.

Contrasting this, both indole and gingipain increased in correlation with pathogenic species and pH, making them excellent candidates for biomarkers for early dysbiosis detection.

## Conclusions

Changes in the local pH and the increase in indole and gingipain showed promising potential as targets for early dysbiosis detection in oral biofilms.

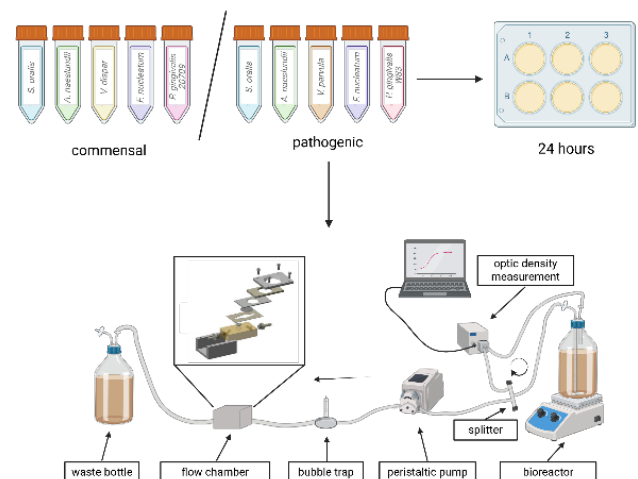


**Figure 1:** Commensal and pathogenic biofilm combinations cultivated statically in well plates and dynamically using the adaptive Hannoverian oral multispecies biofilm implant flow chamber (HOBIC) model.

## References

1. Marsh PD, Zaura E (2017) Dental biofilm: ecological interactions in health and disease. J Clin Periodontol 44 Suppl 18:S12–S22. <https://doi.org/10.1111/jcpe.12679>
2. Marsh PD (2003) Are dental diseases examples of ecological catastrophes? Microbiology (Reading) 149:279–294. <https://doi.org/10.1099/mic.0.26082-0>

## Acknowledgements

The work was funded by the Deutsche Forschungsgemeinschaft (DFG, German Research Foundation) under the Collaborative Research Center SFB/TRR-298-SIIRI (Project ID 426335750).

# Effect of UV irradiation on the flatband voltage of chemical sensors with field-effect structures

T. Yoshinobu <sup>1</sup>, [H. Iken](mailto:iken@fh-aachen.de) <sup>2</sup>, T. Sato <sup>1</sup>, K. Miyamoto <sup>1,3</sup>, T. Wagner <sup>2,4</sup>, M. J. Schöning <sup>2,4</sup>

[iken@fh-aachen.de](mailto:iken@fh-aachen.de)

<sup>1</sup>Tohoku University, 6-6-05 Aza-Aoba, Aramaki, Aoba-ku, Sendai 980-8579, Japan

<sup>2</sup>Institute of Nano- and Biotechnologies (INB), FH Aachen University of Applied Sciences, Campus Jülich, Heinrich-Mußmann-Str. 1, 52428 Jülich, Germany

<sup>3</sup>Okayama University, 3-1-1 Tsushimanaka, Kita-ku, Okayama, 700-8530, Japan

<sup>4</sup>Institute of Biological Information Processing (IBI-3), Forschungszentrum Jülich GmbH, Wilhelm-Johnen-Str., 52425 Jülich, Germany

**Abstract:** Chemical sensors with field-effect structures are used in a wide range of applications. As with all chemical and biological sensors, these require regular calibration. Drift effects in such sensors are caused primarily by shifts in the flatband voltage, in addition to the sensor-active component (receptor layer). Here, we will study the extent to which external UV irradiation can adversely affect three different field-effect layer structures of Al/p-Si/SiO<sub>2</sub>/Ta<sub>2</sub>O<sub>5</sub>, Al/p-Si/SiO<sub>2</sub>, and Al/n-Si/SiO<sub>2</sub>/Si<sub>3</sub>N<sub>4</sub>, respectively.

**Keywords:** ISFET; EISCAP; LAPS; field-effect structure; flatband shift; UV

## Introduction

Ion-sensitive field-effect transistors (ISFETs), light-addressable potentiometric sensors (LAPS), and electrolyte–insulator–semiconductor capacitors (EISCAPs) constitute a family of chemical sensors featuring a field-effect structure [1]. Depending on the bias voltage applied to the electrolyte–insulator–semiconductor (EIS) system, the semiconductor surface transitions through accumulation, depletion, and inversion. Variations in the surface potential of the insulator (reflecting activity of target ions in the solution) are detected as changes in channel conductance in ISFETs, or as capacitance changes within the depletion layer in EISCAPs and LAPS. To compensate for long-term drift, for all such sensors, periodic re-calibration is required. A shift in the flatband voltage is a primary cause of this drift, which is highly dependent on measurement and storage environments. In this study, the effects of UV irradiation on the flatband voltage of the EIS system were investigated, drawing an analogy to similar phenomena in metal-oxide-semiconductor (MOS) systems [2].

## Results and Discussion

Three different layer structures were investigated: (a) Al/p-Si/30 nm SiO<sub>2</sub>/60 nm Ta<sub>2</sub>O<sub>5</sub>, (b) Al/p-Si/30 nm SiO<sub>2</sub>, and (c) Al/n-Si/50 nm SiO<sub>2</sub>/50 nm Si<sub>3</sub>N<sub>4</sub>. An ohmic contact of 300 nm Al was evaporated onto the bottom and annealed at 400 °C for 10 min. Each sample was cut to 10 × 10 mm<sup>2</sup>. The insulator surface was exposed to pH 7 buffer containing a reference electrode. Capacitance–voltage (C–V) curves were acquired by sweeping the bias voltage across the EIS system. After the solution was removed and the insulator surface was dried, the

samples were irradiated with UV light ( $\lambda = 365$  nm with 50 mW/cm<sup>2</sup>) for 20 min. Finally, the insulator surface was again exposed to the solution, and the C–V measurements were repeated. Figure 1 shows the flatband voltage shift of the different EISCAP systems caused by the UV illumination.

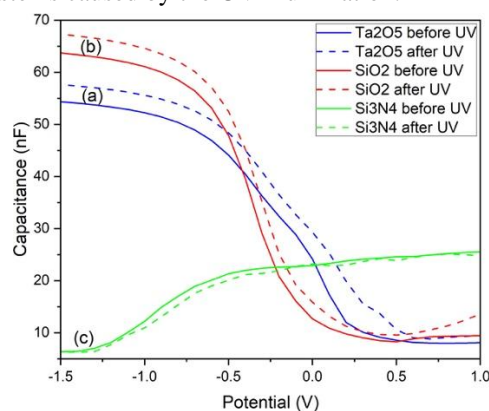


**Figure 1:** Flatband voltage shift of EISCAP systems caused by UV irradiation. (a) Al/p-Si/SiO<sub>2</sub>/Ta<sub>2</sub>O<sub>5</sub>, (b) Al/p-Si/SiO<sub>2</sub>, (c) Al/n-Si/SiO<sub>2</sub>/Si<sub>3</sub>N<sub>4</sub>.

## Conclusions

Effect of UV radiation on flatband voltage shift in field-effect sensors should be taken into account, particularly in long-term measurements. Since there is currently very little information on this topic in the literature, further experiments are planned to contribute to a deeper understanding.

## References

- [1] M.J. Schöning, A. Poghossian. *Electroanalysis* **18** (2006) 1893-1900. doi:10.1002/elan.200603609
- [2] D. Ikeguchi, T. Hosoi, Y. Nakano, et al. *Appl. Phys. Lett.* **104** (2014) 012107. doi:10.1063/1.4860987

# Spin-Dependent Wetting of Chiral Molecules via CISS

Mampi Biswas<sup>1</sup>, Martin Villanueva<sup>1</sup>, Anu Gupta<sup>2</sup>, Ron Naaman<sup>3</sup>, Patricia Losada Pérez<sup>1</sup>, Yves H. Geerts<sup>1</sup>

mampi.biswas@ulb.be

<sup>1</sup>Université Libre de Bruxelles, Plaine Campus, Boulevard du Triomphe, ACC.2, 1050 Brussels, Belgium

<sup>2</sup>The Hebrew University of Jerusalem, Institute of Applied Physics, 9190401 Jerusalem, Israel

<sup>3</sup>Weizmann Institute of Science, Perlman Chemical Sciences Building, 76100 Rehovot, Israel

**Abstract:** The chiral-induced spin selectivity (CISS) effect describes spin-dependent charge transport through chiral molecules. Here, we probe its macroscopic manifestation via time-dependent contact-angle measurements of D- and L-cysteine on Au/Ni spin-polarized substrates under magnetization reversal. Distinct wetting dynamics and contact angles are observed for opposite spin directions, linking spin-chirality coupling to macroscopic interfacial behaviour.

**Keywords:** CISS effect; spin-polarized interfaces; contact angle dynamics; enantiospecific adsorption.

## Introduction

The chiral-induced spin selectivity (CISS) effect links molecular handedness with spin-polarized substrates via spin-dependent charge transfer. Although widely studied using transport and electrochemical methods, its manifestation in macroscopic interfacial properties remains largely unexplored. The contact angle of cysteine solution droplets, governed by interfacial free energies, is not expected to distinguish between enantiomers on non-magnetic surfaces, but it may become sensitive under spin polarization. Here, we investigate whether time-dependent wettability of cysteine enantiomers on Au/Ni substrates can reveal spin-chirality coupling at functional interfaces.

## Results and Discussion

We measured the time-dependent contact angle of different concentrations of D-cysteine and L-cysteine solutions in phosphate buffer on Au/Ni/Ti substrates under an external magnetic field of 448 mT, reversing the magnetization direction beneath the spin-polarized substrate. The phosphate-buffer control showed no measurable response to magnetization reversal. A racemic cysteine solution also showed no spin-dependent wetting, as expected. A polarization was defined from contact angles ( $\theta$ ) as,

$$P(\theta) = \frac{\theta_{\uparrow} - \theta_{\downarrow}}{\theta_{\uparrow} + \theta_{\downarrow}} \times 100\% \quad (1)$$

In contrast, enantiopure samples exhibited opposite wetting dynamics, satisfying  $\theta(D, M \uparrow) \approx \theta(L, M \downarrow)$  and  $\theta(L, M \uparrow) \approx \theta(D, M \downarrow)$ . Kinetics were analysed via plateau contact angle values and single-exponential fits, yielding rate constants and a kinetic polarization,

$$P(k) = \frac{k_N - k_S}{k_N + k_S} \times 100\% \quad (2)$$

These results indicate a chiral contribution to the solid-liquid interfacial free energy, likely arising from spin-dependent interfacial kinetics.

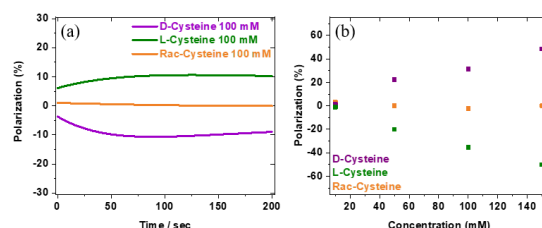


**Figure 1:** (a) Time-dependent polarization for 100 mM cysteine from contact angles (Eq. 1). (b) Concentration-dependent polarization from kinetic analysis (Eq. 2) for D-, L-, and racemic cysteine.

## Conclusions

Contact angle measurements reveal spin-dependent, enantiospecific wetting, supporting the manifestation of CISS effects at macroscopic interfaces.

## References

- [1] B. P. Bloom, Y. Paltiel, R. Naaman, D. H. Waldeck, *Chem. Rev.* 2024, 124, 1950–1991. <https://doi.org/10.1021/acs.chemrev.3c00661>
- [2] Y. Lu, B. P. Bloom, S. Qian, D. H. Waldeck, *J. Phys. Chem. Lett.* 2021, 12, 7854–7858. <https://doi.org/10.1021/acs.jpcclett.1c02087>

## Acknowledgements

Funded by the European Union under the MSCA Doctoral Network CISSE (Grant No. 101071886). Views expressed are those of the authors and do not necessarily reflect those of the EU or REA, which are not liable.

# Building a portable measurement platform to detect per- and polyfluoroalkyl substances (PFAS) in soil and wastewater

T. Karschuck<sup>1</sup>, J. Pettrak<sup>2</sup>, M. J. Schöning<sup>1,3</sup>, T. Wagner<sup>1</sup>

[karschuck@fh-aachen.de](mailto:karschuck@fh-aachen.de)

<sup>1</sup>Institute of Nano- and Biotechnologies (INB), FH Aachen University of Applied Sciences, Campus Jülich, Heinrich-Mußmann-Str. 1, 52428 Jülich, Germany

<sup>2</sup>Institute for Applied Polymer Chemistry (IAP), FH Aachen University of Applied Sciences, Campus Jülich, Heinrich-Mußmann-Str. 1, 52428 Jülich, Germany

<sup>3</sup>Institute of Biological Information Processing (IBI-3), Forschungszentrum Jülich GmbH, Wilhelm-Johnen-Str., 52425 Jülich, Germany

**Abstract:** We present the design of a flow-cell setup for the impedimetric detection of per- and polyfluoroalkyl substances using screen-printed electrodes (SPEs). A prototype of the designed flow-cell was manufactured by selective laser etching of glass. The setup relies on mini-Luer connectors to attach tubing.

**Keywords:** screen-printed electrode; PFAS; impedance

## Introduction

The detection of per- and polyfluoroalkyl substances (PFAS) has gained considerable attention. These synthetic molecules can be found in nature worldwide. This was mainly caused by their high stability and liberal use in industrial applications and consumer products. The aim of the “PFAS-resolve” project is to develop a rapid portable, user-friendly, cost-effective on-site analysis platform. This will enable the mapping of contaminated areas by detecting PFAS in environmental samples. The flow-cell setup (see Figure 1), which is presented here, was designed for Metrohm DropSens 11L sensors [1]. These SPEs were functionalized with molecular imprinting of a polymer to detect perfluorooctanoic acid by Lourenço *et. al* [2,3].

## Results and Discussion

The designed flow-cell was manufactured by selective laser etching of glass using a laser induced etching process (LightFab). The backplate is made of polylactic acid (PLA). An optical microscope (Keyence) was used to investigate the required rinsing volume with colored solutions for various flow rates. The flow-cell was watertight under the tested conditions using a PLA clamp to apply the required mounting pressure. Test impedance measurements of unmodified SPEs were performed with the portable impedance analyzer “Sensit Smart” (PalmSens).

## Conclusions & Outlook

The prototype flow-cell was successfully fabricated out of glass to be corrosion-resistant and heat-tolerant. Testing proved a watertight fluidic setup. In the future, the functionality shall be extended by a temperature control unit and automatic liquid handling. A peripheral solid-phase extraction setup for soil samples will be added.

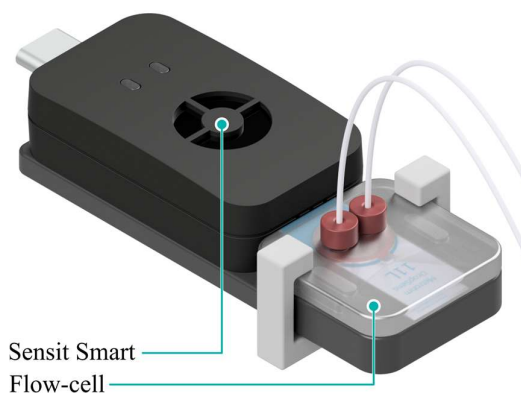


**Figure 1:** Render of the flow-cell concept for the detection of PFAS with screen-printed electrodes (glass flow-cell dimensions: 25 x 25 x 3.3 mm<sup>3</sup>). The Sensit Smart is connected to a laptop via USB-C.

## References

- [1] T. Karschuck, J. Pettrak, M.J. Schöning, T. Wagner. *5<sup>th</sup> European Biosensor Symposium*, Tarragona (2025)
- [2] C. Lourenço, J.W. Lowdon, H. Dilien, T. Cleij, K. Eersels, B. van Grinsven. *16<sup>th</sup> International Workshop on Engineering of Functional Interfaces*, London (2025)
- [3] C. Lourenço, J.W. Lowdon, H. Dilien, T. Cleij, K. Eersels, B. van Grinsven. *5<sup>th</sup> European Biosensor Symposium*, Tarragona (2025)

## Acknowledgements

This work was funded by the Interreg Meuse-Rhine (NL-BE-DE) program under IMR6-00027 – PFAS-resolve. The authors thank S. Schmidt for the 3D model of the Sensit Smart and S. Achtsnicht for technical support.

# Raman-Based Visualization of Diffusion-Driven Delamination at Metal–Polymer–Interfaces of Active Implantable Medical Devices (AIMDs)

Christian Angerer<sup>1</sup>, Adrian Onken<sup>2</sup>, Gunito Fischer<sup>1</sup>, Theodor Doll<sup>2</sup>, Sabine Hild<sup>1</sup>

[Christian.angerer@jku.at](mailto:Christian.angerer@jku.at)

<sup>1</sup>Institute of Polymer Science, Johannes Kepler University, Altenberger Straße 69, 4040 Linz, Austria

<sup>2</sup>NIFE-BioMaterial Engineering, Hannover Medical School, Carl-Neuberg Straße 1, 30625 Hannover, Germany

**Abstract:** Confocal Raman microscopy was used to investigate diffusion-driven degradation at metal–polymer interfaces in active implantable medical devices utilizing a standardized test with embedded metal structures beneath a protective polymer layer to simulate electrolyte-induced interface degradation. Raman imaging provides chemically specific, high-resolution maps of delamination and diffusion-related transformations below the polymer coating. This enables the detection of silver and copper sulfides and oxides, indicating corrosion at the interface, highlighting Raman microscopy as a powerful tool for studying degradation in AIMD materials.

**Keywords:** Confocal Raman microscopy, metal-polymer interface, corrosion, AIMDs

## Introduction

Active implantable medical devices (AIMDs) are a cornerstone of modern medical innovation, enabling life-sustaining and life-enhancing therapies. Despite strict regulatory requirements and extensive safety testing, their long-term reliability remains challenged by body-fluid permeation through protective encapsulation layers. Subsequent ion diffusion can induce reactions at metal–polymer interfaces, promoting corrosion and device malfunction. To investigate these processes, a standardized sample with embedded metallic structures beneath a polydimethylsiloxane (PDMS) layer was developed.<sup>1</sup> Exposure to reactive solutions containing inorganic and organic sulfides enabled systematic investigation of diffusion-driven interface degradation, as these compounds oxidize the metal surface and induce an optical color change. Confocal Raman imaging (CRI) combines spectroscopy with high-resolution imaging, providing a label-free method to chemically resolve these processes. In this way, CRI extends microscopic analysis by enabling chemically specific identification and spatial mapping of corrosion products.

## Results and Discussion

Microscopic investigations (Figure 1a, c) provided an initial overview of the heterogeneous spatial distribution of copper- and silver-based corrosion products within the samples. Surface alterations and deposits indicated the formation of corrosion layers; however, this preliminary assessment, based mainly on color changes, did not allow differentiation between individual corrosion species such as oxides and sulfides. Planar CRI of a silver surface revealed the lateral distribution of Ag<sub>x</sub>O/Ag<sub>y</sub>S-related species

(Figure 1b). In contrast, depth-resolved Raman imaging through the PDMS encapsulation (Figure 1d) revealed a roughened copper surface covered with Cu<sub>x</sub>S<sub>y</sub>-related corrosion products. These findings indicate that corrosion does not proceed homogeneously at the metal-polymer interface.

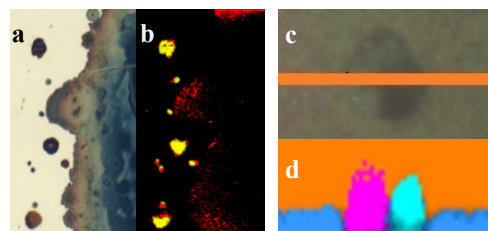


**Figure 1:** Microscopy images of Ag- and Cu- based oxide/sulfide derivatives are shown in Figure (a, c), respectively. Figure (b) highlights the distribution of Ag corrosion products in red and yellow. In Figure (d), the blue region corresponds to Cu<sub>x</sub>S<sub>y</sub>, while purple and turquoise indicate mixed phases; PDMS is shown in orange.

## Conclusions

Optical microscopy revealed surface alterations and spatial distribution of oxide- and sulfide-based corrosion products. Raman imaging enabled their chemical differentiation and confirmed the formation of Ag- and Cu-based species beneath the PDMS layer. Thus, Raman microscopy provides a powerful tool for identifying and spatially mapping chemically distinct corrosion species at metal–polymer interfaces.

## References

- [1] Onken A., et.al., Predicting Corrosion Delamination Failure in Active Implantable Medical Devices: Analytical Model and Validation Strategy. *Bioengineering* 9, 10 (2022) [doi.org/10.3390/bioengineering9010010](https://doi.org/10.3390/bioengineering9010010)

# Effectiveness of deconvolution methods for surface reconstruction in AFM

Lukas Lehnert<sup>a</sup>, Lars Helgest<sup>a</sup>, Eddy Kunnen<sup>b,c</sup>, Ronald Thoelen<sup>b,c</sup>, and Hildegard Möbius<sup>a,\*</sup>

<sup>a</sup>Department of Computer Sciences and Micro Systems Technology, University of Applied Sciences Kaiserslautern, Zweibrücken, Germany

<sup>b</sup>UHasselt, Institute for Materials Research (IUMAT), Martelarenlaan 42, Hasselt, Belgium  
<sup>c</sup>imec, IUMAT, Wetenschapspark 1, Diepenbeek, Belgium

\*E-mail: hildegard.moebius@hs-kl.de

**Abstract:** AFM topography is broadened by tip sample convolution limiting the lateral resolution. In this work the analytical deconvolution methods of Markiewicz et al. and Marques-Moros et al. are compared for nanostructures of different shapes. For fins, Marques-Moros achieves a maximum relative width error of about 18 %, versus about 45 % for Markiewicz; for a 76 nm SiO<sub>2</sub> nanoparticle, both methods give similar widths (75.6 nm and 74 nm). Therefore, Marques-Moros is viable for both types of topography, while Markiewicz is well suited for nanoparticle deconvolution with the advantage that the tip angle does not have to be known.

**Keywords:** Atomic Force Microscopy, nanoparticles, dielectric constant, characterization and analytical techniques

## Introduction

Atomic Force Microscopy is a well-established method for surface characterization with subnanometer accuracy. In AFM the observed topography is always the convolution of real topography of the sample and the shape and size of the tip. To gain the exact topography the size of the tip has to be known precisely. Vice versa, a known topography can be used to reconstruct the size and shape of the tip. This can be done by using a rough sample with high and sharp spikes. With mathematical approaches like Markiewicz et al. and Marques-Moros et al. it is possible to get information about the tip size whilst measuring.<sup>[1,2]</sup> In this work, the well-established method for particles by Markiewicz et al. is compared to the method by Marques-Moros et al. for a rectangular reference structure and for nanoparticles (NP).

## Results and Discussion

Comparing the two deconvolution methods for reconstructing fins it is clearly visible that the method by Marques-Moros et al. is better suited. With their method, the worst error from the width  $w$  is 18 % at 80 nm. This is an improvement by the factor of 2.5 compared to the worst error using Markiewicz et al. with 45 % at 80 nm. The same comparison of deconvolution methods as in Figure 1a was repeated for a 76 nm SiO<sub>2</sub> NP (Figure 1b). In this case the method according to Marques-Moros et al. has similar results as Markiewicz et al. With a particle height of 76.3 nm the total measured width  $w_{tot}$  is 169 nm. The tip used has a radius of 31 nm and a tip angle of 20°. The deconvoluted particle width is 75.6 nm for Markiewicz et al. and 74 nm for Marques-Moros et al.. This difference of 2 % is negligible.

## Conclusions

The method according to Marques-Moros et al. achieves similar results as the method of Markiewicz et al. applied to nanoparticles, but only for well-known tip angles. Therefore, Markiewicz et al. is the preferred choice for tip estimation and deconvolution. For structures like

fins the method of Marques-Moros et al. is preferable due to its significant increase in accuracy compared to Markiewicz et al.

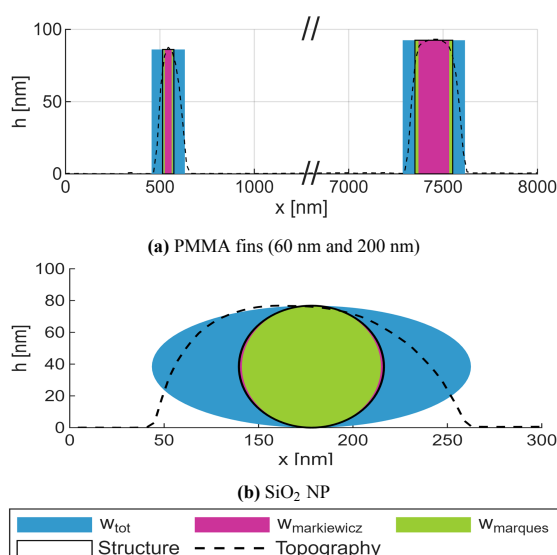


**Figure 1:** Schematic profile of (a) PMMA fins and (b) SiO<sub>2</sub> NP showing total measured width  $w_{tot}$ , width after deconvolution according to Marques-Moros et al.  $w_{marques}$  and Markiewicz et al.  $w_{markiewicz}$ , overlaid with the measured topography

## References

- [1] Peter Markiewicz and M. Cynthia Goh. Atomic force microscopy probe tip visualization and improvement of images using a simple deconvolution procedure. *Langmuir*, 10(1):5–7, 1994.
- [2] Francisco Marques-Moros, Alicia Forment-Aliaga, Elena Pinilla-Cienfuegos, and Josep Canet-Ferrer. Mirror effect in atomic force microscopy profiles enables tip reconstruction. *Scientific reports*, 10(1):18911, 2020.

## Acknowledgements

The authors are grateful for funding of the project "KoM-Bio - Hyperthermiesysteme aus superparamagnetischen Funktionsmaterialien zum kontaktlosen Heizen" (86003140) funded by the European Regional Development Fund and Rhineland-Palatine.

# Biofilm-Dependent Human Osteoblasts Responses in 3D peri-implant model (INTER<sub>b</sub>ACT-B)

Malekhamadi B.<sup>1,2</sup>, Parizi M.<sup>1,2</sup>, Mikolai C.<sup>1,2</sup>, Rahim M.I.<sup>1,2</sup>, Winkel A.<sup>1,2</sup>, Doll-Nikutta K.<sup>1,2</sup>, Menzel H.<sup>4</sup>, Wirth D.<sup>5</sup>, Stiesch M.<sup>1,2</sup>

[Malekhamadi.Behnaz@mh-hannover.de](mailto:Malekhamadi.Behnaz@mh-hannover.de)

<sup>1</sup>Department of Prosthetic Dentistry and Biomedical Materials Science, Hannover Medical School, Hannover, Germany,

<sup>2</sup>Lower Saxony Center for Biomedical Engineering, Implant Research and Development (NIFE), Hannover, Germany

<sup>3</sup>Braunschweig University of Technology, Institute for Sustainable Chemistry, Braunschweig, Germany

<sup>4</sup>Helmholtz Centre for Infection Research, Research Group Model Systems for Infection and Immunity, Braunschweig, Germany

**Abstract:** Infectious biofilms contribute to peri-implant inflammation, bone loss, and implant failure. To investigate host–biofilm interactions, a 3D peri-implant model INTER<sub>b</sub>ACT-B, was developed with fibroblasts, multilayered epithelium, and a scaffold-based hard-tissue compartment with human osteoblasts. Co-cultivation with multispecies commensal or pathogenic biofilms revealed biofilm-dependent changes in tissue responses and osteogenic marker expression, suggesting INTER<sub>b</sub>ACT-B as a clinically relevant platform for studying peri-implant host–biofilm interactions.

**Keywords:** Peri implant diseases; 3D peri-implant model; Oral biofilms; Human osteoblast; HA/TCP scaffold.

## Introduction

The interplay between host tissues and oral microorganisms plays a central role in maintaining peri-implant health as well as to the onset and progression of peri-implant diseases. Although the interest in developing novel therapeutic strategies is increasing, their clinical success will depend on a deeper understanding of host–biofilm interactions. To address this issue, a 3D *in-vitro* model mimicking the physiological soft tissue-implant interface was established (INTER<sub>b</sub>ACT) but was lacking the peri-implant bone compartment (1). Therefore, in this study the model was expanded by integrating a hard tissue scaffold loaded with human osteoblasts into INTER<sub>b</sub>ACT-B, enabling reproducible co-culture experiments with commensal and pathogenic biofilms (2).

## Results and Discussion

The INTER<sub>b</sub>ACT-B construct maintained a stable implant–tissue interface, preserved multilayered tissue architecture, and supported cell viability throughout the culture period. An enhanced osteogenic differentiation within the model resembled by an upregulation of alkaline phosphatase (ALP), a key enzyme involved in early bone matrix mineralization, was observed. Upon biofilm stimulation, this ALP expression was significantly elevated only in case of commensal biofilms but not pathogenic once, suggesting a differential host–biofilm influence on osteogenic activity.

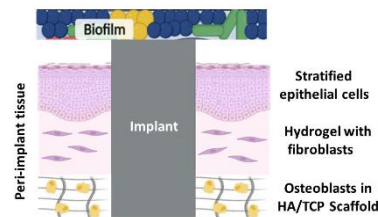


**Figure 1:** Schematic illustration of INTER<sub>b</sub>ACT-B model

## Conclusions

The innovative INTER<sub>b</sub>ACT-B model provides a clinically relevant platform for investigating host–biofilm interactions and evaluating experimental implant surface modifications to enhance peri-implant tissue integration.

## References

- [1] B. Malekhamadi *et al.*, “Establishment of a three-dimensional *in vitro* peri-implant bone-mucosa composite model,” May 15, 2025, In Review. doi: 10.21203/rs.3.rs-6565129/v1.
- [2] N. Heine *et al.*, “Influence of species composition and cultivation condition on peri-implant biofilm dysbiosis *in vitro*,” *Front. Oral Health*, vol. 6, p. 1649419, Sep. 2025, doi: 10.3389/froh.2025.1649419.

## Acknowledgements

This work was funded by the Deutsche Forschungsgemeinschaft DFG, German Research Foundation(-SFB/TRR-298-SIIRI-Project-ID 426335750, Hannover, Germany).

# BDNF-optimized mesenchymal stem cells for therapeutic application in the inner ear

Elena Wiebe<sup>1,2,3</sup>, Sina Christoffers<sup>1,2,3</sup>, Cornelia Blume<sup>1,2,3</sup>

(wiebe@iftc.uni-hannover.de)

<sup>1</sup>Institute for Technical Chemistry, Leibniz University Hannover, Callinstraße 5, 30167 Hannover, Germany

<sup>2</sup>Lower Saxony Center for Biomedical Engineering, Implant Research and Development (NIFE), Stadtfelddamm 34, 30625 Hanover, Germany

<sup>3</sup>Cluster of Excellence Hearing4all, Hannover, Germany

**Abstract:** After cochlear implantation, the regeneration of spiral ganglion neurons and hair cells poses a major challenge for full hearing regeneration. One potential approach to improve recovery is the neuroprotective brain-derived neurotrophic factor (BDNF) secreted from bone-marrow-derived mesenchymal cells (BMSCs), to increase neuronal cell survival and function. Here, we tested whether a CRISPR/Cas9-induced knockout has any influence on cell viability and trilineage differentiation. To clarify the knockout bdnf-expression in the modified cells, qPCR, as well as a cell viability test and cell staining, were performed.

**Keywords:** CRISPR/Cas9 knockout, mesenchymal stem cells, brain-derived neurotrophic factor, selective pressure

## Introduction

The CRISPR/Cas9 system permits modifying native cells to optimize targeted gene expression for clinical research and therapeutic applications [1]. Mesenchymal stem cells have the ability to release neuroprotective factors like BDNF to improve cell survival [2]. An elevated cellular selective pressure could be helpful to insert and overexpress an artificial gene [3] such as the optogenetic system CRY2/CIB to enable light dosage-dependent BDNF-release.

## Results and Discussion

We generated a bdnf-knockout variant with downregulation of the mRNA by up to 60% (Fig.1A). We could show that the modified cells were comparably viable to untreated cells (Fig.1B) and did not substantially lack their original differentiation potency in comparison to native BMSCs (Fig.1C-E). As a next step, we will prove our hypothesis that the bdnf-knockout favours the transfectability of these cells with the optogenetic system.

## Conclusions

The CRISPR/Cas9-mediated knockout decreased the native bdnf-expression in BMSCs without any cell-specific changes in viability or differentiation potential.

## References

[1] Li, T., Yang, Y., Qi, H. et al. *Signal transduction and targeted therapy*, 8(1), 36 (2023). <https://doi.org/10.1038/s41392-023-01309-7>

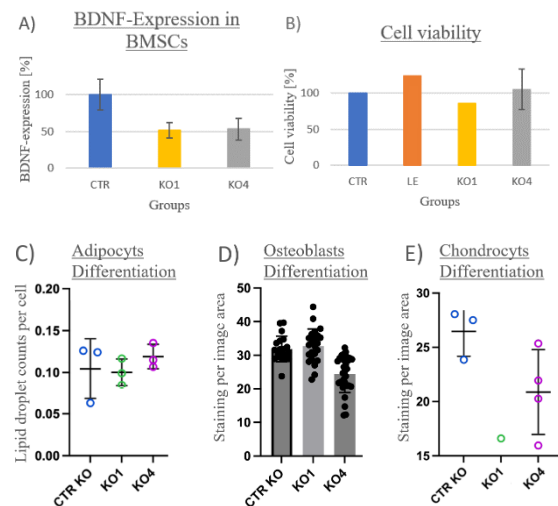


**Figure 1:** A) *Bdnf*-expression in modified BMSCs measured by RT-qPCR (N=2; n=3). B) Cell viability of modified BMSCs (N=1-2; n=3). C-E) Trilineage differentiation of modified BMSCs (N=1; n=1-3). CTR=Control BMSCs without knockout, Le=BMSCs with empty vector, KO1= *Bdnf* knockout variant 1, KO4= *Bdnf* knockout variant 4.

[2] Scheper, V., Schwieger, J., Hamm, A. et al. *Journal of Neuroscience Research*, 97(11), 1414–1429 (2019). <https://doi.org/10.1002/jnr.24488>

[3] Van Damme, A., Thorrez, L., Ma, L. et al. *Stem cells (Dayton, Ohio)*, 24(4), 896–907 (2006). <https://doi.org/10.1634/stemcells.2003-0106>

## Acknowledgements

This project is funded by the Deutsche Forschungsgemeinschaft (DFG, German Research Foundation) under Germany's Excellence Strategy – EXC 2177/1 - Project ID 390895286.

# Development of flexible polyimide devices incorporated with polyvinylidene fluoride for applications as piezoelectric sensors and supercapacitors

G. Badagnani de Carvalho<sup>1,2</sup>, J. R. Siqueira Júnior<sup>1</sup>, M. J. Schöning<sup>2</sup>

gabriel\_badagnani@hotmail.com

<sup>1</sup>Institute of Nano- and Biotechnologies (INB), FH Aachen University of Applied Sciences, Campus Jülich, Heinrich-Mußmann-Straße 1, 52428, Jülich, Germany

<sup>2</sup>Laboratory of Applied Nanomaterials and Nanostructures (LANNA), Federal University of Triângulo Mineiro, Avenida Doutor Randolpho Borges Júnior 1400, 38064-200, Uberaba, Brazil

**Abstract:** The growing demand for miniaturized wearable and implantable electronic devices has driven research into advanced materials with piezoelectric and flexible properties. This work describes sensors and supercapacitors integrated into polyimide (PI) substrates by incorporating polyvinylidene fluoride (PVDF) membranes to generate a device with piezoelectric characteristics. The device assembly was performed using an interdigitated electrode (IDE) structure, a PVA (polyvinyl alcohol)/H<sub>3</sub>PO<sub>4</sub>-based gel electrolyte, and PVDF-based piezoelectric membranes produced by solvent casting. The results point to energy nanogenerator devices with hybrid characteristics such as intermediate power and energy density, fast response times, and low hysteresis.

**Keywords:** Self-charging nanogenerators; PVDF; piezoelectric nanosensor; nanocomposites membranes

## Introduction

Piezoelectric self-charging devices (PENGs) demonstrate a promising way to produce energy in devices that do not require large amounts of power. They are promising candidates for applications in wearable, implantable, Internet of Things (IoT), environmental and medical sensors, where low power consumption and autonomy are essential [1].

## Results and Discussion

A set of four devices was tested to investigate the influence of the composite membrane on the sensor or supercapacitor behavior. Cyclic voltammetry, galvanostatic charge/discharge, and impedance measurements were used to determine the values shown in the Ragone plot (Figure 1) and to understand the capacitive behavior and internal resistance, respectively [2].

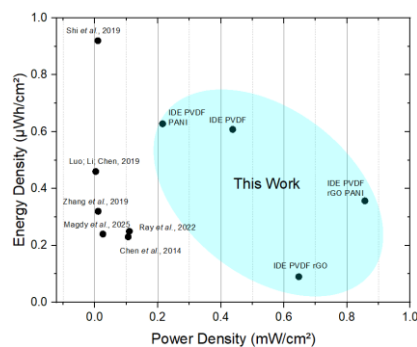


Figure 1: Ragone plot for nanogenerators devices.

Devices with high power density tend to be better sensors in chronopotentiometry at standardized frequency and gradually increasing pressure (see

Figure 2). The device fabricated with PVDF rGO has a high sensitivity, current generation capacity, and low hysteresis of around 22.4 mV/N, 0.12 μA, and 0.14%, respectively.

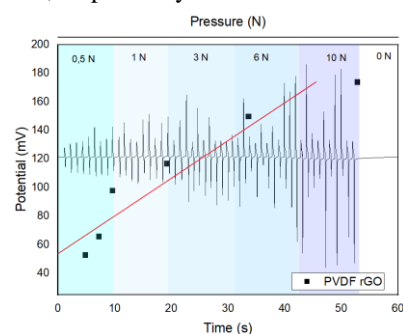


Figure 2: PVDF rGO CP analysis and sensitivity plot.

## Conclusions

Devices manufactured with IDE substrate and PVDF composite membranes are potential candidates for applications as piezoelectric sensors and supercapacitors.

## References

- [1] B. Singh, *et al. J. of Energy Storage*, **47** (2022). doi: 10.1016/j.est.2021.103547.
- [2] C. Shen, *et al. J. Microelectromech. Syst.*, **26** (2017). doi: 10.1109/JMEMS.2017.2723018.

## Acknowledgements

The authors thank FAPEMIG for the grant call 009/2023 - "Promotion of Internationalization of ICTMGs" Process: APQ-05247-23, as well as S. Achtsnicht, H. Iken, and D. Rolka for technical support.

# Neodymium-Samarium alloys with improved mechanical properties

Florian Reiter<sup>1,2\*</sup>, Hüseyin Zengin<sup>2</sup>, Arthur Ernst<sup>1</sup>, Achim Walter Hassel<sup>2,3</sup>

[Florian.Reiter@jku.at](mailto:Florian.Reiter@jku.at)

<sup>1</sup>Institute of Theoretical Physics, Johannes Kepler University Linz, Altenberger Str. 69, 4040, Linz, Austria

<sup>2</sup>Institute of Chemical Technology of Inorganic Materials (TIM), Johannes Kepler University Linz, Altenberger Str. 69, 4040, Linz, Austria

<sup>3</sup>Danube Private University, Steiner Landstraße 124, 3500 Krems an der Donau, Austria

**Abstract:** An alloy of 50 at.% Neodymium (Nd) and 50 at.% Samarium (Sm) was produced by fusion melting. The hardness of the sample was measured using a Vickers hardness tester. The result shows a significantly higher hardness than pure Nd or Sm, while the measured density of the alloy is in agreement with theoretical expectations. Furthermore, a theoretical investigation of the band structure suggests strong magnetic activity of the alloy.

**Keywords:** Neodymium; Samarium; hardness; CPA; magnetism

## Introduction

Nd and Sm possess magnetic properties that are essential for the production of high-strength and stable permanent magnets. Nd is used in Nd-Fe-B alloys for high-strength permanent magnets due to the high magnetic moment of Nd. Sm-Co magnets exhibit a high Curie temperature due to the high anisotropy. A combination of those properties may thus be of high interest for the development of novel permanent magnets. This work thus focuses on examining Nd-Sm alloys and their mechanical properties.

## Results and Discussion

The measured hardness of  $\text{Nd}_{0.5}\text{Sm}_{0.5}$  is  $(70.9 \pm 1.75)$  HV, which is significantly higher than the hardness of pure Nd and Sm, which are 35 HV and 42 HV, respectively [1].

The measured density of the alloy was found to be  $7.256 \text{ g/cm}^3$ , which is in good agreement with the theoretical values of  $7.26 \text{ g/cm}^3$ .

Moreover, the band structure (see figure 1) exhibits relatively flat bands below and near the Fermi level which originate from highly localized 4f electrons. The enhanced density of states near the Fermi level suggests strong magnetic behavior and indicates an increased tendency toward magnetic ordering in the alloy.

## Conclusions

The  $\text{Nd}_{0.5}\text{Sm}_{0.5}$  alloy exhibits a significantly higher hardness than Nd or Sm alone, while the density is in good agreement with theoretical expectations. The flat bands below the Fermi edge suggest enhanced magnetic behavior of the alloy.

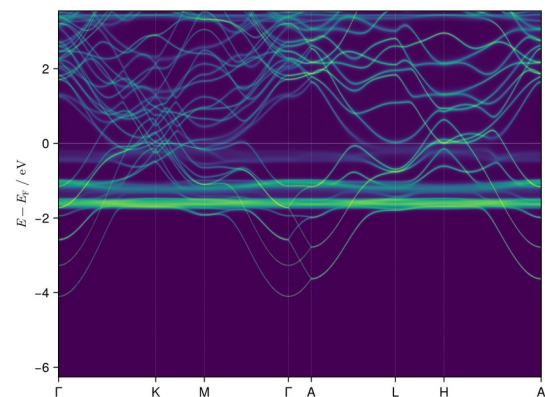


**Figure 1:** Computed band structure of  $\text{Nd}_{0.5}\text{Sm}_{0.5}$  using CPA

## References

- [1] <https://pse-info.de/en> (last access: 2026-05-18)

# Device-to-device matching of extended-gate field-effect transistors with atomic-layer deposited high-k Ta<sub>2</sub>O<sub>5</sub> as pH-sensitive material

M. Knoll<sup>1,2</sup>, A. Poghossian<sup>3</sup>, G. Elias<sup>1</sup>, S. Meier<sup>4</sup>, E. Müllner<sup>4</sup>, M. Keusgen<sup>2</sup>, M. J. Schöning<sup>1</sup>

[Knoll@fh-aachen.de](mailto:Knoll@fh-aachen.de)

<sup>1</sup>Institute of Nano- and Biotechnologies (INB), FH Aachen University of Applied Sciences, Campus Jülich, Heinrich-Mußmann-Str. 1, 52428 Jülich, Germany

<sup>2</sup>Institute of Pharmaceutical Chemistry, Philipps University of Marburg, Wilhelm-Roser-Str. 2, 35032 Marburg, Germany

<sup>3</sup>MicroNanoBio, Von-Guericke-Alle 1, 53125 Bonn, Germany

<sup>4</sup>Texas Instruments Incorporated, Freising, Haggertystr. 1, Germany

**Abstract:** The electrochemical properties of extended-gate field-effect transistors with pH-sensitive gate oxide of Ta<sub>2</sub>O<sub>5</sub> are investigated in this work. Focussing on the matching of the pH-sensing performance, the studied sensors showed outstanding comparability in signal progression, indicating the high and consistent quality of the atomic layer deposited gate oxide.

**Keywords:** extended-gate ISFET; Ta<sub>2</sub>O<sub>5</sub>; ALD; differential measurement

## Introduction

Ion-sensitive field-effect transistors (ISFETs) have been recognized as a promising universal platform for the development of numerous biochemical sensors, ranging from pH, ion concentration and enzymatic sensors over DNA- and immunosensors up to multiplexed multianalyte devices [1]. Their compatibility with standard CMOS (complementary metal-oxide-semiconductor) processes enables scalable, low-cost mass production of robust, miniaturized sensors with minimal power consumption. [2]. Device-to-device variation in ISFETs refers to inconsistencies in electrical and sensing performance (e.g., threshold voltage, sensitivity) between sensors fabricated on the same chip or different batches. These variations are a major obstacle for widespread commercialization of ISFET-based devices, as they necessitate time-consuming and cost-intensive individual calibration for each sensor. In this work, device-to-device variation of extended-gate ISFETs (EGFETs) with Ta<sub>2</sub>O<sub>5</sub> as pH-sensitive material has been studied.

## Results and Discussion

CMOS technology-based sensor chips were used in this experiment, each containing three EGFETs (see Figure 1, upper right). Using atomic layer deposition (ALD), sensors were coated with a 50 nm thick Ta<sub>2</sub>O<sub>5</sub> pH-sensitive layer. A standard pH characterization was performed over the range of pH 5-9 (Figure 1, lower left). Taking into account the capacitive voltage divider, the ALD-Ta<sub>2</sub>O<sub>5</sub>-gate EGFETs exhibited a near-Nernstian pH sensitivity

of  $57.5 \pm 0.1$  mV/pH ( $n = 12$ ). Differential measurements between EGFET pairs over the course of this experiment indicated the excellent matching of these sensors. More details of experiments and obtained results will be presented at the conference.

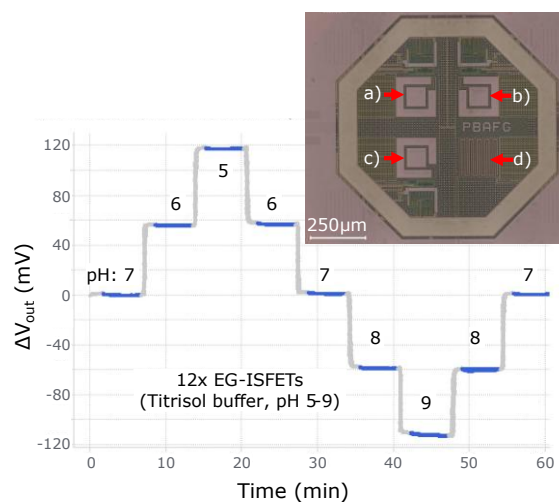


**Figure 1:** pH characterization (pH 5-9) of 12x Ta<sub>2</sub>O<sub>5</sub> EGFETs. Shown is the offset-corrected signal of all 12 sensors (lower left). Sensor chip with 3 EGFETs a), b), c), and onboard temperature sensor d) (upper right).

## References

- [1] A. Poghossian, M.J. Schöning, *Curr. Opin. Electrochem.* **29** (2021) 100811. doi: 10.1016/j.coelec.2021.100811
- [2] M. Douthwaite, N. Moser, P. Georgiou, *IEEE Sens. J.* **21** (2021) 20. doi: 10.1109/JSEN.2021.3094206

# Titanium-hydrogel-interaction in a peri-implant *in-vitro* model

Lars Heine<sup>1,2</sup>, Maya Duitscher<sup>1,2</sup>, Maria Leilani Torres-Mapa<sup>2,3</sup>, Katharina Doll-Nikutta<sup>1,2</sup>, Meike Stiesch<sup>1,2</sup>

[Heine.Lars@mh-hannover.de](mailto:Heine.Lars@mh-hannover.de)

<sup>1</sup> Department of Prosthetic Dentistry and Biomedical Materials Science, Hannover Medical School, Carl-Neuberg-Str. 1, 30625 Hannover, Germany

<sup>2</sup> Lower Saxony Centre for Biomedical Engineering, Implant Research and Development (NIFE), Stadtfelddamm 34, 30625 Hannover, Germany

<sup>3</sup> Institute of Quantum Optics, Leibniz University of Hannover, Welfengarten 1, 30167 Hannover, Germany

**Abstract:** The 3D INTER<sub>b</sub>ACT *in-vitro* model, consisting of an artificial human mucosa, a titanium implant and a bacterial biofilm shows great promise for researching bacterial infections of dental implants. While previous studies analysed the implant-cell-bacteria interaction, this study aims to examine the effect of the hydrogel scaffold simulating the extracellular matrix. Two different hydrogels were investigated in combination with titanium implants in a simplified version of the INTER<sub>b</sub>ACT model. The E-modulus of the hydrogels, surface free energy of the interface between hydrogel and titanium, as well as adhesion forces between implant and scaffold were examined and showed differences, likely due to the differing elasticities of the two materials.

**Keywords:** Hydrogel, Force Spectroscopy, Contact Angle Measurements, INTER<sub>b</sub>ACT model, GelMA

## Introduction

Peri-implantitis is the result of bacterial infections on dental implants, that affect 1 in 4 implants after 5 years of implantation [1]. Researching these infections can be challenging, due to the complex interactions at the peri-implant interface. For this purpose, the INTER<sub>b</sub>ACT model has been developed that combines an implant, a bacterial biofilm and an artificial mucosal tissue made of a cell-containing hydrogel [1]. The model has already been used to analyse the bacteria-cell-material interaction [2]. However, the influence of the selected hydrogel simulating the extracellular matrix has not been analysed so far. Thus, this study aims to specifically examine the hydrogel-implant material interaction by comparing the standard collagen type 1 hydrogel to a Gelatin Methacryloyl (GelMA) hydrogel for their behaviour in combination with titanium.

## Results and Discussion

Simplified versions of the INTER<sub>b</sub>ACT model that focus on the hydrogel-material interaction were created by inserting a titanium disk into the hydrogel scaffolds using both GelMA and type 1 collagen. These models were then analysed at three time points, that were chosen to mimic the six-week assembly protocol of the INTER<sub>b</sub>ACT model.

First, adhesion forces between hydrogel and implant were measured by using a pull-test. Based on initial data, these forces seemed to rise with increased incubation time.

Force spectroscopy with an atomic force microscope was used to examine the E-Modulus of the scaffold.

Overall, the E-modulus of the collagen hydrogel was lower than that of the GelMA hydrogel. In addition, similarly to the adhesion forces, the E-modulus seemed to change with time.

The wettability and surface free energy of the interface between hydrogel and titanium were analysed using contact angle measurements with water and diiodomethane. The surface free energy did not appear to change over time, for both the collagen and the GelMA model.

## Conclusions

Experiments have shown that differences in the implant interaction between the GelMA hydrogel and the collagen hydrogel exist. They can most likely be explained by differences in the hydrogel's elasticity. How this further affects the hydrogel-implant as well as the cell-implant interaction should be analysed in future experiments.

## References

- [1] A. Ingendoh-Tsakmakidis *et al.*, "Commensal and pathogenic biofilms differently modulate peri-implant oral mucosa in an organotypic model," *Cellular Microbiology*, vol. 21, no. 10, p. e13078, 2019, doi: [10.1111/cmi.13078](https://doi.org/10.1111/cmi.13078)
- [2] C. Mikolai, K. Wöll, M. I. Rahim, A. Winkel, C. S. Falk, and M. Stiesch, "Impact of antibacterial therapeutic agents on biofilm-tissue interactions in a 3D implant-tissue-oral-bacterial-biofilm model," *Sci Rep*, vol. 15, no. 1, p. 18979, May 2025, doi: [10.1038/s41598-025-03855-2](https://doi.org/10.1038/s41598-025-03855-2)

## Acknowledgements

The study was supported by the Matrix Evolution project, which is funded by zukunfft.niedersachsen, funding programme of the Lower Saxony Ministry of Science and Culture and the Volkswagen Foundation.

# Structural and Electrochemical Investigation of Electrodeposited PEDOT:PSS Microelectrodes

Qiqi Li<sup>1</sup>, Dongyang Tang<sup>1</sup>, Sven Ingebrandt<sup>1</sup>, Ziyu Gao<sup>1,\*</sup>

\* Corresponding: [ziyu.gao@iwe1.rwth-aachen.de](mailto:ziyu.gao@iwe1.rwth-aachen.de)

<sup>1</sup>Institute of Materials in Electrical Engineering 1, RWTH Aachen University, Otto-Blumenthal-Str. 6, 52074 Aachen, Germany

**Abstract:** This work investigates the influence of electrodeposition voltage on the growth mechanism, microstructural evolution, and electrochemical behavior of PEDOT:PSS electrodeposited on gold (Au) microelectrodes. Electrochemical impedance spectroscopy (EIS) combined with equivalent electrical circuit (EEC) modelling is used to evaluate the voltage-dependent interfacial electrochemical response. Scanning electron microscopy (SEM) reveals morphological evolution, from rough, porous, capacitance-dominated interface to compact structure showing stronger diffusion-related electrochemical responses. Insufficient deposition voltage leads to inhomogeneous film formation, whereas excessively high voltage reduces adhesion of PEDOT:PSS films.

**Keywords:** PEDOT:PSS electrodeposition; Au Microelectrodes; Electrochemical impedance spectroscopy ; Microstructural evolution; Electrode-electrolyte interface; Equivalent electrical circuit

## Introduction

Flexible microelectrode arrays (Flex-MEAs) are promising bioelectronic interfaces, but their performance is often limited by the high impedance of microscale electrodes. PEDOT:PSS coatings can improve electrode-electrolyte coupling by reducing interfacial impedance and enhancing ionic-electronic transport. However, the electrochemical behavior [1] of PEDOT:PSS strongly depends on electrodeposition conditions and the resulting microstructure [2].

## Results and Discussion

Bode plot reveals a strong dependence of interfacial electrochemical properties on the electrodeposition voltage. All electrodeposited PEDOT:PSS microelectrodes exhibited significantly reduced impedance compared with bare Au electrodes. In addition, the phase angles shifted from approximately  $-90^\circ$  to  $-20^\circ$ , indicating enhanced mixed ionic-electronic interfacial coupling.

The Nyquist plot demonstrates distinct low-frequency responses under different deposition conditions. Electrodes deposited at lower voltages exhibit increasingly vertical capacitive tails, suggesting greater capacitance-dominated behavior.

SEM revealed voltage-dependent microstructural evolution. Equivalent electrical circuit (EEC) fitting shows that rough, porous, capacitive-dominated interfaces could be described using an  $R(RQ)Q$  model, while denser interfaces exhibiting diffusion-related behavior are better fitted using an  $R(Q(RW))$  model including a Warburg element.

However, excessively low deposition voltage caused inhomogeneous PEDOT:PSS growth, leading to an unusually strong capacitive response, whereas the 1.0V condition produced compact but less stable coatings with poorer adhesion and reproducibility.

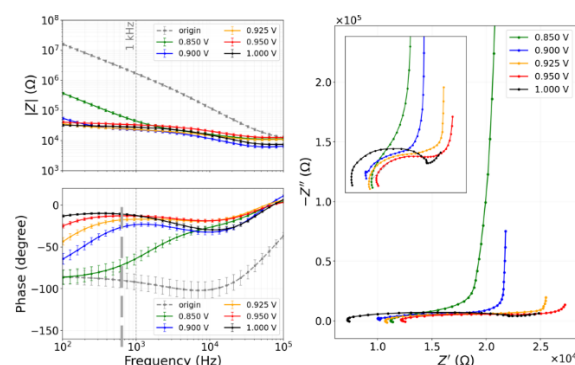


**Figure 1:** Bode plot (left) and Nyquist plot (right) comparing Au microelectrodes and PEDOT:PSS microelectrodes electrodeposited at different electrodeposition voltages.

## Conclusions

This study highlights that electrodeposition voltage strongly influences PEDOT:PSS polymerization, resulting in distinct microstructural and electrochemical properties. Different morphologies and impedance characteristics can be achieved by tuning the electropolymerization parameters. The next step is to evaluate baseline noise and signal-to-noise ratio for in vitro electrophysiological recording and stimulation, including cardiomyocyte and neuronal signal monitoring.

## References

- [1] Jin, R., et al., ACS Appl Mater Interfaces, 2025, 17(50): p. 68389-68399.
- [2] Mousavi, H., et al., Advanced Electronic Materials, 2023, 9.

## Acknowledgements

Authors thank the Federal Ministry of Education and Research (BMBF) and the Ministry of Culture and Science of the German State of North Rhine-Westphalia (MKW) under the Excellence Strategy of the Federal Government and the Länder (ERS-OPSF906).

# Surface functionalization with photoelectrons

Gerrit Janzen<sup>1</sup>, Adrian Onken<sup>1</sup>, Patricia Torgau<sup>1</sup>, Theodor Doll<sup>1</sup>, Marc Müller<sup>2</sup>, Philip Born<sup>3</sup>

Gerrit.janzen@stud.uni-hannover.de

<sup>1</sup> NIFE, BioMaterial Engineering, Hannover Medical School, Carl-Neuberg-Str. 1, 30625 Hannover, Germany

<sup>2</sup> Institute for Multiphase Processes (IMP), Leibniz University Hannover, 30823 Garbsen, Germany

<sup>3</sup>Department of Engineering Science, Jade Hochschule, Friedrich Paffrath Str.101, 26389 Wilhelmshaven

**Abstract:** Neurotechnical implants comprise complex microstructured components, where surface functionalisation is critical to ensure robust and biocompatible integration of dissimilar materials. This study investigates a novel surface functionalisation approach based on photoelectron emission and evaluates its performance in comparison to conventional plasma-based treatments.

**Keywords:** Electron Radiation, photo effect, surface functionalization, bacteria disinfection, Peel-Test

## Introduction

Traditional plasma functionalisation methods are limited in selectivity due to the stochastic interaction of electrons and reactive species with target surfaces. In contrast, photoelectron-based excitation enables the emission of low initial kinetic energy electrons from a thin silver layer under UV-LED irradiation, which can subsequently be accelerated to well-defined energies. This controlled energy transfer is expected to facilitate selective modification of chemical bonding states, thereby enhancing interfacial adhesion. Moreover, as free electrons are known to contribute significantly to plasma-induced sterilisation, photoelectrons may also offer a promising route for surface decontamination. [1] Therefore this study compares plasma functionalisation to the novel approach of electron radiation in two aspects: adhesion and sterilizing ability.

## Method

The experimental setup comprises a UV-LED illuminating a thin silver film deposited on quartz glass, inducing photoelectron emission via the photoelectric effect. A bias voltage of 10 V between the silver layer and a metallic anode accelerates the emitted electrons. The entire system is operated under vacuum conditions to maximise electron mean free path and ensure efficient transport to the anode. The resulting photocurrent is recorded to characterise electron emission behaviour. To evaluate sterilization efficacy, bacterial samples deposited on the anode are exposed to a defined electron dose. Survival rates of *Staphylococcus aureus* (Gram-positive) and *Escherichia coli* (Gram-negative) are evaluated across titanium, stainless steel, and tantalum substrates.

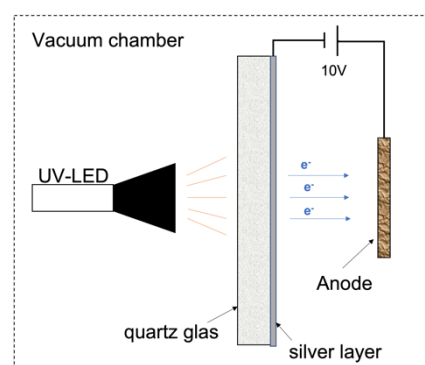


**Figure 1:** Photoelectron-based experimental setup under vacuum conditions.

Adhesion performance is qualified, using a standardized peel test. Adhesive tape is applied to both irradiated and non-irradiated surfaces and removed at constant velocity using a motor-controlled system. The required peel force is measured using a calibrated force sensor to assess changes in interfacial adhesion.

## Outlook

The aim of this proof-of-concept study is to assess the potential of photoelectron irradiation as an alternative method for surface functionalization. Successful results could enable more selective and energy-controlled surface treatment processes in future applications.

## References

- [1] Moisan M, Barbeau J, Moreau S, Pelletier J, Tabrizian M, Yahia LH. Low-temperature sterilization using gas plasmas: a review of the experiments and an analysis of the inactivation mechanisms. *Int J Pharm.* 2001 Sep 11;226(1-2):1-21. doi: 10.1016/s0378-5173(01)00752-9.

## Acknowledgements

Funding by DFG grant No. 527334504 is gratefully acknowledged

# Development of Molecularly Imprinted Polymers as an Indirect Sensing Approach for Spore-Forming Bacteria Detection

A. Guzman-Landero<sup>1</sup>, H. Diliën<sup>1</sup>, B. van Grinsven<sup>1</sup>, R. Arreguin-Campos<sup>1</sup>

[alejandro.guzman@maastrichtuniversity.nl](mailto:alejandro.guzman@maastrichtuniversity.nl)

<sup>1</sup>Maastricht University, Sensor Engineering Department, Duboisdomein 30, 6229GT, Maastricht, The Netherlands

**Abstract:** Molecularly Imprinted Polymers (MIPs) targeting dipicolinic acid (DPA) were developed as an indirect method to detect bacterial endospores. MIPs were synthesized using 3-acrylamidopropyl trimethylammonium chloride as the functional monomer. Rebinding assays and Heat transfer method experiments demonstrated selective binding to DPA in different matrixes. This approach presents a rapid, real-time option for the detection of bacteria endospores in complex environments.

**Keywords:** molecularly imprinted polymers; dipicolinic acid; spore detection; biosensors; food safety

## Introduction

The presence of heat-resistant bacterial spores, such as those from *Bacillus cereus*, poses significant challenges to food safety. Dipicolinic acid (DPA) is a component of bacterial spores, constituting approximately 10 % of their dry weight, and it has been shown to be a key factor in the resistance of spores to wet heat exposure [1-2]. Molecularly Imprinted Polymers (MIPs) offer a stable, easy to prepare selective alternative for detecting small molecules such as DPA [3]. Here, we report the synthesis of MIPs targeting DPA for application in the indirect detection of spore-forming bacteria.

## Results and Discussion

MIPs were prepared using 3-acrylamidopropyl trimethylammonium chloride, ethylene glycol dimethacrylate (EGDMA) as crosslinker, and AIBN as initiator in a DMSO/MeOH system at 60°C. The functional monomer was selected for its permanent positive charge, enhancing electrostatic interactions with the target molecule. Triethylamine (TEA) was added to facilitate deprotonation of DPA during polymerization. Soxhlet extraction using MeOH:AcOH (1:1) and acid washes were used to remove the residual template and base. The binding capacity was evaluated via Rebinding assays (UV-Vis) and Heat transfer method (HTM) experiments in aqueous and diary based DPA solutions. In HTM analysis, MIPs showed higher responses to DPA than NIPs: 0.38% vs 0.23% using a diary DPA 300 nM solution and 0.30% vs 0.13% using an aqueous DPA 450 nM solution (n=3). UV-Vis analysis showed an imprinting factor of 2.60. This approach could contribute to the development of rapid biosensors for detecting heat-resistant bacterial spores in liquid foods, offering potential improvements in food safety monitoring.

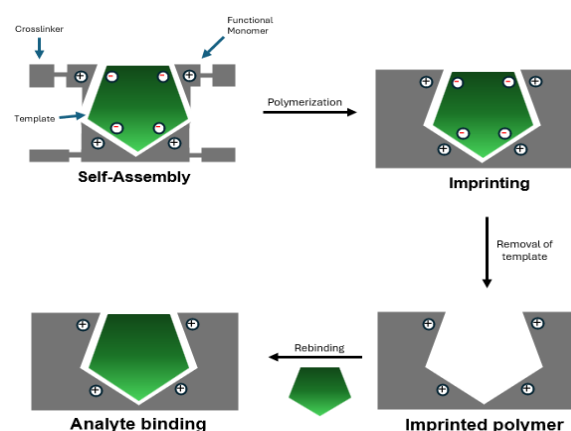


**Figure 1:** Schematic representation of MIP synthesis and DPA rebinding.

## Conclusions

The developed MIPs show promising selectivity toward DPA, indicating their potential for indirect detection of bacterial spores in food matrices. These polymers could form the basis of fast, resource-efficient sensors for early contamination detection, aligning with the objectives of the SenSpores initiative.

## References

- [1] Y. Lai, G. Jiang, T. Liang, X. Huang, W. Jiang, W. Xu, R. Sun, Z. Dai, C. Li, *Anal. Chim. Acta* 1320 (2024) 343034.
- [2] J. Jamroskovic, Z. Chromikova, C. List, B. Bartova, I. Barak, R. Bernier-Latmani, *Front. Microbiol.* 7 (2016) 1791, doi: 10.3389/fmicb.2016.01791.
- [3] K. Eersels, P. Lieberzeit, P. Wagner, *ACS Sens.* 1 (2016) 1171-1187

## Acknowledgements

The authors gratefully acknowledge funding and support from the SenSpores project, the Niederrhein University of Applied Sciences, Maastricht University, Ruhr University Bochum, and industrial partners in the food technology sector.

# Modular Raman Image Analysis of Calcium-Crosslinked Alginate Hydrogels

David Schäffl<sup>1</sup>, Sabine Hild<sup>1</sup>

david.schaeffl@jku.at

<sup>1</sup>Institute for Polymer Science, Johannes Kepler University Linz, Altenberger Straße 69, 4040 Linz, Austria

## Abstract

Hydrogels are soft, water-rich polymer networks used in sensors, electrodes and implant-related materials. Their function can depend on local differences in water content, polymer concentration and inorganic components. This work shows a complete Raman image-analysis workflow for a defined alginate hydrogel series. Alginate concentration is varied and the gels are crosslinked by calcium ions released from calcium carbonate. The samples are measured by Raman microscopy and analysed in Python. The workflow follows Figure 1: hydrogel preparation, Raman measurement, hyperspectral data generation, preprocessing, chemical mapping and plotting of extracted data. The outputs are directly measurable Raman-based maps and plots of alginate-related, water-related and carbonate-related signals. The aim is not to derive a full network model from Raman data alone, but to provide a reproducible route to compare hydrogel formulations and describe chemical heterogeneity.

**Keywords:** Raman imaging; alginate hydrogels; hyperspectral analysis; calcium crosslinking; Python; chemical mapping

## Introduction

Hydrogel interfaces are relevant where hydrated soft materials contact electrodes, sensors, liquids or biological tissue. In such systems, local composition can be more important than the average formulation. Raman microscopy can detect chemical differences without additional labelling, but a Raman image is a hyperspectral dataset: every pixel contains a full spectrum. Therefore, reproducible data processing is required. Here, calcium-crosslinked alginate hydrogels are used as a controlled sample series. The alginate concentration is varied to change the polymer content, while calcium carbonate acts as the internal calcium source for crosslinking. This series is used to test whether different formulations can be measured, processed and compared by the same Raman workflow.

## Results and Discussion

The Python workflow imports Raman image data, displays spectra and maps, removes cosmic rays, corrects background signals, normalizes spectra and generates chemical maps. Selected Raman bands are used for direct mapping, while dimensionality-reduction methods such as principal component analysis or non-negative matrix factorization can be used to explore major spectral differences. Figure 1 summarizes this route from sample preparation to extracted maps and plots.

For the alginate concentration series, the workflow compares measurable Raman signals between formulations. The main outputs are maps of alginate-related spectral regions, water-associated contributions and carbonate-related bands, together with extracted intensity plots or histograms. These outputs show the spatial distribution and heterogeneity of the measured signals. They are interpreted as Raman-based chemical descriptors. Further conclusions about crosslink density, mechanics or network structure require additional measurements such as rheology or swelling experiments.

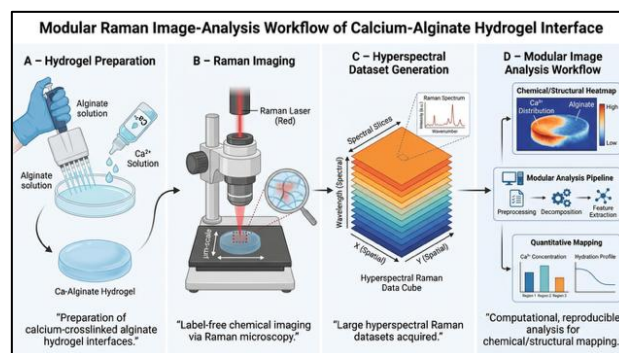


**Figure 1:** Workflow from hydrogel preparation to Raman-based data evaluation. Alginate hydrogels with different polymer concentrations and calcium-carbonate-based crosslinking are prepared, measured by Raman microscopy, processed in Python and converted into chemical maps and extracted intensity plots.

## Conclusions

A modular Python workflow is used to analyse Raman images of calcium-crosslinked alginate hydrogels prepared as a concentration series. The work demonstrates the complete route from hydrogel preparation and Raman measurement to preprocessing, chemical mapping and extracted data plots. This provides a reproducible basis for comparing hydrogel formulations and for future studies of hydrogel heterogeneity and interfaces.

## References

- [1] Jang, J., Seol, Y. J., Kim, H. J., Kundu, J., Kim, S. W., & Cho, D. W. (2014). Effects of alginate hydrogel crosslinking density on mechanical and biological behaviors for tissue engineering. *J. Mech. Behav. Biomed. Mater.*, 37, 69-77.

## Acknowledgements

The author gratefully acknowledges support from the Institute for Polymer Science, Johannes Kepler University Linz.

# PEDOT:PDA as a promising new polymer for the development of MIPs in electrochemical sensors

Martin Wolfgang Konrad<sup>1</sup>, Patrick Wagner<sup>1</sup>, Irene Taurino<sup>2,3</sup>

[martinwolfgang.konrad@kuleuven.be](mailto:martinwolfgang.konrad@kuleuven.be)

<sup>1</sup> Soft Matter and Biophysics, Department of Physics and Astronomy, KU Leuven, 3001 Leuven, Belgium

<sup>2</sup>Micro and Nano Systems (MNS), Department of Electrical Engineering, KU Leuven, 3001 Leuven, Belgium

<sup>3</sup>Semiconductor Physics, Department of Physics and Astronomy, KU Leuven, 3001 Leuven, Belgium

**Abstract:** Molecularly imprinted polymers (MIPs) are a promising class of recognition elements in electrochemical sensors, and novel polymers that offer selectivity, sensitivity and robustness are always in demand. Poly(3,4-ethylenedioxythiophene):polydopamine (PEDOT:PDA) is a conductive polymer that gathered increasing attention recently and promises to enable robust and sensitive MIP design. We report a study on the use of PEDOT:PDA for MIP development to sense hydroxylated polycyclic aromatic hydrocarbons.

**Keywords:** conductive polymer; molecularly imprinted polymers; electrochemistry; PEDOT:PDA

## Introduction

With electrochemical sensors becoming increasingly prevalent for a plethora of different applications, there is a constant demand for novel materials that overcome the obstacles of contemporary technologies. Conductive polymers such as polypyrrole or Poly(3,4-ethylenedioxythiophene) (PEDOT) are integral for use in electrochemical sensors that employ molecularly imprinted polymers (MIPs) as recognition elements [1,2]. Their utilization in MIPs does pose some challenges. Successful polymerization in presence of the imprinting template must not alter the imprinting template; the resulting polymer film must adhere well to the electrode surface, and needs to be stable and conductive in the extraction medium as well as the sample medium. These issues prompted the integration of additional functional monomers for better stability in aquatic media, higher conductivity, and easier polymerization. Recently, the incorporation of polydopamine (PDA) into conductive polymers for improved adhesion and gentler polymerization conditions garnered increased attention for different applications, with PEDOT:PDA in particular showing great promise for use in electrochemical sensors [3-5]. Based on this, we conducted a study to assess the possibility to use PEDOT:PDA in MIPs for electrochemically sensing metabolites of carcinogenic polycyclic aromatic hydrocarbons (PAHs), like hydroxypyrene.

## Results and Discussion

PEDOT:PDA copolymers have been prepared using radical polymerization with ammonium persulfate (APS) as radical starter. The polymerization procedure is depicted in **Figure 1**. The impact of multiple parameters has been studied. This includes the addition of a surfactant for improved miscibility of EDOT and DA, voltage-assisted polymerization, imprinting template concentration, resistance to common extraction media, and reproducibility of the formed polymer film.

## Conclusions

Preliminary results indicate that PEDOT:PDA-based MIPs can be used in an electrochemical sensor for sensing PAH metabolites.

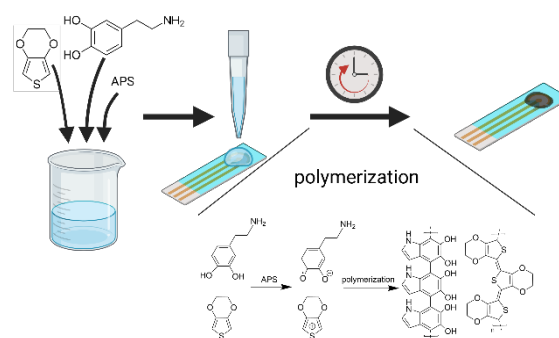


**Figure 1:** Polymerization scheme of PEDOT:PDA.

## References

- [1] G. Wackers *et al.* Electropolymerized Receptor Coatings for the Quantitative Detection of Histamine with a Catheter-Based, Diagnostic Sensor. *ACS Sensors* **6**, 2021.
- [2] A. Hammoud *et al.* A new molecular imprinted PEDOT glassy carbon electrode for carbamazepine detection. *Biosens. Bioelectron.* **180**, 2021.
- [3] Y. He *et al.* Mechanism of Self-Oxidative Copolymerization and its Application with Polydopamine-pyrrole Nano-copolymers. *Small Methods* **8**, 2024.
- [4] Y. Zhou *et al.* Polydopamine-PEDOT-based portable molecularly imprinted sensor for simultaneous ultrasensitive determination of chlorpromazine and norfloxacin. *Chem. Eng. J.* **521**, 2025.
- [5] S. Saghir *et al.* Electropolymerised PEDOT: Polydopamine enables high-performance bioelectrode coatings. *Sci. Rep.* **15**, 2025.

## Acknowledgements

Funding from the Industrial Research Funds (IOF) of KU Leuven (grant C3/23/022) and the Flemish Research Organization (FWO) (Ph.D. fellowship 1S81626N) is gratefully acknowledged.

# Enhanced corrosion stability of Scandium-rich Magnesium alloy thin films in simulated body fluid

Hüseyin Zengin<sup>1\*</sup>, Andrei Ionut Mardare<sup>1,2</sup>, Gianina Popescu-Pelin<sup>2</sup>, Gabriel Socol<sup>2</sup>, Achim Walter Hassel<sup>1,3</sup>

[hueseyin.zengin@jku.at](mailto:hueseyin.zengin@jku.at)

<sup>1</sup>Institute of Chemical Technology of Inorganic Materials (TIM), Johannes Kepler University Linz, Altenberger Str. 69, 4040, Linz, Austria

<sup>2</sup>Lasers Department, National Institute for Lasers, Plasma and Radiation Physics, 077125 Magurele, Romania

<sup>3</sup>Danube Private University, Steiner Landstraße 124, 3500 Krems an der Donau, Austria

**Abstract:** Magnesium (Mg)-Scandium (Sc) thin film library was produced by thermal evaporation technique focusing a compositional spread of Sc up to 20 at.%. The results demonstrated that microstructures primarily consisted of hexagonal facets corresponding to (0002) basal planes. The wall size of these facets showed a significant alteration with increasing Sc concentrations. tests showed that increasing Sc content up to specific composition shifted corrosion potential of Mg toward positive direction and improved the corrosion resistance of Mg. Sc led to the improvement on the protectiveness of the surface layer formed during their exposure to the electrolyte, particularly in SBF.

**Keywords:** magnesium alloys; scandium; scanning droplet cell; microstructure; nanoindentation; corrosion

## Introduction

Mg possess an outstanding biocompatibility and biodegradability, dissolving completely in the human body following the completion of healing process, which eliminates the additional surgical operations for the implant removal. Nevertheless, the widespread use of Mg alloys is severely restricted primarily due to its rapid degradation rate. To mitigate the poor corrosion resistance, rare earth element (RE) additions have been proven to be an effective way [1]. Therefore, in this work, Sc, known as one of the most biocompatible RE, has been employed in Mg at wide compositions range as thin film library.

## Results and Discussion

The SEM microstructures of thin film alloys shows that at low Sc concentrations, the microstructures consist of grains that are generally non-coaxial and lack a specific geometry. As the Sc increases, the facets became more equiaxed and refined. This was also coupled with smoother surface characteristics based on the AFM test results.

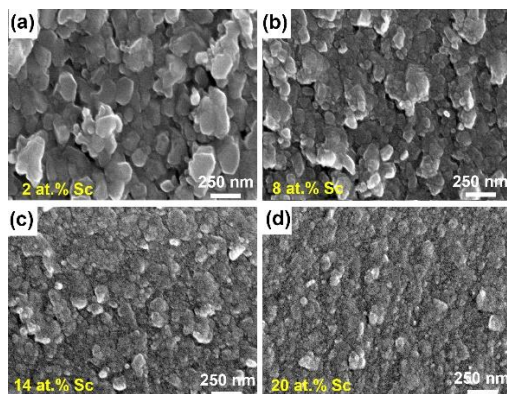


Figure 1: SEM images of Mg-Sc thin film alloys

The Tafel plots shows that the potentials had a tendency to shift to more positive values with increasing Sc content. The sudden drops in the anodic branch of the several samples were due to the depletion of films. At low Sc content, alloys show higher corrosion rates in SBF compared to NaCl whereas higher Sc results in superior corrosion performance in SBF. This is due to the interaction of Sc with complex ions in SBF, forming a much more protective layer of corrosion products on the surfaces.

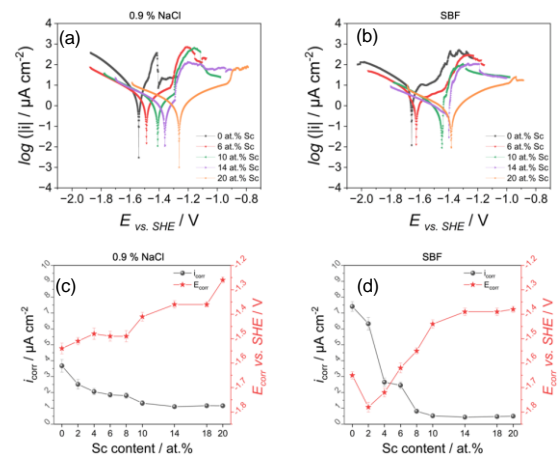


Figure 2: Potentiodynamic polarization test results

## Conclusions

Mg-Sc thin film library revealed a composition-dependent changes in structure and electrolyte-dependent changes in corrosion resistance.

## References

[1] H. Zengin, A.W. Hassel, Corros. Sci. 249 (2025) 112827.

# Studying of Organic Semiconductors in Light-Addressable Potentiometric Sensors (LAPS)

S. Kimoto<sup>1</sup>, Y. Hemmi<sup>2</sup>, A. Ichikawa<sup>2</sup>, H. Matsui<sup>2</sup>, Y. Guo<sup>3</sup>, F. Hirose<sup>4</sup>, C. F. Werner<sup>1</sup>

[werner@kit.ac.jp](mailto:werner@kit.ac.jp), [m25621025@edu.kit.ac.jp](mailto:m25621025@edu.kit.ac.jp)

<sup>1</sup>Electronics, Kyoto Institute of Technology, Kyoto, 606-8585, Japan,

<sup>2</sup>ROEL, Yamagata U., Yonezawa, 992-8510, Japan,

<sup>3</sup>FRIS, Tohoku U., Miyagi, 980-8578, Japan

<sup>4</sup>Graduate School of Science and Engineering, Yamagata U., Yonezawa 992-8510, Japan,

**Abstract:** LAPS is a chemical imaging sensor that utilizes the field effect of semiconductors and can measure local analyte concentrations at specific locations on the sensor surface. While conventional LAPS primarily used inorganic semiconductors such as silicon, these materials are hard and brittle, posing challenges regarding biocompatibility. Organic semiconductors, on the other hand, are flexible materials that conform well to curved surfaces and exhibit high biocompatibility. In this study, we demonstrate for the first time the successful pH responsiveness of an organic LAPS based on PCE12:N2200:SEBS with an Al<sub>2</sub>O<sub>3</sub> pH-sensitive layer.

**Keywords:** Light-addressable potentiometric sensor; ion-sensing; Organic semiconductors;

## Introduction

LAPS is a chemical imaging sensor that utilizes the field effect of semiconductors. It features an electrolyte-insulator-semiconductor (EIS) structure, like that of an ISFET. Compared to similar sensors, LAPS offers the advantage of being able to define the measurement area using light, eliminating the need to integrate microscopic sensor elements and enabling simple, low-cost manufacturing [1]. Traditionally, inorganic semiconductors have been the mainstream choice for LAPS; however, inorganic semiconductors are rigid and present challenges regarding biocompatibility. In contrast, organic semiconductors are flexible, can conform to the curved surfaces of the body, and offer high biocompatibility. They also have the advantage of being manufacturable at standard atmosphere pressure and temperature.

## Results and Discussion

In this study, PCE12:N2200:SEBS was used for the organic semiconductor layer of the sensor, PEDOT:PSS for the transparent electrode, and parylene and Al<sub>2</sub>O<sub>3</sub> for the insulator. Figure 1 shows its structure. For characterization, a self developed real-time LAPS system was used and optimized by selecting a light source (a blue LED with a wavelength of 470 nm) matched to the absorption band of the organic semiconductor and adjusting the bias voltage range to one suitable for organic materials. The photocurrent-voltage (I-V) characteristics were measured using Titrisol (Merck) buffers (pH 5, 7, 9). A shift in the I-V curve was observed when the pH level changed. Figure 2 shows the I-V curve, confirming the pH responsiveness of the OLAPS.

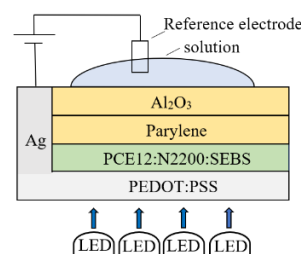


**Figure 1:** Structure of the organic LAPS

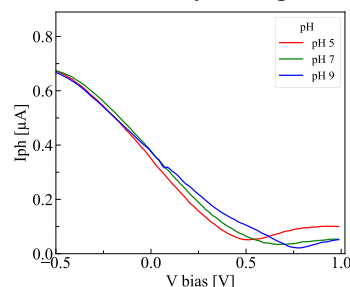


**Figure 2:** I-V curves at different pH levels (LED modulated frequency 1kHz, wavelength 470 nm)

## Conclusions

Using the modified real-time LAPS system, I-V curves were recorded and pH responsiveness was demonstrated with the organic semiconductor. Going forward, we aim to achieve two-dimensional imaging of multiple analytes through surface modification of the sensor.

## References

- [1] M.J. Schöning, T. Wagner, A. Poghossian, K. Miyamoto, C.F. Werner, S. Krause, T. Yoshinobu, Encyclopedia of Interfacial Chemistry, 295-308 (2018), doi:10.1016/B978-0-12-409547-2.13483-3

## Acknowledgements

Part of this research was supported by Grant-in-Aid for Scientific Research (JP24K21336)

# PECVD Preparation of Silicon Carbide Layers as passivating contacts for POLO Solar Cells

Börnert, Steffen<sup>1</sup>, Wunsch, Frank<sup>1</sup>, Peibst, Robby<sup>1,2</sup>, Kähler, Jan-Dirk<sup>3</sup>, Pernau, Thomas<sup>3</sup>, Krügener, Jan<sup>1</sup>

<sup>1</sup>boernert@mbe.uni-hannover.de

<sup>1</sup>Institute of Electronic Materials and Devices, Leibniz University Hannover, Schneiderberg 32, 30167 Hannover, Germany

<sup>2</sup>Institute for Solar Energy Research in Hamelin (ISFH), Am Ohrberg 1, 31860 Emmerthal, Germany

<sup>3</sup>centrotherm international AG, Württemberger Straße 31, 89143 Blaubeuren, Germany

**Abstract:** In this work, a PECVD process for quasi-stoichiometric SiC thin films is established and systematically optimized for use as transparent passivating contacts in polycrystalline silicon on oxide (POLO) solar cells. XPS and Raman measurements confirm an amorphous Si–C network with a near 1:1 Si:C ratio, despite residual oxygen and nitrogen incorporation. Although this work focuses exclusively on photovoltaic applications, the established PECVD deposition process could potentially also serve as a basis for coating in vivo implants, where SiC's chemical inertness and biocompatibility may be of interest [1].

**Keywords:** silicon carbide; PECVD; passivating contacts; thin films; doping; stoichiometry

## Introduction

The primary objective of this work is the establishment of a reproducible PECVD process for thin SiC layers as transparent passivating contacts in POLO-type silicon solar cells. Process parameters are systematically varied to control film stoichiometry, bonding configuration, and impurity incorporation, with emphasis on achieving a near-stoichiometric Si–C network while suppressing phase separation. Structural and chemical characterization by spectroscopic ellipsometry, XPS, and Raman spectroscopy is performed to correlate deposition conditions with material properties. The overarching goal is to define a robust PECVD process window suitable for integration into industrial solar cell architectures.

## Results and Discussion

SiC thin films with a target thickness of approximately 100 nm were deposited by PECVD in a Centrotherm E2000 horizontal furnace using silane (SiH<sub>4</sub>) and acetylene (C<sub>2</sub>H<sub>2</sub>) as reactive precursors and nitrogen as dilution gas. Depositions were carried out on 156 mm pseudo-square crystalline silicon wafers. The influence of key process parameters, including plasma duty cycle and precursor-to-diluent flow ratio, was systematically investigated. By increasing the off-time relative to the on-time, the growth rate decreases from values above 40 nm/min to below 10 nm/min, enabling controlled deposition in the targeted thickness regime as confirmed by spectroscopic ellipsometry.

The Raman spectrum shows no bands in the range of 1300–1600 cm<sup>-1</sup> and no amorphous silicon band at ~480 cm<sup>-1</sup>, indicating the absence of segregated carbon or silicon phases. The combined XPS and Raman results are consistent with the formation of an amorphous Si–C network

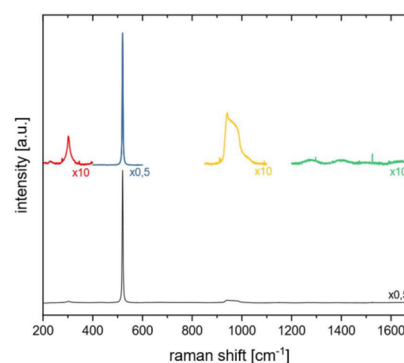


**Figure 1:** Background-corrected Raman spectrum of SiC with magnified views

## Conclusions

A reproducible PECVD process for quasi-stoichiometric amorphous SiC thin films has been established and systematically characterized using a Centrotherm E2000 industrial platform. The resulting amorphous Si–C network provides a solid foundation for further investigation of annealing-induced ordering and passivation performance in POLO-type solar cells. Planned QSSPC measurements will allow correlation of material properties with electrical passivation quality.

## References

- [1] Saddow S. Silicon Carbide Technology for Advanced Human Healthcare Applications. *Micromachines*. 22. Februar 2022;13(3):346. doi:10.3390/mi13030346
- [2] Wang YH, Lin J, Huan CHA. Multiphase structure of hydrogenated amorphous silicon carbide thin films. *Materials Science and Engineering: B*. Juli 2002;95(1):43–50. doi:10.1016/S0921-5107(02)00204-0

## Acknowledgements

We would like to thank the BMWF for funding support.

# Ultrasensitive Electrochemical Detection of Penicillin G Using Electroactive Molecularly Imprinted Polymers for Sepsis Monitoring

Pankaj Singla<sup>1</sup>, Saweta Garg<sup>1</sup>, Timothy Felton<sup>2,3</sup>, Marloes Peeters<sup>1\*</sup>  
[pankaj.singla@manchester.ac.uk](mailto:pankaj.singla@manchester.ac.uk)

<sup>1</sup> Department of Chemical Engineering, Engineering building A, East Booth Street, The University of Manchester, Oxford Road, M13 9PL

<sup>2</sup> Division of Immunology, Immunity to Infection and Respiratory Medicine, School of Biological Sciences, Manchester Academic Health Sciences Centre, University of Manchester, Manchester, Greater Manchester, M1 7DN, UK

<sup>3</sup> Wythenshawe Hospital, Manchester University NHS Foundation Trust, Manchester, Greater Manchester, M23 9LT, UK

**Abstract:** Sepsis is a life-threatening medical emergency requiring rapid and accurate antibiotic treatment, yet antibiotic exposure varies widely between patients.<sup>1</sup> Here, we report a cost-effective electrochemical sensing platform based on electroactive molecularly imprinted polymers (eMIPs) for ultrasensitive detection of penicillin G. Penicillin-specific eMIPs were synthesised and immobilised on graphene electrodes, enabling selective, antibody-free molecular recognition. The sensor achieved a wide detection range (10 fg–10 µg) with a low detection limit of 7.4 fg and excellent selectivity. Reliable performance in penicillin-spiked serum highlights strong potential for rapid point-of-care therapeutic drug monitoring at the bedside.

**Keywords:** Sepsis; Penicillin G; Molecularly imprinted polymers; Graphene electrodes; Electrochemical sensing

## Introduction

Timely and optimised antibiotic therapy is critical in sepsis management, yet real time monitoring of drug concentrations remains challenging in clinical settings.<sup>1</sup> Penicillin G is widely prescribed, but conventional analytical techniques are laboratory intensive and incompatible with rapid decision making. Molecularly imprinted polymers provide a stable, low-cost alternative to biological receptors.<sup>2</sup> Here, we report an eMIP based electrochemical sensor integrated with graphene electrodes for sensitive and selective detection of penicillin G in clinically relevant matrices.

## Results and Discussion

Penicillin-specific eMIPs were synthesised separately and immobilised onto graphene-modified electrodes, providing a conductive and high-surface-area sensing interface. Electrochemical measurements revealed a broad linear response from 10 fg to 10 µg, with a detection limit of 7.4 fg in phosphate-buffered saline. The eMIP sensor demonstrated excellent selectivity, exhibiting negligible interference from structurally related β-lactam antibiotics, while non-imprinted controls showed minimal responses (<5%). Importantly, comparable electrochemical signals were obtained in penicillin G-spiked serum samples, confirming robust performance in complex biological environments relevant to sepsis monitoring.

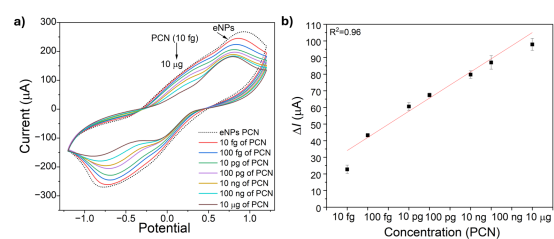


Figure 1: Cyclic voltammetric characterisation of the eNPs-based sensor showing penicillin G-dependent attenuation of the oxidation peak and a linear analytical calibration ( $R^2 = 0.96$ ).

## Conclusions

The eMIP–graphene electrochemical sensor enables highly sensitive and selective detection of penicillin G in serum, offering a robust and antibody free platform for point of care therapeutic drug monitoring in sepsis. The adaptable sensing strategy is readily extendable to other clinically important.

## References

- Huang *et al.*, Postgrad Med J, 2023, 99, 1000–1007.
- Garg *et al.*, Small, 2024, e2403320

## Acknowledgements

This work was supported by the Translation Manchester Accelerator Awards, Confidence for Translation (C4T, 2025/26), as part of the TRIAD project – *Transforming Critical Care through Rapid, Innovative Antibiotic Next-Generation Diagnostics*.

# Superparamagnetic Iron Oxide Nanoparticles in Niosomal Systems for Biomedical Applications

Sandhya Kumar<sup>1</sup>, Viktor Maurer<sup>1</sup>, Georg Garnweitner<sup>1</sup>

sandhya.kumar@tu-braunschweig.de

<sup>1</sup>Institute for Particle Technology, Technische Universität Braunschweig, Germany

**Abstract:** Superparamagnetic iron oxide nanoparticles (SPIONs) exhibit rapid and reversible magnetization, making them relevant for biomedical applications. In this study, SPION-loaded niosomes were synthesized and characterized in terms of particle size, stability, and magnetic behavior. Co-encapsulation of SPIONs with siRNA within niosomal carriers was investigated to evaluate multifunctional delivery potential. The hybrid system is considered for potential application in Magnetic Particle Imaging (MPI) to study nanoparticle biodistribution.

**Keywords:** superparamagnetic nanoparticles; niosomes; magnetic particle imaging; RNA delivery; theranostics.

## Introduction

Multifunctional nanocarriers that integrate therapeutic and imaging capabilities are increasingly important in the development of advanced nanomedicine systems [1]. In this context, niosome-based hybrid nanocarriers offer a versatile platform for combining delivery and diagnostic functions within a single system. Niosomes, composed of non-ionic surfactants, provide a biocompatible vesicular structure capable of encapsulating both hydrophilic and hydrophobic components. The incorporation of SPIONs introduces magnetic responsiveness, enabling controlled delivery and potential imaging applications such as MPI. Integration of nucleic acids further supports their application in gene-based therapeutic strategies. In this study, SPION-loaded niosomes were developed and evaluated for their physicochemical properties and their performance in siRNA-based gene delivery systems.

## Results and Discussion

SPIONs synthesized via thermal decomposition with hydrophobic surface characteristics (Fig. 1A,B) were successfully incorporated into the lipid bilayer of niosomal carriers. The hydrophobic SPIONs showed good compatibility with the membrane, maintaining structural integrity and stability of the niosomes [2]. The resulting hybrid systems efficiently co-encapsulated siRNA and enabled effective cellular uptake in MCF-7 breast cancer cells. Gene silencing studies demonstrated significant downregulation of anti-apoptotic proteins, leading to enhanced apoptotic activity. The application of an external magnetic field further improved intracellular delivery efficiency and amplified the therapeutic response compared to non-magnetic conditions (Fig. 1C). These findings confirm that hydrophobic SPIONs can be integrated into vesicular membranes without compromising functionality, while providing magnetic responsiveness for controlled delivery. Moreover,

the retained magnetic properties suggest potential for future imaging applications, including MPI for tracking nanoparticle biodistribution.

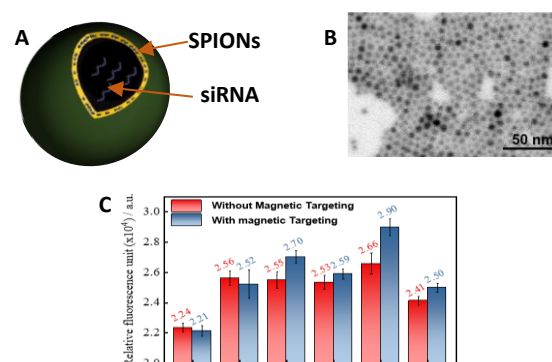


**Figure 1:** A) Schematic illustration of hybrid niosomes; B) hydrophobic SPIONs (<10 nm); C) *in vitro* evaluation of hybrid niosomes.

## Conclusions

This study demonstrates that SPION-loaded niosomes form stable and efficient multifunctional platforms, combining favorable physicochemical properties with retained magnetic functionality while preserving RNA integrity. The system enables enhanced gene delivery under magnetic guidance. Overall, these results underline the potential of SPION-based hybrid carriers for future theranostic applications.

## References

1. Pankhurst, Q. A. et al. Applications of magnetic nanoparticles in biomedicine. *Journal of Physics D: Applied Physics*, 36, R167, (2003).
2. Maurer, V. et al. All-in-one superparamagnetic and SERS-active niosomes for dual-targeted *in vitro* detection of breast cancer cells. *Sensors & Diagnostics*, 1, 469–484, (2022).

## Acknowledgements

This work was supported by the Ministry of Science and Culture of Lower Saxony within the RNApp project funded via Zukunft.Niedersachsen.

# ML-based porous metamaterials design for hip implant stability

B. Ayouch<sup>1</sup>, M. Haertlé<sup>2</sup>, F. Aldakheel<sup>1</sup>

fadi.aldakheel@ibnm.uni-hannover.de

<sup>1</sup>Leibniz Universität Hannover, Institute of Mechanics and Computational Mechanics, Hannover, Germany;

<sup>2</sup>Hannover Medical School, Orthopedic clinic, Hannover, Germany

**Abstract:** Despite major advances in biomaterial compatibility, medical implants still exhibit failure rates that remain high compared to technical systems, largely due to limited understanding of biophysical integration processes, such as bone growth and implant stability. While high-fidelity computational models can provide valuable insights, their computational complexity and cost hinder patient-specific analyses and limit clinical adoption. This contribution presents a machine learning-based inverse design framework for porous metamaterials targeting hip implant stability and bone growth. By combining finite element simulations with real clinical data, surrogate models are developed to efficiently relate microstructural features to effective mechanical and transport properties. In particular, a deep generative diffusion model is developed to enable the inverse design of microstructures with target properties, thereby supporting scalable, patient-specific implant design and clinical decision-making.

**Keywords:** Hip implants, Inverse Design, Machine learning, Implant stability, Porous Metamaterials

## Introduction

The design of hip implants should be tailored to each individual patient, as anatomical structures and biomechanical characteristics vary from person to person. The main goal is to improve implant stability while promoting bone growth and osseointegration. This work focuses on the deep learning-based inverse design of unit cells, which serve as the fundamental building blocks of porous hip implants. Different microstructural designs lead to different mechanical behaviours at the macroscale, enabling the optimization of implant performance for patient-specific applications. Fig. (1) illustrates an example for a hip implant and its microstructure.

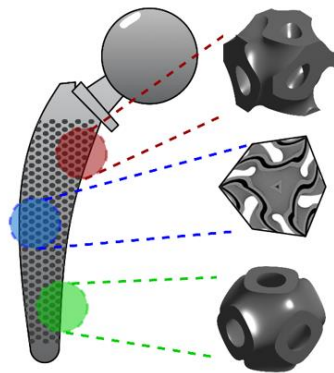


Figure 1: Hip implant and its microstructure in different regions.

## Results and Discussion

A trained diffusion model conditioned on mechanical and hydraulic properties demonstrated a strong ability to generate microstructures with properties closer to the target values. These results are validated by running simulations to evaluate both mechanical and hydraulic properties. One might ask why not simply search the dataset for microstructures with properties closest to the target values. This approach was also tested, but the model is able to explore the design space more effectively

and learn complex mappings. As a result, it generates novel microstructures that are closer to the target properties than those available in the dataset.

The target properties are the principal permeabilities and the normal components of the stiffness tensor with following values:

$$K_{11}^s = 9 \text{ lu}, K_{22}^s = 4.5 \text{ lu}, K_{33}^s = 5.7 \text{ lu}, C_{11} = 16.5 \text{ GPa}, C_{22} = 21 \text{ GPa}, C_{33} = 26 \text{ GPa}$$

Fig. (2) shows the results using the Mean Relative Error (MRE). The blue entries represent the results from the inverse design method, while the grey entries correspond to the closest properties of microstructures in the dataset to the target properties.

$K_{11}^s$ (lu)	$K_{22}^s$ (lu)	$K_{33}^s$ (lu)	$C_{11}$ (GPa)	$C_{22}$ (GPa)	$C_{33}$ (GPa)	MRE (%)
9.17	4.78	5.56	16.56	21.53	26.71	2.61
8.95	4.86	5.36	15	20.5	26.1	4.52
9.09	4.63	6.13	19.62	19.84	25.51	6.32
8.31	4.21	5.94	13.91	21.34	28.17	7.32

Figure 2: Results of the inverse design, compared with microstructures with closest properties to target properties.

## Conclusions

To conclude, the diffusion model-based inverse design approach demonstrates strong generative capabilities at the microstructure level, paving the way for tailored hip implant design. Future research will focus on inverse design at the macroscale and the integration of physics-informed neural networks to achieve improved results.

## References

P. Nguyen, Y. Heider, D. Kochmann, and F. Aldakheel, "Deep learning-aided inverse design of porous metamaterials," *Comput. Methods Appl. Mech. Engrg.* 449 (2026) 118499.

## Acknowledgements

Fadi Aldakheel gratefully acknowledges support for this research by "German Research Foundation" (DFG) through the SFB/TRR-298-SIIRI – Project-ID 426335750

# Influence of various oxygen levels on tissue-biofilm interaction in an implant-tissue-oral-bacterial-biofilm model

Yue Sun<sup>1,2</sup>, Guntram A. Grassl<sup>3</sup>, Marita Meurer<sup>4</sup>, Maren von Köckritz-Blickwede<sup>4</sup>, Andreas Winkel<sup>1,2</sup>, Carina Mikolai<sup>1,2#</sup>, Meike Stiesch<sup>1,2#</sup>

[Sun.Yue@mh-hannover.de](mailto:Sun.Yue@mh-hannover.de)

1 Department of Prosthetic Dentistry and Biomedical Materials Science, Hannover Medical School, Germany

2 Lower Saxony Centre for Biomedical Engineering, Implant Research and Development (NIFE), Hannover, Germany

3 Institute for Medical Microbiology and Hospital Epidemiology, Hannover Medical School, and German Center for Infection Research (DZIF) partner site Hannover-Braunschweig, Germany

4 Institute of Biochemistry, and Research Center for Emerging Infections and Zoonoses (RIZ), University of Veterinary Medicine Hannover, Germany

# These authors contributed equally to this work

**Abstract:** Biofilm-induced peri-implant infections are associated with hypoxia, yet most *in vitro* models ignore clinically relevant oxygen conditions. This study applied normoxic (21% O<sub>2</sub>) and hypoxic (1% O<sub>2</sub>) conditions to the 3D INTER<sub>b</sub>ACT model to investigate the effect of different oxygen levels on tissue–biofilm interactions. While biofilm volume and viability remained unchanged, metabolic activity increased under normoxia. Oxygen levels decreased significantly within tissues, reaching 2% (normoxia) and 0.1% (hypoxia). Hypoxia moderately impaired tissue integrity, and biofilm presence elevated tissue damage. These findings demonstrate that *in vitro* oxygen gradients can affect biofilm and tissue responses in different ways.

**Keywords:** micro physiological system; biofilm; hypoxia; oxygen sensor

## Introduction

Peri-implant infections caused by bacterial biofilms remain a major clinical issue, often accompanied by reduced oxygen availability in peri-implant pocket and surrounding oral mucosa. However, current *in vitro* models largely neglect physiologically relevant (hypoxic) oxygen conditions. To better simulate *in vivo* environments and the subsequent effects for host-biofilm interactions, this study applies, for the first time, reduced oxygen conditions to the existing *in vitro* 3D INTER<sub>b</sub>ACT system [1].

## Results and Discussion

The 3D models were divided in four groups, cultivated with or without a 4-species biofilm for 24 hours under normoxic (21% O<sub>2</sub>) and hypoxic (1% O<sub>2</sub>) conditions. Oxygen levels were measured using PreSens sensors. After co-culture, biofilms were analyzed using LIVE/DEAD staining and resazurin assay. Additionally, tissue morphology and cytokine expression of the tissue were investigated.

Biofilm volume and viability were not significantly affected by oxygen levels, although metabolic activity was higher under normoxia, possibly reflecting adaptive stress responses. Oxygen concentrations decreased substantially over time within both the culture medium and tissue, indicating active consumption. Intra-tissue oxygen dropped as far as 2% under normoxic conditions

without biofilm, in other groups it dropped rapidly towards 0.1%. Hypoxia alone slightly reduced tissue stability, while combined biofilm infection further increased tissue damage, highlighting a synergistic effect.

## Conclusions

These findings demonstrate that oxygen consumption of the tissue for metabolism and functionality can be simulated in an artificial 3D *in vitro* model. Although still in early development, this 3D model hold strong potential to overcome challenges in simulating complex human tissues and organs for clinical research. In the end, this might replace and reduce animal experiments in the investigation of biofilm-associated infections.

## References

- [1] Mikolai, C., Kommerein, N., Ingendoh-Tsakmakidis, A., Winkel, A., Falk, C. S., & Stiesch, M. (2020). Early host–microbe interaction in a peri-implant oral mucosa-biofilm model. *Cellular Microbiology*, 22(8). doi: 10.1111/cmi.13209

## Acknowledgements

This project belongs to the initiative “Replace and Reduce from Lower Saxony – Micro Replace Systems” (R2N-MRS, ID code ZN 4092), which is funded by the Lower Saxony Ministry for Science and Culture (MWK)

# Investigation of TiN<sub>x</sub> Thin film Deposited by Ion Beam Deposition and Sputtering for electronic and bioelectronic applications

Van Hao Vu<sup>1</sup>, Jochen Heiss<sup>1</sup>, Dibyendu Khan<sup>1</sup>, Vivek Pachauri<sup>1</sup>, Sven Ingebrandt<sup>1</sup>, Xuan Thang Vu<sup>1\*</sup>

\*vu@iwe1.rwth-aachen.de; van-hao.vu@iwe1.rwth-aachen.de

<sup>1</sup> Institute of Materials in Electrical Engineering 1 (IWE1), RWTH Aachen University, Otto-Blumenthal-Str. 6, 52074 Aachen, Germany

**Abstract:** Titanium nitride (TiN) is a technologically important material in electronics and bioelectronics due to its tunable electrical conductivity, chemical robustness, and thermal stability, while showing compatibility with CMOS back-end-of-line processing. In this work, TiN<sub>x</sub> thin films were investigated to evaluate how deposition approaches and input parameters influence their structural, morphological, and electrical properties to achieve the desirable material characteristics required for each specialized application.

**Keywords:** TiN, thin film, ion beam deposition, CMOS integration.

## Introduction

TiN is a multifunctional thin-film material widely used in electronics and bioelectronics. In memory applications, it is used as an electrode material for phase change memory fabrication due to its low thermal and beneficial electrical conductivity, which can reduce the RESET power by less thermal loss and higher heating efficiency [1]. TiN can also be utilized for electrode or coating material for biosensors and neural interfaces [2]. This study investigates TiN<sub>x</sub> thin films deposited by ion beam deposition (IBD) and reactive DC magnetron sputtering, assessing their properties and suitability for integrated electronics and bioelectronics applications.

## Results and Discussion

TiN<sub>x</sub> thin films were deposited on SiO<sub>2</sub>/Si, Si, and glass substrates by IBD and reactive DC sputtering at room temperature. The films were investigated for electrical conductivity, surface roughness, thickness, density, crystallographic structure, and surface morphology.

influence of the Ar/N<sub>2</sub> flow ratio on the film properties was systematically investigated. The IBD films were deposited using a SCIA Coat 200 system equipped with a 220 mm-diameter Ti target and reactive N<sub>2</sub> gas. The deposition process was optimized by controlling the primary and secondary ion guns with respect to ion source power, ion beam current, and acceleration voltage.

Figure 1 presents the grazing-incidence X-ray diffraction (GIXRD) patterns (Figure 1A), X-ray reflectivity (XRR) measurements (Figure 1B), and AFM analyses (Figure 1C–D) of 50 nm TiN<sub>x</sub> films deposited on SiO<sub>2</sub>/Si substrates by IBD and DC sputtering. Both deposition methods produced polycrystalline films. XRR results showed clearer, more homogeneous fringes for the IBD films, indicating improved film uniformity. AFM measurements also showed significantly smoother surfaces for the IBD films, with an RMS roughness of  $0.28 \pm 0.04$  nm compared with  $1.59 \pm 0.10$  nm for the sputtered films. The resistivity of the DC-sputtered films strongly depended on the Ar/N<sub>2</sub> flow ratio, increasing with higher N<sub>2</sub> concentrations. In comparison, the IBD films exhibited a lower resistivity of approximately  $230 \mu\Omega \cdot \text{cm}$ .

Further investigations will focus on understanding the influence of deposition parameters on film characteristics and identifying optimized process conditions for specific electronic and bioelectronic applications.

## References

- [1] W. Ren *et al.*, *ECS Trans.*, vol. 60, no. 1, p. 533, Feb. 2014, doi: 10.1149/06001.0533ecst.
- [2] Z. Li *et al.*, *Adv. Mater. Technol.*, vol. 11, no. 8, p. e02242, 2026, doi: 10.1002/admt.202502242.

## Acknowledgements

We acknowledge financial support from Deutsche Forschungsgemeinschaft (DFG, German Research Foundation), grant numbers 424556709/GRK2610 and 528378584/TRR404.

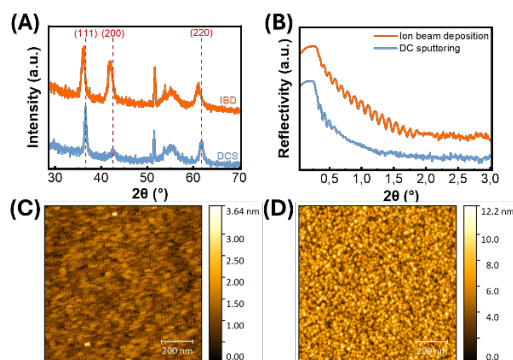


**Figure 1:** Thin film characterizations. (A) GIXRD with  $0.5^\circ$  grazing angle. (B) X-ray reflectivity. (C) AFM of IBD film and (D) AFM of DC sputtered film.

Reactive DC sputtering was performed using an 8-inch Ti target, with N<sub>2</sub> gas introduced into the sputtering chamber to form TiN<sub>x</sub> films. The

# Melt Electrowritten Fibrous Scaffolds for Bone Tissue Engineering: From Architectural Design to Dynamic Cell Culture

Mehwish Yousaf<sup>1</sup>, Stephan Reichl<sup>1,2</sup>, Iordania Constantinou<sup>1</sup>

[mehwish.yousaf@tu-braunschweig.de](mailto:mehwish.yousaf@tu-braunschweig.de)

<sup>1</sup>Institut für Mikrotechnik, Technische Universität Braunschweig

<sup>2</sup> Institut für Pharmazeutische Technologie und Biopharmazie, Technische Universität Braunschweig

**Abstract:** Melt electrowriting (MEW) enables the fabrication of highly ordered microfibrillar scaffolds with tunable architecture, offering a promising platform for bone tissue engineering. This study examines how MEW scaffold design parameters like fiber alignment, lay-down angle, and pore geometry, influence the mechanical properties and osteogenic differentiation of human mesenchymal stem cells (hMSCs) under both static and dynamic perfusion conditions. A novel bone-on-chip device integrating MEW scaffolds is introduced to deliver controlled fluid flow-induced shear stress.

**Keywords:** melt electrowriting, scaffold architecture; osteogenesis; dynamic culture

## Introduction

Bone is a mechanically active tissue whose regeneration depends critically on both scaffold microarchitecture and dynamic mechanical cues [1]. Melt electrowriting (MEW) has emerged as a high-resolution fabrication technique capable of producing microfibrillar PCL scaffolds with precisely tunable fiber alignment and pore geometry that closely mimic native bone extracellular matrix [2]. Despite growing evidence that architectural parameters profoundly influence osteogenic cell behaviour, the effect of MEW scaffold design on stem cell differentiation under physiologically dynamic conditions remains unexplored.

This study aims to: (i) fabricate and mechanically characterise MEW scaffolds across systematically varied architectural configurations; (ii) assess how these architectures influence attachment and osteogenic differentiation of human mesenchymal stem cells (hMSCs) under static and dynamic culture conditions.

## Results and Discussion

Mechanical characterisation via tensile and compression testing confirms that both pore size and fiber lay-down architecture markedly affect scaffold mechanical performance. Tensile modulus and ultimate strength decrease substantially with increasing pore size, while lay-down angle independently governs stiffness anisotropy. These findings inform biologically relevant scaffold selection and confirm MEW as a tool for generating bone scaffolds with tuneable, predictable mechanical properties. hMSC seeding and osteogenic differentiation experiments, alongside dynamic chip-based culture, are currently underway.

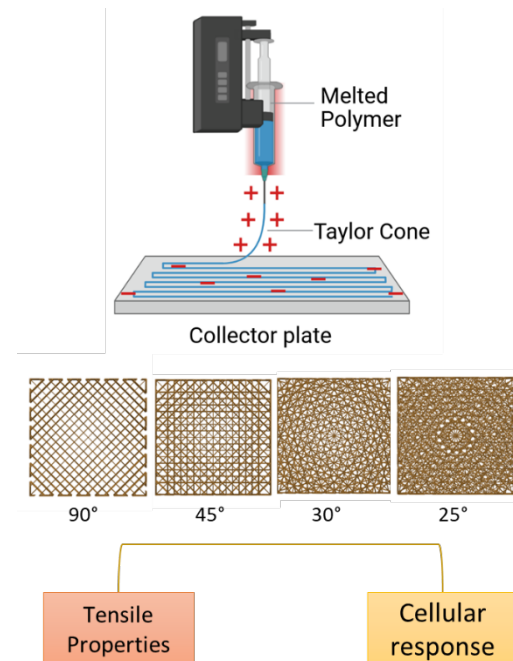


**Figure 1:** Graphical representation of Melt Electrowriting principle and how it is utilized to create scaffolds with varying mechanical properties and cellular responses.

## Conclusions

This work presents the first integration of MEW scaffolds within a dynamic platform, addressing a critical gap in physiologically relevant *in vitro* bone models and offering a powerful tool for rational scaffold design and bone regeneration research.

## References

- [1] Josephson, T.O. & Morgan, E.F. *Frontiers in Physiology* 14, 1232698 (2023). <https://doi.org/10.3389/fphys.2023.1232698>
- [2] Loewner, S. *et al.* *Frontiers in Bioengineering and Biotechnology* 10, 896719 (2022). <https://doi.org/10.3389/fbioe.2022.896719>

# An Advanced Three-Dimensional Peri-implant Tissue Model to Investigate Host-Microbe Interactions

Amit Gaikwad<sup>1,2</sup>, Muhammad Imran Rahim<sup>1,2</sup>, Andreas Winkel<sup>1,2</sup>, Dagmar Wirth<sup>3</sup>, Henning Menzel<sup>4</sup>, Meike Stiesch<sup>1,2,5</sup>

[Steisch.Meike@mh-hannover.de](mailto:Steisch.Meike@mh-hannover.de)

<sup>1</sup>Department of Prosthetic Dentistry and Biomedical Materials Science, Hannover Medical School, Germany

<sup>2</sup>Lower Saxony Centre for Biomedical Engineering, Implant Research and Development (NIFE), Germany

<sup>3</sup>Research Group Model Systems for Infection and Immunity, Helmholtz Centre for Infection Research, Braunschweig, Germany

<sup>4</sup>Institute for Sustainable Chemistry, Braunschweig University of Technology, Braunschweig, Germany

**Abstract:** An immunocompetent advanced 3D peri-implant tissue model, comprising soft- and hard-tissue-like compartments, was established to study host-microbe interactions. The model maintained its tissue architecture even after biofilm challenge and showed inflammatory and osteogenic marker changes. Biofilm characterization further indicated altered biofilm volume and bacterial membrane integrity in the macrophage-integrated model. This platform may support future biomaterial and sensor-actuator testing.

**Keywords:** dental implant; host-biofilm interactions; macrophages; multi-species biofilm; organotypic model

## Introduction

The peri-implant interface is biologically complex, and conventional models including monoculture or even simple co-culture systems do not capture host-implant-microbe interactions well. Hence, clinically relevant 3D models are needed to better reproduce the spatial organization of peri-implant tissues and their response to microbial challenge. This work aimed to establish and characterize an advanced 3D peri-implant tissue model for investigating host-microbe interactions at the implant interface.

## Results and Discussion

After 48 h of co-culture with a multi-species bacterial biofilm, key components of the peri-implant interface were preserved, including the stratified epithelium, collagen-rich connective tissue, macrophages, and an osteoblast-populated porous scaffold. Macrophage integration was confirmed by immunohistochemistry, with macrophages confined to the collagen-rich soft tissue compartment. Under biofilm-challenged conditions, macrophages formed inflammatory foci migrating towards the epithelial compartment, suggesting an active immune-associated response. In the hard tissue compartment, osteoblasts remained well distributed within the porous hydroxyapatite scaffold, indicating preservation of the bone-like component of the model even after co-culture with bacterial biofilm. Molecular analysis by RT-qPCR demonstrated a pro-inflammatory response, reflected by elevated IL-1 $\beta$  and TNF- $\alpha$  expression, together with decreased osteocalcin and alkaline phosphatase expression, suggesting reduced osteogenic activity under biofilm-challenged conditions. Biofilm characterization showed increased biofilm volume accompanied by reduced bacterial membrane integrity within macrophage-integrated model, suggesting that macrophage

integration influences both the host inflammatory response and bacterial viability within the 3D peri-implant system.

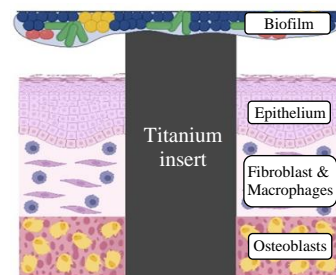


**Figure 1:** Schematic representation of an advanced three-dimensional peri-implant tissue model.

## Conclusions

Overall, the established 3D peri-implant tissue model enables investigation of host-microbe interactions at the implant interface and provides a translational platform for testing future biomaterial and sensor-actuator systems.

## References

- [1] Malekhamdi, B., Kheirmand-Parizi, M., Mikolai, C., Winkel, A., Rahim, M. I., Doll-Nikutta, K., Kampmann, A., Gellrich, N. C., Wirth, D., Menzel, H., & Stiesch, M. (2026). Establishment of a three-dimensional in vitro peri-implant bone-mucosa composite model. *BMC oral health*, 26(1), 91. <https://doi.org/10.1186/s12903-025-06930-2>
- [2] Chen S, Rahim MI, Mikolai C, Paasch D, Winkel A, Doll-Nikutta K, et al. Macrophage-mediated control of implant-associated biofilms in a three dimensional human oral mucosa model. *Materialia*. 2025. <https://doi.org/10.1016/j.mtla.2025.102452>

## Acknowledgements

Deutsche Forschungsgemeinschaft (DFG, German Research Foundation) DFG-SFB/TRR-298-SIIRI-Project-ID 426335750.

# Diabetes-Associated Host Dysregulation at the Peri-Implant Tissue Interface in an Immunocompetent 3D Cell Culture Model

Tayyaba Nawaz<sup>1,2</sup>, Muhammad Imran Rahim<sup>1</sup>, Raunak Lohar<sup>1</sup>, Hermann Haller<sup>2</sup>, Meike Stiesch<sup>1</sup>

[Nawaz.Tayyaba@mh-hannover.de](mailto:Nawaz.Tayyaba@mh-hannover.de)

<sup>1</sup> Department of Prosthetic Dentistry and Biomedical Materials Science, Hannover Medical School, Carl-Neuberg-Straße 1, 30625 Hannover, Germany

<sup>2</sup> Department of Nephrology and Hypertension, Hannover Medical School, Carl-Neuberg-Straße 1, 30625 Hannover, Germany

**Abstract:** Biofilm-associated implant infections are aggravated under hyperglycemic conditions due to impaired immune responses and chronic inflammation. Using the human 3D peri-implant model INTERbACT, this study investigated host–biofilm interactions and evaluated probiotic-derived filtrates as non-antibiotic therapeutics. Hyperglycemia enhanced oral biofilm formation and IL-1 $\beta$  expression, while probiotic-derived filtrates reduced biofilm biomass and modulated macrophage responses, highlighting their potential for managing implant-associated infections in diabetic patients.

**Keywords:** biofilms; hyperglycemia; probiotics; peri-implant model; macrophages; inflammation

## Introduction

Implant-associated infections are more common in diabetic patients, where hyperglycemia promotes chronic inflammation and impaired immune responses. Due to the lack of clinically relevant in vitro models, host–biofilm interactions under hyperglycemic conditions remain poorly understood. In this study, the human 3D peri-implant model INTERbACT was used to investigate host–biofilm interactions and evaluate probiotic-derived filtrates as alternative non-antibiotic therapeutics.

## Results and Discussion

Probiotic-derived filtrates showed antibacterial and immunomodulatory effects against oral biofilms. Hyperglycemia increased IL-1 $\beta$  expression in epithelial cells and significantly enhanced biofilm biomass and volume in the 3D model, indicating greater tissue susceptibility to biofilm colonization. Treatment with probiotic-derived filtrates effectively reduced biofilm biomass. Ongoing cytokine and gene expression analyses aim to further elucidate the molecular mechanisms underlying hyperglycemia-driven biofilm persistence and inflammatory responses.

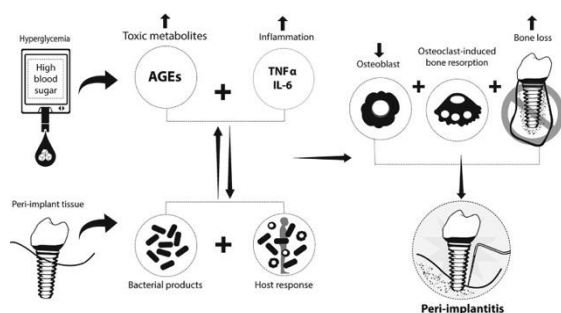


**Figure 1:** Schematic illustration of hyperglycemia-driven peri-implantitis progression. Hyperglycemic conditions promote the formation of advanced glycation end products (AGEs), inflammatory cytokine release, and dysregulated host immune responses, enhancing bacterial activity and peri-implant inflammation. These processes contribute to osteoblast dysfunction, increased bone resorption, and ultimately peri-implant bone loss and peri-implantitis (Oliveira-Neto et al., 2020).

## Conclusions

Probiotic-derived filtrates appear to be promising antibacterial and immunomodulatory agents. Hyperglycemia upregulated IL-1 $\beta$  expression in epithelial cells and increased biofilm thickness and volume in the 3D model. Further cytokine and gene expression analyses will clarify the effects of hyperglycemia on tissue responses.

## References

- [1] Isler, S. C., et al. (2025). Long-term outcomes of peri-implantitis reconstructive therapy: 7-year survival and success. *Clin. Oral Implants Res.*, 36, 1202–1218.
- [2] Trullenque-Eriksson, A., et al. (2025). Association between diabetes and peri-implantitis: Evidence from a Swedish register-based study. *J. Clin. Periodontol.*, 52, 1650–1661.
- [3] Chen, S., et al. (2025). Macrophage-mediated control of implant-associated biofilms in a 3D human oral mucosa model. *Materialia*, 41, 102452.

## Acknowledgements

- SIIRI – Safety-Integrated and Infection-Reactive Implants (SFB/TRR 298 – Project-ID 426335750)
- Prof. Hermann Haller (Department of Nephrology, Hannover Medical School)

# Interface-induced shear control for enhanced flow of shear-thinning silicones in micro-annular printheads

Thorben Schulz<sup>1</sup>, Adrian Onken, Ralf Johow, Yuesi Xi, Tobias Biermann, Theodor Doll

thorbenschulz@t-online.de

<sup>1</sup>NIFE, BioMaterial Engineering, Hannover Medical School, Carl-Neuberg-Str. 1, 30625 Hannover, Germany

**Abstract:** Controlling the flow of highly viscous silicone elastomers is a key challenge in extrusion-based additive manufacturing. This work explores a micro-annular printhead design with a rotating inner core to actively reduce viscosity via shear. Analytical modeling, simulations, and experiments show that moderate rotational speeds increase flow rate at constant pressure.

**Keywords:** shear-thinning; micro-annulus; additive manufacturing; silicone elastomers; flow control

## Introduction

Extrusion-based additive manufacturing of silicone elastomers is essential for personalized medical devices [1-3]. However, the high viscosity and pronounced shear-thinning behavior of these materials limit process stability and achievable resolution. While shear-thinning reduces viscosity under deformation, conventional extrusion provides limited control over local shear conditions in micro-scale nozzles [2]. This work investigates a rotating inner boundary to induce additional shear and reduce apparent viscosity (Figure 1). The concept is related to Couette-Poiseuille flow, where pressure- and shear-driven transport interact [2,3]. Previous studies on non-Newtonian flows have demonstrated that localized shear can reduce apparent viscosity and improve flow efficiency [2]. Despite this, the application of rotational shear in micro-annular systems for highly viscous silicone elastomers remains insufficiently explored in terms of rotational speed and geometric confinement. This work investigates the influence of inner-cylinder rotation on flow enhancement in micro-annular geometries, combining modeling, simulation, and experimental validation to identify relevant operating regimes.

## Results and Discussion

The results show that rotational motion of the inner cylinder can enhance the volumetric flow rate at constant pressure, attributed to shear-induced viscosity reduction. The relationship between rotational speed and flow rate is nonlinear ranging from flow enhancement speeds towards saturation at higher speeds. The flow behavior can be described by a generalized Newtonian model, where viscosity decreases with increasing shear rate:

$$\eta \propto \dot{\gamma}^{n-1} \quad (1)$$

with  $n < 1$  for shear-thinning fluids. This relationship explains the strong sensitivity of the system to imposed shear.

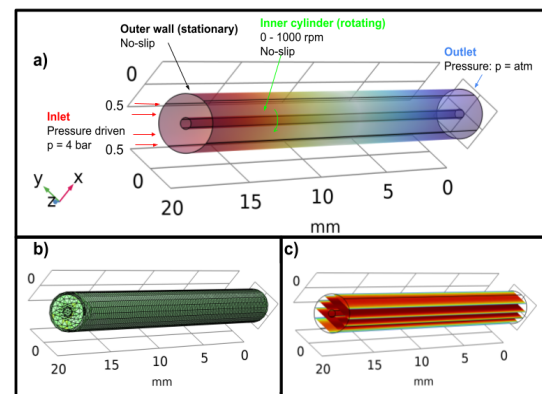


**Figure 1:** CFD model of the concentric annulus showing (a) applied boundary conditions (b) the mesh, and (c) the resulting velocity magnitude distribution along the channel at 0 rpm.

## Conclusions

Rotational shear in micro-annular geometries enhances flow in shear-thinning silicone elastomers by reducing apparent viscosity. The effect is strongest at moderate rotational speeds, depends on geometric confinement, and shows saturation at higher speeds. This approach provides a practical method to improve flow control in extrusion-based additive manufacturing without increasing pressure, offering potential benefits for high-resolution silicone printing and related applications.

## References

- [1] Y. Li and B. Li, *Oxford Open Materials Science*, vol. 2, no. 1, 2022.
- [2] R. B. Bird, W. E. Stewart, and E. N. Lightfoot, *Transport Phenomena*, Wiley, 2007.
- [3] F. M. White, *Fluid Mechanics*, McGraw-Hill, 1999.

## Acknowledgements

Parts of this work was done within the Cluster of Excellence H4a PhoenixD [EXC2122] and funded by the trinational Project 511765241

# COMPUTATIONAL MODELING OF STENT FAILURE DURING CRIMPING AND DEPLOYMENT IN CORONARY ARTERIES

Alexandros Tragoudas<sup>1</sup>, Gerhard A. Holzapfel<sup>2,3</sup> and Fadi Aldakheel<sup>1</sup>

[alexandros.tragoudas@ibnm.uni-hannover.de](mailto:alexandros.tragoudas@ibnm.uni-hannover.de)

<sup>1</sup>Institute of Mechanics and Computational Mechanics, Leibniz Universität Hannover, Hannover, Germany

<sup>2</sup>Institute of Biomechanics, Graz University of Technology, Austria

<sup>3</sup>Department of Structural Engineering, Norwegian University of Science and Technology, Trondheim, Norway

**Abstract:** This study develops a 3D phase-field fracture framework to simulate failure in coronary stents during crimping and balloon deployment. It combines finite-strain elastoplasticity with a ductile fracture model, implemented via UEL in Abaqus and validated against experimental data. A second arterial model captures anisotropic hyperelastic behavior of vessel layers. Fully coupled simulations of the stent-balloon-artery system reproduce realistic loading sequences, revealing that damage initiates during crimping and progresses during expansion. Results highlight how stent design, coronary artery geometry and material behavior influence failure, providing a tool for optimizing stent performance and patient-specific treatment strategies.

**Keywords:** Phase-field; Large-deformation; Coronary artery; Stent; Crimping and deployment

## Introduction

Crimping and deployment of coronary stents involve large deformations, contact, and complex loading cases affecting structural integrity. This study presents a 3D phase-field fracture framework combining finite-strain elastoplasticity with ductile fracture [1], implemented as a user element in Abaqus and validated with experimental data to simulate stent behavior. A second computational model is implemented to describe the anisotropic hyperelastic arterial wall [2]. Coupled simulations capture the full crimping and expansion process, showing fracture initiates during crimping and deployment.

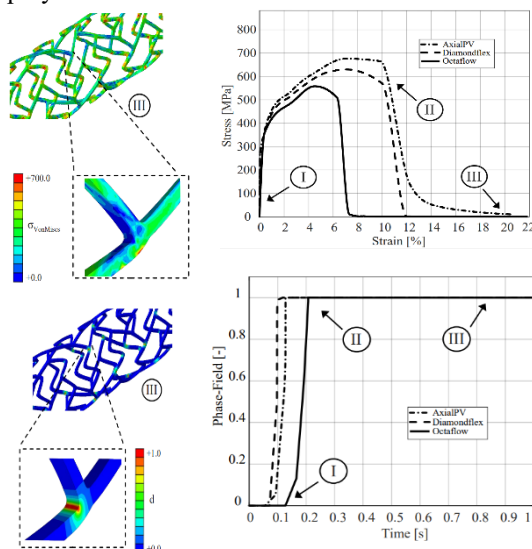


**Figure 1:** Crimping under extreme conditions reveals stress evolution for three stent designs, with contour plots illustrating key deformation stages I–III.

## Results and Discussion

The results show that the proposed framework accurately captures elastoplastic behavior, fracture initiation, and damage evolution during both

crimping and deployment. In particular, Fig. (1) highlights that under extreme conditions, phase-field damage initiates at stress concentration zones and evolves differently depending on stent design. Comparisons between designs reveal significant variations in strength and fracture resistance, emphasizing the critical role of geometry.

## Conclusions

Simulations show that crimping-induced stresses and stent–artery interaction drive fracture initiation, stress redistribution, inelastic deformation, and recoil, with outcomes strongly dependent on stent design and arterial properties. The current model focuses on core mechanics but will be extended to include in vivo effects such as pre-stretch, remodeling, residual stresses, and realistic layered artery structures. Future work will address fatigue, biodegradation, corrosion, and physics-based machine learning for optimization of stent design. Ultimately, the framework aims the development of smart stents integrating mechanical performance, material behavior, and patient-specific functionality.

## References

- [1] Dittmann, M., Aldakheel, F., Schulte, J., Wriggers, P., & Hesch, C. (2018). Variational phase-field formulation of non-linear ductile fracture. *Computer Methods in Applied Mechanics and Engineering*, 342, 71-94.
- [2] Mortier, P., Holzapfel, G. A., De Beule, M., Van Loo, D., Taeymans, Y., Segers, P., ... & Verheghe, B. (2010). A novel simulation strategy for stent insertion and deployment in curved coronary bifurcations: comparison of three drug-eluting stents. *Annals of biomedical engineering*, 38(1), 88-99.

## Acknowledgements

Fadi Aldakheel gratefully acknowledges support for this research by the “German Research Foundation” (DFG) through the SFB/TRR-298-SIIRI – Project-ID 426335750

# Biodegradable nanoMIP Interfaces Enable Selective IL-6 Detection in Human Perilymph

Minh-Hai Nguyen<sup>1</sup>, Theodor Doll

minh-hai.nguyen@stud.uni-hannover.de

<sup>1</sup>Department of Otolaryngology, Hannover Medical School, Carl-Neuberg-Straße 1, 30625 Hannover, Germany

**Abstract:** Chronic inflammation significantly limits the long-term performance of cochlear implants (CIs). As a first step toward future multi-template molecularly imprinted polymer (MIP) sensing platforms, we developed a conductive, biocompatible, and biodegradable nanoparticle molecularly imprinted polymer (nanoMIP)-based sensing layer for the selective detection of interleukin-6 (IL-6) in perilymph. The nanoMIPs achieved sensitivities down to 2 pg/mL in *in-vivo* samples while maintaining high selectivity against common perilymph constituents. Embedded within a chitosan matrix, the sensing layer is fully compatible with existing CI electronics and designed to biodegrade after monitoring, enabling electrode release without additional surgical intervention.

**Keywords:** Cochlear implant, spraycoating, nanoMIPs, chitosan

## Introduction

Cochlear implants (CIs) restore auditory perception through micro-electrode arrays interfacing directly with the auditory nerve. Despite their clinical success, post-implantation inflammatory responses remain a major challenge, as they are governed by complex cascades of multiple biomarkers that can progressively compromise the electrode-tissue interface and long-term device performance [1]. Integrating multiplex biosensing capabilities into CI electrode arrays is further constrained by the extremely limited implant surface area and the risk of electrical cross-talk interfering with neural stimulation fidelity. To address these limitations, nanoMIPs were investigated as a scalable sensing strategy toward future multi-template MIP platforms for localized inflammatory monitoring. In this proof-of-concept study, IL-6 was selected as a representative inflammatory biomarker and selectively detected using epitope-imprinted nanoMIPs embedded within a biodegradable chitosan coating deposited onto electrode surfaces via spray coating. NIP coatings were prepared as controls [2,3].

## Method

Epitope-imprinted nanoMIPs were incorporated into a biodegradable chitosan matrix and spray-deposited onto screen-printed electrodes (SPEs) to fabricate a compact electrochemical sensing platform. Electrochemical impedance spectroscopy (EIS) was employed to evaluate IL-6 recognition across varying target concentrations in PBS. Sensor selectivity was investigated using physiologically relevant interferents, including HSA, IL-9, and IL-1 $\beta$ . To assess translational applicability, measurements were additionally performed in *ex-vivo* human perilymph samples collected during CI procedures. The degradation behaviour and functional stability of the nanoMIP-chitosan coatings were monitored over four weeks under aqueous incubation at 37 °C using longitudinal EIS measurements. Finally, biocompatibility studies were conducted to evaluate the suitability of the sensing platform for implantable bioelectronic applications.

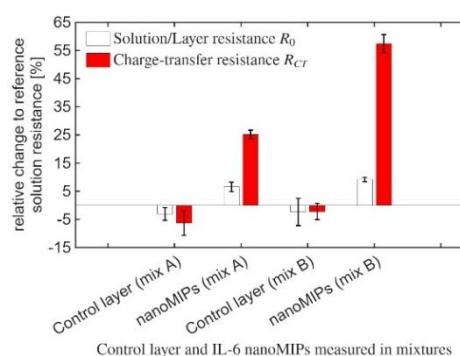


**Figure 1:** EIS-based IL-6 detection in human perilymph showing relative changes in  $R_0$  and  $R_{ct}$

## Results and Conclusions

The nanoMIP-based sensing platform enabled selective and concentration-dependent IL-6 detection using EIS. A nanoMIP:chitosan ratio of 1:8 achieved the highest sensing performance with an imprinting factor of  $8.1 \pm 0.6$ . IL-6 was reliably detected down to 29 pg/mL in PBS and 2 pg/mL in *ex-vivo* human perilymph samples. Selectivity studies against HSA, IL-1 $\beta$ , and IL-9 yielded selectivity factors of  $9.6 \pm 3.1$ ,  $8.2 \pm 2.1$ , and  $6.9 \pm 2.4$ , respectively, confirming strong preferential recognition of IL-6. The sensing platform maintained functionality over four weeks under physiological conditions while exhibiting good biocompatibility. These findings demonstrate the potential of biodegradable nanoMIP-based interfaces as a foundation for future multiplex inflammatory biomarker monitoring in CIs.

## References

- [1] K. Eersels, P. Lieberzeit, P. Wagner, *ACS Sens.* **1** (2016) 1171-1187
- [2] C. C. Mardare, A. W. Hassel, *Phys. Status Solidi A*, **216** (2019) 1900047, doi: 10.1002/pssa.201900047
- [3] M-H. Nguyen, T. Doll, *Sens. Bio-Sens. Res.* **51** (2026), doi: 10.1016/j.sbsr.2026.100990.

## Acknowledgements

This study is funded by the “Cluster of Excellence Hearing4All” (EXC2077).

# Microwave-Assisted Preparation of Bone Regeneration Materials

H. Christmann<sup>1,2</sup>, M. Widerspan<sup>1,2</sup>, M. Lietzow<sup>1,2</sup>, P. Behrens<sup>†</sup>, Nina Ehlert<sup>1,2</sup>

nina.ehlert@acb.uni-hannover.de

<sup>1</sup>Institute of Inorganic Chemistry, Leibniz University Hannover, Callinstr. 9, 30167 Hannover, Germany  
<sup>2</sup>NIFE, Lower Saxony Centre for Biomedical Engineering, Implant Research and Development, Stadtfelddamm 34, 30625 Hannover, Germany

**Abstract:** Critical-sized bone defects, caused *e.g.* by trauma or infections, require regenerative materials that combine bioactivity, mechanical stability, biodegradability and osteoinductive properties to ensure full recovery. Here, we present a composite material consisting of bioactive glass and the polymer poly(glycerol sebacate), that fulfils these requirements. A novel microwave-assisted synthesis route was employed to facilitate and accelerate polymer preparation. The developed composite demonstrates strong potential as a promising candidate for future applications in regenerative bone tissue engineering.

**Keywords:** bone regeneration material; microwave synthesis; bioglass; poly(glycerol sebacate)

## Introduction

Critical size defects in bones can no longer be fully healed by the body and only cartilage is formed [1]. The implantation of a bone regeneration material supports the healing process and facilitates bone formation and thus complete recovery. This work presents a bioactive, porous and elastic composite material consisting of a silica-calcium based bioactive glass and the synthetic biopolymer poly(glycerol sebacate) (PGS) as a suitable bone regeneration material. A porous structure enables vascularisation while the biodegradable nature of the material allows for the substitution with the newly formed bone [2,3].

PGS is an elastic and biodegradable polymer. As the conventional synthesis entails time-intensive heating, microwave synthesis offers a suitable alternative. While the preparation of the prepolymer in the microwave is already established [4], its use for the solvent-free crosslinking of PGS has yet to be mastered.

## Results and Discussion

PGS was prepared from glycerol and sebacic acid using either conventional heating or microwave irradiation for the preparation of the prepolymer and the crosslinking. The mechanical properties are similar for both preparation methods, while the preparation time could be reduced significantly. Successful crosslinking could also be shown by IR.

The bioactive glass was produced using the sponge-template method, yielding a brittle material with open macro- and mesopores as shown in Figure 1. The mechanical stability was increased and biocompatibility as well as degradation behaviour were optimized by the polymer coating, while the macroporous structure was still intact.

Biocompatibility was shown for the composite material using a CellTiter-Blue™ assay.

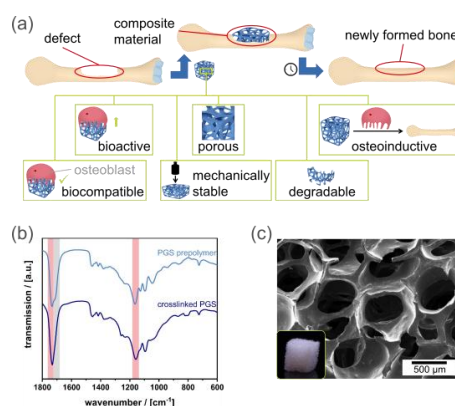


**Figure 1:** a) Scheme depicting the use and properties of the composite as bone regeneration material. b) IR spectra of the PGS prepolymer and crosslinked polymer showing successful crosslinkage. c) SEM image and photograph of the composite material.

## Conclusions

By successfully crosslinking the polymer in a microwave synthesis, a composite bone regeneration material consisting of bioactive glass and poly(glycerol sebacate) was prepared.

## References

- [1] E. Roddy, M. R. DeBaun, A. Daoud-Gray, Y.P. Yang, M.J. Gardner *Eur. J. Orthop. Surg. Traumatol.*, 2018, 28, 351-362.
- [2] T. Albrektsson, C. Johansson *Eur. Spine J.*, 2001, 10, 96-101.
- [3] H. Qu, H. Fu, Z. Han, Y. Sun *RSC Adv.*, 2019, 9, 26252-26262.
- [4] H. M. Aydin, K. Salimi, Z. M. O. Rzaev, E. Piskin *Biomater Sci.*, 2013, 1, 503-509.

## Acknowledgements

This work was funded by Leibniz University Hannover.

# Direct Detection of *Staphylococcus aureus* via Microparticle Imprinted Polymers

Tessa V. M. Bogaardt<sup>1</sup>, H. Diliën<sup>1</sup>, B. van Grinsven<sup>1</sup>, R. Arreguin-Campos<sup>1</sup>

[tessa.bogaardt@maastrichtuniversity.nl](mailto:tessa.bogaardt@maastrichtuniversity.nl)

<sup>1</sup>Sensor Engineering Department, Faculty of Science and Engineering, Maastricht University, P.O. Box 616, 6200 MD Maastricht, Netherlands

**Abstract:** Surface-imprinted polymers (SIPs) were developed for the direct detection of *S. aureus* using polystyrene particles as synthetic templates, eliminating the need for pathogenic bacteria during fabrication and simplifying the imprinting process. The resulting binding cavities, matching the morphology of the bacteria, were shown to enable semi-quantitative direct detection of *S. aureus*. A limit of detection of  $5 \times 10^4$  CFU/mL shows clear promise for further development of microparticle imprinted polymers for bacteria detection.

**Keywords:** *Staphylococcus aureus*, bacteria detection, microparticles, surface-imprinted polymer, HTM

## Introduction

Detection of bacterial pathogens is essential for public health, food quality, and environmental safety. Surface-imprinted polymers (SIP) offer a promising sensing platform, providing selective binding cavities that match the shape and size of bacteria. This research introduces a novel approach to surface imprinting, using polystyrene (PS) microparticles as a synthetic template for bacteria detection. This method prevents the need for live pathogens during SIP fabrication, making the process simpler, faster, and cheaper by eliminating the need for specialised laboratory equipment.

## Results and Discussion

For the detection of *S. aureus*, a SIP has been prepared using PS microparticles as templates to imprint polydimethylsiloxane (PDMS). By adapting the previously reported interfacial imprinting method<sup>[1]</sup>, the surface coverage was improved, and variability between samples was decreased by a factor of four. Characterisation via optical microscopy showed that 98% of the PS particles were effectively removed through sonication, thereby exposing binding cavities that correspond to the morphology of *S. aureus*. Using the heat-transfer method (HTM), the binding of *S. aureus* to the PS-imprinted SIPs was investigated (see Figure 1).

HTM measurements performed in triplicate for both imprinted (SIP) and non-imprinted (NIP) layers showed significantly higher effect size values for the SIP layer, indicating that the resulting cavities allow for more bacteria binding. The limit of detection (LoD) was calculated according to the CLSI guidelines<sup>[2]</sup>, leading to an LoB value of 0.098% and an LoD value of  $5 \times 10^4$  CFU/mL.

To further show the importance of binding cavities of matching morphology to the target bacteria, the binding of rod-shaped *Escherichia coli* bacteria to

the spherical cavities showed significantly less binding to the imprinted layers than *S. aureus*.

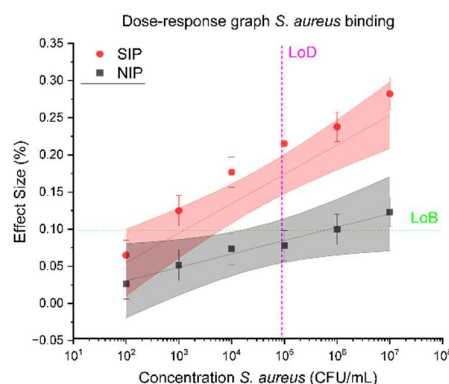


**Figure 1:** Dose-response graph of *S. aureus* binding to PS imprinted (SIP) and non-imprinted (NIP) layer ( $n=3$ ). Error bars: signal noise. Linear regression models with 95% CI bands are shown for both SIP and NIP. Limit of blank (LoB) is indicated in green, and limit of detection (LoD) is shown in magenta.

## Conclusions

Using PS particles for the imprinting of binding cavities matching the shape and size of *S. aureus*, a semi-quantitative sensor has been developed. The limit of detection shows the importance of shape-specific binding cavities for the direct detection of bacteria.

## References

- [1] R. Arreguin-Campos, K. Eersels, R. Rogosic, T. J. Cleij, H. Diliën, B. van Grinsven, *ACS Sensors*, **7** (2022) 1467-1475
- [2] D.A. Armbruster & T. Pry, *The Clinical Biochemist Reviews*, **29** (2008) S49-S52

## Acknowledgements

This work was supported by Maastricht University and the Sensor Engineering Department.

# Biocompatible surface modification of dental implants

Evelin Miller<sup>1</sup>, Chaymae Boukari<sup>1,2</sup>, Michael Veith<sup>1</sup>

[Evelin.miller@studmail.w-hs.de](mailto:Evelin.miller@studmail.w-hs.de), [chaymae.boukari@w-hs.de](mailto:chaymae.boukari@w-hs.de), [michael.veith@w-hs.de](mailto:michael.veith@w-hs.de)

<sup>1</sup>Laboratory of Molecular Biophysics, Westphalian University of Applied Sciences, August-Schmidt-Ring 10, 45665 Recklinghausen & <sup>2</sup>Department of Prosthetic Dentistry and Biomedical Materials Science, Hannover Medical School, Carl-Neuberg-Str. 1, 30625 Hannover, Centre for Biomedical Engineering, Implant Research and Development (NIFE), Stadtfelddamm 34, 30625 Hannover, Germany

**Abstract:** Biocompatible surface modification of dental implants aims to enhance soft-tissue integration while reducing bacterial colonization. Biotinylated fibronectin was immobilized on streptavidin-coated surfaces to promote gingival healing. Fourier-transform infrared spectroscopy confirmed that the protein's secondary structure remained intact after modification, indicating preserved biological activity. Surface plasmon resonance spectroscopy demonstrated successful fibronectin adsorption and revealed irreversible adhesion of lactic acid bacteria to titanium, underscoring the risk of biofilm formation. These results validate the structural integrity of modified fibronectin and highlight biophysical methods for characterizing protein and bacterial interactions on implant surfaces.

**Keywords:** Biofunctionalization; Fourier-transform infrared spectroscopy; surface plasmon resonance spectroscopy; dental implant

## Introduction

When using implants, infection-preventive and integration-promoting properties are equally important; however, achieving both simultaneously is usually not feasible. For this reason, the Molecular Biophysics Research Group at the Westphalian University of Applied Sciences developed a biofunctionalization method that can combine both aspects [1,2]. Immobilized biotinylated fibronectin (Fig. 1 A) is intended to support the healing of a dental implant abutment into the gingiva.

## Results and Discussion

Fibronectin is a key glycoprotein in wound healing, supporting cell adhesion, migration, and differentiation. To ensure that biotinylation does not impair its function, Fourier-transform infrared spectroscopy was used to compare native and modified fibronectin. The nearly identical distribution of secondary structure elements indicates preserved structural integrity and biological activity.

Using surface plasmon resonance spectroscopy, the adsorption behaviour was characterized in situ and in real time at a molecular level. The first measurement observes the immobilization of biotinylated fibronectin on a streptavidin monolayer. All free proteins were removed by a washing step. The reduced reflectivity indicates a surface altered by adsorption, which is desirable for the biofunctionalization of implants. The second measurement shows the adhesion of lactic acid bacteria to a titanium surface. The persistent change in reflectivity indicates an irreversible binding of the bacteria. In the case of a titanium dental implant, this can lead to the formation of a biofilm, which in turn can trigger an infection of the surrounding tissue.

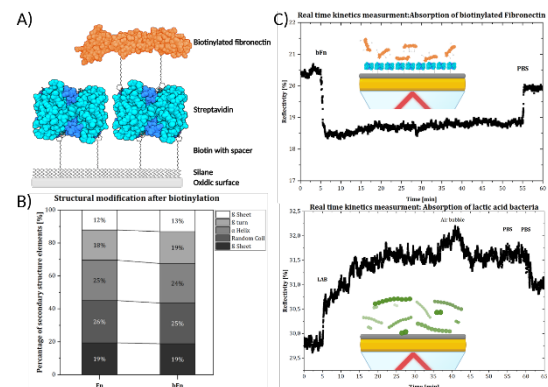


**Figure 1:** A) Biofunctionalized molecular multilayer system; B) Percentage distribution of secondary structure features in native and modified fibronectin; C) Real-time kinetics measurements.

## Conclusions

Biophysical studies confirm intact protein folding and provide a method for characterizing adhesion, which can also determine anti-adhesive effects and the extent of coverage by bacteria or proteins.

## References

- [1] Ettelt V, Veith M., et al Streptavidin-coated surfaces suppress bacterial colonization by inhibiting nonspecific protein adsorption. *J Biomed Mater Res A* 2018; 106(3): 758–68 [https://doi.org/10.1002/jbm.a.36276] [PMID: 29055106]
- [2] Ettelt V, Veith M., et al 2018. Enhanced selective cellular proliferation by multi-biofunctionalization of medical implant surfaces with heterodimeric BMP-2/6, fibronectin, and FGF-2. *J Biomed Mater Res Part A* 2018;106A:2910–2922. [https://doi.org/10.1002/jbm.a.36480].

# Optimized implants through control of stem and immune cells: modulation of TAK1 activity

Y. Roger<sup>1,2</sup>, J. Libnow<sup>1,2</sup>, N. Lachmann<sup>3</sup>, S. Immenschuh<sup>4</sup>, A. Hamm<sup>1,2</sup>, A. Hoffmann<sup>1,2</sup>

roger.yvonne@mh-hannover.de (Corresponding e-mail address)

1 Hannover Medical School, Department of Orthopedic Surgery, Biological Basics for Biohybrid Implants, Anna-von-Borries-Straße 1-7, 30625 Hannover, Germany

2 Lower Saxony Center for Biomedical Engineering, Implant Research and Development (NIFE), 30625 Hannover, Germany

3 Hannover Medical School, Department of Pediatric Pulmonology, Allergology, and Neonatology, Carl-Neuberg-Straße 1, 30625 Hannover, Germany

4 Hannover Medical School, Institute of Transfusion Medicine and Transplant Engineering, Carl-Neuberg-Straße 1, 30625 Hannover, Germany

**Abstract:** Intracellular signalling crucially influences cell behaviour and thereby responses to biomaterials. The kinase TAK1 plays a central role as node factor in various signalling pathways of stem and immune cells. The analysis of three TAK1 inhibitors revealed cell-type-specific characteristics. Inflammatory M1 macrophages demonstrated massive cell death in response to two of these inhibitors. Furthermore, pro- and anti-inflammatory programs of macrophages were affected, with the surface markers CD38 and CD206 showing reduced expression and altered cytokine secretions. RNA-sequencing revealed differential effects of all TAK1 inhibitors.

**Keywords:** human mesenchymal stromal cells, human monocyte-derived macrophages, signal transduction

## Introduction

Over the last decades, diseases, which require medical implants have increased rapidly. There are many different types of implants for a wide variety of areas within the human body, and typically there is a risk of failure due to various adverse reactions. One major problem results from foreign body reactions and fibrosis (figure 1) - the inflammatory process involving immune cells.

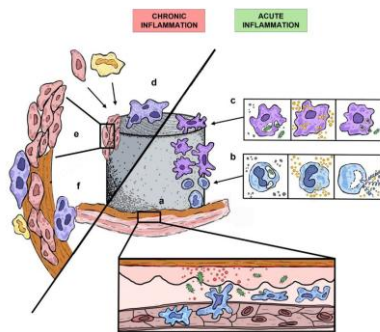


**Figure 1: Foreign body reaction in implants.** Acute inflammation (right) and chronic inflammation (left). **a** acute inflammation: Signalling substances from damaged cells lead to vasodilation, migration of immune cells and plasma proteins, activation and recruitment of further immune cells to the matrix. **b** neutrophils: phagocytosis, cytokine secretion and degranulation, NETosis. **c** monocyte-derived macrophages: phagocytosis, cytokine secretion, antigen presentation. **d** Fusion of macrophages into multinucleated giant cells. **e** Formation of granulation tissue. **f** Formation of scar-like, fibrous capsule. Implant: grey cylinder (central). Cells: red: erythrocytes, blue (under a): immune cells (in general), blue (under b): neutrophils, purple: macrophages, yellow: fibroblasts, brown: vascular endothelial cells. Soluble factors/granula/particles: red: plasma proteins (a), grey: wear particles from implant (b, c), yellow: cytokines (b, c). Bacteria in case of an infection are shown in dark green. Drawing by Johanna Libnow.

## Results and Discussion

Since TAK1 plays a critical role in many different signalling pathways, the analysis of various commercially available inhibitors (Oxozaenol, Takinib and HS-276) is of enormous importance to understand TAK1 signalling more closely. The results of our studies demonstrate a cell type-specific role of TAK1. The inhibition by Oxozaenol or HS-276 led to severe cell loss in M1 macrophages, presumably due to disruption of survival signals and apoptosis. The inhibition by Takinib showed lower cytotoxicity, which could indicate reduced functionality and limited cell permeability. TNF- $\alpha$  expression and secretion were greatly reduced by Oxozaenol and HS-276. At the same time, TAK1 inhibition reduced the expression of cell surface markers such as CD38 and CD206, indicating impairment of pro- and anti-inflammatory programs. In osteoclasts, cell viability remained largely stable during TAK1 inhibition; however, during differentiation, a shift in the expression of specific markers was detected (CD51<sup>low/high</sup>, CD86, CD206).

## Conclusions

Overall, the results underscore the cell type-specific function of TAK1: in macrophages, it regulates survival and proinflammatory activation; in osteoclasts, it regulates differentiation and maturation. The data provide valuable insights for the targeted, context-dependent modulation of TAK1 as a potential therapeutic approach in inflammatory diseases, including implant-associated tissue reactions.

## Acknowledgements

This work was funded by the Deutsche Forschungsgemeinschaft (DFG, German Research Foundation).

# Simulation of Biofilm Growth and Drug-Induced Degradation

Oliver Höchel<sup>1</sup>, Rumjhum Mukherjee<sup>2,3</sup>, Meisam Soleimani<sup>1</sup>, Meike Stiesch<sup>2</sup>, Szymon P. Szafranski<sup>2,3</sup>, Philipp Junker<sup>1</sup>

hoechel@ikm.uni-hannover.de

<sup>1</sup>Institute of Continuum Mechanics, Leibniz Universität Hannover, 30823 Garbsen, Germany

<sup>2</sup>Department of Prosthetic Dentistry and Biomedical Materials Science, Medizinische Hochschule Hannover, 30625 Hannover, Germany

<sup>3</sup>Lower Saxony Centre for Biomedical Engineering, Implant Research and Development (NIFE), 30625 Hannover, Germany

**Abstract:** *In vitro* reproduction of implant-associated biofilm dynamics is challenging and often low-throughput. Numerical simulation techniques help in overcoming methodological limitations. Therefore, this project aims to create an *in silico* experiment setup that simulates multi-species biofilm growth with consideration of its inner dynamics. This is achieved in a nested design: A macro-scale continuum model simulates *spatial* growth, while a nested meso-scale cascade model simulates dynamics *within* biofilm, e.g., cross-protection.

**Keywords:** biofilm growth; biofilm ecology; multi-species biofilm simulation; phage-antibiotic synergy

## Introduction

Biofilms developing on oral implant surfaces contribute to inflammation or even severe long-term peri-implant diseases. This poses a major problem for their longevity and the overall patient health. Better understanding of biofilm growth could enable the deduction of new treatments. This can be achieved by supporting established *in vitro* experiments with novel *in silico* ones, which can simulate even very complex setups.

## Results and Discussion

First step is designing a *macro*-scale continuum model to describe spatial growth of biofilm, based on the surrounding concentration of nutrients<sup>1</sup>. This assumes a homogeneous biofilm, disregarding internal dynamics. It consists of partial differential equations that are derived from the extended Hamilton principle:

$$\mathcal{H}[\mathbf{u}, \xi, \theta] = \int_I (G + C - B + D) dt \rightarrow \text{stat.}_{\mathbf{u}, \xi} \quad (1)$$

To account for effects within biofilm, a second model at the *meso*-scale is nested within the growth model, describing ecological relationships within a representative set of bacteria. Interactions between species can be modelled as a complex network of sequential and parallel biochemical reactions. This *cascade* is efficiently described using the Hamilton principle. Conceptually, this approach not only allows consideration of biochemical reactions, but also of their activation energy within such a cascade.

The nesting of different scales allows for detailed simulation of biofilm growth, considering not only concentration of nutrients, but also internal reactions of the colonizing species to global changes. This facilitates testing of new anti-biofilm therapeutics against, e.g., cross-protection.

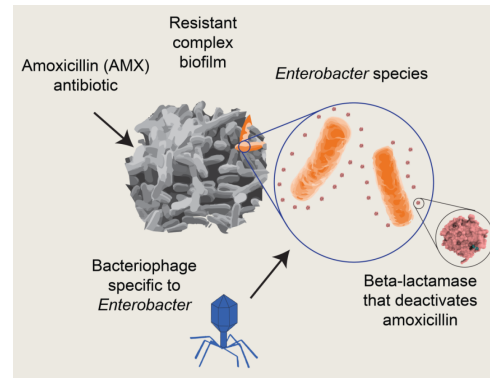


**Figure 1:** Phage-antibiotic combination therapies to inhibit  $\beta$ -lactamase driven cross-protection.

## Conclusions

While this project is still work in progress, major milestones are already achieved. The development of the continuum growth model is finished and following research on this *in silico* model, new setups for *in vitro* investigation were found as well<sup>2</sup>. New strategies of phage-antibiotic combination therapies against cross-protecting biofilm cultures were found, which will be further investigated after application of the cascade model.

## References

- [1] F. Klempt, M. Soleimani, P. Wriggers, et al. A Hamilton principle-based model for diffusion-driven biofilm growth. *Biomechanics and Modeling in Mechanobiology* 23, 2091–2106 (2024). <https://doi.org/10.1007/s10237-024-01883-x>
- [2] T. Qu, L. Koch, R. Mukherjee, et al. Laser-assisted microbial culturomics. *Nature Communications* (2025). <https://doi.org/10.1038/s41467-024-55444-2>

## Acknowledgements

Funded by the Deutsche Forschungsgemeinschaft (DFG, German Research Foundation) – SFB/TRR-298-SIIRI – Project- ID 426335750

# Photovoltaic-Driven Organo-Electronic Ion Pump for Wireless Retinal Ionic Stimulation

Kalyani Devkota<sup>1</sup>, Sven Ingebrandt<sup>1</sup>, Ziyu Gao<sup>1</sup>

ziyu.gao@iwe1.rwth-aachen.de

<sup>1</sup> Institute of Materials in Electrical Engineering 1 (IWE1), RWTH Aachen University, Otto-Blumenthal-Str. 6, 52074 Aachen, Germany

**Abstract:** Organic electronic ion pumps (OEIPs) enable precise, electrophoresis-based ionic transport, and their wireless photovoltaic operation has recently been demonstrated[1]. Here, a silicon photovoltaic-driven OEIP is presented as an in vitro research platform, incorporating a PEDOT:PSS channel on glass slide. Ionic conductivity across KCl, NaCl, LiCl, acetylcholine (ACh), and GABA was characterised at varying light intensities, successfully proving the concept. The platform will be miniaturised to the microscale for investigating ionic signalling and its interaction with retinal cells.

**Keywords:** Organic electronic ion pump; PEDOT:PSS; Photovoltaics; Ion transportation; Retinal stimulation

## Introduction

Ionic and neurotransmitter signalling underpins retinal neural communication, and developing platforms capable of delivering precise, controlled ionic species to retinal tissue remains an open challenge in bioelectronics[2]. OEIPs have emerged as a compelling solution, enabling electrophoresis-driven transport of small charged species, including neurotransmitters such as acetylcholine and GABA, with high spatiotemporal resolution, and their wireless photovoltaic operation has recently been demonstrated[1]. Nevertheless, systematic platforms characterising ionic conductivity across biologically relevant species, driven by silicon photovoltaics and integrated at the microscale for interfacing with retinal cells, remain largely unexplored.

## Results and Discussion

The silicon photovoltaic-driven OEIP demonstrated light-modulated ionic transport through the PEDOT:PSS channel (Figure 1). Under LED illumination, ionic current increased sharply and reproducibly from the room-light baseline (~20  $\mu\text{A}$ ), reaching peak values of ~140  $\mu\text{A}$  for KCl and ~120  $\mu\text{A}$  for LiCl, before returning to baseline upon switching off the light source. The photovoltaic cell enables on/off tuning of the ionic pump, with the two dark periods in the room-light phase confirming that transport is driven exclusively by the photovoltaic bias rather than passive diffusion. The distinct current levels for KCl and LiCl are consistent with the known ionic mobility sequence  $\text{K}^+ > \text{Li}^+$  in cation exchange membranes[3], demonstrating species-dependent transport, a key requirement for future investigation of biologically relevant ions in the context of retinal signalling.

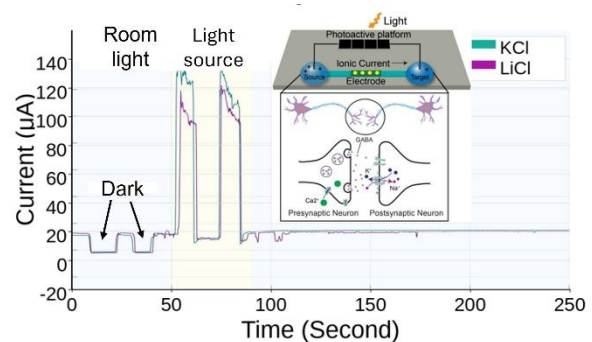


**Figure 1:** Ionic current over time for KCl and LiCl (30 mM) under dark, room light, and LED illumination. (Inset) Device schematic and targeted neurotransmitter delivery concept.

## Conclusions

The silicon photovoltaic-driven OEIP successfully proved wireless, light-controlled ionic transport through a PEDOT:PSS channel, establishing a functional in vitro characterisation platform that will be miniaturised to the microscale for systematic investigation of ionic signalling and its interaction with retinal cells.

## References

- [1] M. Jakešová, et al. *npj Flex. Electron.* 2019;3(1):14. doi:10.1038/s41528-019-0060-6.
- [2] A.E. Medina Arellano, et al. *J. Neurochem.* 2025;169(8):e70198. doi:10.1111/jnc.70198.
- [3] T.A. Sjöström, et al. *Adv. Mater. Technol.* 2018;3(5):1700360. doi:10.1002/admt.201700360.

## Acknowledgements

This work was supported by the DFG-funded graduate school “Innovative Retinal Interfaces for Optimized Artificial Vision” (GRK2610, Grant No. 424556709).

# Development of an integration process for a high-density electrode array for future retinal implant

Fatemeh Molasarvestani<sup>1</sup>, Sven Ingebrandt<sup>1</sup>, Xuan Thang Vu<sup>1\*</sup>

[f.molasarvestani@iwe1.rwth-aachen.de](mailto:f.molasarvestani@iwe1.rwth-aachen.de); [vu@iwe1.rwth-aachen.de](mailto:vu@iwe1.rwth-aachen.de)

<sup>1</sup> Institute of Materials in Electrical Engineering 1 (IWE1), RWTH Aachen University, Otto-Blumenthal-Str. 6, 52074 Aachen, Germany

**Abstract:** The project aims to develop a high-density microelectrode array (HD-MEA) for vision restoration of patients affected by irreversible photoreceptor degeneration. A row-column transistor array is designed on silicon-on-insulator (SOI) wafers to individually address each electrode (up to 1024 electrodes), overcoming interconnection limitations of HD-MEA. The fabricated array is transferred onto a flexible polyimide substrate for mechanical conformability and biocompatibility with retinal tissue. The planar electrodes are further transformed into three-dimensional (3D) structures to enhance the tissue-electrode interface and improve stimulation efficiency. The design targets high spatial resolution, a wide field of view, and simultaneous stimulation and recording capability.

**Keywords:** High-density microelectrode array; Vision restoration; Biocompatibility; 3D electrodes;

## Introduction

Retinitis Pigmentosa (RP) and age-related macular degeneration (AMD) are leading causes of photoreceptor degeneration and severe vision loss [1]. Silicon-on-insulator (SOI)-based transistor technology offers low leakage current, high switching speed, and reduced power consumption while allowing for superior transistor scaling. The high-density transistor array will be realized on top-silicon layer of SOI wafer. The inherent rigidity of SOI technology necessitates to remove the bulk silicon and transfer the device layer onto a flexible polyimide substrate.

## Results and Discussion

In this work, we pursue a one-transistor-one-electrode (1T1E) cell configuration to address the electrodes. The transistors are arranged in rows and columns for selecting electrodes, while the electrode is directly connected to the drain of the transistor, the gate and source are for switching the corresponding transistor on and off (Figure 1).

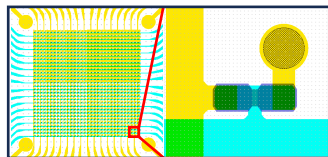


**Figure 1:** Row-column transistor array with 32×32 1T1E cell configuration

In parallel with the fabrication of the 1T1E device, we are developing a process for transferring the array from SOI to a flexible polyimide film. Pseudo-chips were fabricated by metallization on a 290 nm-thick thermal oxide layer on a silicon wafer. The front side of the wafer was passivated with polyimide. The bulk silicon on the backside was

subsequently etched away using a combination of wet and dry etching. In Figure 2a, the result of etching bulk silicon is presented.

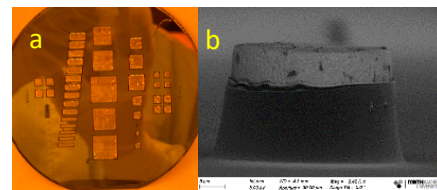


**Figure 2:** a) The result of etching silicon windows with different sizes. b) 3D microelectrode with sidewalls passivation

In Figure 2b, a 21 μm high 3D electrode is presented. The 3D structure was realised by electroplating gold onto planar electrodes, and the electrode sidewalls were then passivated with a thin layer of polyimide.

## Conclusions

Future work will focus on complementary p- and n-type transistors to enable charge-balanced biphasic stimulation. In parallel, the thinned silicon device will be transferred onto a flexible polyimide substrate and packaged for physiological experiments.

## References

[1] E. Butt, et al. J Neural Engineering 21 (2024). <https://doi.org/10.1088/1741-2552/ad2a37>

## Acknowledgements

We acknowledge financial support from Deutsche Forschungsgemeinschaft (DFG, German Research Foundation), grant numbers 424556709/GRK2610.

# Electrostatics of Thin-Film MOS Devices for Gas Electroadsorption

Víctor M. Fuenzalida<sup>1</sup>, M. Moreno-Gutberlet<sup>1</sup> and Theodor Doll<sup>2</sup>

vfuenzal@ing.uchile.cl

<sup>1</sup>Surf. Sci. Lab. FCFM, Universidad de Chile, Av. Beauchef 850, 8370449, Santiago, Chile

<sup>2</sup>Hannover Medical School MHH - BioMaterial Engineering, Cluster of Excellence Hearing 4 All, NIFE Building, Stadtfeldamm 34, 30625 Hannover, Germany

**Abstract:** Electric control of gas adsorption has been reported using metal oxide semiconductor structures, where the electric field at the free semiconductor surface acts as the driving force for adsorption. A preliminary electrostatic model is presented that allows estimation of the electric field emerging from the semiconductor surface for thin-film devices.

**Keywords:** adsorption, electroadsorption, semiconductors, surface science

## Introduction

The influence of electric fields on gas adsorption has attracted interest since the 1950s [1]. It has been observed by electrical measurements and by X-ray photoelectron spectroscopy on a semiconductor surface under electrical polarization [2]. In the test of Fig. 1 a potential is applied to the back of the sample, while the guard ring is grounded, acting as a reservoir of electrons or holes as well as fixing the potential of a region of the surface. A key aspect is that the semiconductor thickness  $w$  is of the order of the Debye screening length  $L_D$ , allowing the electric field to extend across the semiconductor.

Despite the observation of changes in the chemical states of the adsorbate [2, 3] depending on the back potential, the detailed electrostatic behavior of the device is still not fully understood and we report here on recent efforts to model it.

## Results and Discussion

Even though the MOS has been studied since the 1960s, work focused on the channel just below the gate. The Poisson-Boltzmann equation for the p-MOS [4] in dimensionless variables is

$$d^2u/dx^2 = 1 - e^{-u} + e^v(e^u - 1) \quad (1)$$

where  $u$  is the potential,  $x$  is expressed in units of  $L_D$  and  $v$  is the onset potential of strong inversion;  $v$  is the only parameter depending on the semiconductor properties. Eq. (1) can be integrated once, yielding an expression of the form

$$du/dx = G(u, f) \quad (2)$$

where the parameter  $f$  is the non-dimensional field evaluated at the grounded side of the device ( $x=w$ ): it vanishes in the thick-device limit [4]. It was numerically calculated (from an integral equation) for gate potentials spanning from accumulation to strong inversion [5], allowing a straightforward numerical calculation of the potential and carrier densities.

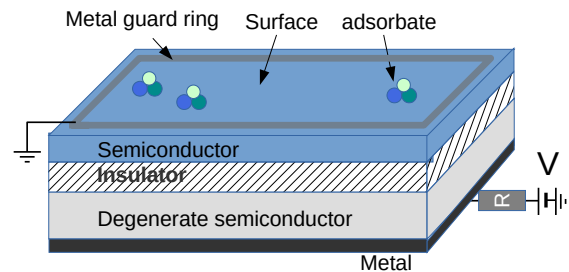


**Figure 1:** MOS device for gas electroadsorption measurements

## Conclusions

The main conclusion is that the field at the grounded surface is non-negligible and can extend beyond the semiconductor into the vacuum if the grounded electrode is not in contact with the surface. This geometry, however, cannot be described by a 1D model and calculations for a 3D device are currently in progress.

## References

- [1] T. Wolkenstein, *The Electron Theory of Catalysis on Semiconductors*, Pergamon, Oxford, 1963.
- [2] T. Doll, J.J. Velasco-Velez, D. Rosenthal, J. Avila, and V. Fuenzalida, *CHEMPHYSICHEM* 14(11) 2505-10 2013. <https://doi.org/10.1002/cphc.201201013>
- [3] A. Ibáñez-Landeta, Thesis, U. de Chile, 2017. <https://repositorio.uchile.cl/handle/2250/145200>
- [4] J.P. Colinge and C.A. Colinge, *Physics of Semiconductor Devices*, Kluwer, NY, 2002
- [5] M. Moreno-Gutberlet, Thesis, U. De Chile, 2025. <https://repositorio.uchile.cl/handle/2250/207092>

## Acknowledgements

We acknowledge support from the German and Chilean governments, through grants DFG 527334504 and ANID-DFG220012, respectively.

# Single Enzyme Nanocapsules for Highly Stable & Robust Biosensing

Dhanjai<sup>1,2</sup>

[dhanjai@allduniv.ac.in](mailto:dhanjai@allduniv.ac.in)

<sup>1</sup>Department of Chemistry, University of Allahabad, Prayagraj 211002, India, <sup>2</sup>KU Leuven, Laboratory for Soft Matter and Biophysics, Celestijnenlaan 200 D, B-3001, Leuven, Belgium

**Abstract:** This study demonstrates the use of highly stable single-molecule enzyme nanocapsules (SENs) instead of traditional native enzyme as biorecognition element in enzyme-based biosensors. The main purpose of this study is to resolve the major obstacle and challenge in the biosensor field, i.e., the poor stability of enzyme-based biosensors, including thermal stability, organic solvent tolerance, long-term operational stability, etc. For this purpose, highly active and robust SENs of glucose oxidase (GOx, as a model enzyme) were synthesized (nGOx) using an *in-situ* polymerization strategy in an aqueous environment and used for the detection of glucose.

**Keywords:** Single enzyme nanocapsule (SEN); biosensors; glucose oxidase; glucose.

## Introduction

Biomolecules such as glucose, adrenaline, dopamine are integral elements of living organisms and control many biochemical functions of the body. Such biomolecules are generally termed as biomarkers for body metabolite or disease detection. Increasing imbalance in the natural metabolism of human body results in irregular secretion/absorption and alteration in biomolecule concentration which may lead to various genetic, metabolic, and cancerous diseases. Therefore, there is a great need for highly sensitive, accurate and stable detection platforms for their fast and specific detection.

## Results and Discussion

Highly active and robust enzyme nanocapsules were synthesized using a simple two-step *in-situ* polymerisation method. In the first step polymerizable vinyl/acryloyl groups were engineered on the enzyme (protein) surface by acryloxylation. The second step involved the subsequent *in situ* polymerization in aqueous environment encapsulating acryloxyated enzyme molecules. Each enzyme nanocapsule consists of a protein (enzyme) core and a thin permeable shell. The polymer shells effectively stabilized the interior enzyme by enabling rapid substrate transportation resulting in a novel class of biocatalytic nanocapsules with outstanding stability and activity.

## Conclusions

Synthesized single molecule enzyme nanocapsules (SENs) of GOx enzyme and successfully applied to fabricate novel class of stable and robust nano(bio)sensors. Thin polymer layer around the enzyme molecule was highly permeable to glucose substrate which did not restrict the substrate movement. This work demonstrates a new class of nano(bio)sensors based on SENs for biosensing applications at different working environment.

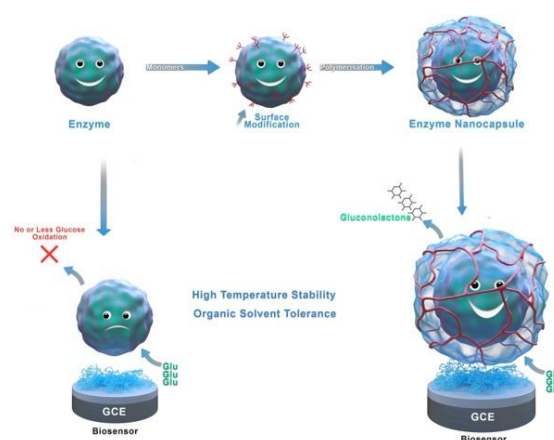


**Figure 1:** Schematic illustration showing preparation, application and stability of single molecule enzyme nanocapsules.

## References

- [1] L. Liu, W. Yu, D. Luo, Z. Xue, X. Qin, X. Sun, J. Zhao, J. Wang, T. Wang, *Adv. Funct. Mater.* 2015, 25, 5159-5165.
- [2] A. Belouqui, A.Y. Kobitski, G.U. Nienhaus, G. Delaitre, *Chem. Sci.* 2018, 9, 1006-1013.
- [3] Z. Gu, M. Yan, B. Hu, K. Joo, A. Biswas, Y. Huang, Y. Lu, P. Wang, Y. Tang, *Nano Lett.* 2009, 9, 4533-4538.

## Acknowledgements

Dr. Dhanjai gratefully acknowledges the support of the Research Foundation–Flanders (FWO) through a Travel Grant (Grant for a Scientific Stay in Flanders), Grant ID V505626N, for visiting KU Leuven as a Visiting Researcher.

# Characteristic pH profiles in a dual-species biofilm model associated with musculoskeletal implant infections

Lisan Püttmann<sup>1,2</sup>, Maya Duitscher<sup>1,2</sup>, Nils Heine<sup>1,2</sup>, Meike Stiesch<sup>1,2</sup>, Katharina Doll-Nikutta<sup>1,2</sup>

puettmann.lisan@mh-hannover.de

<sup>1</sup>Department of Prosthetic Dentistry and Biomedical Materials Science, Hannover Medical School, Carl-Neuberg-Straße 1, 30625 Hannover, Germany

<sup>2</sup>Lower Saxony Centre for Biomedical Engineering, Implant Research and Development (NIFE), Stadtfelddamm 34, 30625 Hannover, Germany

**Abstract:** Implant-associated infections, a challenging-to-detect inflammation of the tissue surrounding implants, are often caused by bacterial biofilms and can lead to severe medical complications. To enable early detection and treatment, this study aims to define baseline pH values and changes within the biofilm upon external triggers for the development of a sensor for pH-dependent autonomous drug release systems. For this purpose, mono- and dual-species biofilms of the most common species found in musculoskeletal implant biofilms were ratiometrically stained and pH values were determined in three-dimensions by microscopy and digital image analysis, showing typical gradients and species-specific differences.

**Keywords:** implant-associated infection, bacterial biofilm, pH sensor, fluorescence microscopy

## Introduction

Implant-associated infections, often caused by bacterial biofilms, can lead to severe complications like implant loss and sepsis. Early detection of bacterial colonization by their metabolic products would enable timely treatment and implant preservation. In biofilms of musculoskeletal implants, like hip and knee endoprostheses, *Staphylococcus epidermidis* and *Enterococcus faecalis* are the most common dual-species biofilms, while *Staphylococcus aureus* is the most common mono-species biofilm strain [1]. This study aims to obtain three-dimensional pH profiles of the different model biofilms to define specific thresholds for infection sensor development.

## Results and Discussion

The dual-species biofilm was established under laboratory conditions and analysed using fluorescence-*in-situ*-hybridisation (FISH) staining, revealing an approximately 1:1 distribution after 16 h of cultivation [Figure 1]. Afterwards, pH-sensitive, ratiometric fluorescence staining SNARF-4F 5-(and 6) Carboxylic Acid (SNARF-4F), confocal laser scanning microscopy and digital image analysis could demonstrate pH gradients within the biofilms of all species as previously evaluated for oral biofilms [2]. The acidification is most probably attributed to an increase in lactic acid production, a metabolic byproduct from all examined strains.

## Conclusions

In the present study, an orthopaedic dual-species biofilm was successfully developed and characteristic pH gradients could be detected. In the future, this model can be used to analyse the influence of different environmental conditions (e.g.

nutrients or wear particles) to define parameters for infection sensor development.

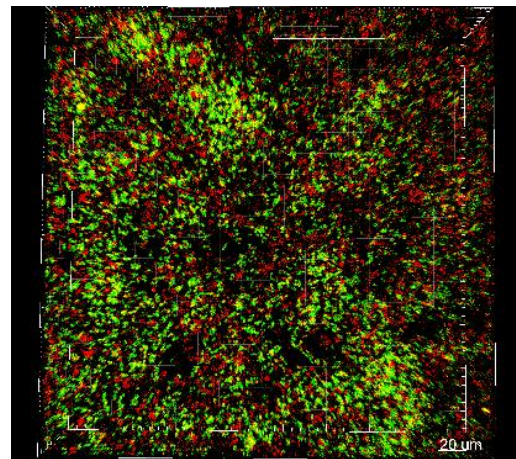


**Figure 1:** Dual-species biofilm of *S. epidermidis* (red) and *E. faecalis* (green) after 16h of growth. Stained with fluorescence-*in-situ*-hybridization. Scalebar shows 20  $\mu\text{m}$ .

## References

- [1] Flurin L, Greenwood-Quaintance K. E, Patel R. Microbiology of Polymicrobial prosthetic joint infection. *Dmb.* 2019;94(3), 255-259 <https://doi.org/10.1016/j.diagmicrobio.2019.01.006>
- [2] Doll-Nikutta K, Weber SC, Mikolai C, et al. Gradual Acidification at the Oral Biofilm–Implant Material Interface. *Journal of Dental Research.* 2025;104(2):164-171 <https://doi.org/10.1177/00220345241290147>

## Acknowledgements

The work was funded by the Deutsche Forschungsgemeinschaft (DFG, German Research Foundation) under the Collaborative Research Center SFB/TRR-298-SIIRI (Project ID 426335750).

# Electrospun SLIPS as Anti-Adhesive Biomaterial Coatings: Effects on Wettability and Biological Interactions

Tom Bode<sup>1</sup>, Jan Drexler<sup>1</sup>, Gerrit Paasche<sup>2</sup>, Birgit Glasmacher<sup>1</sup>, Marc Mueller<sup>1</sup>

t.bode@imp.uni-hannover.de

<sup>1</sup>Institute for Multiphase Processes, Leibniz University, An der Universität 1, 30823 Garbsen, Germany

<sup>2</sup>Otorhinolaryngology, Hannover Medical School, Carl-Neuberg-Straße 1, 30625 Hannover, Germany

**Abstract:** Electrospun slippery liquid-infused porous surfaces (SLIPS) were evaluated for their ability to modulate wettability, protein adsorption, and cellular adhesion. Porous polymer substrates infused with various lubricants were characterized by contact and sliding angles, spectroscopy, and microscopy. SLIPS reduced fibroblast adhesion and metabolic activity and altered blood-related interactions compared to untreated substrates. However, protein adsorption and cell attachment were not consistently suppressed across all fluids and material systems. The findings indicate that SLIPS performance is strongly dependent on substrate–lubricant combinations and environmental conditions, resulting in reduced but not eliminated biological adhesion.

**Keywords:** SLIPS, electrospun implant coatings, protein adsorption, fibroblasts, surface functionalization

## Introduction

Protein adsorption and subsequent cell adhesion remain a critical limitation of many implant surfaces [1]. Slippery liquid-infused porous surfaces (SLIPS) have emerged as an approach to modify interfacial interactions by introducing a liquid layer that prevents direct contact between the substrate and the surrounding biological medium [2]. However, the effectiveness of SLIPS depends strongly on material combinations and environmental conditions, and their performance in complex biological media remains insufficiently understood [3]. The aim of this study was to evaluate electrospun SLIPS systems with respect to their wettability, protein adsorption, and cell adhesion. Electrospun substrates based on polycaprolactone (PCL), polyvinylidene fluoride-Trifluoroethylene (PVDF), and polyurethane (PU) were infused with different lubricants (Almond, coconut and silicone oil) to create SLIPS and exposed to blood, plasma, and artificial perilymph. In addition, NIH/3T3 fibroblast adhesion, viability, and metabolic activity were assessed.

## Results and Discussion

Oil infusion significantly reduced water contact angles from approximately 130° for the untreated substrates (PCL, PVDF, PU) to 80.9–86.9° for the SLIPS systems. Sliding angles decreased substantially from no sliding (untreated substrates) to sliding angles as low as 10.2° (PCL-Coconut). However, variability in sliding behavior and microscopic observations indicate inhomogeneous lubricant distribution and partial exposure of the electrospun substrate, suggesting limitations in surface uniformity. Protein adsorption showed a strong dependence on both the biological medium and the material–lubricant combination. While all SLIPS systems exhibited reduced adsorption relative to untreated substrates, no consistent

suppression across all fluids and exposure times was observed. Fibroblast culture demonstrated reduced cell density and metabolic activity on all SLIPS compared to reference surfaces (pristine fiber mats, PDMS thin films), while maintaining overall cell viability. This indicates that SLIPS attenuate cell adhesion and proliferation without inducing cytotoxic effects, consistent with reduced surface accessibility rather than complete inhibition of biological interaction.

## Conclusions

Overall, the results highlight that electrospun SLIPS systems can mitigate biological adhesion processes, but their performance is governed by the interplay of substrate properties, lubricant characteristics, and environmental conditions. Consequently, anti-adhesive behavior remains variable and system-dependent rather than universally effective and requires further optimization to achieve reliable and durable anti-adhesive functionality in biomedical applications.

## References

- [1] M. J. Foggia, et al. Intracochlear fibrosis and the foreign body response to cochlear implant biomaterials. *Laryngoscope Investigative Otolaryngology*. 2019;4:678–683. doi: 10.1002/liv.2.329.
- [2] C. Howell, et al. Designing liquid-infused surfaces for medical applications: A review. *Advanced Materials*. 2018;30:e1802724. doi: 10.1002/adma.201802724.
- [3] W. Yao, et al. Recent developments in slippery liquid-infused porous surface. *Progress in Organic Coatings*. 2022;166:106806. doi: 10.1016/j.porgcoat.2022.106806

## Acknowledgements

This study was partly funded by the German Research Foundation (DFG) – 60443918.

# Bioimpedance Model Fitting for Clinical Biomarker Quantification

Johannes Bruning<sup>1</sup>, Thomas Hilbel<sup>1</sup>, Michael Schlüter<sup>1</sup>

Johannes.Bruning@w-hs.de

<sup>1</sup> Dept. Electrical Engineering and Applied Natural Sciences, Westphalian UAS, Gelsenkirchen, Germany

**Abstract:** This work focuses on modeling bioimpedance data for biomarker quantification, using lactate as an example. Impedance spectra (1 MHz–100 MHz) at different concentrations show clear, concentration-dependent behavior. Iterative least-squares fitting was applied. More complex models, such as the double Cole model and the Randles circuit, achieved sufficient fits throughout model assessments.

**Keywords:** Biosensors, impedance spectroscopy, Electrical Equivalent Circuit, Lactate, Model Fitting

## Introduction

Point-of-care biomarker detection remains challenging due to reliance on invasive methods. Although bioimpedance spectroscopy offers a non-invasive alternative, it requires robust modelling to distinguish the effects of biomarkers from the dominant influences of tissue and electrolytes. Electrical equivalent circuits (EECs) are commonly used to describe impedance data, though model validity and efficiency remain critical [1,2].

For evaluation, saline solutions with physiological lactate concentrations were measured using electrochemical impedance spectroscopy. The dataset is used to assess the suitability of different modelling approaches for biomarker quantification.

## Results and Discussion

The dataset comprises impedance spectra from 1 MHz to 100 MHz at five lactate concentrations, showing clear concentration-dependent differences (Fig. 1). In this work this dataset functions as evaluation for general bioimpedance modelling with EECs.

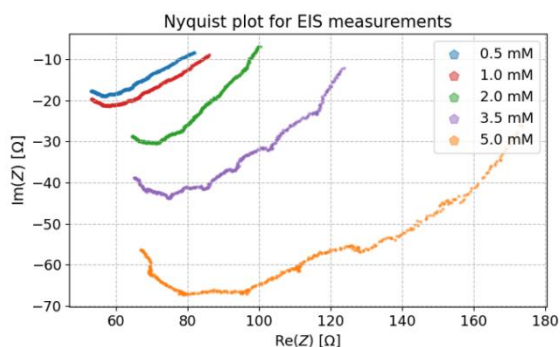


**Figure 1:** Lactate concentration measurements

An iterative least-squares method with random initialization was applied, suitable for low computational cost. Initially, all data were fitted using a single Cole model [3]. However, the model failed to capture the spectral complexity, resulting in significant deviations. Therefore, more complex models were evaluated [2,4]. Both the double Cole model (DCM) and the Randles circuit provide improved fits (Fig. 2). The mean squared error

(MSE) is 4.24  $\Omega$  for the double Cole model and 4.40  $\Omega$  for the Randles circuit; summed over all measurements, 62.163  $\Omega$  and 63.427  $\Omega$ , respectively, indicating a slightly better fit for the DCM. While both models describe the data adequately, further constraints and application-specific parameter bounds are required for reliable quantification and real-time analysis.

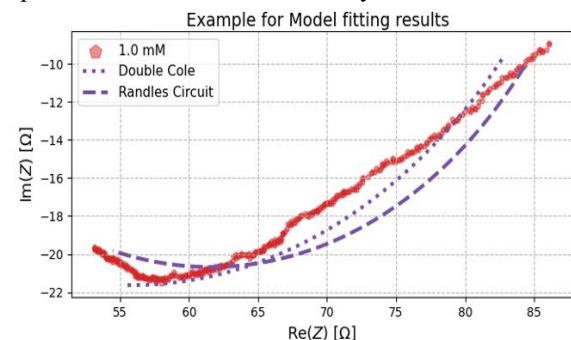


**Figure 2:** Fitted Models for measurement example

## Conclusions

This work addresses a component of the quantification pipeline for biomarkers using bioimpedance measurements. The results show that multiple modelling approaches are viable; however, model complexity must be sufficient to reliably capture the underlying biophysical behaviour. The findings align with existing proof-of-concept studies on lactate detection via bioimpedance and support the extension toward quantitative estimation of lactate and potentially other biomarkers.

## References

- [1] Y. Ding et al., *Sensors*, 25(4):1045, 2025, doi:10.3390/s25041045.
- [2] M. Kunaver et al., *Processes*, 9:1859, 2021, doi:10.3390/pr9111859.
- [3] T. J. Freeborn, *Pers. Ubiquit. Comput.*, 23(2):279–285, 2019, doi:10.1007/s00779-019-01203-6.
- [4] A. Lazanas and B. P. Simon, *Sensors*, 25(19):6260, 2025, doi:10.3390/s25196260.

## Acknowledgements

This work was funded by internal research funding of the Westphalian University of applied sciences.

# A CFD–DEM Framework for Predicting Thermo-Mechanical Drying Behaviour of mRNA-LNP Vaccine Droplets

Jiqian Guo<sup>1,\*</sup>, Silas Wolf<sup>1</sup>, Jan Henrik Finke<sup>1</sup>, Carsten Schilde<sup>1</sup>  
jiqian.guo1@tu-braunschweig.de

<sup>1</sup> Institute for Particle Technology, Technical University Braunschweig, Braunschweig, Germany

**Abstract:** Spray drying is a promising route for improving the storage stability of mRNA-LNP vaccines, but rapid heating, evaporation and particle aggregation are difficult to observe experimentally. We develop a CFD–DEM framework to simulate a single vaccine-like droplet exposed to hot air. The model couples VOF-resolved evaporation, thermodynamic wet-bulb cooling, vapor transport and discrete particle motion. Simulations reveal how gas temperature, humidity and flow velocity affect droplet shrinkage, thermal history and LNP-like particle rearrangement. This digital approach supports process design for thermally sensitive nano-medicines.

**Keywords:** mRNA vaccine; LNP; CFD–DEM; spray drying; digital twin; nano-medicine

## Introduction

mRNA-LNP vaccines are highly sensitive to thermal and mechanical stress during manufacturing and storage. Spray drying may improve their long-term stability, but the process involves fast evaporation, strong temperature gradients and particle redistribution inside micron-scale droplets [1,2]. These coupled effects are difficult to measure directly. Therefore, a predictive digital model is useful for understanding how drying conditions influence the thermal and mechanical history of vaccine-like droplets.

## Results and Discussion

A three-dimensional CFD–DEM model was developed for a water-based droplet containing embedded LNP-like particles. The liquid–gas interface is resolved by a VOF method, while the particle phase is tracked by DEM. Evaporation is driven by a thermodynamic wet-bulb temperature model and localized at the droplet interface. This model builds on previous numerical work on droplet heating, evaporation and particle segregation during spray drying [1,3].

The simulations show that droplet temperature is controlled by both hot-air heating and evaporative cooling. Higher gas temperature and stronger airflow accelerate shrinkage, whereas higher vapor content reduces the evaporation driving force. After the initial heating stage, the droplet diameter follows the expected  $d^2$ -law trend. The DEM particles move with the internal flow, concentrate during shrinkage and finally form agglomerated structures. In flowing-air cases, asymmetric heating and vapor transport lead to directional particle migration and shell-like accumulation.

## Conclusions

The proposed CFD–DEM framework provides a digital tool for studying evaporation, heat transfer and particle rearrangement in mRNA-

LNP-like droplets during spray drying. It can help identify drying conditions that reduce thermal stress while controlling final particle morphology.

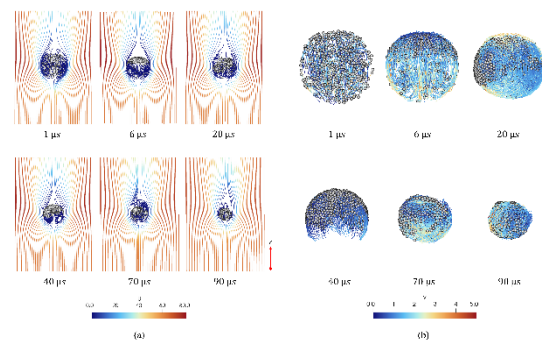


**Figure 1:** A single droplet evaporating in flowing hot air with streamline and particle trajectory visualized.

## References

- [1] Sazhin, S. S. (2006). Advanced models of fuel droplet heating and evaporation. *Progress in energy and combustion science*, 32(2), 162-214.
- [2] Boel, E., Koekoekx, R., Dedroog, S., Babkin, I., Vetrano, M. R., Clasen, C., & Van den Mooter, G. (2020). Unraveling particle formation: From single droplet drying to spray drying and electrospraying. *Pharmaceutics*, 12(7), 625.
- [3] Wolf, S., Kühn, N., Ivanov, D., Levy, A., & Schilde, C. (2025). Numerical study of particle segregation during spray drying of binary suspension droplets. *Powder Technology*, 459, 121019.

## Acknowledgements

This work was supported by the Deutsche Forschungsgemeinschaft (DFG, German Research Foundation) and by zukunfft.niedersachsen.

# The Corrosion of Titanium Dental Implants in Dental Hygiene Products

Andreas Greul<sup>1</sup>, Christoph Kleber<sup>2</sup>, Constantin von See<sup>2</sup>, Achim Walter Hassel<sup>1,2</sup>

[andreas.greul@jku.at](mailto:andreas.greul@jku.at)

<sup>1</sup>Institute of Chemical Technologies of Inorganic Materials (TIM), Johannes Kepler University, Altenberger Straße 69, 4040 Linz, Austria

<sup>2</sup>Danube Private University (DPU), Steiner Landstraße 124, 3500 Krems an der Donau, Austria

**Abstract:** This study focuses on assessing the influence of commercial mouth rinse solutions on the stability of titanium dental implant screws. While titanium remains the gold standard for dental implantology, factors that can influence its corrosion have to be explored thoroughly. In these experiments, 5 commercial mouth rinse solutions have been tested and compared to artificial saliva. Tafel analysis made it possible to determine an upper limit of titanium release caused by the solutions. Furthermore, electrochemical impedance spectroscopy revealed surface changes to the implants caused by some of the solutions.

**Keywords:** implant, dental, corrosion, electrochemistry

## Introduction

Titanium dental implants are the gold standard for modern dental implantology. The oral cavity provides a highly demanding environment, with fluctuating temperatures, pH values and a wide range of different chemicals, which all influence the corrosion of an implant [1]. One chemical factor are commercial dental hygiene products such as mouth rinse solutions. They often contain aggressive agents, such as HOCl or other components which are not widely tested in terms of their influence on corrosion. This study investigates 5 different commercial mouth rinse solutions and their influence on the corrosion of titanium dental implant screws.

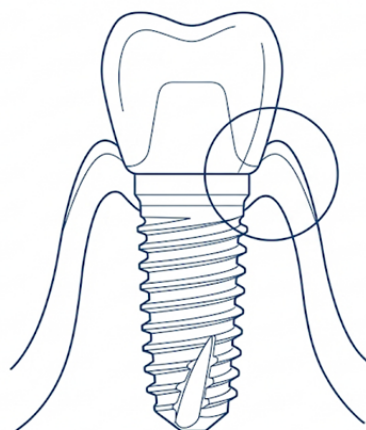


*Figure 1: Drawing of a dental screw indicating the implant area exposed to mouth rinse solutions during everyday use. (\*AI generated)*

## Results and Discussion

The experiments were performed on 5 different mouth rinse solutions with various compositions and active agents. As a first step, linear polarisations were performed on the solutions to test their redox behaviour at relevant potentials. In order to establish a base line all corrosion tests were additionally performed in Fusayama/Meyer solution (artificial saliva for corrosion tests). Implant screws were mounted in a self-designed testing cell to simulate the electrolyte exposure it would face in an implanted state. The temperature of the electrolyte was held at 33°C for all tests. In this setup the corrosion rate and corrosion potential were determined by Tafel analysis. Further, electrochemical impedance spectroscopy was performed after extended immersion times in order to assess possible changes to the passive oxide layer.

## Conclusions

The tests made it possible to give an assessment of the upper limit of conceivable titanium release caused by the solutions. While some solutions caused a clearly elevated corrosion rate, the linked titanium release stayed at benign levels for all solutions. The impedance measurements indicated surface changes to the implants, linked to certain ingredients such as phosphates. Ultimately, the test gave valuable insight into the influence of dental hygiene products on the stability of dental implants. Knowledge of these factors are essential for patient safety and future product development alike.

## References

- [1] J.C.M. Souza, K. Apaza-Bedoya, C.A.M. Benfatti, F.S. Silva, B. Henriques, *Metals*, **10** (2020) 1272

# Influence of Thiol-Based Self-Assembled Monolayers on the Electrochemical Behavior of Combinatorial Ag-Cu Thin Films

Maria Lukina<sup>1</sup>, Manuel Hofinger<sup>1</sup>, Dominik Farka<sup>2</sup>, Achim Walter Hassel<sup>1,3</sup>, Andrei Ionut Mardare<sup>1,4</sup>

[marriialukina@gmail.com](mailto:marriialukina@gmail.com)

<sup>1</sup>Institute of Chemical Technology of Inorganic Materials, Johannes Kepler University Linz, Altenberger Str. 69, 4040, Linz, Austria

<sup>2</sup>PřF Department of Chemistry, University of South Bohemia, Branisovská 31, 370 05, České Budejovice, Czech Republic

<sup>3</sup>Faculty of Medicine and Dentistry, Danube Private University, Steiner Landstraße 124, 3500 Krems an der Donau, Austria

<sup>4</sup>National Institute for Lasers, Plasma and Radiation Physics, Atomistilor Str. 409, 077125, Magurele, Romania

**Abstract:** This study investigates the influence of self-assembled monolayers (SAMs) with thiol-groups on combinatorial Ag-Cu thin film libraries. The thin films were fabricated by thermal co-evaporation of Ag and Cu on glass with a Cr adhesion layer. A compositional gradient of Ag ranging from 83 to 99 at. % was obtained. The alloys surface modification was achieved by SAM adsorptions via solution immersion. The electrochemical properties were characterized by electrochemical impedance spectroscopy (EIS), Tafel analysis, and cyclic voltammetry (CV). EIS and Tafel analysis were repeated after one CV cycle to assess the stability of the monolayer. The results were compared to a reference Ag-Cu thin film. The increase in charge transfer resistance ( $R_{ct}$ ) and reduction of corrosion rate (CR) for specific alloy compositions indicated that SAMs act as effective surface protective layers. These results highlight the potential of SAMs as surface modifiers for corrosion protection applications.

**Keywords:** Ag-Cu combinatorial thin film; self-assembled monolayers; corrosion protection;

## Introduction

Surface properties strongly influence the electrochemical behavior of thin films, particularly their corrosion resistance. SAMs can tailor these properties by forming ordered molecular monolayers with specific chemical functionalities. Acting as charge transfer barriers at the film-electrolyte interface, SAMs reduce corrosion rates. Beyond corrosion protection, the choice of terminal functional groups enables applications in sensing, catalysis and other areas requiring controlled interfacial interactions, such as anodic memristors. [1]

## Results and Discussion

Three thiol-based SAMs: adamantylthiol (AD), mercaptotrytil (TRT) and mercapto (pentafluorophenyl) (5F), were electrochemically investigated on combinatorial Ag-Cu thin films. EIS measurement revealed an overall increase in  $R_{ct}$  for the AD- and 5F- modified samples, particularly in the compositional range from 90 to 95 at. % Ag. This increase in  $R_{ct}$  was accompanied by a significant reduction in the CR compared to the unmodified Ag-Cu thin film. In contrast, the TRT-modified sample exhibited the opposite trend. CVs showed considerably lower currents at higher Ag compositions for AD- and 5F-samples (when compared to the uncoated alloys), and at lower Ag

compositions for TRT-sample, indicating suppressed electrochemical activity. In all cases, the observed behavior was strongly dependent on alloy composition.

## Conclusions

Thiol-based SAMs significantly influenced the electrochemical behaviour of combinatorial Ag-Cu thin films. AD and 5F provided the most effective surface passivation at high Ag composition, as evidenced by an increase in  $R_{ct}$  and a reduction of CR compared to the reference sample.

## References

[1] Sabaghian, Z., Arefinia, R., & Davoodi, A. (2025). Surface modification of copper by the formation of self-assembled monolayers at different concentrations of octadecanethiol in order to study aging process in 3.5 wt.% NaCl solution. *Thin Solid Films*, 830, 140808. <https://doi.org/10.1016/j.tsf.2025.140808>

## Acknowledgements

This research was funded in whole or in part by the State of Upper Austria through the Linz Institute of Technology [project COMSENS, LIT-2023-12-SEE-111].

# Insights in Biomedical Applications of Magnetic Nanoparticles from Nonequilibrium Dynamic Relaxation Simulations

Ulrich M. Engelmann<sup>1</sup>, Sandra Bolte<sup>1</sup>, Beril Simsek<sup>1</sup> and Mohamad Bilal Abbas<sup>1</sup>

engelmann@fh-aachen.de

<sup>1</sup>Department of Medical Engineering and Applied Mathematics, FH Aachen, 52428 Jülich, Germany

**Abstract:** Magnetic nanoparticles (MNP) drive innovative diagnostics with magnetic particle imaging (MPI) and biosensing as well as therapies using MNP as heating agents. Such application relies on the magnetic relaxation of MNP in alternating magnetic fields, whose physics can be predicted using nonequilibrium dynamic magnetization simulations, enabling insights into setup instrumentation, MNP design, and *in-vivo* applicability.

**Keywords:** Biosensing; FMMD; Magnetic nanoparticles; MPS; MPI; MFH; Theranostics

## Introduction

Magnetic nanoparticles (MNP) are miniaturized magnets with unique superparamagnetic properties leading to nonlinear relaxation processes under alternating magnetic fields (AMF) [1]: Applying different frequencies of AMF enable detection, localization and heating of MNP, inspiring biomedical applications spanning diagnostics with magnetic particle spectroscopy (MPS) & imaging (MPI) as well as biosensing and therapeutic treatment options like magnetic fluid hyperthermia (MFH) [1-2], even allowing combined application in theranostics [3]. Exciting MNP with dual-frequency AMF adds intermodulation frequencies to the MNP's magnetic response, enabling multiplexing capabilities to biosensing applications – known as frequency mixing magnetic detection (FMMD) [2]. Managing and predicting the MNP relaxation response depends on the materials properties, (micro-)environmental factors and the AMF itself, as summarized in Figure 1. Also, above biomedical applications imply *in-vivo* use in blood, cells or tissue [4], leading to immobilization and clustering of MNP that change their binding states, hindering rotation and increasing magnetic interactions [5]. Stochastic Néel-Brownian-coupled nonequilibrium dynamic magnetization simulations emerged as a potent tool for systematically predicting MNP signal generation in MPS/MPI, MFH and FMMD [1,2].

## Results and Discussion

Preliminary results from simulations suggest that...  
... larger individual magnetic core sizes generate higher signal in all applications (cf. Fig. 1, inset) [3].  
... increased viscosity and particle immobilization (modelling immersion with blood or cells) slightly reduce MPS and FMMD signal, largely independent of excitation conditions (cf. Fig. 1, inset) [6].  
... the combined effects of viscosity and shell thickness indicate an optimal signal “sweet spot” in MPS for MNP with thin shells [4].  
... particle interactions decrease the net MPS signal; but strongest for largest core sizes, thus smaller cores could yield relatively higher signal *in-vivo* [5].

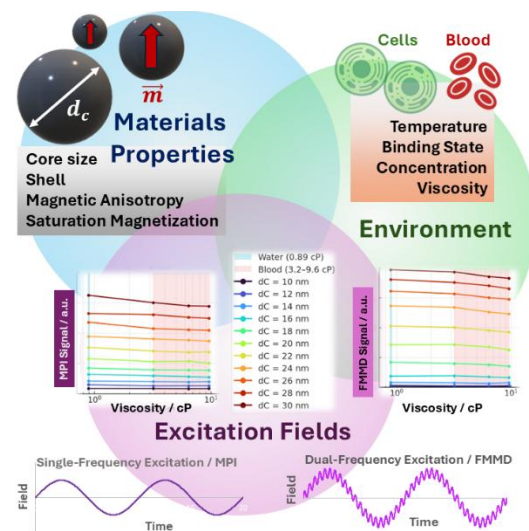


**Figure 1:** Schematic of interplaying factors optimizing application of MNP; incl. preliminary simulation results on MPS / MPI and FMMD (inset).

## References

- [1] U. M. Engelmann, et al. *Magnetic Nanoparticle Relaxation in Biomedical Application* in *Magnetic Nanoparticles in Human Health and Medicine*, 1st ed., C. Caizer, Ed. Wiley & Sons, (2021). <https://doi.org/10.1002/9781119754725.ch15>
- [2] H.-J. Krause, U. M. Engelmann *Adv. Sci.* 12, 2416838 (2025). <https://doi.org/10.1002/adv.202416838>
- [3] Simsek et al. *Int. J. Magn. Part. Imaging* 11, Suppl 1 2503049 (2025). <https://doi.org/10.18416/IJMPI.2025.2503049>
- [4] S. Bolte et al. *Int. J. Magn. Part. Imaging* 12, Suppl 1, 2603047 (2026). <https://doi.org/10.18416/IJMPI.2026.2603047>
- [5] M. B. Abbas et al. *Int. J. Magn. Part. Imaging* 12, Suppl 1, 2603015 (2026). <https://doi.org/10.18416/IJMPI.2026.2603015>
- [6] M. B. Abbas et al. *Int. J. Magn. Part. Imaging* 11, Suppl 1, 2503033 (2025). <https://doi.org/10.18416/ijmpi.2025.2503033>

## Acknowledgements

Funded by DFG – project number 574089568.

# Impact of ionophore concentration on sensor performance of Na<sup>+</sup>-ion sensitive field-effect capacitors

S. Beging<sup>1</sup>, P. Liegmann<sup>1</sup>, K. Miyamoto<sup>2,3</sup>, T. Wagner<sup>1,4</sup>, T. Yoshinobu<sup>2</sup>, M. J. Schöning<sup>1,4</sup>

[beGING@fh-aachen.de](mailto:beGING@fh-aachen.de)

<sup>1</sup>Institute of Nano- and Biotechnologies (INB), FH Aachen University of Applied Sciences, Campus Jülich, Heinrich-Mußmann-Str. 1, 52428 Jülich, Germany

<sup>2</sup>Tohoku University, 6-6-05 Aza-Aoba, Aramaki, Aoba-ku, Sendai 980-8579, Japan

<sup>3</sup>Okayama University, 3-1-1 Tsushimanaka, Kita-ku, Okayama, 700-8530, Japan

<sup>4</sup>Institute of Biological Information Processing (IBI-3), Forschungszentrum Jülich GmbH, Wilhelm-Johnen-Str., 52425 Jülich, Germany

**Abstract:** Capacitive field-effect EMIS (electrolyte-membrane-insulator-semiconductor) sensors have been studied for the detection of Na<sup>+</sup> ions in solutions. As sensor membrane, polyvinyl chloride (PVC) incorporating different amounts of the sodium ionophore X, has been prepared via drop-casting on field-effect structures of Al/p-Si/SiO<sub>2</sub>/Ta<sub>2</sub>O<sub>5</sub>. Sensor characterization has been performed by means of impedance spectroscopy, capacitance-voltage- (C-V), and constant-capacitance (ConCap) methods in terms of Na<sup>+</sup>-ion sensitivity, signal stability, hysteresis, and cross-sensitivity towards interfering ions (K<sup>+</sup>, Ca<sup>2+</sup>).

**Keywords:** sodium sensor; capacitive field-effect sensor; PVC membrane; sodium ionophore X

## Introduction

A sodium-ion sensitive capacitive field-effect sensor was introduced recently; in this study, a key focus was on investigating the structure of the sensor chip using different gate insulator materials (SiO<sub>2</sub>, Si<sub>3</sub>N<sub>4</sub>, and Ta<sub>2</sub>O<sub>5</sub>) [1].

As former studies with field-effect sensors with an incorporated potassium ionophore demonstrated, ionophore concentration strongly influences the overall sensor behavior [2]. Therefore, to further optimize sensor performance, running experiments address the influence of membrane cocktail composition with regard to ionophore concentration (0.7%, 2%, and 3%). The Na<sup>+</sup>-ion EMIS sensors will be characterized in terms of Na<sup>+</sup>-ion sensitivity, signal stability, hysteresis, and cross-sensitivity towards interfering ions (K<sup>+</sup>, Ca<sup>2+</sup>).

## Results and Discussion

The Al/p-Si/SiO<sub>2</sub>/Ta<sub>2</sub>O<sub>5</sub> field-effect capacitors were prepared as described in [1]. The polymeric membrane cocktail with different concentrations of 0.7%, 2%, and 3% of sodium ionophore X was fabricated via drop-casting on the sensor surface after silanization with hexamethyldisilazane.

Electrochemical sensor characterization started in different Na<sup>+</sup>-ion concentrations (10<sup>-1</sup> M – 10<sup>-6</sup> M) in 1 M TRIS buffer, pH 8.

Figure 1 shows representative ConCap (constant capacitance) responses of three Na<sup>+</sup>-sensitive EMIS sensors with a sensitivity of 44.0 mV/pNa for 0.7%

(black line), 53.7 mV/pNa for 2% (red line), and 24.3 mV/pNa for 3% (blue line) of ionophore X.

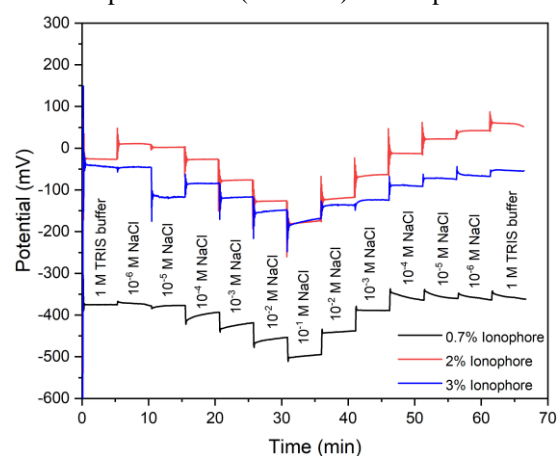


**Figure 1:** Exemplary ConCap measurements of three EMIS sensors with different quantities of sodium ionophore X.

## References

- [1] S. Beging, K.-I. Miyamoto, T. Wagner, T. Yoshinobu, M. J. Schöning, 16<sup>th</sup> EnFI Conference, London 2025.
- [2] Y. Mourzina, T. Mai, A. Poghosian, Y. Ermolenko, T. Yoshinobu, Y. Vlasov, H. Iwasaki, M. J. Schöning, *Electrochimica Acta* **48**, 3333 (2003). doi: 10.1016/S0013-4686(03)00402-X.

## Acknowledgements

TU Research-Oriented Incoming Student (ROIS) Scholarship is acknowledged. The authors thank S. Achtsnicht for valuable discussions.

# Analysing functionalisation of FETs used in biosensing with KPFM

Wiktor Łuczak<sup>1,2</sup>, Achim Walter Hassel<sup>1,2</sup>, Roger Hasler<sup>1</sup>, Christoph Kleber<sup>1,2</sup>

[wiktor.luczak@dp-uni.ac.at](mailto:wiktor.luczak@dp-uni.ac.at)

<sup>1</sup> Department of Physics and Chemistry of Materials, Danube Private University, 3500 Krems-Stein, Austria

<sup>2</sup> Institute of Chemical Technology of Inorganic Materials, Johannes Kepler University, 4040 Linz, Austria

**Abstract:** Biosensors are of interest in diagnostic field due to their promise for fast, precise, and direct detection of target analytes while being compact and easy to use. Kelvin Probe Force Microscopy (KPFM) analysis of the biosensors can provide a wealth of information on surface properties. Topography and Kelvin potential of deposited active channel materials on field-effect transistors (FETs) has been investigated.

**Keywords:** atomic force microscopy; field-effect transistors; graphene oxide; hydrogel

## Introduction

Lab-on-a-chip technology is of great interest in the field of diagnostics due to its ability to deliver rapid, accurate, and direct results once analytes are introduced into the compact device, which is easy to store, operate, and interpret. Different compounds can be used in manufacturing of devices applied in non-destructive sensing of the biological molecules, biomarkers, e.g. nanoparticles, polymers, hydrogels (Figure 1)[1]. KPFM allows for investigation of the surface topography together with the surface Kelvin potential of active sensor surface.

## Results and Discussion

Surface characterisation of FETs functionalised with graphene oxide (GO), reduced GO (rGO – used as active transistor channel material) and hydrogel (pNIPAAm – used for functionalisation of the channel) has been conducted with KPFM under ambient conditions. Challenges in defining relation between the thickness of the deposited material and Kelvin potential detected on surface have been identified. Three different times of wet casting of GO on the substrate have been analysed: 10 min, 30 min and 60 min. Analysis of Kelvin potential across the different thicknesses of the layer of GO/rGO showed dependence of surface potential on thickness of the deposited material. For instance, the Kelvin potential between the substrate (Si/Si<sub>3</sub>N<sub>4</sub>) and the deposited material was approximately 10-130 mV (for 2-6 nm of rGO after 60 min), while 10-40 mV (2-4 nm of rGO after 10 min). The dependence of the potential on thickness of the GO/rGO can directly influence the signal that is acquired by the biosensors [2]. Hence, the input of the data can be affected, leading to change in the quality of the attained data. With application of KPFM for characterisation, it is possible to optimise the fabrication process.

The next step in creation of the biosensors includes functionalisation of the channel allowing for binding chemical/biological analytes [3]. The deposition of the hydrogel has been, with mean step size of dry hydrogel approximately equal to 85 nm.

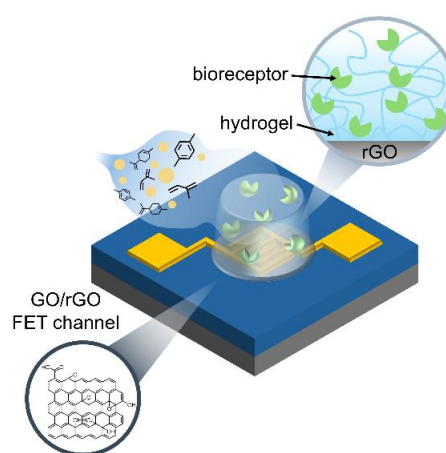


**Figure 1:** Principle behind the concept of hydrogel deposited on FET used for biosensing – reception of volatile organic compounds in exhaled breath.

## Conclusions

Functionalisation of the FETs used in biosensing is allowing for enhancement of the sensor properties. KPFM was successfully used in characterisation of the surface of the FETs with GO/rGO compounds and hydrogels used respectively as active channel material and for functionalisation thereof.

## References

- [1] H.H. Bay, R. Vo, X. Dai, et al. Nano Lett. 19(4) 2019. <https://doi.org/10.1021/acs.nanolett.9b00431>
- [2] E.A. Chiticaru, L. Pilan, C.-M. Damian et al. Biosensors 9(4) 2019. <https://doi.org/10.3390/bios9040113>
- [3] E. Danielson, V.A. Sontakke, A.J. Porkovich et al. Sens Actuators B Chem 320 2020. <https://doi.org/10.1016/j.snb.2020.128432>

## Acknowledgements

This work was supported by the Austrian Research Promotion Agency (FFG) within the COMET project „PI-SENS“ (Project No 915477) as well as by the Federal Provinces of Lower Austria and Tirol.

# Towards tuneable biomineralization: Raman Confocal study of calcium carbonate formation in silk based solutions

Anika Hauseder<sup>1</sup>, David Schäffl<sup>1</sup>, Ghazal Javanshir<sup>1</sup>, Sabine Hild<sup>1</sup>

anika.hauseder@jku.at

<sup>1</sup> Institute of Polymer science, Johannes Kepler University, Altenbergerstraße 69, 4040 Linz, Austria

**Abstract:** Biomineralized hydrogel systems are of particular interest for biomaterials applications, as they provide suitable substrates for cell culture, while calcium carbonate (CaCO<sub>3</sub>) formation can promote specific cell attachment and enhance material functionality. CaCO<sub>3</sub> precipitation was studied under fibroin and sericin mediated mineralisation and compared to reference experiments without the presence of proteins. Confocal Raman spectroscopy allows identification of crystal phases, spatial distinction between organic and inorganic regions and enables distinction between different polymorphs of CaCO<sub>3</sub>.

**Keywords:** biomineralization; silk; Raman; precipitation

## Introduction

The interest in silk fibroin (SF) and sericin from *Bombyx mori* silkworms as versatile and highly biocompatible material for biomedical applications, has increased significantly in recent years. [1] Investigating biomineralization processes within organic matrices contributes to the development of sustainable manufacturing strategies for functional materials in the field of biomedical engineering. [2] Silk proteins interact with ions in solution, thereby influencing nucleation, crystal growth and polymorph selection of CaCO<sub>3</sub>, which makes them an attractive model system for bio inspired material development. [3]

In this study, the influence of proteins with varying concentrations in solution and within an oriented matrix on CaCO<sub>3</sub> precipitation will be investigated. The experiments will be conducted under varying pH conditions and salt concentrations that are similar to physiological environments.

## Results and Discussion

Initial experiments were conducted by precipitating of CaCO<sub>3</sub> in the presence of fibroin. Briefly, a 0.2 mol L<sup>-1</sup> calcium chloride solution was added to a fibroin solution (2 g L<sup>-1</sup>) under continuous stirring. Subsequently, a 0.2 mol L<sup>-1</sup> sodium carbonate solution was added dropwise. The resulting crystals were collected after different precipitation times varying from 10 minutes to 20 hours. Reference samples were prepared following the same procedure, in the absence of protein. Raman spectroscopy was employed to identify the resulting CaCO<sub>3</sub> polymorphs.

Figure 1. depicts the obtained spectra, where calcite was identified as the dominant polymorph, as indicated by characteristic peaks (a,b,c,d). All spectra were normalized on the symmetric stretching vibration of the carbonate ion  $\nu(\text{CO}_3^{2-})$ . Differences between samples were mainly observed in peak intensities, particularly in the low wavenumber

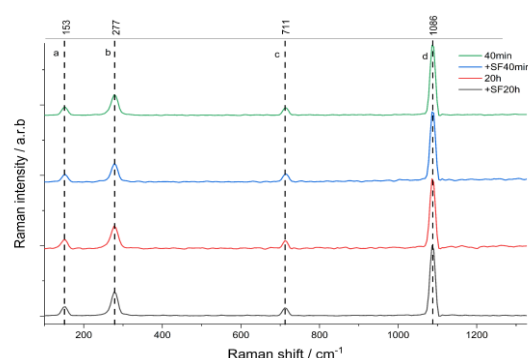


**Figure 1:** Raman Spectra of CaCO<sub>3</sub> with and without fibroin after different reaction times, executed by using WITec alpha 300RA, 532nm

region. A precipitate was observed only after 30 minutes, no precipitation occurred prior to this point.

## Conclusion

A systematic precipitation approach enables controlled biomineralization in the presence of silk proteins, with calcite as the predominant polymorph under the investigated conditions. Future work will focus on tuning polymorph formation and extending the study to fibroin and sericin hydrogels to investigate mineralization at interfaces and within three-dimensional matrices.

## References

- [1] H. Zheng, B. Zuo, Functional silk fibroin hydrogels: preparation, properties and applications, 2021, Royal Society of Chemistry, doi: 10.1039/d0tb02099k.
- [2] E. Asenath-Smith, H. Li, E. C. Keene, Z. W. Seh, L. A. Estroff, Crystal growth of calcium carbonate in hydrogels as a model of biomineralization, 2012, Adv. Funct. Mater., doi: 10.1002/adfm.201200300.
- [3] W. Hao, D. Porter, X. Wang, Z. Shao, Silk fibroin-mediated biomineralization of calcium carbonate at the air/water interface, CrystEngComm, 2014, doi: [10.1039/C4CE01092B](https://doi.org/10.1039/C4CE01092B)

# A multiplexed impedimetric biosensor platform for lung-disease biomarker detection in exhaled breath condensate

S. Bakhshi Sichani<sup>1</sup>, M. Khorshid, J. Hürttlen, M.M. Menger, J.M. Hohlfeld, G. Pohlmann, P. Lieberzeit, and P. Wagner

soroush.bakhshisichani@kuleuven.be

<sup>1</sup>KU Leuven, Laboratory for Soft Matter and Biophysics, Celestijnenlaan 200D, 3001 Leuven, Belgium

**Abstract:** A multiplexed, biomimetic biosensor system is presented for the non-invasive analysis of inflammatory biomarkers in exhaled breath condensate (EBC). Three targets, 3-nitrotyrosine, hexanal, and neutrophil elastase are detected using integrated molecularly imprinted polymers and aptamer-based receptors on a multi-electrode chip. EBC is rapidly collected and conditioned to enable reliable impedimetric measurements. The system is evaluated on clinical EBC samples from healthy individuals and COPD patients. Elevated biomarker levels and responses to environmental exposure are observed, demonstrating the potential for quantitative breath-based diagnostics.

**Keywords:** impedimetric biosensor, molecularly imprinted polymers, aptamers, exhaled breath condensate

## Introduction

Chronic respiratory diseases such as chronic obstructive pulmonary disease (COPD) and cystic fibrosis (CF) require improved tools for early diagnosis and monitoring. Exhaled breath condensate (EBC) provides a promising non-invasive approach, enabling repeated sampling of biomarkers linked to inflammation and oxidative stress [1]. Using a low-cost condenser, EBC can be collected within a few minutes with minimal burden to patients [2]. However, accurate quantification remains challenging due to low biomarker concentrations and sample variability. In addition, environmental factors such as air pollution can influence biomarker levels and disease progression [3]. These challenges highlight the need for sensitive, multiplexed biosensor systems for reliable EBC analysis.

## Results and Discussion

The developed biosensor system enables sensitive and selective detection of 3-nitrotyrosine (3-NT), hexanal, and neutrophil elastase (NE) in exhaled breath condensate (EBC). As shown in **Fig. 1**, the platform combines a low-cost EBC collection unit, a multiplexed multi-electrode chip, and a portable impedimetric readout system. Calibration with spiked samples demonstrates picomolar detection limits, below concentrations expected for healthy individuals, while covering elevated levels reported for COPD and CF patients.

The integration of molecularly imprinted polymers and aptamer-based receptors allows simultaneous detection of multiple biomarkers with minimal cross-interference, confirming specific molecular recognition. Measurements on human-derived EBC show higher concentrations of 3-NT and hexanal in COPD patients compared to healthy volunteers. Temporal variations are observed, with indications

that exposure to polluted urban air increases 3-NT levels.

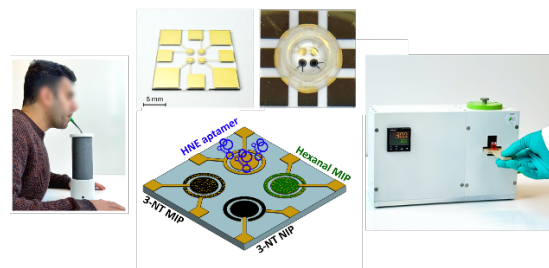


**Figure 1:** Overview of the biosensor platform, including EBC collection, multiplexed multi-electrode chip, and impedimetric readout system.

## Conclusions

A multiplexed, impedimetric biosensor for non-invasive analysis of lung disease biomarkers in EBC has been demonstrated. The system enables sensitive, selective, and portable detection of multiple targets. Clinical observations indicate its potential for real-time monitoring of disease progression and environmental effects, supporting future development toward point-of-care diagnostics.

## References

- [1] F. Ghelli, M. Panizzolo, G. Garzaro, G. Squillaciotti, V. Bellisario *et al.*, *Int. J. Mol. Sci.* **23**, art. no. 9820 (2022).
- [2] M. Khorshid, S. Bakhshi Sichani, D.L. Barbosa Estrada *et al.*, *Adv. Sens. Res.* **3** (7), art. no. 2400020 (2024).
- [3] M. Benjdir, É. Audureau, A. Beresniak, P. Coll, R. Epaud *et al.*, *Environ. Epidemiol.* **5** (4), art. no. e165 (2021).

## Acknowledgements

This work was supported by the European Union's Horizon 2020 (REMEDIATION, Grant No. 874753) and by KU Leuven (C2 project ThermoSens, Grant No. 3E230544).

# Innovative Sensing to Optimise Parkinson's Disease Management

Xinlu Liu<sup>1</sup>, Oliver Jamieson<sup>1</sup>, Alex Casson<sup>1</sup>, and Marloes Peeters<sup>1</sup>

[marloes.peeters@manchester.ac.uk](mailto:marloes.peeters@manchester.ac.uk)

<sup>1</sup>School of Engineering, University of Manchester, Oxford Road, M13 9PL Manchester, United Kingdom

**Abstract:** Parkinson's disease is commonly treated with levodopa; however, its short half-life and fluctuating concentrations in patients often lead to inconsistent symptom control. This work focuses on developing a portable electrochemical sensing platform for levodopa detection using screen-printed electrodes functionalised with molecularly imprinted polymers. The sensor is designed to enhance selectivity and sensitivity toward levodopa while maintaining adaptability across different solution environments and experimental conditions. Electrochemical measurements demonstrate a limit of detection of 2.32  $\mu\text{M}$ , with a rapid response time. These results highlight the potential of the platform as a flexible sensing system under varying analytical conditions.

**Keywords:** Electrochemical biosensor, Molecularly imprinted polymer nanoparticles (nanoMIPs), Parkinson's Disease, Screen Printed Electrodes (SPEs), Medical diagnostics

## Introduction

Parkinson's disease (PD) affects millions worldwide and places a growing burden on healthcare systems and associated costs.<sup>1</sup> Levodopa remains the primary treatment; however, its narrow therapeutic window means that deviations in concentration can lead to loss of symptom control.<sup>2</sup> This motivates the need for improved monitoring. Detection in complex biofluids is challenging due to interfering species, requiring selective recognition elements such as molecularly imprinted polymers (MIPs).<sup>3</sup>

## Results and Discussion

Electroactive nanoMIPs were synthesised using a bulk polymerisation method with L-tyrosine as a dummy template to mimic levodopa's structure.<sup>4</sup> Pyrrole served as the functional monomer, forming a conductive matrix capable of recognising levodopa via shape and interaction-specific cavities.

The MIPs were drop-casted onto SPEs to create a disposable sensing. Cyclic voltammetry (CV) measurements in Figure 1 showed an increasing current change with rising levodopa concentrations, demons.

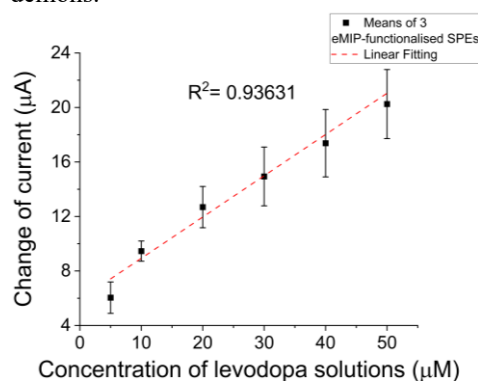


**Figure 1:** CV responses of MIP-functionalised SPEs at varying levodopa concentrations (PBS, pH=7.4)

To enhance sensitivity and achieve a faster electrochemical response, square wave voltammetry (SWV) was also employed. Figure 2 presents representative SWV curves obtained under different buffered solutions, illustrating that the sensing platform can be used repeatedly in different buffer solutions without loss of performance, demonstrating the adaptability of the approach.

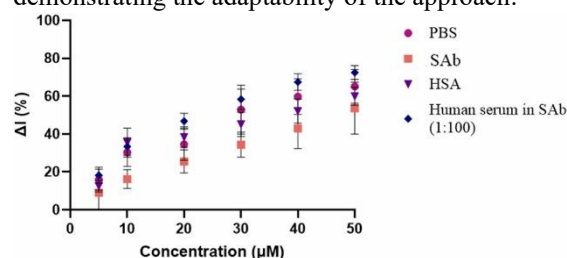


**Figure 2:** SWV calibration curves of the sensor in different sample medium

## Conclusions

This study demonstrates a rapid and robust electrochemical platform for the detection of levodopa using pyrrole-based MIP sensors. The system shows potential for integration into portable and miniaturised devices. Future work will focus on improving sensor sensitivity to enable reliable performance in more complex analytical contexts.

## References

- [1]. Poewe, W. *et al.* Parkinson disease. *Nat. Rev. Dis. Primer* **3**, 17013 (2017).
- [2]. Probst, D., Batchu, K., Younce, J. R. & Sode, K. Levodopa: From Biological Significance to Continuous Monitoring. *ACS Sens.* **9**, 3828–3839 (2024).
- [3]. BelBruno, J. J. Molecularly Imprinted Polymers. *Chem. Rev.* **119**, 94–119 (2019).
- [4]. Jamieson, O. *et al.* Label-Free Electrochemical Levodopa Detection via Dummy Imprinted Polymers for Advanced Disease Monitoring. *Anal. Chim. Acta* 345174 (2026) doi:10.1016/j.aca.2026.345174.

# In vitro investigation of electrospun PVDF-TrFE fiber mats regarding their influence on electrical impedance and cell proliferation

Vinzent Braemer<sup>1,2</sup>, Jan Drexler<sup>3</sup>, Lisa Kötter<sup>1,2</sup>, Birgit Glasmacher<sup>2,3</sup>, Gerrit Paasche<sup>1,2,4</sup>

[Braemer.vinzent@mh-hannover.de](mailto:braemer.vinzent@mh-hannover.de)

<sup>1</sup>Department of Otorhinolaryngology, Head and Neck Surgery, Hannover Medical School, 30625 Hannover, Germany

<sup>2</sup>Lower Saxony Center for Biomedical Engineering, Implant Research and Development, 30625 Hannover, Germany

<sup>3</sup>Institute for Multiphase Processes, Leibniz University Hannover, 30823 Garbsen, Germany

<sup>4</sup>Hearing4all, Hannover Medical School, 30625 Hannover, Germany

**Abstract:** Cochlear implant electrodes are frequently surrounded by connective tissue due to surgical trauma and foreign body response, which can reduce electrical stimulation efficiency. This study evaluated electrospun fiber mats produced as surface modifications to limit such insulation. Increasing mat thickness led to higher impedance values. Surface wetting was accelerated by adding ethanol. Although fibroblast proliferation was reduced on the fiber mats compared to the standard culture substrates after seven days, cell growth was only delayed, indicating that these coatings may help mitigate tissue formation without completely inhibiting cellular activity.

**Keywords:** cochlear implant, electrode surface modification, electrospinning, electrical conductivity, cell-material response

## Introduction

Cochlear implants (CIs) are used to treat patients with severe to profound sensorineural hearing loss by restoring auditory function. However, insertion of the implant and the resulting foreign body response can lead to the formation of connective tissue around the electrode array. This tissue acts as an electrical barrier, reducing the effectiveness of auditory nerve stimulation. One potential strategy to address this issue is to modify the electrode surface to minimize tissue adhesion. In this study, model electrodes were fabricated and coated with fiber mats made from the hydrophobic polymer poly(vinylidene fluoride-trifluoroethylene) (PVDF-TrFE). In vitro investigations regarding the influence of the fiber mat on electrical conductivity and fibroblast growth on their surfaces were evaluated.

## Results and Discussion

For the electrical characterization platinum-iridium model electrodes were manually fabricated to equal the surface area of conventional CI electrodes (0.38 mm<sup>2</sup>) [1]. Mean surface area of the model electrodes was  $0.384 \pm 0.003$  mm<sup>2</sup>. Afterwards the electrodes were embedded in silicone and coated with fiber mats of either three different thicknesses or fiber diameters. The impedance value for the embedded electrodes without coating was  $1119 \pm 142.8$   $\Omega$ . The additional layer of fibers increased the impedance in a thickness dependent matter (between 3-4 k $\Omega$  in increase) with the highest impedance measured for the thickest fiber mat. The best results

for accelerating the wetting process of the fiber mat were achieved by adding 30% v/v ethanol to the physiological sodium chloride solution used for the electrical characterization. The growth of fibroblasts was reduced on the electrospun fiber mats compared to the surrounding cell culture material (fiber mat  $70.8 \pm 10.9$  average fluorescence intensity,  $82 \pm 2.9$  % cell covering after 7 days), (surroundings  $79.5 \pm 5.7$  average fluorescence intensity,  $92.2 \pm 0.7$  % cell covering after 7 days).

## Conclusions

Model electrodes approximating the surface area and impedance values of CI stimulation electrodes were successfully fabricated. The coating with a thin layer of electrospun PVDF-TrFE seems to have the potential to reduce fibroblast growth on stimulating contacts of CI electrodes without increasing the electrode impedance too much for certain thicknesses. For the application on a CI, other wetting strategies or the wetting behavior in vivo have to be investigated.

## References

- [1] C. Newbold et al. J. Neural Eng. Vol. 1, no. 4 (2004). <https://doi.org/10.1088/1741-2560/1/4/005>

## Acknowledgements

This project has been funded by the German Research Foundation (project number: 507870341).

# Long-Term Human Brain-Slice Electrophysiology using a Flexible Microelectrode Interface

Bisruta Chowdhury<sup>1</sup>, Henner Koch<sup>2</sup>, Sven Ingebrandt<sup>1</sup>, Ziyu Gao<sup>1</sup>, Frank Sommerhage<sup>1</sup>

sommerhage@iwe1.rwth-aachen.de

<sup>1</sup> Institute of Materials in Electrical Engineering 1 (IWE1), RWTH Aachen University, Otto-Blumenthal-Straße 6, 52074 Aachen, Germany

<sup>2</sup> Department of Epileptology, University Hospital RWTH Aachen University, Pauwelsstraße 30, 52074 Aachen, Germany

**Abstract:** Flexible microelectrode arrays provide mechanically compliant interfaces for long-term electrophysiological recordings. In this study, in-house flexible MEA devices were evaluated for long-term recordings from human brain slices alongside the development of an automated analysis pipeline incorporating artifact removal, spike detection, waveform quality control, firing-rate estimation, ISI characterization, and spike sorting. The combined flexible neural interface and automated analysis workflow supports functional bioelectronic investigations in disease-relevant neural models.

**Keywords:** flexible interface; microelectrode array; brain slice recording; electrophysiology; signal analysis

## Introduction:

Comprehending brain dynamics currently requires not only conventional methodologies but also supplementary knowledge of neural activity with high spatial and temporal resolution over prolonged durations to achieve comprehensive insights [1]. Recent advancements in high-density and flexible microelectrode arrays have improved large-scale brain recordings [2]. Nonetheless, the increasing complexity and volume of electrophysiological data pose significant obstacles for reliable neural signal interpretation [3].

## Results and Discussion

Figure 1A & B show the in-house flexible MEA, which allows long-term electrophysiological recordings from the top-side of human brain slices. Between most of the 128 microelectrodes (bright dots) are large openings (dark circles) which facilitate the diffusion of oxygen and nutrients into the brain slice, while waste material is removed.

An electrophysiological data analysis pipeline was implemented to process the recordings. During preprocessing, median absolute deviation (MAD)-based noise estimation was implemented to derive appropriate spike detection thresholds [4]:

$$\sigma_n = \frac{\text{median}(|x_i - \text{median}(x)|)}{0.6745}$$

Where  $\sigma_n$  reflects estimated background noise. Spikes were thus identified using an adaptive threshold:

$$V_{thr} = -k\sigma_n$$

with  $k = 4.5$ . The pipeline also includes artifact masking, filtering, spike identification, waveform extraction, firing frequency estimation and inter-spike interval (ISI) analysis. Figure 1C shows a raster plot demonstrating a 24-hour recording

feasibility. The application of tetrodotoxin (red line) terminated the neuronal activity.

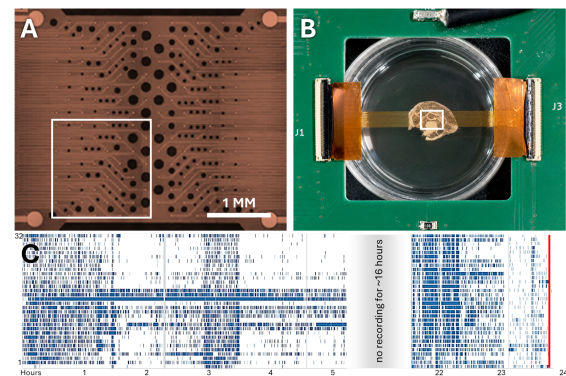


**Figure 1:** Long-term brain slice electrophysiology. (A) Flexible MEA; dark circles are openings to aid diffusion; bright circles are electrodes; white square marks recording area for data shown in C. (B) Setup with brain slice; white rectangle marks the area shown in A. (C) Raster plot of slice activity over 24 hours; red line marks application of tetrodotoxin.

## Conclusions

The flexible MEA platform and analytic pipeline allowed successful long-term electrophysiological recordings and brain signal characterisation.

## References

- [1] J.E. Chung, et al. *Neuron*. 2019;101(1):21–31. doi:10.1016/j.neuron.2018.11.002.
- [2] H. Frese, et al. *Curr Dir Biomed Eng*. 2023;9(1):375–378. doi:10.1515/cdbme-2023-1094.
- [3] A.P. Buccino, et al. *Prog Biomed Eng*. 2022;4:022005. doi:10.1088/2516-1091/ac50cc.
- [4] D. Valencia, et al. *J Neural Eng*. 2022;19(4). doi:10.1088/1741-2552/ac8077.

## Acknowledgements

This work was supported by the DFG-funded graduate school “Innovative Retinal Interfaces for Optimized Artificial Vision” (GRK2610, Grant No. 424556709).

# Qualification of a Swellable Hydrogel–Silicone Bimorph for Implantable Actuation

Esma Dosdogru<sup>1</sup>, Adrian Onken<sup>1</sup>, Patricia Torgau<sup>1</sup>, Marc Müller<sup>2</sup>, Theodor Doll<sup>1</sup>

Esma.dosdogru@stud.uni-hannover.de

<sup>1</sup> NIFE, BioMaterial Engineering, Hannover Medical School, Carl-Neuberg-Str. 1, 30625 Hannover, Germany

<sup>2</sup> Institute for Multiphase Processes (IMP), Leibniz University Hannover, 30823 Garbsen, Germany

**Abstract:** Hydrogel particles are promising fillers for stimuli-responsive silicone composites. By qualifying a swellable hydrogel–silicone bimorph, this research establishes a framework for implantable actuators. This study systematically investigates the influence of filler loading and curing conditions on swelling kinetics and structural integrity. A key focus is the impact of hydrogel purification on cytocompatibility. Using WST-1 assays, the study evaluates how removing impurities via washing enhances cell viability. Overall, the research demonstrates how processing parameters and purification steps affect the functional performance and biological safety of these adaptive composite structures.

**Keywords:** silicone–hydrogel hybrids, biocompatibility, stimuli-responsive hydrogels, swelling behavior

## Introduction

Despite the potential of bimorph hydrogel-silicone configurations for soft actuators, the reliability of these systems is often limited by inconsistent swelling behavior and varying biocompatibility results. It remains unclear whether these issues stem from intrinsic material properties, processing parameters, or leachable components.

To address these uncertainties, this work systematically qualifies hydrogel-silicone bimorphs by investigating the influence of curing conditions and washing procedures. By comparing hybrid systems with silicone reference samples, this study disentangles process-related effects to ensure reproducible performance and biological safety for future medical applications.

## Results and Discussion

The experimental results reveal a clear correlation between hydrogel content, swelling kinetics, and cytocompatibility. Notably, cell viability improved with increasing hydrogel fractions. This can be attributed to a synergistic shielding effect: the hydrated particles reduce direct contact with the silicone matrix and minimize non-specific protein adsorption, while simultaneously acting as a physical and biochemical barrier against residual silicone components [1-3].

The washing process of the hydrogel enhanced cell viability, confirming that the removal of residual impurities and monomers is essential for biological safety.

Regarding the functional properties, the water uptake capacity increased with higher hydrogel loading, as expected for a percolating network.

However, a distinct difference was observed between the two purification states: unwashed hydrogel particles exhibited higher water uptake. This increased swelling potential in unwashed specimens likely stems from the presence of osmotic active residuals that further drive water absorption. These findings demonstrate that a balance between maximum swelling performance and biological safety must be struck through controlled purification and processing parameters.

## Conclusions

This study establishes that purifying hydrogel fillers is essential for balancing actuation performance and biological safety. While unwashed particles enhance swelling through osmotic effects, washed hydrogels ensure superior cytocompatibility and stable kinetics. By optimizing filler loading and swelling behavior, these silicone-based composites provide a reliable material platform for the development of responsive, implantable medical actuators.

## References

- [1] Fei Tan, et al.: GelMA/PEDOT:PSS Composite Conductive Hydrogel-Based Generation and Protection of Cochlear Hair Cells through Multiple Signaling Pathways. [10.3390/biom14010095](https://doi.org/10.3390/biom14010095)
- [2] Ryan Horne, et al.: Reducing the foreign body response on human cochlear implants and their materials in vivo with photografted zwitterionic hydrogel coatings. [10.1016/j.actbio.2023.05.011](https://doi.org/10.1016/j.actbio.2023.05.011)
- [3] Hyun Joon Kong, et al.: Designing alginate hydrogels to maintain viability of immobilized cells. [10.1016/s0142-9612\(03\)00295-3](https://doi.org/10.1016/s0142-9612(03)00295-3)

## Acknowledgements

The authors gratefully acknowledge Dr. Johannes Aucktor and Unavera Chemlab GmbH for the generous donation of the hydrogel powder.

# Medium-dependent Mg ion release and biological responses to WE43 magnesium alloy

Qiushuo Duan<sup>1,2</sup>, Raunak Lohar<sup>1,2</sup>, Winkel Andreas<sup>1,2</sup>, Meike Stiesch<sup>1,2</sup>

[Duan.qiushuo@mh-hannover.de](mailto:Duan.qiushuo@mh-hannover.de)

<sup>1</sup>Department of Prosthetic Dentistry and Biomedical Materials Science, Hannover Medical School, Hannover, German

<sup>2</sup>Lower Saxony Centre for Biomedical Engineering, Implant Research and Development (NIFE), Hannover, Germany

**Abstract:** WE43 magnesium alloy may regulate peri-implant microenvironments through medium-dependent degradation and Mg ion release, thereby affecting oral bacteria and host bone-related cells. We assessed pH, Mg ion release, bacterial metabolic activity, MG-63 LDH/CellTiter-Blue responses, and F-actin/DAPI morphology using WE43/Mg materials, Ti-6Al-4V controls, alloy-conditioned media, and MgCl<sub>2</sub>. Mg release was higher in biological media, while high Mg exposure reduced bacterial metabolic activity and induced time-dependent MG-63 cytotoxicity with cytoskeletal alterations. Ion-conditioned media and MgCl<sub>2</sub> confirmed soluble Mg ions as key contributors, supporting future studies on Mg-mediated peri-implant remodeling under bacterial challenge.

**Keywords:** WE43 magnesium alloy; Mg ion release; MG-63 cells; oral bacteria; cytotoxicity; metabolic activity

## Introduction

Biodegradable magnesium alloys release bioactive Mg ions but may alter peri-implant microbial and host-cell responses. This study investigated the effects of WE43 magnesium alloy and Mg-derived ions on oral bacteria and MG-63 cells. [1,2].

## Results and Discussion

SEM confirmed the surface morphology of WE43/Mg materials and the Mg particle size range used in this study (Figure 1). Mg degradation was strongly medium-dependent, with greater pH changes in water and PBS, stronger buffering in BHI and  $\alpha$ -MEM, and higher Mg ion release in biological media. High Mg exposure reduced bacterial metabolic activity in *S. oralis*, commensal, and pathogenic multispecies biofilm models.

In MG-63 cells, direct WE43/Mg exposure induced concentration- and time-dependent cytotoxicity, reflected by increased LDH release, reduced CellTiter-Blue viability, and disrupted F-actin organization. Ion-conditioned media and MgCl<sub>2</sub> controls reproduced these effects, confirming soluble Mg ions as key contributors to the observed cellular response.

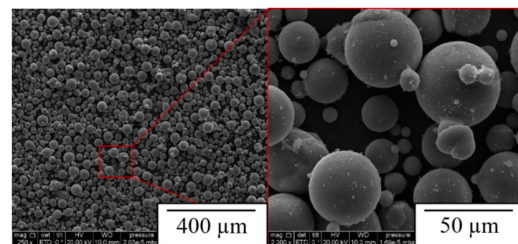


**Figure 1:** SEM images showing WE43 alloy surface morphology and Mg particle size.

## Conclusions

WE43 magnesium alloy showed medium-, concentration-, and time-dependent effects on bacteria and MG-63 cells. High Mg exposure reduced bacterial metabolic activity but compromised cell viability and cytoskeletal organization. Ion-conditioned media and MgCl<sub>2</sub> confirmed soluble Mg ions as key contributors, highlighting the importance of balancing antibacterial activity with host-cell compatibility.

## References

- [1] F. Witte, The history of biodegradable magnesium implants: A review. *Acta Biomaterialia* 6, 1680-1692 (2010).
- [2] N.T. Kirkland, N. Birbilis, M.P. Staiger, Assessing the corrosion of biodegradable magnesium implants: A critical review. *Acta Biomaterialia* 8, 925-936 (2012).

## Acknowledgements

Funded by the Deutsche Forschungsgemeinschaft (DFG, German Research Foundation) – Research Unit 5250 – Project-ID 449916462 as well as SFB/TRR-298-SIIRI – Project-ID 426335750.

# Double-Imprinted nanoMIPs for Targeted Drug Delivery in NSCLC

Shreya Tiwari<sup>1</sup>, Saweta Garg<sup>1</sup>, Huda Hammad Rattu<sup>2</sup>, Pankaj Singla<sup>1</sup>, Tim Witney<sup>2</sup>, Marloes Peeters<sup>1</sup>  
marloes.peeters@manchester.ac.uk

<sup>1</sup>The University of Manchester, Department of Chemical Engineering, Manchester, M13 9QS, UK

<sup>2</sup>King's College London, School of Biomedical Engineering & Imaging Sciences, London, SE1 7EH, UK

**Abstract:** This study reports the development of nano-sized, double imprinted molecularly imprinted polymers for targeted drug delivery in non-small cell lung cancer (NSCLC). The nanoMIPs were synthesised against a resistance-associated receptor epitope and subsequently imprinted with a chemotherapeutic agent. They exhibited high binding affinity towards the targeted epitope and cytotoxic effects in the receptor overexpressing cancer cell lines. These findings demonstrate the potential of double-imprinted nanoMIPs as a selective platform for overcoming drug resistance in NSCLC.

**Keywords:** Molecularly imprinted polymers; double imprinting; drug delivery; cancer; receptor-targeting

## Introduction

Non-small cell lung cancer (NSCLC) remains a leading cause of cancer-related mortality, primarily driven by therapeutic resistance. Targeted drug delivery systems offer significant potential to enhance treatment specificity and efficacy. Molecularly imprinted polymers (MIPs), particularly in nano-sized formats, provide high selectivity through tailored recognition sites. In this study, double-imprinted nanoMIPs were developed by incorporating a resistance-associated epitope and a therapeutic payload, enabling targeted and efficient drug delivery.

## Results and Discussion

This study reports the development of nano-sized, double-imprinted molecularly imprinted polymers (NMs) for targeted drug delivery in non-small cell lung cancer [1]. An epitope of a resistance-linked receptor was employed for solid-phase synthesis of the NMs, followed by a second imprinting step with the chemotherapeutic agent doxorubicin (DOX), denoted as D-NMs [2]. Alternatively, NMs were synthesised with fluorescein and denoted as F-NMs. The NMs were characterised for size and morphology using DLS and SEM, revealing spherical nanoparticles with hydrodynamic diameters of  $220 \pm 3$  nm (PDI = 0.136) and  $190 \pm 3$  nm (PDI = 0.118). The D-NMs exhibited a drug loading capacity of 12.02% and released up to  $94.52 \pm 0.5\%$  of DOX under tumour microenvironment conditions (pH 6.5, 37 °C) over 84 h. SPR analysis demonstrated approximately 50-fold higher binding affinity of D-NMs toward the targeted epitope ( $32 \pm 53$  nM) compared to a non-specific epitope ( $1570 \pm 2473$  nM). Evaluation in receptor-high and receptor-low cell lines via MTT assay showed lower cell viability in receptor-high cells, correlating with higher F-NMs binding observed by flow cytometry. These results highlight the potential of double-imprinted NMs as a precise and effective platform for targeted drug delivery in NSCLC.

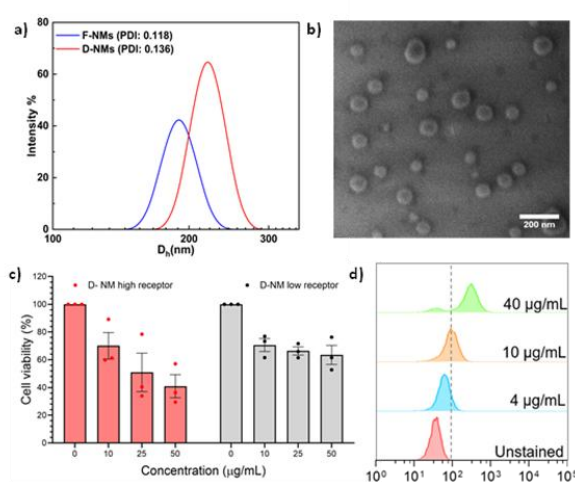


**Figure 1:** (a) DLS showing the hydrodynamic diameter of the NMs. (b) SEM image of D-NMs displaying spherical morphology. (c) MTT assay of D-NMs in receptor-high and low cell lines after 24 h treatment. (d) Flow cytometry binding analysis of F-NMs in receptor-high cells.

## Conclusions

This study demonstrates the successful development of double-imprinted nanoMIPs for targeted drug delivery in NSCLC. The nanoparticles exhibited selective binding, controlled drug release, and enhanced cytotoxicity in receptor-overexpressing cells. The double-imprinting strategy effectively integrates targeting and therapeutic functions within a single platform. These findings highlight the potential of nanoMIPs to overcome drug resistance and improve treatment specificity.

## References

- [1] Canfarotta, F., et al., Nano Letters, 2018, 18(8).
- [2] Singla, P., et al., Advanced Science, 2024, 11(36).

## Acknowledgements

The authors acknowledge financial support from MRC grant MR/Y008421/1.

# Accurate concentration prediction in multispecies bacterial samples using FTIR spectroscopy and deep learning

Katharina Anna Frings<sup>1,2</sup>, Emilie Baron<sup>1,2</sup>, Lars Baumann<sup>1,2</sup>, Nils Heine<sup>2,3</sup>, Katharina Doll-Nikutta<sup>2,3</sup>, Maria Leilani Torres-Mapa<sup>1,2</sup> Alexander Heisterkamp<sup>1,2</sup>

[frings@iqo.uni-hannover.de](mailto:frings@iqo.uni-hannover.de)

<sup>1</sup>Institute of Quantum Optics, Leibniz University Hannover, Hannover, Germany <sup>2</sup>Lower Saxony Center for Biomedical Engineering, Implant Research and Development (NIFE), Hannover, Germany <sup>3</sup>Department of Prosthetic Dentistry and Biomedical Materials Science, Hannover Medical School, Hannover, Germany

**Abstract:** FTIR spectroscopy in combination with machine learning is a powerful and well-established tool for the classification of bacterial species with high discriminatory power even at strain level. However, in clinical applications bacteria are often encountered in mixed biofilms which are difficult to distinguish with classical machine learning algorithms. For this purpose, we propose a 1D Convolutional Autoencoder Regressor Network, that is capable of predicting the concentration of six oral bacterial species with an MAE of 0.013 in mixed samples.

**Keywords:** multispecies samples, oral bacteria, classification, FTIR, deep learning, 1D-CNN

## Introduction

Oral diseases, like periodontitis, are associated with multispecies biofilms. The composition of these biofilms plays a crucial role in their pathogenicity.[1] Fourier transform infra-red spectroscopy (FTIR) is a label-free method, that probes the chemical composition of a given sample. It has proven to be capable of classifying bacterial species with high accuracy especially in combination with machine learning (ML) in single species samples.[2] FTIR spectra of mixed samples, however, show subtle differences that linear ML algorithms are not able to extract. In contrast, deep learning algorithms are capable of extracting and learning these highly non-linear features.

## Results and Discussion

The network, developed in this work, contains several convolutional layers and an autoencoder for feature extraction. The last layer is a regression layer, that assigns a concentration value to each component in the mixture as the output. The dataset used to train and test the network consisted of 10 samples, each containing six species at varying concentrations. Two additional samples, containing the same species but at previously unknown concentrations was used to stress test the network. To evaluate the performance, the mean absolute error (MAE) was calculated. The network was able to predict the concentrations of the test set with high accuracy and a MAE of 0.013. In the next step, the ability of the network to generalize the learned features was tested by predicting unknown concentrations. The prediction results can be seen in Figure 1. The MAE of the predictions increased slightly to 0.041.

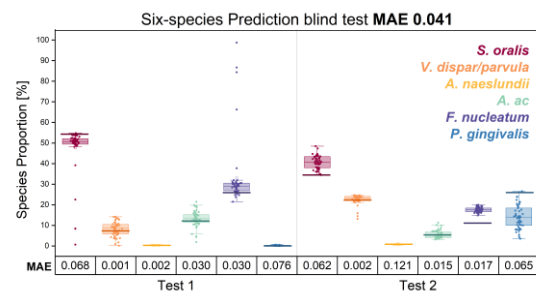


**Figure 1:** Predictions of unknown samples containing six different oral bacterial species. Coloured bars denote the real concentrations, boxes represent the predicted values.

## Conclusions

The analysis pipeline developed in this work, based on FTIR and deep learning allows for highly accurate prediction of concentration in multispecies samples. It shows high potential to be a label free and fast method for the composition analysis of mixed bacterial samples in laboratory settings.

## References

- [1] S. S. Socransky et. al., "Periodontal microbial ecology," *Periodontol.* 2000, 38, 135–187, 2005, doi: 10.1111/j.1600-0757.2005.00107.x.
- [2] Â. Novais, et. al., "Fourier transform infrared spectroscopy: unlocking fundamentals and prospects for bacterial strain typing," *Eur. J. Clin. Microbiol. Infect. Dis.*, 38, 3, 427–448, 2019, doi: 10.1007/s10096-018-3431-3.

## Acknowledgements

Funded by the Deutsche Forschungsgemeinschaft (DFG, German Research Foundation) – SFB/TRR-298-SIIRI – Project-ID 426335750

# Effective contact-area investigation in polymer-based TENGs

Philipp Mattauch<sup>1</sup>, Annika Hilgert<sup>2</sup>, Stephan Tremmel<sup>2</sup>, Gerhard Fischerauer<sup>1</sup>

Philipp.Mattauch@uni-bayreuth.de

<sup>1</sup>Measurement and Control Systems and Center for Energy Technology (ZET), Faculty of Engineering Science, University of Bayreuth, Universitätsstraße 30, 95447 Bayreuth, Germany

<sup>2</sup>Engineering Design and CAD, Faculty of Engineering Science, University of Bayreuth, Universitätsstraße 30, 95447 Bayreuth, Germany

**Abstract:** This study investigates the relationship between the electrical output produced by triboelectric nanogenerators (TENGs) due to contact electrification and the effective contact area during sliding motion. Polymer foils were tested against aluminium in controlled process and environmental conditions. The results show a clear trend between increasing transferred charge and an estimated larger contact area. Time-resolved measurements suggest that changes in contact conditions (e.g. due to flattening or wear) play a key role in electrical output.

**Keywords:** contact electrification; sliding mode; surface charge density; effective contact area

## Introduction

Contact electrification describes the process of two materials exchanging charges when brought into contact. The number of charges exchanged mainly depends on the specific materials used and, supposedly, the effective contact area [1]. Separating the two materials generates a voltage due to the charge accumulation and the resulting electric field. Adding electrodes to the materials and connecting them with a load impedance generates an electric current due to charge induction. In the special case of short-circuited electrodes this current is proportional to the relative movement of the contact partners [2].

In this work, we investigate the connection between the electrical output and the effective contact area at constant process and environmental conditions. We use Polyimide (PI) and Polytetrafluorethylen (PTFE) foils with thicknesses of 75  $\mu\text{m}$  and 80  $\mu\text{m}$ , respectively, and a cross-sectional area of 20 x 30  $\text{mm}^2$ . The contact partner is always aluminium foil with a thickness of 80  $\mu\text{m}$ . All experiments were carried out at a sliding rate of 3 Hz and a normal preload of 3 N for 1 hour, the ambient temperature was 20  $^{\circ}\text{C} \pm 1^{\circ}\text{C}$  and the relative humidity 45 %RH  $\pm$  5 %RH.

## Results and Discussion

Figure 1a shows the number of charges transferred during each sliding cycle over the estimated contact area calculated from microscopic images and laser scanned height profiles. Although there is a high variance both in the electrical output and the estimated contact area, a strong trend where higher contact areas lead to higher electrical outputs is observed. However, regarding Figure 1b we see that the behavior over the testing duration of 1 h is very different between specimen. Although almost all

specimen show a characteristic running-in behavior, presumably flattening the contact surfaces and therefore increasing the real contact area, some show a huge decrease that might be caused by severe wear.

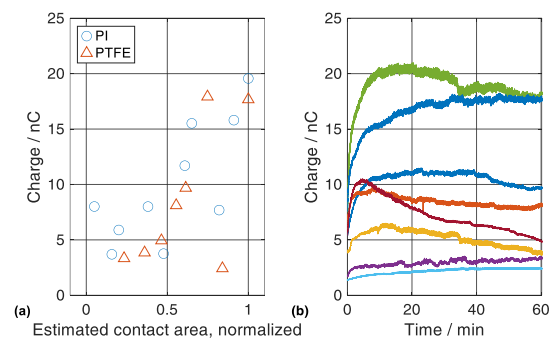


**Figure 1:** (a) Transferred charge per sliding cycle after 1 hour over the estimated contact area. (b) Comparison of the time-resolved evolution of the transferred charges generated by PTFE.

## Conclusions

The results suggest a high correlation between the number of charges transferred and the estimated contact area based on wear tracks. Further investigations are needed to understand the contact mechanisms behind the running-in and falling-off behaviours.

## References

- [1] Y. Zi, S. Niu, J. Wang, et al. Nat Commun 6, 8376 (2015). <https://doi.org/10.1038/ncomms9376>
- [2] D. Mulvihill, R. Mukherjee, Y. Xu, et. al. Adv. Energy Mater 15, 44 (2025). <https://doi.org/10.1002/aenm.202502920>

## Acknowledgements

Funded by the Deutsche Forschungsgemeinschaft (DFG, German Research Foundation) – 527445509

# Finite element modelling for gentle removal of total hip arthroplasties by means of induction heating

P. Evers<sup>1</sup>, M. Reulbach<sup>2</sup>, S. Herbst<sup>1</sup>, E. Jakubowitz<sup>2</sup> and F. Nuernberger<sup>1</sup>  
evers@iw.uni-hannover.de

<sup>1</sup>Institut für Werkstoffkunde (Materials Science), Leibniz Universität Hannover, An der Universität 2, 30823 Garbsen, Germany

<sup>2</sup>Laboratory for Biomechanics and Biomaterials (LBB), Department of Orthopaedic Surgery, Hanover Medical School, Anna-von-Borries-Strasse 1-7, 30625 Hanover, Germany

**Abstract** This work describes a finite element model for the induction heating of hip endoprostheses for facilitated intentional removal during revision surgery. The aim of the procedure is the softening of the thermoplastic bone cement around the endoprostheses to lower extraction forces and thus conserve surrounding tissue, while facilitating the removal of cemented implants from the medullary cavity. This has the potential to significantly reduce recovery times and improve the stability of revision arthroplasties.

**Keywords:** total hip arthroplasty; induction heating; revision surgery; finite element modelling

## Introduction

Revision surgeries account for approximately 10 % of all total hip arthroplasty procedures in OECD countries [1]. In this procedure a defective hip implant is removed from its seat through hammering and chiseling, carrying a significant risk of damaging the surrounding femur, which leads to increased convalescence periods and decreased stability of the newly implanted endoprosthesis [2]. A promising approach to reduce the necessity of mechanical removal techniques is the use of alternating magnetic fields to increase the implant temperature and thus soften the surrounding bone cement [3], reducing extraction forces. To not thermally damage the femur, heating must be applied precisely and homogeneously. For prediction of the temperature distribution with regard to inductor geometry, a finite element model was created in ANSYS Mechanical.

## Results and Discussion

A three-dimensional finite element simulation was built using ANSYS Mechanical 2025 R2. For this, a simplified implant geometry adapted from a Zimmer Biomet Mueller straight stem was positioned inside a helical inductor. A single-plane symmetry was used. The solution step was split into an electromagnetic and a thermal task, which were run alternately. In this way, the influence of temperature increase on the material properties could be accounted for. A validation of the model was conducted by means of heating experiments of the aforementioned implant geometry in a testbed with an induction heating generator eldec MFG 30. The surface temperature of the implant was measured using infrared thermography and compared to the computations with regard to absolute maximum temperature and temperature distribution.

The resulting surface temperature distribution is depicted exemplarily for a heating time of 16.5 s in Figure 1a for the simulation and in Figure 1b as determined in the experiment.

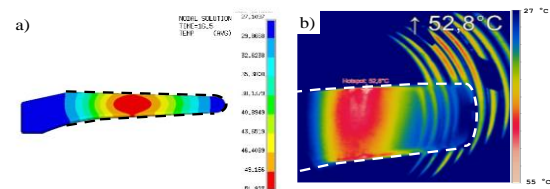


**Figure 1:** Simulated (a) and experimentally determined (b) temperature distributions on the surface of the hip implant.

Thus, the in-silico model was successfully validated with thermography measurements.

## Conclusions

The finite element model enables prediction of temperature distributions for induction heating of hip implants in revision surgeries. This allows for the design of implant specific inductors and heating regimens to facilitate intentional implant removal with minimal thermal and mechanical damage of the surrounding tissue.

## References

- [1] A. Grimberg, J. Lützner, O. Melsheimer, et al., EPRD Jahresbericht 2023. DE: EPRD Endoprothesenregister Deutschland, 2023
- [2] B. A. Masri, P. A. Mitchell, and C. P. Duncan, “Removal of Solidly Fixed Implants During Revision Hip and Knee Arthroplasty” J. Am. Acad. Orthop. Surg., 2005;13(1):18–27, doi: 10.5435/00124635-200501000-00004
- [3] M. Reulbach et al., “Implications of ageing effects on thermal and mechanical properties of PMMA-based bone cement for THA revision surgery,” J. Mech. Behav. Biomed. Mater. 2023, doi: 10.1016/j.jmbbm.2023.106218.

## Acknowledgements

This work has been funded by the Deutsche Forschungsgemeinschaft (German Research Foundation) SFB/TRR 298 SIIRI Project ID 426335750.

# Green Chemistry Meets Thermal Sensing: Sustainable Metal MIP-based Sensors for L-Leucine Detection

Ana I. Furtado<sup>1</sup>, Joseph W. Lowdon<sup>1</sup>, Vasco D.B. Bonifácio<sup>2</sup>, Raquel Viveiros<sup>3</sup>, Teresa Casimiro<sup>3</sup>, Bart van Grinsven<sup>1</sup>

[ana.carreirofurtado@maastrichtuniversity.nl](mailto:ana.carreirofurtado@maastrichtuniversity.nl) (Corresponding e-mail address)

<sup>1</sup>Sensor Engineering department, Maastricht University, Institute, University, Duboisdomein 30, 6229 GT, Maastricht, The Netherlands

<sup>2</sup>iBB–Institute for Bioengineering and Biosciences and i4HB–Institute for Health and Bioeconomy, Instituto Superior Técnico, University of Lisbon, Portugal

<sup>3</sup>LAQV–REQUIMTE, Chemistry Department, NOVA School of Science & Technology, NOVA University of Lisbon, Campus de Caparica, 2829–516, Caparica, Portugal

**Abstract:** A combination of green, scalable strategies were developed for fabricating metal MIP-based receptor layers on thermal sensors. Mechanochemistry was employed for the solvent-free synthesis of metal-based monomers and MIPs. The resulting MIP particles were then deposited onto aluminium substrates via a microcontact method. In parallel, supercritical carbon dioxide (scCO<sub>2</sub>)-assisted polymerization was also used to produce MIP particles, which were subsequently deposited onto aluminium substrates. Additionally, scCO<sub>2</sub>-assisted polymerization on plasma-activated aluminium substrates was explored for direct MIP grafting. All types of sensors were applied for the selective isomeric recognition of L-leucine (LEU).

**Keywords:** Mechanochemistry; Supercritical fluids; Plasma activation; Molecular Imprinting; Thermal biosensors .

## Introduction

Plastic antibodies, known as Molecularly Imprinted Polymers (MIPs), enable the selective recognition of target molecules in biosensors [1]. Conventional MIP synthesis often relies on organic solvents, extensive post-processing, and complex substrate functionalization, which limit scalability and sustainability [2]. Mechanochemistry operates under solvent-free conditions using low-cost equipment and enables rapid polymerization, overcoming solubility issues and reducing production costs [3]. On the other hand, scCO<sub>2</sub> acts as a tunable, green solvent, enabling efficient polymerization and template removal, while plasma activation promotes direct surface functionalization [4]. These green technologies were employed to fabricate metal MIP-based receptor layers on thermal sensors.

## Results and Discussion

Using L-leucine (LEU) as a model analyte and MIPs incorporating metal-based monomers, such as beryllium complexes, were produced. The MIPs particles exhibited high binding affinity (imprinting factors of 12 for the scCO<sub>2</sub> approach and 5 for the mechanochemical approach). Thermal sensors were successfully fabricated, achieving isomeric selectivity factors against L-isoleucine of 1.8, 3.8, and 1.7 for ball-milled MIP particle-deposited substrates, scCO<sub>2</sub> MIP particle-deposited substrates, and grafted substrates, respectively, which are comparable/superior to reported sensors.

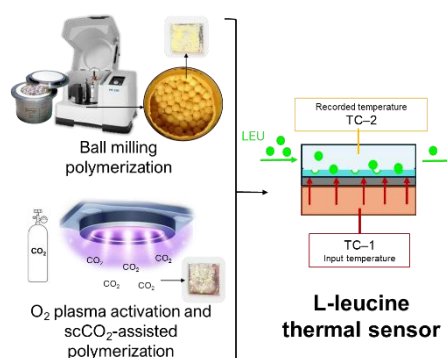


**Figure 1:** The used green technologies for the fabrication of MIP-based L-leucine thermal sensors.

## Conclusions

These strategies showed to be promising for sustainable, cost-effective routes for large-scale MIP-based biosensing platforms.

## References

- [1] Li Y. et al., *Biosens. Bioelectron.*, 2024, 249, 116018. <https://doi.org/10.1016/J.BIOS.2024.116018>.
- [2] Cutiaia A., Alberti G., *Polymers*, 2026, 18, 512. <https://doi.org/10.3390/polym18040512>
- [3] Furtado A.I. et al., *Biosens. Bioelectron.* X, 2025, 1, 100605. <https://doi.org/10.1016/J.BIOSX.2025.100605>.
- [4] Furtado A.I. et al., *Molecules*, 2024, 29, 926. <https://doi.org/10.3390/MOLECULES29050926>.

## Acknowledgements

A.I.F. PhD grant (SFRH/BD/150696/2020) from SPQ and FCT/MCTES, YERUN 2022 award and STSM grant funded by COST under CA21101 Action.

# Mussel-Inspired Nanoprecipitation Coatings for Complex Geometries

Maren Leuker<sup>1</sup>, Romina Berger<sup>1</sup>, Marie Weinhart<sup>1,2</sup>

maren.leuker@pci.uni-hannover.de, marie.weinhart@pci.uni-hannover.de

<sup>1</sup>Institute for Physical and Electrochemistry, Leibniz Universität, Callinstraße 3a, 30167 Hanover, Germany

<sup>2</sup>Institute for Chemistry and Biochemistry, Freie Universität Berlin, Takustraße 3, 14195 Berlin, Germany

**Abstract:** The need to prevent device-associated infections (DAIs) motivates the development of innovative surface coatings. We established a long-term stable, protein-repellent hydrogel coating on polydimethylsiloxane (PDMS), generated via straightforward nanoprecipitation and catechol crosslinking, that is now translated to complex 3D geometries such as cochlear implants. Furthermore, this coating approach is extended to cationic polymers, enabling surfaces with inherent contact-active antimicrobial properties.

**Keywords:** functional surface coating; PDMS; implant coating; bioactive coatings

## Introduction

PDMS is widely used in medical devices for its flexibility and biocompatibility. However, its inherent hydrophobicity and chemical inertness promote protein adsorption and subsequent bacterial adhesion, thereby contributing to DAIs.<sup>[1]</sup> To address this, we developed a long-term stable ( $\geq 90$  days) mussel-inspired copolymer coating based on the protein-repellent poly(hydroxyethyl acrylamide) (P1, Figure 1B). Additionally, incorporated catechol units mediate coating formation by nanoprecipitation with simultaneous crosslinking and surface immobilization (Figure 1A). In defined solvent/non-solvent mixtures, polymer colloids form and deposit on plasma-activated PDMS, yielding covalently anchored hydrogel films upon thermal crosslinking (coating thickness:  $44 \pm 7$  nm, water contact angle (WCA):  $61 \pm 16^\circ$ ).<sup>[2]</sup>

Building on this coating strategy, we aim to extend the nanoprecipitation platform to 3D geometries using cationic polymers that confer additional contact-active<sup>[3]</sup> antimicrobial function.

## Results and Discussion

The contact-active polymers (Figure 1C), where prepared from either poly(dimethylaminoethyl methacrylate) (P2) or poly(dimethylaminopropyl methacrylamide) (P3) by quaternization of the amino groups, providing a permanent positive charge to the catechol-bearing copolymers.

Given the polyelectrolyte nature of these systems, solvent/non-solvent composition, ratio and ionic strength were adjusted to enable an efficient coating process. Both cationic polymers formed smooth coatings with WCAs of  $63 \pm 10^\circ$  and tuneable thicknesses of 35-135 nm on planar PDMS.

To adapt the coating procedure to clinically relevant 3D geometries, we investigate the coating of tubular PDMS substrates via controlled rotation. Initial

experiments, employing a coating duration analogous to planar substrates, demonstrated a  $\sim 30^\circ$  decrease in WCA compared to uncoated controls, indicating effective transfer to cylindrical geometries. Rotation speed and coating time are now systematically investigated to optimize film formation.

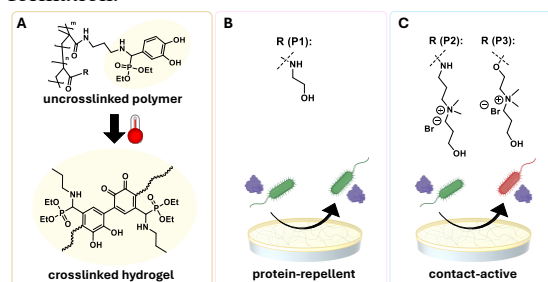


**Figure 1:** A) Nanoprecipitation and subsequent catechol-mediated thermal crosslinking, provides access to covalently anchored B) protein-repellent or C) contact-active coatings on PDMS.

## Conclusions

Transition from protein-repellent to contact-active PDMS coatings with 3D-transferability highlights the versatility of the nanoprecipitation approach. Furthermore, hydroxyl groups present in all polymers enable subsequent functionalization for advanced applications.

## References

- [1] I. Miranda, et al, Properties and Applications of PDMS for Biomedical Engineering: A Review. *J Funct Biomater.* **2021** doi: 10.3390/jfb13010002.
- [2] R. Berger, et al. Stable, bioactive hydrogel coating on silicone surfaces for non-invasive decontamination via photochemical treatment. *Bioactive Materials.* **2025** doi: 10.1016/j.bioactmat.2025.07.052.
- [3] Y. Xue, et al. Antimicrobial Polymeric Materials with Quaternary Ammonium and Phosphonium Salts. *Int J Mol Sci.* **2015** doi: 10.3390/ijms16023626.

## Acknowledgements

We gratefully acknowledge financial support from the DFG via TRR 298 "SIIRI" (Project B08; project number 426335750).

# MatrixModel: Building a Computational Model of the HSPC Niche

Julia Käsehagen<sup>1</sup>, Sophia Rudolf<sup>1</sup>

kaeshagen@cell.uni-hannover.de

<sup>1</sup>Institute of Cell Biology and Biophysics, Leibniz University Hannover, Herrenhäuser Straße 2, 30419 Hannover, Germany

**Abstract:** Hematopoietic stem and progenitor cells (HSPCs) rely on finely tuned adhesion to the extracellular matrix (ECM) in the bone marrow niche to maintain quiescence, self-renewal, and differentiation. As part of the MatrixEvolution consortium, Matrix Model develops a multiscale computational framework to predict how ECM composition, architecture and mechanics regulate HSPC behaviour. We implemented pipelines to use and adapt models by other groups: (i) a mechanochemical ODE model of integrin-talin-vinculin adhesion dynamics [1] and (ii) a hybrid Cellular-Potts-Bead-Spring model of ECM fibre networks [2].

**Keywords:** hematopoietic stem cells, extracellular matrix, computational modelling, adhesion dynamics

## Introduction

The bone marrow niche is soft heterogenous, and fibre-rich (fibronectin, laminins, collagens). HSPCs use specific integrins and rapid, small adhesions, rather than large focal adhesions, to maintain in contact with their microenvironment. How ECM density, stiffness, and fibre alignment jointly govern HSPC adhesion strength remains poorly quantified. We address this with a dual-model strategy spanning molecular adhesion kinetics to cell-matrix mechanics.

## Results and Discussion

The model of adhesion formation by Honasoge et al. [1] consists of 17 coupled ODEs capturing integrin activation and binding, talin engagement and unfolding, and vinculin recruitment. The mechanics include force-dependent on/off rates, load sharing across molecular clutches, and feedback from talin extension. With this model we can calculate adhesion lifetimes, traction per adhesion, and reinforcement kinetics. We can predict sensitivity to perturbations.

This output will be used to derive adhesion rules that will then be put into the hybrid cellular-Potts-Bead-Spring model by Tsingos et al. [2]. The Cellular Potts model models the HSP-cell based on shape, area conservation, and adhesion energy. The matrix is modelled as a bead-spring fibre network. The cell and ECM fibres are coupled through integrin-mediated links between cell membrane and nearby fibres. We will adapt the model, so that adhesions are dynamic and can be assembled and disassembled during simulation. With the adapted model we can predict migration speed, contact area, traction patterns, and ECM remodelling.

## Conclusions

By combining two different computational frameworks, we will gain mechanistic insights into how ECM mechanics and architecture regulate HSPC anchorage and motility. We want to produce

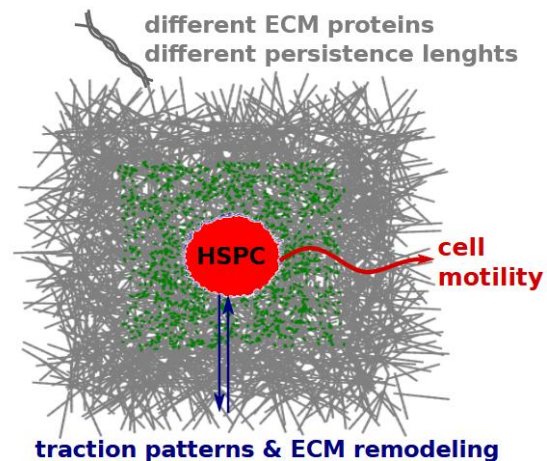


**Figure 1:** Visualisation of the hybrid Cellular-Potts-Bead-Spring model. HSPCs interact with the surrounding ECM fibres. Depending on the ECM stiffness and architecture, HSPCs remodel the ECM. Cell motility is influenced by matrix stiffness.

predictive maps that can guide microenvironment engineering for HSPC maintenance and expansion in vitro.

## References

- [1] K.S. Honasoge et al., PLoS Comput Biol 19, 10, (2023). <https://doi.org/10.1371/journal.pcbi.1011500>
- [2] E. Tsingos et al, Biophysical Journal, 122 (2023). <https://doi.org/10.1016/j.bpj.2023.05.013>

## Acknowledgements

This work is funded by zukunft.niedersachsen, the joint science funding program of the Lower Saxony Ministry of Science and Culture and the Volkswagen Foundation. J.K. is supported by the Caroline Herschel Programm of the Leibniz Universität Hannover.

# Adjacent Hydrogel Thin-Films for a competitive cell culture assay

Julian Baron<sup>1</sup>, Chaymae Boukari<sup>1,2</sup>, Evelin Miller<sup>1</sup>, Christian Hiepen<sup>1</sup>, Michael Veith<sup>1</sup>  
[julian.baron@w-hs.de](mailto:julian.baron@w-hs.de)

<sup>1</sup>Dept. Engineering and natural sciences, Westphalian University of Applied Sciences, August-Schmidt-Ring 10, 45665 Recklinghausen, Germany

<sup>2</sup>Dept. of Prosthetic Dentistry and Biomedical Materials Science, Hannover Medical School, Carl-Neuberg-Str. 1, 30625 Hannover, Germany

**Abstract:** This project presents a novel spin-coating approach for the fabrication of laterally adjacent hydrogel thin films using a custom-designed spin coater attachment. The system enables the sequential deposition of two distinct hydrogel formulations on a single substrate, resulting in vertically defined interfaces with tuneable physicochemical properties. Current efforts focus on optimizing hydrogel composition and spin-coating parameters to achieve reproducible and well-defined film thicknesses. Subsequently, the platform will be applied to 2D cell culture studies to investigate cell adhesion and migration behaviour on bioactive hydrogel interfaces under controlled conditions.

**Key words:** bioink, spin-coater, surface, coating, attachment, cell culture

## Introduction

In this project, a method for coating two laterally adjacent hydrogel thin films was developed. The process is enabled through the design of a novel attachment for a spin coater (Fig. 1). The surfaces are coated with a hydrogel-based system that has been developed as a prospective bioink for the 3D bioprinting of organoids. In particular, the material and cell-biological properties are critical determinants of cellular behaviour in culture systems<sup>[1]</sup>. The primary objective is to prevent migration between different cell types located in two adjacent layers.

## Results and Discussion

For the application of hydrogels in the spin-coating process, key physicochemical parameters are critical to ensure the reproducible fabrication of films with defined thicknesses. The film thickness of a non-Newtonian fluid can be approximated using the fundamental spin-coating equation<sup>[2]</sup>:

$$h = \left( \frac{K}{\rho\omega t} \right)^{\frac{n}{2n+1}}$$

The resulting film thickness is predominantly determined by both material-specific and process-related parameters.

Figure 1 illustrates the technical drawing of the spin coater attachment, which is designed for coating standard-sized glass slides and is fabricated from polypropylene (PP). During the coating process, one half of the glass slide is covered by a rigid aluminum plate with minimal mass and fixed in place using PP screws. Once the hydrogel has gelled, the aluminum plate is removed and repositioned to cover the already coated region.

A second spin coating step is then performed, in which the previously uncoated half of the substrate is functionalized with a different hydrogel. This process enables the formation of a lateral separated interface between two distinct hydrogels with tuneable and differential properties

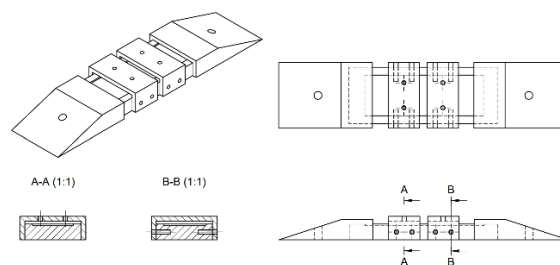


**Figure 1:** Spin coater attachment for the coating process of laterally adjacent polymer-based thin films

## Conclusion

Initial experiments using the developed spin coater attachment have already been successfully conducted. The system demonstrated stable and reliable operation without disruptive effects during rotation. The initially produced layers already exhibited the desired formation of vertically defined hydrogel interfaces. Nevertheless, both the process parameters and the hydrogel composition require further optimization in order to reliably achieve well-defined and reproducible film thicknesses.

## References:

- [1] Revach OY, Grosheva I, Geiger B. Biomechanical regulation of focal adhesion and invadopodia formation. *J Cell Sci.* 2020 Oct 22;133(20):jcs244848. doi: 10.1242/jcs.244848. PMID: 33093229.
- [2] Chen, D., Yoon, J., Chandra, D., Crosby, A.J. and Hayward, R.C. (2014), Stimuli-responsive buckling mechanics of polymer films. *J. Polym. Sci. Part B: Polym. Phys.*, 52: 1441-1461. <https://doi.org/10.1002/polb.23590>

# Establishment of personalized immunocompetent 3D peri-implant-mucosa models using patient-derived macrophages

Raunak Lohar<sup>1</sup>, Amit Gaikwad<sup>1</sup>, Andreas Winkel<sup>1</sup>, Szymon Piotr Szfranski<sup>1</sup>, Muhammad Imran Rahim<sup>1</sup>, Meike Stiesch<sup>1</sup>

Lohar.raunak@mh-hannover.de

<sup>1</sup>Department of Prosthetic Dentistry and Biomedical Materials Science, Lower Saxony Centre for Biomedical Engineering, Implant Research and Development (NIFE), Hannover Medical School, Hannover, Germany

**Abstract:** Biomaterial-associated infections remain a major clinical challenge. Here, a primary cell-based peri-implant 3D model, incorporating patient-derived macrophages and human gingival fibroblasts, was developed to investigate biohybrid implants and host-biofilm interactions. Co-cultivation of the 3D with patient-derived biofilm demonstrated reduced bacterial burden, improved tissue attachment to titanium, and preserved tissue integrity, highlighting its potential for studying host-implant-biofilm interactions and evaluating next-generation biohybrid implant surfaces.

**Keywords:** dental implants; peri-implantitis; oral mucosa model; primary monocytes; macrophages; oral biofilms

## Introduction

Biomaterial-associated infections remain a major clinical challenge, as conventional antibiotic treatments often exhibit limited effectiveness against biofilm-associated pathogens. To address this problem, biohybrid titanium implants with anti-biofilm, immunomodulatory, and osteoregulatory properties were previously developed and evaluated in 3D INTER<sub>b</sub>ACT model [1]. Here, a patient-derived primary macrophage-based 3D model was developed to better replicate physiological host responses for testing biohybrid implants and assessing interpatient variability related to age and gender.

## Results and Discussion

Primary monocytes were isolated from the blood of patients using PBMC density-gradient separation and CD14<sup>+</sup> magnetic sorting. Following differentiation into macrophages, cells were incorporated with autologous gingival fibroblasts into a collagen-based matrix to establish a patient-derived oral peri-implant tissue model. Titanium cylinders were implanted into the tissues prior to 24h exposure to a host-derived multispecies oral biofilm.

Preliminary results (Figure 1) showed significantly reduced OD<sub>600</sub> values in macrophage-containing cocultures compared with macrophage-free controls, indicating reduced bacterial burden. Histological analysis further demonstrated improved mucosal attachment to titanium in macrophage-enriched tissues. Together, these findings suggest that primary macrophages remained functional within the host-implant-biofilm model and contributed to preservation of tissue integrity under biofilm challenge.

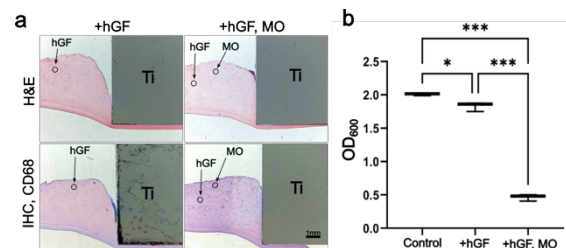


**Figure 1:** a. Histology of mucosa models after 24 h biofilm exposure showing fibroblast and macrophage distribution (CD68-HRP stained) within the tissue matrix (pink/violet). b. OD<sub>600</sub> values of tissue-biofilm coculture media.

## Conclusions

The patient-derived macrophage-based oral peri-implant model provides a clinically relevant platform for studying host-implant-biofilm interactions. Incorporation of primary macrophages reduced bacterial burden, improved tissue attachment to titanium, and preserved tissue integrity under biofilm challenge, supporting its use for evaluating next-generation biohybrid implant surfaces.

## References

- [1] Lohar et al., Commensal Microbiota-Coated Biohybrid Implants Induce Antibiofilm, Osteogenic, and Immunomodulatory Responses in a Human 3D Immunocompetent Model. Preprint: <http://dx.doi.org/10.2139/ssrn.5507958>

## Acknowledgements

Funded by the Deutsche Forschungsgemeinschaft (DFG, German Research Foundation) – SFB/TRR-298-SIIRI – Project-ID 426335750 and ALLEGRO program funded by the Lower Saxony Ministry for Science and Culture, Germany.

# Systematic study of Ytterbium influence in binary alloying systems

Manuel Hofinger<sup>1</sup>, Achim Walter Hassel<sup>1,2</sup>

manuel.hofinger@jku.at

<sup>1</sup> Institute of Chemical Technology of Inorganic Materials, Johannes Kepler University Linz, Altenberger Straße 69, 4040 Linz, Austria

<sup>2</sup> Danube Private University, Steiner Landstraße 124, 3500 Krems an der Donau,

## Abstract:

The presented work employs combinatorial approaches to investigate how Yb alloying influences properties in Al-, Mg-, and Ti-binary alloys. Microstructure, crystallography and morphology of thin film libraries with compositional gradients and corresponding bulk alloys were investigated. Scanning droplet cell microscopy was performed for the measurements of corrosion properties and the characterisation of the oxide layer. The high throughput analysis showed a generally beneficial influence on the corrosion resistance on thin film libraries and a segregation of the oxide layers through anodisation.

**Keywords:** Ytterbium, combinatorial studies, microelectrochemistry, binary alloys

## Introduction

Rare earth elements (REE) attracted special interest in recent years in different research areas and industrial applications. While light REE like Nd or Sm are already established in the industry for different applications like magnets or electric motors, the utilization of heavy REE remains still quite narrow [1]. This thesis focuses on alloying of the heavy REE Yb and how it can be employed to enhance certain properties of different metals and alloys. Due to the selected combinatorial approaches in this work, different material properties were studied in alloys containing a variety of Yb concentrations.

## Results and Discussion

Alloy composition, crystallography, morphology, microstructure and elemental distribution were studied by employing different methods such as energy dispersive X-ray (EDX), spectroscopy, X-ray diffraction (XRD), scanning electron microscopy (SEM), transmission electron microscopy (TEM) or X-ray photoelectron spectroscopy (XPS). Also, inductively coupled plasma optical emission spectroscopy (ICP-OES) was used for the analysis of corrosion products during electrochemical testing in various electrolytes.

However, the main focus was set on electrochemical testing of co-deposited thin film libraries with a compositional gradient in binary alloy systems. Additionally, bulk alloys were studied to compare the similarity of the properties to combinatorial thin films. Scanning droplet cell microscopy (SDCM) was used for the analysis of the libraries to generate a high compositional resolution of different tested

alloys and ensure a high throughput investigation of the systems.

The behaviour of Yb was investigated in alloys containing either Al, Mg or Ti. With this microelectrochemical approach, the oxide formation through anodization and the corrosion behaviour were studied in these systems. Through stepwise potentiodynamic polarization the film-formation factor  $k$  and the dielectric constant  $\epsilon_r$  were investigated in an Al-Yb thin film library [2]. For Mg the influence of Yb on the corrosion behaviour before and after anodization was compared and the reproduction on bulk was investigated. Ti-Yb thin films were investigated in regards of  $k$  and  $\epsilon_r$ , as well as on the change of the corrosion rate  $cr$  and the corrosion potential  $E_{\text{corr}}$  during the anodization process. Anodic memristors were subsequently produced from this system due to the findings of the oxide layer segregation in this system.

## Conclusions

It was found that alloying these elements with Yb has generally a beneficial influence on the corrosion behaviour and leads to segregations in the oxide during anodization. These findings can be further used for defect engineering and provides the opportunity to use these alloys for novel application such as anodic memristors.

## References

- [1] V. Balaram, Geosci. Front. 10, 4 (2019) 1285-1303. <https://doi.org/10.1016/j.gsf.2018.12.005>
- [2] M. Hofinger, A.I. Mardare, J. Duchoslav, et al. Electrochim. Acta 540 (2025) 147018. <https://doi.org/10.1016/j.electacta.2025.147018>

# Fully Additive Neural Implants ... and understanding why they fail

Adrian Onken<sup>1</sup>, Esma Dosdogru, Boutaina Zerrik, Emily Eiken, Theo Doll

Onken.Adrian@mh-hannover.de

<sup>1</sup>NIFE; BioMaterial Engineering, Hannover Medical School, Carl-Neuberg-Str. 1, 30625 Hannover, Germany

**Abstract:** This work presents a fully additive manufacturing approach for flexible neural implants using multi-material direct ink writing. Besides fabrication and functional integration, diffusion-driven degradation processes at polymer–metal interfaces were investigated to better understand long-term failure mechanisms. Combining additive fabrication with interface analysis enables iterative design improvements towards more reliable bio-integrated implant systems.

**Keywords:** 3D printing; neural interfaces; diffusion-driven degradation; PDMS; implant engineering

## Introduction

Additive manufacturing offers a promising route towards flexible, application-specific neural implants with integrated functionality. Compared to conventional fabrication methods, direct ink writing enables the deposition of multiple materials within a single process, allowing the realization of soft, multilayer electrode architectures. A fully additive manufacturing workflow based on multi-material direct ink writing was developed to fabricate flexible neural implants using PDMS as structural material and conductive paste for electrical traces. The process enables layer-by-layer deposition of functional structures and direct integration onto flexible printed circuit boards, eliminating the need for post-fabrication contacting. In parallel, simplified model systems were employed to investigate diffusion-driven degradation mechanisms at polymer–metal interfaces, with particular focus on the interaction between encapsulation layers and conductive elements. These degradation processes are considered a critical factor for long-term implant reliability and therefore need to be addressed already during device design and manufacturing.

## Results and Discussion

Functional 20-channel neural implants for rat models were successfully fabricated and integrated into experimental setups, demonstrating reliable electrical performance and mechanical flexibility while maintaining a comparatively high electrode density. The additive workflow enables high design freedom and scalable production of application-specific devices. At the same time, diffusion studies revealed that fluid ingress at polymer–metal interfaces can initiate delamination processes, leading to accelerated degradation and potential failure. These findings highlight the importance of minimizing interfacial pathways and structural inhomogeneities during fabrication. Consequently, design and process adaptations were derived to improve structural integrity and reduce susceptibility to diffusion-driven damage.

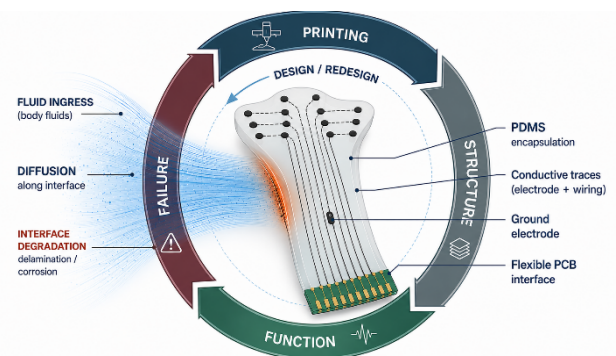


**Figure 1:** Design concept of a fully additive neural implant workflow, linking fabrication, functional performance, diffusion-driven degradation, and iterative redesign within a continuous engineering feedback loop.

## Conclusions

This work demonstrates the feasibility of fully additive neural implant fabrication while emphasizing the necessity of integrating material-level understanding into the design process. Future developments will focus on advanced material systems, such as hydrogel-based encapsulation strategies, to further improve biocompatibility and long-term stability. The combination of fabrication and failure analysis represents a key step towards robust, next-generation bio-integrated implant systems.

## References

- [1] Li Y, Li B. Direct ink writing 3D printing of polydimethylsiloxane-based soft and composite materials: a mini review. *Oxford Open Materials Science*2022; [https://doi.org/10.1093/oxfmat/itac008]
- [2] Stieghorst J, Doll T. Toward 3D Printing of Medical Implants: Reduced Lateral Droplet Spreading of Silicone Rubber under Intense IR Curing. 2016; [https://doi.org/10.1021/acsami.5b12728]

## Acknowledgements

This study was funded by (DFG, German Research Foundation) – EXC 2177/1–Project ID 390895286

# Continuous Millifluidic Synthesis of ZnO Nanostructures

*Lena Arndt<sup>1</sup>, Sherif Okeil<sup>1</sup> and Georg Garnweitner<sup>1</sup>*

lena.arndt@tu-braunschweig.de

<sup>1</sup>Institute for Particle Technology and Laboratory for Emerging Nanometrology, Technische Universität Braunschweig, 38104 Braunschweig, Germany

**Abstract:** ZnO is a semiconductor material for which numerous synthesis protocols have been developed, including non-aqueous methods using benzyl alcohol. Here, ZnO nanostructures were synthesized in a continuous millifluidic system, enabling reduced reaction times. Process parameters affect both the particle size and aggregation behavior. Flow experiments reveal nucleation on precursor-derived structures followed by nanorod growth, aggregation, and breakup, providing new insight into the formation mechanism of ZnO nanostructures.

**Keywords:** ZnO; millifluidics; continuous flow; nanorods; non-aqueous synthesis

## Introduction

Due to the importance of ZnO as a semiconductor material that is used in many applications from gas sensing to biomedicine, a lot of synthesis protocols have been developed, including non-aqueous synthesis methods in benzyl alcohol [1,2]. However, the transfer of such non-aqueous approaches to continuous systems is still limited, despite their advantages of better reaction control and shorter reaction times due to enhanced heat transfer.

## Results and Discussion

In this work, the non-aqueous synthesis of ZnO nanostructures via the benzyl alcohol route was successfully implemented in a continuous millifluidic system, enabling significantly reduced reaction times. Variations in process parameters have an influence on the primary particle size and aggregation behavior. The system features efficient heat transfer, increased reaction kinetics, and straightforward variation of the residence time from 30 s to 5 min through adjustment of the flow rate. This provides an insight into the temporal evolution of ZnO nanostructures formed from zinc acetylacetonate hydrate in benzyl alcohol and offers the possibility to elucidate the growth mechanism in detail.

Continuous flow experiments indicate that ZnO nucleates on precursor-derived structures, which subsequently evolve into aggregated nanorod structures. With increasing residence time, the growing nanorods can reach high aspect ratios and form characteristic star-shaped aggregates (Figure 1), followed by breakup into individual nanorods. Higher temperatures and increased precursor concentrations accelerate this process. Compared to batch experiments, similar evolution occurs only at higher concentrations or longer reaction times, highlighting the accelerated reaction in the millifluidic system.

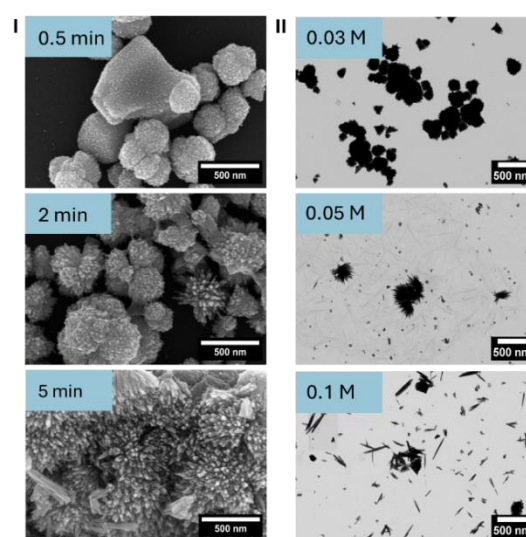


**Figure 1:** SEM (I) and STEM (II) images of ZnO nanostructures synthesized at 180°C for different residence times (I) and at different precursor concentrations after 2 min (II).

## Conclusions

Overall, these results highlight the potential of simple millifluidic reactor synthesis, due to its ability to easily vary reaction parameters and facilitate the observation of nanostructure evolution under different process conditions.

## References

- [1] B. Ludi, M. J. Süess, I. A. Werner and M. Niederberger, Mechanistic aspects of molecular formation and crystallization of zinc oxide nanoparticles in benzyl alcohol, *Nanoscale*, **2012**, 4, 1982–1995.
- [2] S. Okeil, J. Ungerer, H. Nirschl and G. Garnweitner, Synthesis of Anisotropic Metal Oxide Nanoparticles via Non-Aqueous and Non-Hydrolytic Routes, *KONA Powder Part. J.*, **2024**, 41, 197–220.

## Acknowledgements

This work was supported by the Deutsche Forschungsgemeinschaft (DFG, German Research Foundation (project No. 542142265).

# Corrosion Sensing for Cochlear Implants

Tatiana Blank<sup>1</sup>, Nils Prenzler<sup>2</sup>, Thomas Lenarz<sup>2</sup>, Christian Klose<sup>1</sup>, Hans Jürgen Maier<sup>1</sup>

[blank@iw.uni-hannover.de](mailto:blank@iw.uni-hannover.de)

<sup>1</sup>Institut für Werkstoffkunde (Materials Science), Leibniz Universität Hannover, An der Universität 2, 30823, Garbsen, Germany

<sup>2</sup>Department of Otolaryngology, Hannover Medical School, Carl-Neuberg-Strasse 1, 30625 Hannover, Germany

**Abstract:** Cochlear implants use platinum-based electrodes, which are prone to electrochemical corrosion; this impairs speech perception and poses cytotoxic risks due to the release of platinum. In the present study, electrochemical analysis of platinum is coupled with microstructural investigation. The aim is to link impurities, grain orientation, and mechanical deformation to corrosion. Preliminary data indicate that grain-boundary density is a key parameter. In addition, thiol-functionalised gold electrodes were developed as *in-situ* sensors, detecting platinum degradation via impedance changes. Ongoing work is examining the stability of gold layers and alternative coatings, such as protein-scavenging coatings, to deliver safer, more reliable implants.

**Keywords:** electrochemistry; material degradation; sensory electrode; platinum

## Introduction

Cochlear implants are a widely used solution for patients with profound hearing loss [1]. However, they face durability issues due to corrosion reactions affecting platinum electrodes. This corrosion diminishes the implants' effectiveness by impairing speech comprehension and overall functionality, and also introduces safety concerns due to the cytotoxic effects of dissolved platinum [2, 3].

## Results and Discussion

In order to investigate the cause of corrosion, various influencing factors, such as mechanical deformation, surface roughness, and grain boundary density, must be considered. The data obtained demonstrates that higher surface roughness and grain boundary density, as well as defects, worsen the corrosion behavior of the electrodes.

Additionally, long-term studies were conducted on cochlear implants, and the results were compared with those from explants. These clearly showed that, after just four weeks, the corrosion effects in the explants were similar to those in the implant.

To monitor corrosion and intervene early by adjusting the stimulation parameters a functional coating was developed. For this sensory electrode, which is intended to replace one of the existing electrodes, cf. Figure 1, various coatings were bound to the gold surface via a thiol linker. Electrochemical impedance spectroscopy demonstrated that this coating can capture platinum from the solution.

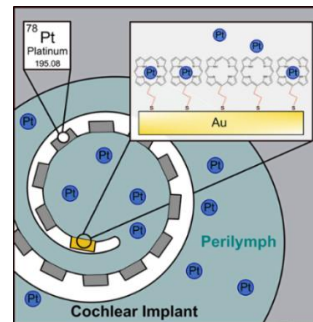


**Figure 1:** Schematic diagram illustrating how a sensory gold electrode works in a cochlear implant.

## Conclusions

The successful development of a coating that can be detected by impedance spectroscopy opens up the possibility of functionalizing it in different ways. For instance, it could be used to target proteins that are usually linked to inflammation. At the same time, the principle of this coating could be applied to other implant systems in the future.

## References

- [1] T. Lenarz, A. Büchner, A. Illg, *Laryngorhinootologie*, 101(S 01): S36-S78, (2022), doi: 10.1055/a-1731-9321
- [2] K. Wissel, G. Brandes, N. Pütz, G.L. Angrisani, J. Thieleke, T. Lenarz, M. Durisin, *PLOS ONE*, 5: e0196649, (2018), doi: 10.1371/journal.pone.0196649
- [3] R.K. Shepherd, P.M. Carter, Y.L. Enke, A. Thompson, B. Flynn, E.P. Trang, A.N. Dalrymple, J.B. Fallon, *J Neural Eng.*, 17:56009, Epub 2020/10/08, (2020), doi: 10.1088/1741-2552/abb7a6

## Acknowledgements

Financial support for this study by Deutsche Forschungsgemeinschaft (project number 426335750) is gratefully acknowledged.

# Streptavidin-based anti-adhesive biofunctionalization for dental implants

Chaymae Boukari<sup>1,2</sup>, Evelin Miller<sup>2</sup>, Dr. Katharina-Nikutta Doll<sup>1</sup>, Prof. Dr. Meike Stiesch<sup>1</sup>, Prof. Dr. Michael Veith<sup>2</sup>

Chaymae.boukari@w-hs.de

<sup>1</sup>Department of Prosthetic Dentistry and Biomedical Materials Science, Hannover Medical School, Carl-Neuberg-Str. 1, 30625 Hannover, Germany/Lower Saxony Centre for Biomedical Engineering, Implant Research and Development (NIFE), Stadtfeldamm 34, 30625 Hannover & <sup>2</sup>Department of Molecular Biophysics, Westphalian University of Applied Sciences, August-Schmidt-Ring 10, 45665 Recklinghausen, Germany

**Abstract:** Titanium surfaces were biofunctionalized to confer anti-adhesive properties using streptavidin. The resulting nanometer-scale supramolecular architecture was characterized by contact angle measurements and surface plasmon resonance. Reduced bacterial adhesion was further confirmed using the dental commensal bacterium *Streptococcus oralis*.

**Keywords:** Biofunctionalization; dental implant; abutment; biophysical; *S.oralis*

## Introduction

Implant-associated infections arise from the formation of bacterial biofilms on the implant body, particularly in the area of the abutment. Therefore, there is a need for new biofunctionalizations of dental implants that inhibit biofilm formation. The patented biofunctionalization based on streptavidin (SAv) developed by the Molecular Biophysics Group at the Westphalian University of Applied Sciences exhibits anti-adhesive and antibacterial effects that are well suited for this purpose (Fig. 1A) [1].

## Results and Discussion

The successful biofunctionalization of the titanium surface was verified by changes in the contact angle (Fig. 1B images). The contact angle changed significantly after each functionalization step. Surface plasmon resonance kinetic measurements showed that SAv physisorbs directly onto the substrate (Fig. 1B box plots). However, after a rinsing step, the majority of the SAv desorbs again. Compared to the biofunctionalized surface with biotinylated silane, the direct physisorption of SAv results in a significantly lower degree of surface coverage. The results confirm previous work, including that by Ettelt et al. [2]. Only the molecularly intact, specific bond on the surface between SAv and biotin provides a stable functionalization that reduces bacterial adhesion. Furthermore, microscopic images of the commensal bacterium *S. oralis* on a biofunctionalized titanium sample, showed a visually reduced bacterial adhesion compared to a titanium reference sample (Fig. C).

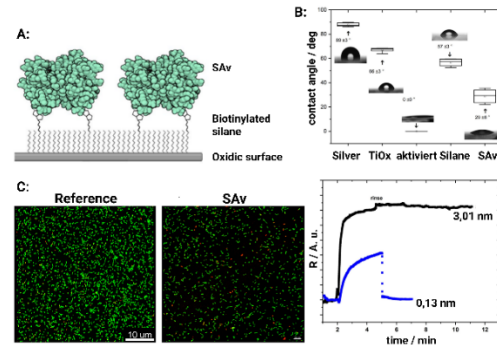


**Figure 1:** A: Biofunctionalization scheme B: Contact angle changes during biofunctionalization and corresponding kinetic measurements. C: Microscopic images of *S. oralis* (live cells green, dead cells red; created in BioRender.com).

## Conclusions

Biophysical analysis confirmed successful biofunctionalization, while microscopic images revealed reduced bacterial adhesion.

## References

- [1] Ettelt V, Ekat K, Kämmerer PW, Kreikemeyer B, Epple M, Veith M. Streptavidin-coated surfaces suppress bacterial colonization by inhibiting nonspecific protein adsorption. *J Biomed Mater Res A* 2018; 106(3): 758–68 [https://doi.org/10.1002/jbm.a.36276] [PMID: 29055106]
- [2] Boukari C. Biophysical characterization of biofunctionalized dental implant surfaces. Master's thesis. Westphalian University of Applied Sciences [Recklinghausen]; [2024].

## Acknowledgements

I acknowledge the Hans Böckler Foundation for my PhD scholarship, and Deutsche Forschungsgemeinschaft (DFG, German Research Foundation) under the Collaborative Research Center SFB/TRR-298-SIIRI – Project ID 426335750 for supporting my doctoral research.

# Advancing a multi-sensor array platform for real-time drinking water quality surveillance

D. Özsoylu<sup>1</sup>, E. Börmann-El Kholy<sup>1</sup>, S. Achtsnicht<sup>1</sup>, M. J. Schöning<sup>1,2</sup>

[oezsoylu@fh-aachen.de](mailto:oezsoylu@fh-aachen.de)

<sup>1</sup>Institute of Nano- and Biotechnologies (INB), FH Aachen, Campus Jülich, Heinrich-Mußmann-Str. 1, 52428 Jülich, Germany

<sup>2</sup>Institute of Biological Information Processing (IBI-3), Forschungszentrum Jülich GmbH, Wilhelm-Johnen-Str., 52425 Jülich, Germany

**Abstract:** Reliable access to safe drinking water is fundamental for public health. To identify water quality variations and potentially hazardous contamination events at an early stage, a remotely accessible online system for continuous multi-parameter monitoring is required. The work presented here addresses this need through the development of such a system.

**Keywords:** Ion-selective electrode (ISE); water quality; continuous monitoring; ground water

## Introduction

Securing drinking water quality increasingly requires monitoring approaches that move beyond periodic laboratory analysis toward continuous and decentralized surveillance. Conventional control strategies rely largely on offline sampling, which may delay the recognition of sudden changes or contamination events. Sensor-based early warning concepts therefore gain growing relevance for resilient water infrastructure. Despite established protection measures and regulatory supervision, deviations from prescribed quality thresholds are still reported in routine assessments [1-3]. This underlines the need for analytical platforms capable of tracking multiple water quality indicators (such as pH, dissolved ions, toxins and heavy metals) simultaneously and in real-time. Within this context, the presented work focuses on the development of a multi-parameter sensing platform that combines complementary electrochemical and physico-/chemical detection principles in a single monitoring system. The objective is to enable continuous assessment of water status and support rapid identification of abnormalities through integrated online measurements.

## Results and Discussion

An initial demonstrator featuring a flow-through configuration for simultaneous detection of multiple ions (such as copper, nitrate, sodium and chloride) within the same liquid sample will be introduced (Figure 1). The demonstrator consists of two serially connected measurement cells: one integrating sensors for temperature, pH, and conductivity, while the second accommodates the ion-selective electrodes. In addition, the performance of the developed system has been evaluated under continuous flow conditions through long-term testing to assess its stability and functionality for online monitoring applications.

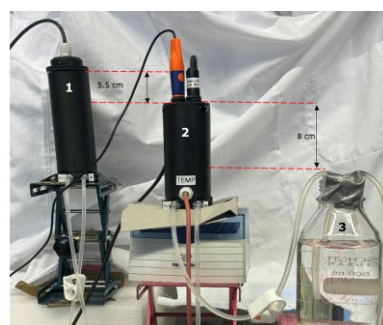


**Figure 1:** Multi-electrode measurement setup for continuous drinking water quality assessment. 1, measurement cell equipped with ISEs; 2, measurement cell including physico-/chemical sensors such as for pH, conductivity and temperature; 3, drinking water under examination.

## References

- [1] <https://www.umweltbundesamt.de/en/themen/wasser/gewassertyp-des-jahres/water-body-type-of-the-year-2022-groundwater#importance-of-groundwater>, last accessed 28.04.2025
- [2] Drinking Water Ordinance of 20 June 2023 (Federal Law Gazette 2023 I No. 159)
- [3] Bericht des Bundesministeriums für Gesundheit und des Umweltbundesamtes an die Verbraucherinnen und Verbraucher über die Qualität von Wasser für den menschlichen Gebrauch (Trinkwasser) in Deutschland (2020-2022)

## Acknowledgments

The authors thank the Central Innovation Program (project number:16KN0996445) for small and medium-sized enterprises (SMEs) funded by the German Federal Ministry for Economic Affairs and Climate Action (BMWK) and also the project partners, INCOstartec GmbH, LANTECH Informationstechnik GmbH, Fraunhofer IGB, and Stadtwerke Klingenberg.

# Evaluation of Host Responses to Biofilms with Distinct Pathogenic Potential Using a 3D Macrophage-Containing INTER<sub>b</sub>ACT Model

Shuli Chen<sup>1,2</sup>, Muhammad Imran Rahim<sup>1,2</sup>, Andreas Winkel<sup>1,2</sup>, Katharina Nikutta<sup>1,2</sup>, Meike Stiesch<sup>1,2</sup>

[stiesch.meike@mh-hannover.de](mailto:stiesch.meike@mh-hannover.de)

<sup>1</sup>Department of Prosthetic Dentistry and Biomedical Materials Science, Hannover Medical School, Hannover, Germany

<sup>2</sup>Lower Saxony Centre for Biomedical Engineering, Implant Research and Development (NIFE), Hannover, Germany

**Abstract:** Peri-implant diseases involve dysbiotic interactions between biofilms and host immune responses. Three-dimensional (3D) implant–tissue–oral bacterial biofilm *in vitro* models incorporating macrophages provide a clinically relevant representation of the peri-implant microenvironment and can be used to investigate host responses to biofilms with distinct bacterial compositions, including commensal and pathogenic biofilms. The role of macrophages in modulating immune activity was confirmed according to changes in both biofilm and tissue reaction within the 3D setting. Therefore, this model provides a unique platform to study immune regulation in peri-implant environments in the context of basic and translational research.

**Keywords:** 3D model, peri-implant, biofilm, macrophages, host–biofilm interaction

## Introduction

The peri-implant environment is continuously exposed to microbial biofilms, which under healthy conditions usually exist in balance with surrounding host tissues. However, shifts in biofilm composition toward more pathogenic or dysbiotic states may trigger inflammatory responses and contribute to the development of peri-implant diseases. Macrophages are key immune cells in peri-implant tissues, where they regulate inflammation and contribute to host responses following bacterial challenge. Using a previously established macrophage-containing 3D peri-implant model (INTER<sub>b</sub>ACT [1]), complex interactions between host tissues, microbial Biofilms and implant materials can be investigated under controlled conditions. Within this system, macrophages play an important role in shaping tissue responses to biofilms with different pathogenic potential.

## Results and Discussion

THP-1-derived macrophages were incorporated into a 3D peri-implant model consisting of a matrix containing gingival fibroblasts, and a titanium implant overlaid with a multilayered epithelium. The model was successfully co-cultured with two oral multispecies biofilms representing health and pathologic conditions [2][3] for at least 48 hours. Histological analysis indicated that the presence of macrophages contributed in general to the maintenance of tissue integrity. Biofilm staining demonstrated reduced biofilm viability and alterations in biofilm structure in the presence of macrophages, confirming macrophage-mediated antimicrobial effects that were dependent on the bacterial community applied. These observations

further highlight the potential to simulate the adapted host response with distinct consequences usually observed for peri-implant inflammation processes in the patient in the 3D model as well. In addition, gene expression analysis revealed changes in macrophage-associated markers during co-culture, suggesting possible polarization of macrophages, supporting the evidence of macrophage plasticity under the experimental conditions.

## Conclusions

The macrophage-containing INTER<sub>b</sub>ACT model was established as a 3D platform to study immune–biofilm–implant interactions in details. The findings indicate that host responses vary depending on biofilm composition, highlighting the influence of biofilm composition on both microbial behavior and tissue responses. Within this system, macrophages contribute to immune modulation, while the model provides a valuable tool to investigate how biofilms with different pathogenic potential shape host responses in peri-implant environments.

## References

- [1] S. Chen, M.I. Rahim, C. Mikolaj, et al. *Materialia* 41, (2025). <https://doi.org/10.1016/j.mta.2025.102452>
- [2] N. Kommerein, S.N. Stumpp, M. Müsken, et al. *PLoS One* 12(3), e0173973 (2017). <https://doi.org/10.1371/journal.pone.0173973>
- [3] N. Heine, K. Bittroff, S.P. Szafranski, M. Duitscher, W. Behrens, C. Vollmer, et al. *Front. Oral Health* 6, (2025). <https://doi.org/10.3389/froh.2025.1649419>

## Acknowledgements

Funded by the Deutsche Forschungsgemeinschaft (DFG, German Research Foundation) – SFB/TRR-298-SIIRI – Project-ID 426335750.

# Controlling Adhesion of Bacteria and Host Tissue Cells by Polyelectrolyte Multilayer Coatings on Titanium-based Biomaterials

Ye Guo<sup>1,2</sup>, Tonya Andreeva<sup>3</sup>, Anne Jahn<sup>4</sup>, Osman Akbas<sup>1,2</sup>, Diana Strauch<sup>1,2</sup>, Henning Hartwig<sup>1,2</sup>, Andreas Greuling<sup>1,2</sup>, Andreas Winkel<sup>1,2</sup>, Rumen Krastev<sup>3</sup>, Meike Stiesch<sup>1,2</sup>

Stiesch.meike@mh-hannover.de

<sup>1</sup>Department of Prosthetic Dentistry and Biomedical Materials Science, Hannover Medical School, Hannover, Germany

<sup>2</sup>Lower Saxony Centre for Biomedical Engineering, Implant Research and Development (NIFE), Hannover, Germany

<sup>3</sup>Reutlingen University, Faculty Life Sciences, Reutlingen, Germany

<sup>4</sup>Laser Zentrum Hannover e.V., Hannover, Germany

**Abstract:** Additively manufactured dental implants were developed to improve patient-specific prosthetic care. Polyelectrolyte multilayer coatings allow for the targeted adaptation of the surface properties of implant systems to optimize cytocompatibility and antibacterial efficacy. *In vitro* studies of tissue cell adhesion on the one hand, and bacterial adhesion and biofilm formation on the other, identified suitable coating strategies for the application to customized implant materials. Finally, the results will be transferred to the organotypic 3D model INTER<sub>b</sub>ACT (Implant-tissue-oral bacterial biofilm model) to gain insights into the changes in the peri-implant host-biofilm interaction caused by these surface modifications.

**Keywords:** additively manufactured titanium, polyelectrolyte multilayer coating, cytocompatibility, bacterial adhesion

## Introduction

Innovations in dental implantology, such as the use of new materials, alloys or additive manufacturing in order to enable new applications and improved care, must always keep an optimal interaction with the immediate environment in mind. In many cases, this necessitates various surface modifications through sandblasting and etching, as well as coatings applied after implant body fabrication, to minimize negative effects on peri-implant tissue adhesion and bacterial colonization. In this study, we investigated the *in vitro* influence of different coatings on the adhesion of tissue cells and oral bacteria.

## Results and Discussion

Discs of Ti<sub>6</sub>Al<sub>4</sub>V were additively manufactured, sandblasted and acid etched to simulate surfaces expected in customized implant strategies. The samples were then coated with different polymers (PSS, PAA, PAH, HA, chitosan) in various combinations to generate specific surface properties. Initially, primary human osteoblasts (NHOst) as well as individual bacterial species and multispecies communities [1] were applied and the adhesion and activities on the surfaces were examined microscopically and molecularly. Only some coatings showed advantageous properties with regard to improved cell adhesion combined with antibacterial effect [2]. To further confirm this and to better consider the clinically relevant, complex

interaction of tissue, implant and biofilm at the same time, the most promising coating will also be incorporated into the 3D model INTER<sub>b</sub>ACT and examined in more detail [3,4].

## Conclusions

With polyelectrolyte multilayer coatings a physical and chemical uniformity of titanium alloy can be designed to achieve improved cytocompatibility as well as modified bacterial adhesion while preserving specific morphology and micro-roughness of the underlying implant material.

## References

- [1] Kommerein N et al. PLoS One. 2017 Mar 15;12(3):e0173973. doi: 10.1371/journal.pone.0173973.
- [2] Andreeva T et al. In Vivo. 2025 May-Jun;39(3):1786-1798. doi: 10.21873/invivo.13980. S. Chen, M.I. Rahim, C. Mikolai, et al. *Materialia* 41, (2025). <https://doi.org/10.1016/j.mtla.2025.102452>
- [3] Chen S et al. *Materialia* 41 (2025): 102452. doi: 10.1016/j.mtla.2025.102452
- [4] Malekhamadi B et al. BMC Oral Health. 2026 Jan 14;26(1):91. doi: 10.1186/s12903-025-06930-2.

## Acknowledgements

Funded by the Deutsche Forschungsgemeinschaft (DFG, German Research Foundation) – Research Unit 5250 – Project-ID 449916462.

# Adhesion characteristics of *Candida albicans* on polymer-based materials

Saba Tamjiddash<sup>1,2</sup>, Laura Brose<sup>3</sup>, Meike Stiesch<sup>1,2</sup>, Sebastian Hahnel<sup>3</sup>, Katharina Doll-Nikutta<sup>1,2</sup>, Nadine Kommerein<sup>1,2</sup>

Tamjiddash.saba@mh-hannover.de

1 Department of Prosthetic Dentistry and Biomedical Materials Science, Hannover Medical School, Hannover, Germany

2 Lower Saxony Centre for Biomedical Engineering, Implant Research and Development (NIFE), Hannover, Germany

3 Department of Prosthetic Dentistry, UKR University Hospital Regensburg, Germany

**Abstract:** *Candida albicans* (*C. albicans*) adhesion to polymer-based surfaces is a key factor in denture-related stomatitis. This study investigated adhesion to polyvinyl chloride (PVC) and polytetrafluoroethylene (PTFE) using single-cell force spectroscopy (SCFS) and qRT-PCR. In addition, prosthetic materials—polymethyl methacrylate (PMMA), polyether ether ketone (PEEK), and 3D-printed dimethacrylate-based resin (DMA)—were subjected to artificial aging and analysed using scanning electron microscopy (SEM). Results showed that adhesion is influenced by saliva and surface properties like roughness and hydrophobicity, affecting adhesion strength and cell distribution. The findings highlight the importance of physicochemical surface characteristics in developing anti-adhesive denture materials.

**Keywords:** *Candida albicans*; adhesion; single-cell force spectroscopy; scanning electron microscopy

## Introduction

Denture-related *Candida* stomatitis is an inflammatory condition of the oral mucosa beneath removable dental prostheses, primarily caused by the fungal pathogen *C. albicans* [1]. A key factor in the development of these infections is the initial adhesion of *C. albicans* to polymer-based surfaces, followed by the formation of biofilms [2]. However, the mechanisms underlying fungal adhesion to different polymer-based materials are not yet fully understood. The aim of this study is therefore to investigate these interactions at multiple levels.

## Results and Discussion

Adhesion forces of *C. albicans* on PVC and PTFE surfaces were quantified using SCFS [3], and gene expression was analysed via qRT-PCR. Additionally, the number of cells on prosthetic materials was assessed using SEM, considering surface hydrophobicity and roughness with and without artificial saliva pre-treatment. The results showed that PTFE exhibited higher adhesion than PVC when coated with saliva, independently of roughness, whereas PVC adhesion was strongly dependent on roughness. Gene expression analysis revealed increased *ALSI* expression and low *HWPI* levels. SEM analyses demonstrated material-dependent effects: without saliva, ageing and smoother surfaces reduced cell numbers on PMMA and DMA, but increased them on PEEK. Cell aggregation generally increased on aged samples and was further enhanced by saliva, particularly on 3D-printed materials. [Figure 1]

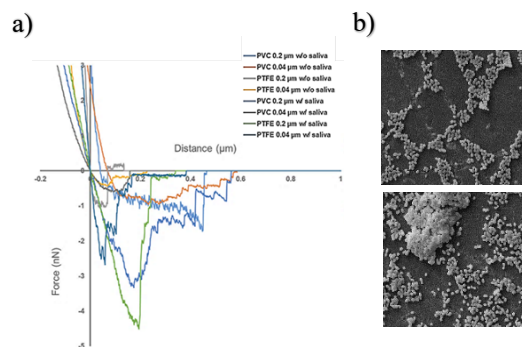


**Figure 1:** a) Representative force–distance curves for PVC and PTFE at different roughness. b) SEM images of thermally aged PMMA (no saliva, top) and DMA45° (with saliva, bottom), both at 0.04 μm.

## Conclusions

Smooth surfaces, as well as high surface polarity and surface energy, can reduce *C. albicans* adhesion. Saliva has a significant influence on the process and must be taken into account.

## References

- [1] Le Bars, P. et al. *Microorganisms* 2022, 10, 1437. <https://doi.org/10.3390/microorganisms1007437>.
- [2] Zhang, Y. et al. *PLOS ONE* 2023, 18, e0308705. <https://doi.org/10.1371/journal.pone.0308705>.
- [3] Doll, K. et al. *J. Dent. Res.* 2020, 99, 1071–1079. <https://doi.org/10.1177/0022034520916397>.

## Acknowledgements

This research was funded by the Deutsche Forschungsgesellschaft (DFG, German Research Foundation), project ID 470769735.

# Development of an electrochemically synthesized RNA sensor

Niclas Gellert<sup>1</sup>, Martina Knabel, Daniela Andrea Contreras Pérez, Theodor Doll

[Gellert.niclas@mh.hannover.de](mailto:Gellert.niclas@mh.hannover.de)

<sup>1</sup>NIFE, BioMaterial Engineering, Hannover Medical School, Carl-Neuberg-Str. 1, 30625 Hannover, Germany.

**Abstract:** Sensitive and selective ribonucleic acid (RNA) detection is important for future diagnostic applications. This work proposes a proof-of-concept sensor based on electrochemically synthesized molecularly imprinted polymers (MIPs) on screen-printed electrodes (SPE). The RNA template is incorporated during polymerization to create selective recognition sites in a thin, controllable film. The concept is designed for low sample volumes and aims at fast, reproducible, and potentially biocompatible sensor fabrication. Future work will focus on optimizing imprinting conditions, evaluating selectivity, and testing transferability to different RNA targets.

**Keywords:** RNA, *in-vivo* sensor, molecularly imprinted polymer

## Introduction

The sensitive and selective detection of ribonucleic acid (RNA) is becoming increasingly important in biomedical research, diagnostics, and therapeutic monitoring, as RNA molecules provide dynamic information about gene expression, cellular regulation, and disease-related processes. In contrast to more stable biomolecules, RNA levels can change rapidly in response to physiological or pathological conditions, making them highly valuable biomarkers for early detection and real-time analysis. However, RNA analysis remains challenging because of its low abundance, structural complexity, susceptibility to degradation, and the presence of closely related sequences in complex biological environments. Molecularly imprinted polymers (MIPs) have emerged as a promising synthetic recognition strategy for addressing these challenges. By forming template-specific binding sites, MIPs can provide selective recognition while offering advantages such as chemical stability, low cost, and the potential for integration into robust sensing platforms. These properties make MIPs particularly attractive for the development of RNA sensors intended for biomedical and potentially *in vivo* applications. <sup>[1,2]</sup>

## Method

A proof-of-concept approach is proposed for the electrochemical detection of RNA using Poly(3,4-ethylenedioxythiophene) polystyrene sulfonate (PEDOT:PSS) based MIPs on screen-printed electrodes (SPE) (Fig. 1). The concept relies on the electrochemical polymerization of EDOT in the presence of the RNA target to create a thin, controllable recognition layer with selective binding sites. A key advantage of the approach is the use of a very small sample volume, enabling both the imprinting process and subsequent detection in a compact, low-volume format.

Before experimental validation, the interaction between EDOT, the RNA template, and the resulting polymer matrix are currently evaluated conceptually

to identify suitable synthesis conditions and assess the feasibility of template incorporation and removal. The electrochemical polymerization strategy bears a high potential to provide a fast and reproducible route to *in situ* film formation with precise control over thickness and growth. In the next step, the sensor platform will be adapted to evaluate selectivity, sensitivity, and transferability to different RNA targets, with the long-term goal of developing a biocompatible and potentially wireless or point-of-care compatible sensing system.

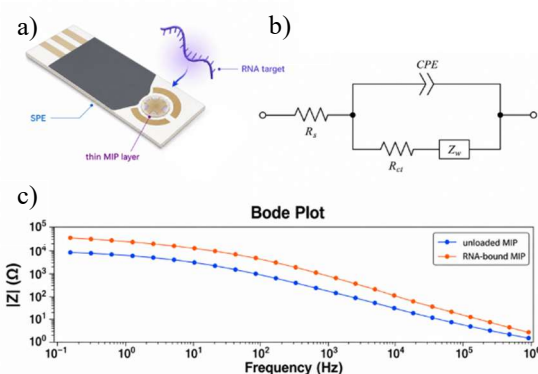


**Figure 1:** a) Schematic of the RNA detection using a MIP on a SPE b) Randles equivalent circuit used to model the sensor response c) Theoretical Impedance curve of an RNA detecting MIP

## References

- [1] Islam et al. Small Methods (2017). <https://doi.org/10.1002/smt.201700131>
- [2] Nguyen et al. ACS Omega (2024). <https://doi.org/10.1021/acsomega.4c02906>

## Acknowledgements

This work has been funded by the Graduate School RNApp (zukunft.niedersachsen)

# Plasma-Engineered Coatings for the Reduction of Biomaterial Adhesion

Johanna Reus<sup>1,2</sup>, Denise Püllmann<sup>1</sup>, Jan Henrik Finke<sup>1,2,3</sup>, Kristina Lachmann<sup>1,2</sup>

Johanna.reus@ist.fraunhofer.de

<sup>1</sup>Fraunhofer Institute for Surface Engineering and Thin Films, Riedenkamp 2, 38108 Braunschweig, Germany,

<sup>2</sup>Center of Pharmaceutical Engineering, TU Braunschweig, Franz-Liszt-Str. 35a, 38106 Braunschweig, Germany

<sup>3</sup>Institute for Particle Technology, TU Braunschweig, Volkmaroder Str. 5, 38104 Braunschweig, Germany

**Abstract:** Interactions between biological materials and surfaces can compromise the performance and biocompatibility of medical devices. This project develops plasma-assisted coatings and analytical methods to quantify and reduce surface residues. Initial results show that tailored surfaces properties can effectively reduce biomolecular adhesion.

**Keywords:** biomolecular adhesion, surface coatings, surface engineering, plasma-assisted thin films

## Introduction

Interactions between biological materials and surfaces can significantly affect the performance, stability and biocompatibility of medical devices. Undesired adhesion of biomolecular structures can trigger fouling processes, immune response or loss of functionality. These results aim to develop an anti-adhesive surface coating with the focus on plasma-deposited thin films to minimize biomaterial adhesion. Initially, the influence of these coatings on the adhesion behaviour of model substances will be systematically investigated. In addition, suitable analytical methods will be established to detect and quantify residues on surfaces. These insights will contribute to the design of advanced anti-fouling coatings for biomedical applications.

## Results and Discussion

Initial experiments were carried out on model polymeric surfaces (Polypropylene, *PP*) and glass slides. Different plasma-assisted thin films were applied to these surfaces to detect changes in the adhesive properties of such materials. The results show that plasma-based coatings can be a useful tool to neutralize surfaces which could be shown by measuring the isoelectric point of various materials before and after coating processes. When looking at the surface free energy (SFE) on surfaces, depending on the coating agents the SFE could either be increased or decreased after the coating process. Both the surface charge and the SFE are well known in literature to hugely impact the adhesion behaviour of biological materials [1].

Initial fluorescence-based detection of PolyA-LNP adhesion demonstrated residual signals on borosilicate glass and polymer substrates after storing PolyA-LNPs on the surface and binding lipophilic fluorescence marker onto the surface. After coating these materials using PEG-Silane a reduction of unspecific adsorption processes could

be detected (see figure 1). These findings underline the influence of surface chemistry on biomolecule and LNP interactions, guiding future material design. The resulting insights will steer the future design of optimized surfaces.

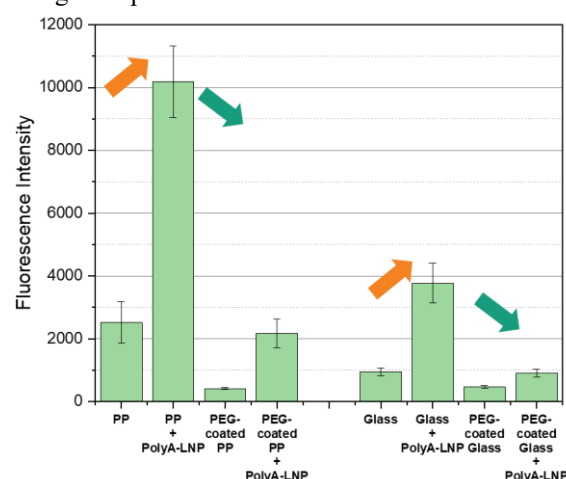


**Figure 1:** Preliminary adsorption tests of PolyA-LNPs on PEG-coated glass and Polypropylene (*PP*) surfaces.

## Conclusions

Preliminary studies on surface properties relevant to biomedical applications show that plasma-assisted coatings can modulate surface charge, surface free energy and thereby reduce biomolecular adhesion. These results support the development of anti-adhesive coatings for medical devices, particularly to improve their long-term performance.

## References

- [1] F. Song, H. Koo, D. Ren. *J. of Dental Research* 94, 8 (2015). <https://doi.org/10.1177/0022034515587690>

## Acknowledgements

RNAp is funded under grant number ZN4345 by the zukunft.niedersachsen program.

# A Biosensor with Simplified Target Recognition for Early Detection of Leprosy from Serum of Household Contacts

Flavia Di Scala, Augusto Parreiras de Jesus, Alejandro Guzman Landero Renteria, Thomas Houben, Hanne Dilien, Thomas Cleij, Valerii Myndrul, Bart van Grinsven

flavia.discal@maastrichtuniversity.nl

Sensor Engineering Department, Faculty of Science and Engineering, Maastricht University, Maastricht, P.O. Box 616, 6200 MD, The Netherlands

**Abstract:** In this study, we developed a biosensor for the early detection of Leprosy before symptoms appear using a self-assembled monolayer (SAM) on a screen-printed gold electrode (SPGE) that contained a peptide specifically designed to detect leprosy's IgG and IgM. Once we have ascertained that the immunocomplex responds to the electrochemical test We will incorporate FCVJ within a polymer matrix of Polydimethylsiloxane (PDMS) and lauric acid (LA) to introduce an optical redout.

**Keywords:** molecular rotors, electrochemistry, self-assembled monolayer

## Introduction

In this study, we developed a biosensor for the early detection of Leprosy before symptoms appear, aiming to prevent severe disabilities. Leprosy is a neglected tropical disease (NTD) caused by the acid-fast bacilli (AFB) of the *Mycobacterium leprae* complex [1], affecting the skin, peripheral nerves, mucosa of the upper respiratory tract, and eyes [2]. According to the World Health Organization (WHO), approximately 200,000 cases of leprosy are reported annually in more than 120 countries [3]. However, leprosy is curable, and various studies [4] show a connection between the severity of disabilities and delays in diagnosis, which occur in 60-70% of patients.

## Results and Discussion

We used a self-assembled monolayer (SAM) on a screen-printed gold electrode (SPGE) containing a peptide designed to detect leprosy IgG and IgM. One end of the peptide was modified with methylene blue (MB) as a redox probe, while the other end had a thiol group (-SH) for binding to the gold surface. We added 6-mercapto-1-hexanol (C6-OH) as a backfill agent to reduce non-specific adsorption and maintain the peptide's orientation. Figure 1 illustrates the MB current variations in response to different sample matrices, including buffer solutions, healthy human plasma, and plasma from asymptomatic "contacts" of leprosy patients, who show specific antibodies via ELISA. Upon confirming the immunocomplex's response to the electrochemical test, the functionalized electrode will be embedded in a thermo-optical flowcell. We will incorporate FCVJ within a Polydimethylsiloxane (PDMS) and lauric acid (LA) matrix to enhance heat transfer changes resulting from antibody-peptide binding at the electrode surface.

## Conclusions

The MR's fluorescent sensitivity to temperature and viscosity alterations will be used to detect antibody-associated changes in serum samples of the flow cell.

## References

- [1] M. B. Maymone, M. Laughter, S. Venkatesh, M. M. Dacso, P. N. Rao, B. M. Stryjewska, J. Hugh, R. P. Dellavalle, C. A. Dunnick, Leprosy: clinical aspects and diagnostic techniques, *Journal of the American Academy of Dermatology* 83 (1) (2020) 1–14.
- [2] World Health Organization, Leprosy, <https://www.who.int/news-room/fact-sheets/detail/leprosy>, accessed: 2025-06-04 (2024). URL <https://www.who.int/news-room/fact-sheets/detail/leprosy>.
- [3] W. H. Organization, Leprosy (hansen disease), accessed: 2025-06-04 (2025). URL <https://www.who.int/data/gho/data/themes/topics/leprosy-hansens-disease60>
- [4] B. M. Masresha, H. B. Biresaw, Y. A. Moyehodie, S. S. Mulugeta, Time-to-disability determinants among leprosy patients enrolled for treatment at alert center, addis ababa, ethiopia: A survival analysis, *Infection and Drug Resistance* (2022) 2729–2741.
- [5] de Jesus, Augusto César Parreiras, et al. "Identifying promising peptide targets for leprosy serological tests: From prediction to ELISA." *Journal of Genetic Engineering and Biotechnology* 23.1 (2025): 100475.

# New platform for microfluidic structuring in glass

Benno Schneider<sup>1</sup>, M.J. Schöning, T. Wagner

[benno.schneider@fh-aachen.de](mailto:benno.schneider@fh-aachen.de)

<sup>1</sup>University of Applied Sciences Aachen, Heinrich-Mußmann-Str. 1, 52428 Jülich, Germany

**Abstract:** Selective Laser-Induced Etching (SLE) is an innovative two-stage process for the precise microstructuring of glass. In the first stage, ultrashort laser pulses locally modify the chemical etchability of the material. In the second stage, wet chemical etching selectively removes the modified regions, yielding complex three-dimensional microstructures. With selectivities exceeding 500:1 in quartz glass, SLE enables the fabrication of fine, high-aspect-ratio microchannels with minimal conicity. This platform opens new possibilities for microfluidic applications, lab-on-chip systems, and advanced microstructured components in life sciences and chemical analysis.

**Keywords:** microfluidic; laser; glass etching

## Introduction

The demand for precise, scalable, and cost-effective microstructuring techniques in glass is growing steadily, driven by applications in microfluidics, lab-on-chip technologies, and bioanalytical systems. Conventional methods for glass structuring, such as photolithography combined with wet etching or mechanical drilling, face significant limitations regarding three-dimensional complexity, achievable channel aspect ratios, and surface quality. Selective Laser-Induced Etching (SLE) has emerged as a powerful alternative, overcoming many of these constraints by combining ultrashort pulse laser processing with subsequent chemical etching. This contribution presents a novel platform based on SLE for the fabrication of complex microfluidic structures in glass, offering high selectivity, geometric freedom, and scalability for industrial and scientific applications.

## Results and Discussion

The Selective Laser-Induced Etching process is a two-stage process:

First, transparent material is exposed to laser radiation in such a way that the chemical etchability is increased at these points. To ensure that this is achieved without cracking, a short pulse duration (fs-ps) and a small focus volume (a few  $\mu\text{m}^3$ ) are required. The focus is then moved through the material until a contiguous volume in contact with the outer surface of the workpiece is exposed.

In the second process step, the material modified by the laser radiation is selectively removed by wet chemical etching, the structure is essentially developed. Selectivity the etching rate of the modified material in relation to the etching rate of the unmodified material is essential for structural accuracy.

Quartz glass typically has a selectivity greater than 500:1, enabling the creation of fine, long channels

with low conicity. SLE technology can therefore be used to create complex 3D cavities in glass, which form the basis for various products, such as microfluidics and microstructured components.

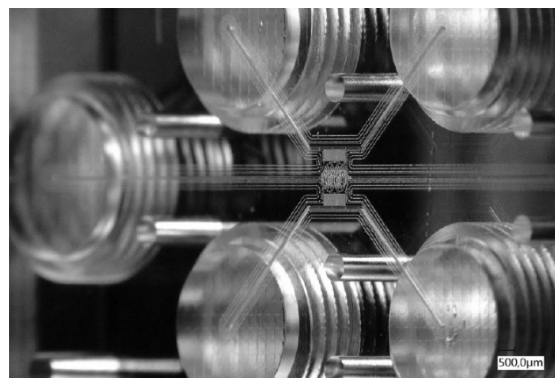


**Figure 1:** Small channels (width 5  $\mu\text{m}$ , length 2000  $\mu\text{m}$ ) and chambers, fully structured in glass.

## Conclusions

SLE constitutes a highly capable and versatile platform for the fabrication of complex microfluidic architectures in glass. Achieving high precision and large aspect ratios in microfluidic channels nevertheless requires careful CAD (computer-aided design) and CAM (computer-aided manufacturing) preprocessing, alongside the development of optimized processing protocols to ensure reproducible, high-quality fabrication outcomes. These methodologies and process workflows are currently under active development and provide promising opportunities for future collaborative research activities.

## Acknowledgements

The authors would like to thank the Aachen University of Applied Sciences for its financial support.

# Hormone-Driven Modulation of Implant-Associated Biofilms

Rumjhum Mukherjee<sup>1,2</sup>, Marie Thomsen<sup>1,2</sup>, Meike Stiesch<sup>1,2</sup>, Szymon P. Szafranski<sup>1,2</sup>

[Szafranski.szymon@mh-hannover.de](mailto:Szafranski.szymon@mh-hannover.de)

<sup>1</sup>Department of Prosthetic Dentistry and Biomedical Materials Science, Hannover Medical School (MHH), Hannover, Germany

<sup>2</sup>Lower Saxony Center for Biomedical Engineering, Implant Research and Development (NIFE), 30625 Hannover, Germany

**Abstract:** Peri-implant diseases are driven by dysbiotic biofilms and remain a major limitation for long-term implant success. This project investigates how host-derived sex hormones modulate microbial metabolism, interspecies interactions, and virulence within implant-associated biofilms. Using synthetic biofilm communities, metatranscriptomics, advanced imaging, and functional assays, hormone-responsive pathways linked to pathogen persistence and biofilm resilience will be systematically characterized. The study aims to establish a mechanistic framework connecting endocrine signaling with peri-implant dysbiosis and infection susceptibility, providing a foundation for precision prevention strategies and next-generation infection-responsive implant interfaces.

**Keywords:** peri-implant infections; biofilms; microbial endocrinology; oral microbiome; metatranscriptomics

## Introduction

Biofilm-associated peri-implant diseases are among the leading causes of implant failure and are strongly influenced by complex host–microbe interactions. Recent studies indicate that microbial metabolism and interspecies cross-feeding contribute to the persistence of pathogenic oral biofilms. At the same time, endocrine factors such as estradiol and progesterone are increasingly recognized as modulators of microbial physiology and virulence. However, the mechanistic relationship between host hormonal status and implant-associated dysbiosis remains poorly understood. This project addresses this gap by investigating hormone-responsive microbial pathways and their role in peri-implant biofilm development, with relevance for personalized and infection-reactive implant systems [1,2].

## Results and Discussion

The project combines *in vitro* synthetic biofilm models, metatranscriptomic analyses, microscopy, and functional assays to characterize hormone-driven changes in microbial community dynamics. Particular focus is placed on the modulation of redox-associated metabolic pathways and interspecies interactions that support the expansion of opportunistic pathogens. Preliminary observations suggest that physiologically relevant hormone concentrations may enhance biofilm resilience and virulence-associated traits in peri-implant communities. The planned investigations will establish a mechanistic framework linking endocrine signaling with microbial dysbiosis and implant-associated infection susceptibility. These findings are expected to support the development of targeted preventive and therapeutic strategies for functional implant interfaces.

## Conclusions

This work explores the interplay between host endocrine signaling and implant-associated microbial ecology. By integrating microbiology, transcriptomics, and biofilm modeling, the project aims to advance the understanding of hormone-mediated dysbiosis in peri-implant disease. The findings may contribute to future precision approaches for infection prevention and implant longevity in susceptible patient populations.

## References

- [1] Neuman H, Debelius JW, Knight R, Koren O. Microbial endocrinology: the interplay between the microbiota and the endocrine system. *FEMS Microbiology Reviews*. 2015;39(4):509–521.
- [2] Hajishengallis G, Liang S, Payne MA, et al. Low-abundance biofilm species orchestrates inflammatory periodontal disease through the commensal microbiota and complement. *Cell Host & Microbe*. 2011;10(5):497–506.

## Acknowledgements

Funded by the Deutsche Forschungsgemeinschaft (DFG, German Research Foundation) – SFB/TRR-298-SIIRI – Project-ID 42633575. This project was funded by the MHH start-up grant for young researchers ('HiLF').

# Photoelectrochemical sensing and mapping of flow velocity in microfluidics

Yunpeng Fang <sup>1</sup>, Ruixiang Li, Bo Zhou, Jon Gorecki, Jiazhe Zhao, Joe Briscoe, Karin Hing, Steffi Krause

y.fang@qmul.ac.uk, s.krause@qmul.ac.uk

School of Engineering and Materials Science, Queen Mary University of London, London, E1 4NS, UK

**Abstract:** This study presents zinc oxide nanorod (ZnO NR)-based photoelectrochemical sensing for ultralow microfluidic flow detection and local flow velocity mapping. Under UV illumination and applied bias, the ZnO NR sensor showed reproducible flow-dependent photocurrent responses, with distinguishable signals down to 0.006 mL/min. This sensitivity is attributed to piezo-photoelectrochemical coupling, where flow-induced deformation modulates interfacial charge transfer and photocurrent generation. By integrating ZnO NRs with photoelectrochemical imaging (PEI), local flow velocity distributions were mapped in microchannels, showing stronger photocurrent near the channel centre, consistent with laminar flow behaviour. This platform offers a promising route for real-time flow monitoring and future studies of cell adhesion under well-defined shear stress conditions.

**Keywords:** ZnO nanorods; ultralow flow sensing; flow mapping; photoelectrochemical imaging

## Introduction

Accurate local flow measurement is important in microfluidics, where bulk flow rate cannot fully represent spatial variations in velocity and shear stress. PEI enables label-free, spatially resolved mapping of photocurrent responses at semiconductor/electrolyte interfaces. ZnO NRs have been used as light-addressable sensor substrates for bioanalytical applications, including pH sensing and real-time monitoring of enzymatic polymer degradation<sup>1</sup>. Their photoelectrochemical, charge transport, and piezoelectric properties make them promising for flow-responsive sensing<sup>2</sup>. Here, we exploit this piezo-phototronic effect for flow sensing.

## Results and Discussion

ZnO NR sensor responses were measured at different flow rates using an Autolab potentiostat under UV illumination and applied bias. As shown in Figure 1, reproducible photocurrent changes were observed when flow was switched on and off, with distinguishable signals obtained at ultralow flow rates down to 0.006 mL/min. This confirms the high sensitivity of ZnO NRs to weak fluid motion.

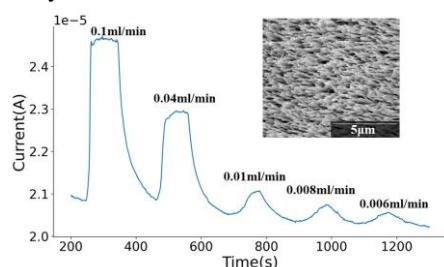


**Figure 1:** Photocurrent measurements with ZnO NRs grown on FTO coated glass at different flow rates in a microfluidic channel.

The response is attributed to piezo-photoelectrochemical coupling, where flow-induced deformation modulates interfacial charge transfer

and photocurrent generation. Based on this sensitivity, ZnO NRs were combined with PEI to map local flow velocity distributions. Figure 2 shows stronger photocurrent near the channel centre and weaker signals near the edges, consistent with laminar flow.

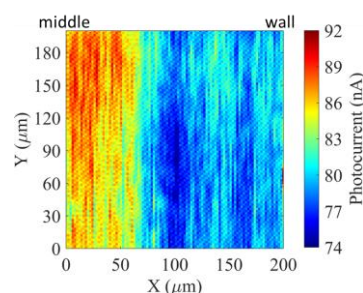


**Figure 2:** PEI mapping of local flow velocity in a microchannel at 0.05 mL/min flow rate, showing increased photocurrent towards the channel centre, consistent with laminar flow.

## Conclusions

ZnO NRs were demonstrated as sensitive photoelectrochemical flow sensors, detecting ultralow flow rates down to 0.006 mL/min. Combined with PEI, they enabled spatial mapping of local flow velocity in microchannels. This platform offers a route for real-time microfluidic flow monitoring and future studies of shear stress-regulated cell adhesion.

## References

- [1] Y. Tu et al., Anal. Chem. 90, 8708–8715 (2018).
- [2] Y. Wang et al., Micromachines 14, 47 (2022).

## Acknowledgements

Thanks to the China Scholarship Council for PhD studentships for RL, JZ and YF and to EPSRC (EP/R035571/1) for funding.

# Creating biomimetic 3D *in vitro* models of the bone-marrow / implant interface

Milan Brockert<sup>1</sup>, Jan Mathis Hornbostel<sup>1</sup>, Dr. Marco Haertlé<sup>2</sup>, Prof. Dr. Andrea Hoffmann<sup>2</sup>, Prof. Dr. Cornelia Lee-Thedieck<sup>1</sup>

onur.milan.brockert@stud.uni-hannover.de

<sup>1</sup>Institute of Cell Biology and Biophysics, Leibniz University Hannover, Herrenhäuser Straße 2, Hannover

<sup>2</sup>Department of Orthopaedic Surgery, Hannover Medical School, Anna-von-Borries-Straße 1-7, Hannover

**Abstract:** Aseptic implant loosening is the most common cause of implant failure. Aseptic loosening involves the appearance of wear particles, which induce cellular and molecular reactions. Since the clinical symptoms of aseptic implant loosening occur in the later stages of this process, the molecular processes involved in the onset of this condition are not well understood. Although models of the interface between implants and stiff tissue have been developed, only 2D models resembling the interface between implants and soft tissue exist. This project aims to develop a 3D model of the bone marrow/implant interface to study the molecular and cellular responses to wear particles.

**Keywords:** Aseptic implant loosening; in-vitro model; bone marrow; wear particles

## Introduction

Approximately 22% of joint revision surgeries are due to aseptic implant loosening. While it has been demonstrated that wear debris disturbs the microenvironment of hard tissue, this project aims to investigate its effects on bone marrow at the implant site. This imbalance can disrupt the local microenvironment, impair implant function and worsen bone-related diseases. To study the changed microenvironment at the interface between bone marrow and the implant, this project aims to build an *in vitro* model of this microenvironment. The model will use a hydrogel based on cationized BSA (cBSA) as a scaffold, which will be seeded with different bone marrow cell types to study their interaction and responses in this environment.

## Results and Discussion

To mimic the porous architecture of trabecular bone and the protein-rich nature of bone marrow, a protein-based, macroporous hydrogel scaffold was developed. Through the process of cationization, BSA was converted to cell-adhesive cBSA. Co-cultures of bone marrow stem cells responsible for regenerative processes, namely hematopoietic stem and progenitor cells (HSPCs) and mesenchymal stem/stromal cells (MSCs) were successfully established in these scaffolds [1]. To enable studies on bone remodelling, cocultures of bone-building osteoblasts and bone-resorbing osteoclasts were set up. These co-culture systems will be extended toward 3D triple co-cultures including macrophages, which play an important role in the immune response to wear particles. Macrophages will be obtained by differentiation from peripheral blood mononuclear cells (PBMCs).

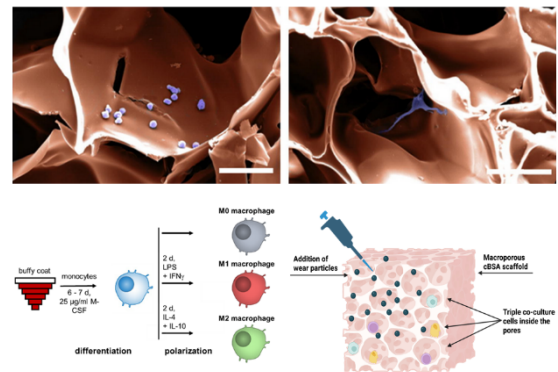


**Figure 1:** Top: SEM images of a cBSA scaffold seeded with hematopoietic cells (left) and MSCs (right). The cells are located inside of the pores of the scaffold and adhere to the scaffold material. Lower left: Isolation, differentiation and polarization of monocyte-derived macrophages. Lower right: Triple co-culture inside cBSA scaffold with added wear particles.

## Outlook

Once established, the bone marrow-mimetic 3D cocultures systems will be used to study the molecular and cellular responses to wear particles in this environment.

## References

- [1] Raic, A. *et al.* Biomimetic 3D *in vitro* model of biofilm triggered osteomyelitis for investigating hematopoiesis during bone marrow infections. *Acta Biomaterialia* 73, 250–262 (2018).

## Acknowledgements

This project is funded by the Deutsche Forschungsgemeinschaft (DFG, German Research Foundation) – SFB/TRR-298-SIIRI – Project-ID 426335750.

# Direct 3D Printing of Soft Neural Implants onto Flexible PCB Substrates

Boutaina Zerrik<sup>1</sup>, Adrian Onken, Theodor Doll

Zerrik.Boutaina@mh-hannover.de

<sup>1</sup> NIFE, BioMaterial Engineering, Hannover Medical School, Carl-Neuberg-Str. 1, 30625 Hannover, Germany

**Abstract:** A fully integrated additive manufacturing workflow for the direct deposition of soft neural implants onto flexible printed circuit boards (FlexPCBs) is presented. Using a multi-material direct ink writing process with polydimethylsiloxane and conductive epoxy paste, conductive traces are deposited directly onto FlexPCB footprint pads during fabrication, eliminating post-fabrication contacting steps. A custom alignment stage, an in-situ alignment procedure, and a two-part printing strategy were developed to achieve sub-millimetre registration and reliable electrical integration.

**Keywords:** neural implants; direct ink writing; PDMS; 3D printing; printed electrodes

## Introduction

Soft neural implants based on PDMS offer mechanical compliance well-suited to neural tissue, reducing chronic foreign body responses compared to other materials [1]. Direct ink writing (DIW) enables multi-material deposition in a single workflow without custom tooling. Previous work demonstrated multi-layer EEG electrode arrays for rodent models using a bioplotter-based DIW process, with electrical connection achieved via anisotropic conductive film (ACF) tape bonding [2]. This approach suffers from delamination susceptibility and operator-dependent sub-millimetre alignment, resulting in low fabrication yield. The present work aims to eliminate post-fabrication contacting through direct printing functional implant layers directly onto the FlexPCB contact pads.

## Results and Discussion

A custom alignment stage was designed and fabricated to position the FlexPCB (0.15 mm thickness, polyimide substrate) flush with the adjacent glass substrate on the bioplotter print bed. A PCB alignment and calibration procedure was developed exploiting the partial transparency of the polyimide board for visual registration, achieving consistent sub-millimetre alignment between printed trace endpoints and footprint pads. The implant design was reconstructed in an inverted orientation so that conductive traces are deposited first, directly onto the FlexPCB contact pads. A two-part printing strategy was implemented to address surface non-uniformity and bridging line constraints inherent to the full multilayer design. Both implant parts were fabricated successfully and combined by folding to yield a complete integrated device, as shown in Figure 1(c). In-situ PDMS curing on the heated platform (80°C, 13 min) eliminated positional errors arising from holder remounting,

confining all precision-critical deposition steps to a single uninterrupted session.

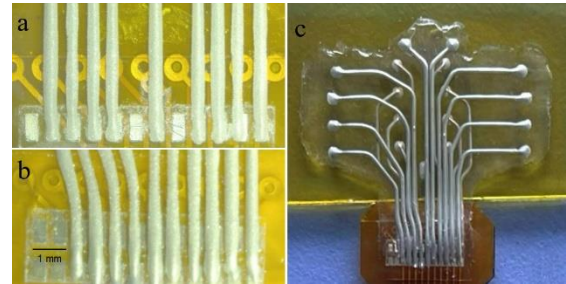


**Figure 1:** Optical microscopy images of conductive traces of the first and second implant parts deposited directly onto the FlexPCB footprint pads (a & b). (c) Completed implant after folding both parts into a single integrated structure.

## Conclusions

Direct additive fabrication of soft neural implants onto FlexPCBs has been demonstrated, eliminating post-fabrication contacting and improving alignment reproducibility over ACF tape bonding. Future work will focus on the integration of a sacrificial release layer for atraumatic implant detachment and a redesign of the FlexPCB to serve as the primary print substrate.

## References

- [1] L. Zhou, et al. Flexible, Ultrathin Bioelectronic Materials and Devices for Chronically Stable Neural Interfaces. *Brain-X*. 2023;1(4):e47.
- [2] A. Onken, , et al. 3D Printing of Scaled Neural Implants: Additive Fabrication Tailored to Rodent Skulls. *EnFI* 2025.

## Acknowledgements

Parts of this work was done within the Cluster of Excellence H4a PhoenixD [EXC2122] and funded by the trinational Project 511765241

# Fabrication and preliminary optimization of an in situ written PEGDA membrane in a quartz glass microfluidic chip

Lisa M. Ehlers, Lukas Rennpferdt, Hoc Khiem Trieu

[Lisa.ehlers@tuhh.de](mailto:Lisa.ehlers@tuhh.de)

Institute of Microsystems Technology, Hamburg University of Technology, Hamburg, Germany

**Abstract:** A hybrid microfluidic platform combining a quartz glass chip fabricated by selective laser-induced etching (SLE) with an in situ written poly(ethylenglykol)diacrylate (PEGDA) hydrogel membrane using two-photon polymerization (2PP) is presented. A cylindrical quartz glass through-channel served as the confined volume for membrane integration. The circular membrane was designed with 30  $\mu\text{m}$  target pores. Because the 2 mm membrane exceeds the sub-millimeter region of consistent writing fidelity, stitching is required to preserve pore uniformity. Initial experiments show that membrane morphology and pore formation depend strongly on laser power, slicing-line spacing, and writing speed.

**Keywords:** microfluidics; selective laser-induced etching; 2PP; PEGDA; quartz glass; hydrogel membrane

## Introduction

Hybrid microfluidic systems combining rigid substrates with soft functional materials are of growing interest for filtration and bioanalytical applications [1]. Quartz glass offers high optical transparency, chemical resistance, and can be fabricated with high geometric precision, while PEGDA hydrogels provide tuneable properties and can be micropatterned using 2PP. Inspired by recent work on stacked microporous glass membranes in 3D glass microfluidics [2], the present study transfers the glass membrane concept to an in situ written hydrogel structure, addressing the challenge of combining high resolution 2PP with comparatively large millimeter structures.

## Results and Discussion

A 2 mm through-channel was fabricated in 2.4 mm thick quartz glass using a LightFab 3D printer (femtosecond laser with 1030 nm wavelength, 765 kHz, 0.5 ps, 200 mm/s), followed by etching in 8 mol/L KOH at 82 °C for 24 h. For membrane integration, PEGDA 700 with 1% IC2959 was introduced into the channel and polymerized in situ line-by-line using 2PP over a millimeter-scale area at a wavelength of 515 nm, 10 MHz, 0.289 ps, and 1 or 5 mm/s. Unpolymerized material was removed by ethanol development and DI water rinsing. The circular membrane was designed with a nominal pore diameter of 30  $\mu\text{m}$ . Higher pulse energy (e.g. 3 nJ) produced thicker, more brittle membranes with non-through pores (Figure 1, Left), whereas lower pulse energy (e.g. 1 nJ) yielded finer, shape-stable structures with open 30  $\mu\text{m}$  pores (Figure 1, Right). The main limitation occurred in the stitching regions, where reduced membrane thickness created mechanical weak points. At a slicing-line spacing of 5  $\mu\text{m}$ , individual lines remained visible and partially

detached at lower exposure. This was prevented by reducing the spacing to 1  $\mu\text{m}$  and increasing the writing speed from 1 to 5 mm/s. The results indicate that membrane fidelity strongly depends on pulse energy, slicing-line spacing and writing speed.

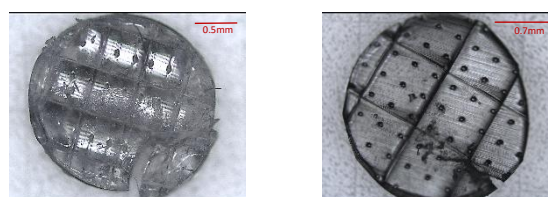


**Figure 1:** (Left) Membrane written at 3 nJ, 5  $\mu\text{m}$  slicing-line spacing, 1 mm/s writing speed, and 0.5 x 0.5 mm<sup>2</sup> writing field. (Right) Membrane written at 1 nJ, 1  $\mu\text{m}$  slicing-line spacing, 5 mm/s writing speed, and 0.7 x 0.7 mm<sup>2</sup> writing field.

## Conclusions

In situ integration of a patterned PEGDA membrane into a microfluidic chip was demonstrated. Structural fidelity improved at lower pulse energy, smaller slicing-line spacing, and higher writing speed, while stitching regions remained the main limitation. The results show that a membrane with micrometer-scale resolution can be integrated into a millimeter-scale fluidic structure, exceeding the capabilities of standard additive manufacturing.

## References

- [1] Lin, J., Cui, L., Shi, X., & Wu, S. (2025). Emerging Trends in Microfluidic Biomaterials: From Functional Design to Applications. *Journal of Functional Biomaterials*, 16(5), 166. <https://doi.org/10.3390/jfb16050166>
- [2] Duran-Arteaga, D., Chen, W., Rackus, D.G. et al. Selective laser etching fabrication of stacked microporous membranes for multisize particle separation in 3D microfluidics. *Sci Rep* 15, 36236 (2025). <https://doi.org/10.1038/s41598-025-20267-4>

## Acknowledgement

This project is funded by the Deutsche Forschungsgemeinschaft (DFG, German Research Foundation) - SFB 1615 - 503850735.

# Bacteria-surface interaction on smooth and rough titanium: Correlation between surface characteristics and bacterial adhesion

Sophia Awerbuch<sup>1,2</sup>, Florian Fuchs<sup>3</sup>, Meike Stiesch<sup>1,2</sup>, Katharina Doll-Nikutta<sup>1,2</sup>

[Awerbuch.sophia@mh-hannover.de](mailto:Awerbuch.sophia@mh-hannover.de)

<sup>1</sup>Department of Prosthetic Dentistry and Biomedical Materials Science, Hannover Medical School, Carl-Neuberg-Straße 1, 30625 Hannover, Germany

<sup>2</sup>Lower Saxony Centre for Biomedical Engineering, Implant Research and Development (NIFE), Stadtfelddamm 34, 30625 Hannover, Germany

<sup>3</sup>Department for Dental Prosthetics and Materials Science, University Hospital Leipzig, Liebigstraße 12, 04103 Leipzig, Germany

**Abstract:** Biofilm-associated infections on dental implants remain a major challenge in modern dentistry with implant surface properties having a direct impact on bacterial colonization. This study investigated the influence of titanium surface roughness on the adhesion and biofilm formation of *Streptococcus oralis* and *Actinomyces naeslundii*. By correlating physical surface characteristics with microbiological results, a distinct influence of surface polarity as well as nanoscale but not microscale surface roughness could be identified.

**Keywords:** titanium, oral biofilms, bacterial adhesion, dental implants, surface roughness

## Introduction

Peri-implant infections are caused by oral bacteria colonization of the dental implant surface. They form three-dimensional structures, called biofilms, that protect the cells from the host immunity and antibacterial substances. Titanium is widely used for dental implants due to its biocompatibility and mechanical stability. It is commonly assumed that smoother implant surfaces reduce bacterial adhesion and therefore lower the risk of infection [1]. However, several studies describe no clear correlation between roughness and biofilm formation or even increased bacterial attachment on nano-smooth surfaces [2]. For this purpose, this study aimed to systematically analyse the influence of titanium surface roughness on the adhesion and biofilm formation of two oral bacteria species.

## Results and Discussion

In this study, titanium discs with three different surface roughness spanning two powers of ten were investigated. Micro- and nano-scale roughness were assessed by confocal laser-scanning microscopy (CLSM, Fig. 1). Additionally, surface wettability was characterized by contact angle measurements using water and diiodomethane. The results show distinct differences in the surface' free energy polar fraction but not disperse fraction. Adhesion and biofilm formation of the commensal oral bacteria *Streptococcus oralis* and *Actinomyces naeslundii* were analysed by live/dead fluorescence staining and CLSM (Fig. 1). Interestingly, bacterial colonization was increased on smooth but not nano-smooth surfaces for both species, while bacterial viability showed species-specific patterns.

## Conclusions

Correlation analysis revealed that especially surface polarity and nanoscale, but not microscale surface roughness significantly influenced bacterial adhesion and biofilm formation on titanium surfaces.

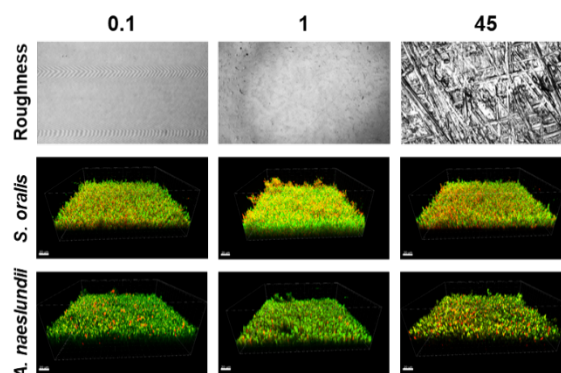


**Figure 1:** CLSM images of surface topography (top row, 190x95  $\mu\text{m}^2$ ) and biofilm formation of indicated strains. Live cells appear green, dead cells appear yellow/red. Scale bar 20  $\mu\text{m}$ .

## References

- [1] Yu J, Zhou M, Zhang L, Wei H. Antibacterial Adhesion Strategy for Dental Titanium Implant Surfaces: From Mechanisms to Application. *J Funct Biomater.* 2022; 13:169. doi: 10.3390/jfb13040169.
- [2] Ma J, Li K, Gu S. Selective Strategies for Antibacterial Regulation of Nanomaterials. *RSC Adv.* 2022; 12:4852-3864. doi: 10.1039/d1ra08996j.

## Acknowledgements

The work was funded by the Deutsche Forschungsgemeinschaft (DFG, German Research Foundation) under the Collaborative Research Center SFB/TRR-298-SIIRI (Project ID 426335750).